

**Laptev Sea System:
Expeditions in 1995**

Edited by Heidemarie Kassens

The TRANSDRIFT III Expedition: Freeze-up Studies in the Laptev Sea
H. Kassens, I. Dmitrenko, L. Timokhov & J. Thiede

Expedition to the Lena and Yana Rivers
V. Rachold, E. Hoops, A. M. Alabyan, V. N. Korotaev & A. A. Zaitsev

Ber. Polarforsch. 248 (1997)
ISSN 0176 - 5027

Heidemarie Kassens & Jörn Thiede, GEOMAR Forschungszentrum für marine
Geowissenschaften, Wischhofstraße 1-4, D-24148 Kiel

Igor Dmitrenko & Leonid Timokhov, State Research Center - Arctic and Antarctic
Research Institute, 38 Bering str., 199397 St. Petersburg, Russia

Volker Rachold & Erich Hoops, Alfred Wegener Institute for Polar and Marine
Research, Research Department Potsdam, Telegrafenberg A 43, D-14773
Potsdam

Andrey M. Alabyan, Vladislav N. Korotaev and Alexander A. Zaitsev, Moscow State
University, Geography Department, Scientific Research Laboratory of Erosion
and Fluvial Processes, 119899 Moscow, Russia

Contents

The TRANSDRIFT III Expedition: Freeze-up Studies in the Laptev Sea

H. Kassens, I. Dmitrenko, L. Timokhov & J. Thiede pages 1 - 192

Expedition to the Lena and Yana Rivers

V. Rachold, E. Hoops, A.M. Alabyan, V.N. Korotaev
& A.A. Zaitsev pages 193 - 210

The TRANSDRIFT III Expedition: Freeze-up Studies in the Laptev Sea



Edited by

H. Kassens, I. Dmitrenko, L. Timokhov & J. Thiede

ABSTRACT

The Russian icebreaker KAPITAN DRANITSYN carried out the TRANSDRIFT III expedition to the Laptev Sea (October 1 to 30., 1995), the largest ice factory in the Arctic Ocean and source region of the Transpolar Drift. In this shelf region, ice free for only three months a year, a comprehensive interdisciplinary working program concerning the causes and effects of annual freeze-up was performed.

Unlike our previous expeditions to the Laptev Sea, which focused on oceanographical, hydrochemical, ecological, and sedimentological processes during the brief ice-free period in summer, this expedition studied these processes during the extreme physical change through the onset of ice formation in autumn. This is the first study of its kind under these conditions, and gave important clues to the rapid (14 to 40 days) freeze-up, which has significant year-round effects for the Laptev Sea and global environment.

Freeze-up began one month later than usual (a 40 year record) close to the Novosibirskie Islands in low salinity surface waters due to heat stored in an intermediate water layer between 10 and 25 m water depth. Later, huge tracts of turbid, dirty ice were found off the Lena Delta where an unusually high phytoplankton concentration for this time of year occurred. The origin of these anomalies, and whether they are anomalies at all, and their relationship to global environment in real time are the focus of continuing research.

TABLE OF CONTENTS

Introduction.....	1
••Море Лаптевых - многоликий регион Арктики	1
••Laptev Sea System - An Overview	4
••The TRANSDRIFT III Expedition: Freeze-up Studies in the Laptev Sea	7
••Properties of the Laptev Sea, Key Results and Highlights 1995.....	10
••The KAPITAN DRANITSYN, Icebreaker Equipped for Research.....	16
Scientific Results	19
• Sea-Ice Conditions during the TRANSDRIFT III Expedition.....	19
••Meteorological Research and Synoptical Support of the Expedition.....	20
• Ocean-Atmosphere Interaction Processes.....	25
••Aerosol Measurements	25
••Sea-Ice Remote Sensing.....	28
••Side-Looking Airborne Radar and Aerial Video Recording of Sea Ice.....	29
••Dirty Sea-Ice Studies.....	31
• Crystal Structure and Physical and Mechanical Properties of Laptev Sea Ice at the Initial Period of Ice Formation.....	34
••Oceanographic Processes in the Laptev Sea during Autumn	44
• The Distribution of Chlorophyll Fluorescence Intensity in the Laptev Sea: Results of Hydrooptical Measurements.....	62
••Hydrochemical Observations	68
••Biological Investigations	69
••Multiprobe Suspension and Current Speed Measurements: Aspects of Sediment Dynamics during Freeze-up Studies in the Laptev Sea	75
• The Depositional Environment of the Laptev Sea	79
• Micropaleontological Studies	89
••Physical Properties of Near-Surface Sediments in the Laptev Sea.....	90
• Geochemical Pathways.....	93
••Pore-Water Geochemistry	97
References.....	99
Acknowledgements.....	102
Appendix	103
••Participants aboard the KAPITAN DRANITSYN for TRANSDRIFT III	104
••Station List of the TRANSDRIFT III Expedition.....	107
••Ice Stations Occupied by Ship and Helicopter during the TRANSDRIFT III Expedition	116

- Helicopter Flights during the TRANSDRIFT III Expedition..... 118
- Ice Observations aboard KAPITAN DRANITSYN 123
- List of Water and Sea Floor Samples Taken during the
TRANSDRIFT III Expedition 141
- List of Ice Samples Taken during the TRANSDRIFT III Expedition..... 152
- Description of Sediment Cores Taken during the
TRANSDRIFT III Expedition 154

INTRODUCTION

Море Лаптевых - многоликий регион Арктики

Л. А. Тимохов
Арктический и антарктический научно-исследовательский институт,
С.-Петербург, Россия

Арктика играет важную роль в формировании климата на нашей планете, так как эта полярная область не только быстро реагирует на глобальные изменения окружающей среды, но также вместе с этими изменениями активно воздействует на управляющие механизмы климата Земли. Причиной этому являются, прежде всего, морские льды, которые покрывают круглый год большую часть Северного ледовитого океана. Они влияют на взаимодействие между атмосферой и океаном, на циркуляцию океана, разрушают берега и являются важным фактором, влияющим на структуру осадков в океане.

Главной научной задачей российско-германского проекта "Система моря Лаптевых" является исследование региона моря Лаптевых как одного из важных элементов природной среды Арктики. Это море вместе с Восточно-Сибирским является "фабрикой льда" для Северного ледовитого океана. Сюда впадают крупные сибирские реки: Лена, Яна, Хатанга, Индигирка и др., выносящие в океан большое количество пресной речной воды, минеральных и органических веществ и антропогенных загрязнений. Здесь располагается самый обширный в Арктике мелководный шельф, аккумулирующий выносимые реками взвешенные вещества, захватываемые затем образующимся морским льдом и путешествующие в нем через Северный ледовитый океан. Сток рек, гидрологические и ледовые процессы в этом регионе влияют на положение и интенсивность Трансарктического течения, участвуя таким образом в изменениях климата Северного ледовитого океана.

Проект "Система моря Лаптевых" является крупнейшим среди выполняемых в рамках межправительственного соглашения о сотрудничестве в полярных и морских исследованиях. Всего в проекте принимают участие ученые более 40 научных институтов из России и Германии, причем это представители многих научных дисциплин: океанологи, палеогеографы, химики, геологи, биологи и др. Координация исследований осуществляется Арктическим и антарктическим НИИ (Санкт-Петербург) с российской стороны и Центром морских геонаук Кильского университета (ГЕОМАР) - с германской. Финансирование проекта осуществляется совместно министерствами науки России и Германии.

Реализация проекта разбита на этапы, на каждом из которых решаются конкретные научные проблемы. Так, в 1993 году основной целью было получение комплексной океанографической и метеорологической информации, включая оценки загрязненности моря Лаптевых в навигационный период, исследование биологических, литологических и геологических процессов на шельфе моря и устьевых участках рек.

Основной задачей экспедиции в 1994 году было определение границ выноса речных вод и связанных с этим явлением ареалов распространения различных биологических сообществ, особенностей распределения донных отложений и их геохимического состава. Установив по результатам предыдущей экспедиции ключевые районы, исследователи сконцентрировали свое внимание на физических процессах и механизмах, формирующих обнаруженные ранее региональные особенности природных явлений в море Лаптевых.

В октябре 1995 года, в отличие от прежних летних экспедиций, морская среда исследовалась в экстремальных физических условиях отрицательных температур воздуха, фазовых переходов и нарастания льда. Главные задачи экспедиции состояли в изучении образования и распространения льда, его состава, процессов "захвата"

взвешенных частиц и осадков льдом при его формировании, изменений термохалинных и химических характеристик морской воды в период образования льда, влияния ледовых процессов на биопродуктивность моря.

В истории изучения моря Лаптевых никогда еще ученые не проводили комплексные морские исследования по всей акватории в суровый переходный период от осени к зиме. Для выполнения научных задач в столь трудный сезон года был арендован ледокол Мурманского морского пароходства "Капитан Драницын". Выбор судна оказался очень удачным: мощные судовые двигатели, хорошая ледопробиваемость и маневренность позволили без задержек по ледовым и метеорологическим условиям эффективно решать оперативные планы экспедиции. Ледокол имеет неплохое палубное оборудование, которое успешно использовалось для ледоисследовательских, биологических и геологических работ. В немалой степени успешным исследованиям способствовал большой профессионализм и доброжелательность экипажа ледокола во главе с капитаном О. И. Агафоновым.

Уже с первых дней экспедиция ощутила властную мощь природы: арктические моря 48 лет не знали такой легкой ледовой обстановки, а накопленный морями запас тепла сдвинул сроки начала ледообразования в среднем на месяц позже климатических сроков.

Но этот "каприз" природы не изменил существенно выполнение основных задач экспедиции. График же работ научных отрядов стал еще более напряженным, поскольку ученые не могли упустить редчайшую удачу: дополнительно к плану исследовать подробно последствия аномально малой ледовитости и теплого лета.

Сюрпризы не заставили себя ждать. Уже на широтном разрезе к острову Бельковский температура воды на поверхности 10 октября была такой же, как летом 1994 года. А на глубинах от 15 до 20 метров были измерены удивительно высокие значения температуры воды до $+3,8^{\circ}$, что никогда раньше не отмечалось в этом районе и на таких глубинах даже в период максимального прогрева летом. Аномальным было также распределение морской воды в северо-восточной части моря Лаптевых. Так, к северу от острова Котельный соленость морской воды была на 40% меньше среднепогодной.

Анализ результатов океанографической съемки, выполненной экспедицией, показал, что в восточной части моря гидрологический фронт занимал меридиональное положение. Это свойственно второму основному типу гидрологического режима, который формируется при доминирующем влиянии арктического антициклона, как это наблюдалось и в 1995 году. Но величины значений параметров морской среды и обостренность их градиентов параметров в этом году были особенно большими. Впервые зарегистрированная такая большая осенняя аномалия должна особенно сильно повлиять на будущее развитие ледово-гидрологических процессов и заложить значимый климатический сигнал. Учет аномальных состояний арктических морей летом-осенью 1995 года позволит лучше понять формирование макроциркуляционных процессов в Арктике и оценить дальнейшее их влияние на погоду не только на Севере, но и в Европе.

Несмотря на то, что природа преподнесла сюрприз, отодвинув начало замерзания на более поздние сроки, экспедиция успешно провела исследования инкорпорации веществ в лед при его образовании и росте толщины. Уже в начале экспедиции в мелководной губе Драгоценная на севере острова Котельный в отобранных образцах льда оказалось большое количество инкорпорированного вещества. Захваченное в воде вещество льдом при его образовании и росте отмечалось во всех образцах льда, отобранных в устьевых областях рек Яны, Оленька, Хатанги. Но особенно много его было зафиксировано в колонках льда вблизи северной части дельты реки Лена. Уже предварительный анализ полученных результатов подтверждает одну из главных идей российско-германской программы, что льды моря Лаптевых являются мощным геологическим фактором в захвате и переносе взвешенных веществ и седиментов моря

на огромные расстояния вплоть до Северного полюса и пролива Фрама.

Биологические исследования позволили закрыть одно из белых пятен природной среды моря. Впервые к северу от острова Котельный были проведены количественные исследования экосистем макробентоса. В центральной части моря впервые выявлено сезонное уменьшение биомассы организмов макробентоса в 1.2 - 2.8 раза. Этот экспериментальный факт несколько необычен и требует еще своего объяснения. По результатам биологических исследований удалось установить, что ранее определенная для летнего сезона зависимость распределения биомассы макробентоса от солености и плотности придонных вод в целом характерна и для осеннего периода. Однако при уменьшении биомасс в одних и тех же районах минимум биомассы осенью наблюдался при солености 30.4 промили, а не 30 промилей как для летнего периода.

Экспедиция 1995 года еще раз продемонстрировала многоликость этого региона Арктики и важность изучения структуры и изменчивости природной среды море Лаптевых. Есть все основания полагать, что природные процессы в море Лаптевых дают кладут начало многим аномалиям, инициирующим изменения климата в Арктике, которые определяют погодные и ледовые условия, например, на трассе Северного морского пути.

Laptev Sea System - An Overview

The impact of the polar regions on global climate development has been established. Modern climate models as well as paleoclimatic reconstructions have shown that the waxing and waning of the continental ice caps and changes in sea-ice distribution influence the renewal of deep and intermediate water masses and, therefore, thermohaline ocean circulation. However, our knowledge of the climate impact in the Arctic Ocean, e.g., of the influence of climate changes on sea-ice formation, is very limited, thus making it difficult to predict the impact of possible future global climate changes. This holds true in particular for the Siberian shelf seas, which, for logistical and political reasons, have long been inaccessible to the international scientific community. Large amounts of Arctic sea ice are formed on these shelves, which is underscoring the central importance of these processes for the climate system.

The Laptev Sea is of particular interest because it's a source area for both the Transpolar Drift (Fig. 1) and sediment-loaded sea ice. In the Laptev Sea, it might be possible to demonstrate the extent to which global ocean circulation and climate development are influenced by extremely large influxes of freshwater from the Siberian river systems. Current oceanographic models have not yet considered such a direct terrestrial impact on the global climate.

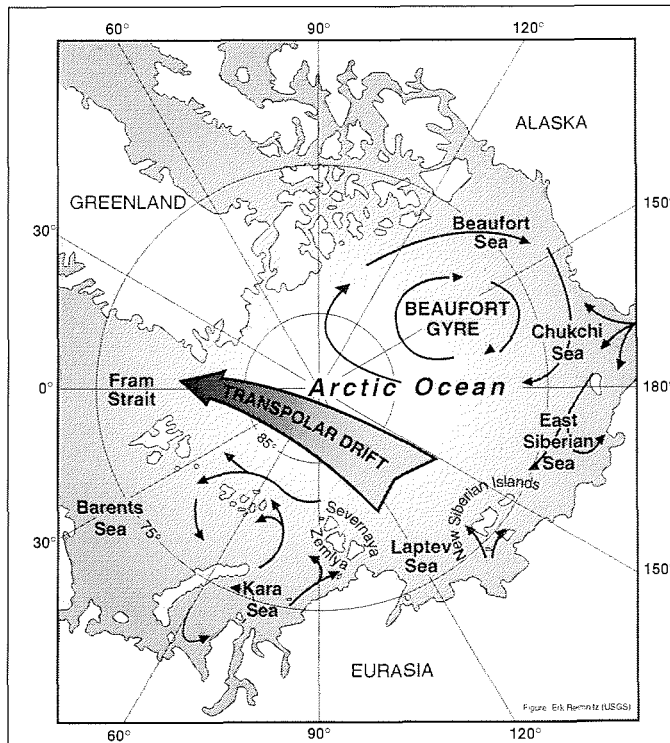


Fig. 1: Overview of ice drift patterns in the Arctic Ocean and its adjacent shelf seas.

In 1994, a major multidisciplinary research program 'Laptev Sea System' was designed as a cooperation effort of Russian and German institutions in order to understand the Arctic environment and its significance for the global climate. Ongoing bilateral research activities include land and marine expeditions to the Laptev Sea area during different seasons of the year as well as workshops and the exchange of scientists. The GEOMAR Research Center for Marine Geosciences in Kiel, Germany and the State Research Center for Arctic and Antarctic Research in St. Petersburg (AARI), Russia, are jointly responsible for organizing and coordinating the multidisciplinary project, which is funded by the Russian and German Ministries of Science and Technology.

The success of the pilot phase (AMEIS'91 to Kotel'nyi, ESARE'92 to the Lena Delta and the Novosibirskie Islands, and TRANSDRIFT I onboard RV IVAN KIREEV to the Laptev Sea in 1993) as well as the LENA'94 expedition to the River Lena and the TRANSDRIFT II expedition to the Laptev Sea onboard RV PROFESSOR MULTANOVSKY in 1994 was very encouraging (Dethleff et al., 1993, Kassens und Karpiy, 1994; Kassens, 1995). This promoted the next expedition, TRANSDRIFT III, to be planned for the autumn to study freeze-up processes in the Laptev Sea; a first for this time of year. Consequently, the expedition logistics were extremely difficult. The expedition out of Murmansk on the Russian icebreaker KAPITAN DRANITSYN had 52 scientists from Russia and Germany (Fig. 2, Tab. A1) and took place from October 1 to 30, 1995.

The TRANSDRIFT III expedition mainly targeted the coastal areas of the eastern Laptev Sea, e.g., the Lena Delta and the region of the Laptev Sea polynya. The highest priority program objectives were to study:

- extent and composition of sea ice,
- incorporation processes of various particulates into new ice,
- influence of sediment load in new ice on its albedo,
- alteration of oceanographic and hydrochemical processes during ice formation,
- impact of ice cover on the biological productivity,
- influence of freeze-up on the depositional environment in the Laptev Sea.

The TRANSDRIFT III expedition was joined by (i) the international ARK XI-1 expedition of RV POLARSTERN to the continental slope of the Laptev Sea (Rachor, 1997), and (ii) the LENA'95 expedition to one of the main source areas of the eastern Laptev Sea, the Lena and Yana rivers (Rachold et al., this volume). These joint research activities were performed in close cooperation between many Russian and German scientific institutions and succeeded in drawing a detailed picture of the important processes shaping the 'Laptev Sea System'. In this report we have compiled some of the pertinent data of the TRANSDRIFT III expedition, and hope to offer some clues as to why the Laptev Sea froze so late in 1995.

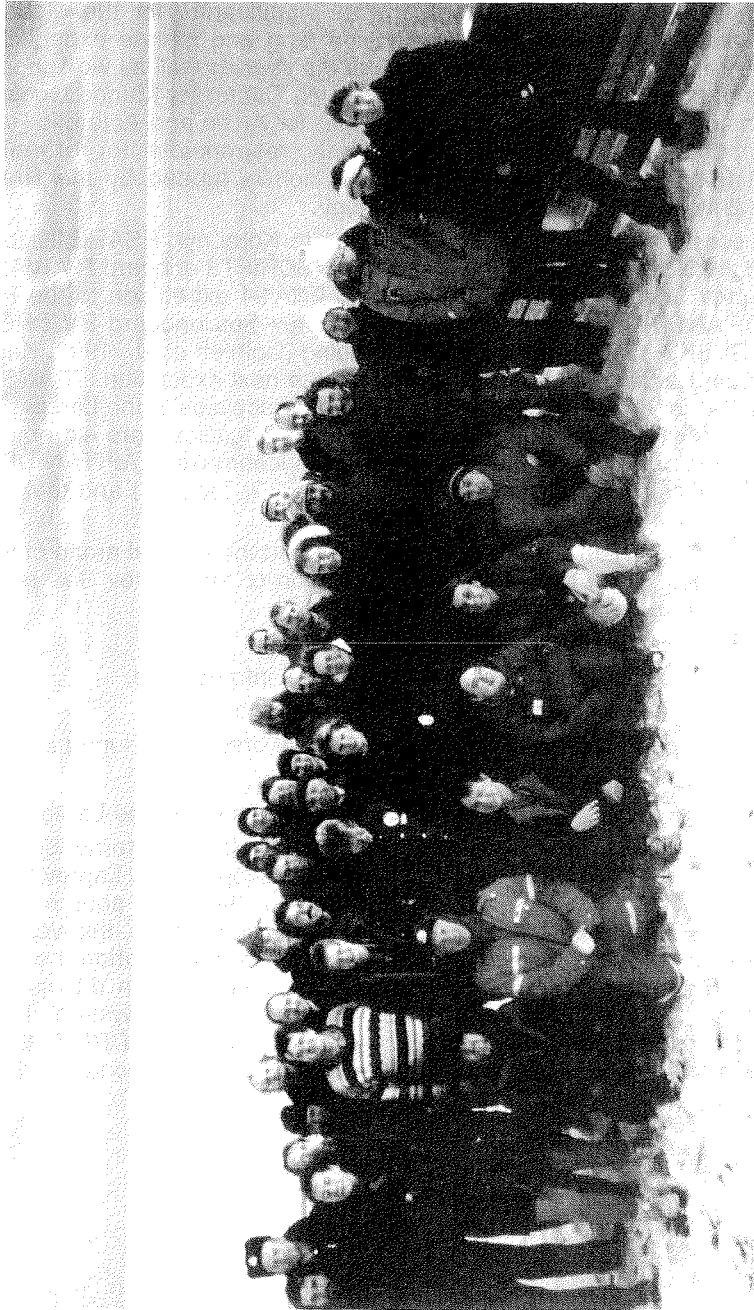


Fig. 2: Participants of the TRANSDRIFT III expedition (Photo - M. Antonow).

The TRANSDRIFT III Expedition: Freeze-up Studies in the Laptev Sea

The Laptev Sea (Fig. 3) is one of the most important sea-ice producing areas in the Arctic where large amounts of sediment can be entrained into the ice cover of the Transpolar Drift (e.g. Pfirman et al., 1990; Wollenburg, 1993; Nürnberg et al., 1994; Reimnitz et al., 1994; Eicken et al., 1997). Mechanism and processes being responsible for sediment entrainment, such as scavenging of suspended matter from the water column by frazil ice crystals, anchor ice formation or river spilling on sea ice in coastal regions, as well as their seasonal and interannual variability are of great importance for ice and sediment dynamics. The research program during the TRANSDRIFT III expedition concentrated on the autumn freeze-up and its impact on the depositional environment. Sea-ice formation processes were studied considering the effects on biological productivity, entrainment of particulate and dissolved matter, and hydrodynamic processes. Meteorological boundary conditions and the influence of river outflow were continuously recorded. Multi-disciplinary experiments were performed comprising:

- ice observations by remote sensing techniques and continuous ship- and helicopter-based ice monitoring,
- measurements of physical and chemical properties of the water column, its suspension and ice load by CTD, current meters, underwater photography, and water sampling,
- observations of the ice structure by drilling and subsequent investigation of various physical, chemical, and biological characteristics,
- bio-ecological studies including the biota's reaction on new-ice formation and ice coverage, and
- sedimentological investigations of the seafloor deposits, suspended particulate matter and sea-ice sediments.

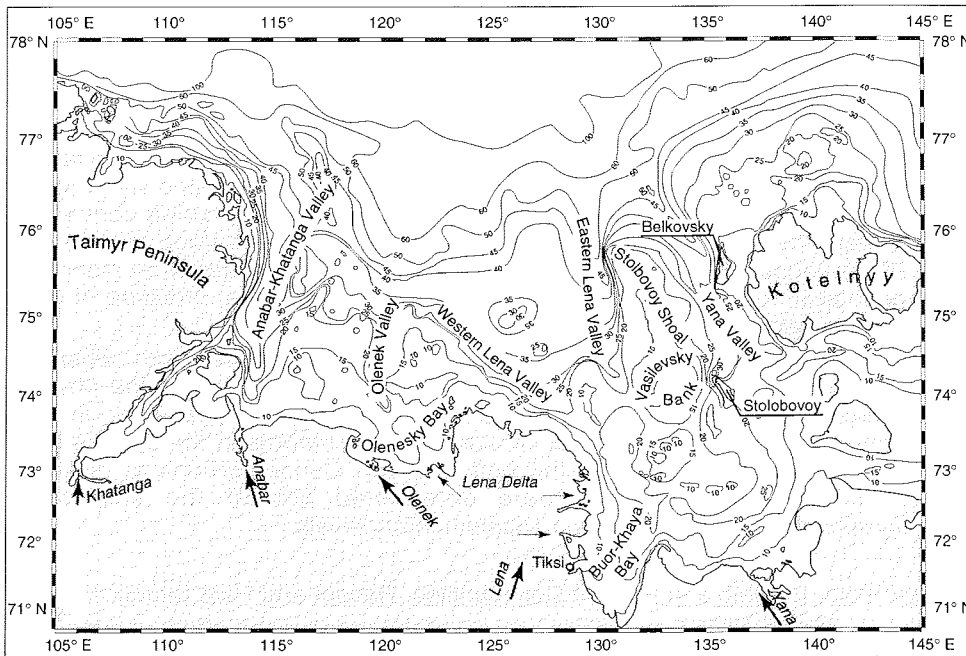


Fig. 3: Bathymetry map of the Laptev Sea.

Remote Sensing and Aerial Reconnaissance:

Information on the regional and meso-scale distribution of new ice areas down to small scale processes during ice formation was obtained from real-time satellite data. Aboard the KAPITAN DRANITSYN, large-scale information from the satellites OKEAN as well as from RADARSAT, ERS-2, and AVHRR were obtained. Further information on ice distribution, e.g. width and length of frazil streaks, and extent of congealed ice, was determined from side-looking airborne radar and visual observation. Determination of surface temperatures was achieved by spectral radiometric measurements (e.g. thermal infrared determination) providing information on the albedo.

Sea-Ice Studies

The TRANSDRIFT III expedition was designed to investigate the sediment entrainment processes active during formation and growth of sea ice and the subsequent export to the Transpolar Drift. Research on the ice was performed directly from the ice floes, and when the young ice was too thin, from the ship (gangway, mummy chair) (Fig. 4). The in situ observations mainly focussed on processes responsible for the entrainment of dissolved and particulate matter. Apart from systematic glaciological (properties of various ice types, ice mechanic characteristics), sedimentological studies (characterization of the sediment freight) and biological studies (e.g. chlorophyll measurements, faunal and floral studies), emphasis was placed on chemical studies, and the quantification of dissolved matter within the sea ice and the water column below. Small-scale fluxes of sediment during the formation of frazil ice were observed by an underwater particle camera and an "optical backscatter" nephelometer probe supported by sampling of the water column. Studies on the mesoscale ice formation, advection and accretion were conducted from air-borne observations in close coordination with meteorological and oceanographic observations.

Oceanography and Hydrochemistry

Small and mesoscale oceanographic processes under growing ice of different thickness as well as in ice-free zones are of considerable interest, since hydrophysical processes evolving in the surface layer during autumn significantly drive the intensity of suspension incorporation into sea ice. Wind and wave action, in this respect, is of outstanding importance and causes deep-going convection, which affects the vertical thermohaline structure of the sea surface layer. In the frame of the various TRANSDRIFT expeditions, studies concentrated on monitoring the hydrological conditions influenced by river runoff processes, radiation of water mass cooling, and convective processes.

The oceanographic investigations were run partly from the ship and - when ice-coverage was too dense - directly from the ice-floes. In addition to the physico-oceanographic studies, chemical analyses were carried out on sea water, in order to determine the annual biochemical consumption of nutrients in the surface layer, within the main halocline and in the bottom layer. Concentrations of dissolved oxygen, silica and phosphate were determined aboard the ship at all oceanographic sites at standard and supplementary levels.

Sea-Ice Biota, Benthic and Pelagic Communities: Recent and Past Situation

Previous TRANSDRIFT expeditions revealed the pronounced effect of river runoff on the distribution of benthic and pelagic communities. Hence, biological studies performed during TRANSDRIFT III focused on sea-ice and sub-ice biology, on

phytoplankton and zooplankton, as well as on benthic life in relation to seasonal changes. The characterization and quantification of the ice and sub-ice biota, including habitat structure and feeding behaviour of organisms, was derived by ice coring, sampling below ice floes with a sub-ice net, and *in situ* observations of the ice-water interface with a video-endoscope.



Fig. 4: Freeze-up studies by using the "mummy chair" of KAPITAN DRANITSYN during the TRANSDRIFT III expedition.

Estimations of the phytoplankton biomass based on chlorophyll *a* measurements throughout the water column by continuous water sampling as well as on measurements of *in situ* fluorescence. Zooplankton distribution patterns and biomass calculations will be carried out from Bongo net and Nansen net samples. Ongoing studies on grazing activities of zooplankton organisms are performed at the home lab. Various seabottom sampling gears (Van Veen grab, Sigsby trawl, bottom dredge) were applied to quantify the macro- and megabenthos inventory.

Organic Carbon Budget and the Carbonate System

In order to evaluate the importance of organic carbon storage on the Laptev Sea

shelf, the flux of marine and terrigenous organic matter in relation to environmental changes and paleoclimate was estimated. In addition to the differentiation of organic carbon into marine and terrigenous components (HI-indices, C/N ratios), various proxies for terrigenous input (long-chain n-alkanes, lignin) and marine productivity (alkenones, dinosterols, fatty acids, biogenic silica, Ba/Al ratios) will be applied to the shelf sediments after the cruise. Benthic fluxes of recycled organic carbon were quantified by estimating respiration rates from oxygen gradients across the water/sediment interface and ΣCO_2 measurements within the pore water. Due to the importance of both the carbonate system for the global carbon budget and for tracing water masses into the deep basins, total carbonate together with alkalinity dissolved and particulate organic carbon were analyzed in water samples.

Sediment Dynamics

The Laptev Sea shelf is a fast changing depositional environment characterized by excess sedimentation, tidal currents, erosion, and large-scale sediment reworking. Tidal changes, storm-wave processes (re-suspension of seafloor deposits), as well as density stratification due to river runoff and intense bottom and surface currents shape the sedimentary regime in close interrelation with intense ice activity, e.g. ice-gouging and iceberg ploughing. Sedimentological investigations were performed on material recovered by Van Veen grab, giant box core and vibro-core. Due to the harsh conditions during autumn, the over consolidated seafloor deposits, and ice-bonded surface sediments (permafrost) we recovered sediment cores no longer than 2.3 m. Investigations aboard the ship (microscopic investigations, coarse fraction analyses, bio-zonation) revealed distinct temporal changes in the depositional environment, which will further be characterized by grain size investigations (settling velocities, fine fraction granulometry), as well as clay and heavy mineral analyses (X-ray diffraction).

Properties of the Laptev Sea, Key Results and Highlights 1995

Because of the commercial importance of the Northern Sea Route from Europe to the Far East, Russian scientists routinely try to predict the freeze-up of the various segments of the Eurasian shelf seas; however, these predictions are usually available only 1 month ahead of time. For the Laptev Sea, freeze-up is known to usually occur during late September/early October (Fig 5). In Figure 6 we show the prediction for 1995 indicating that new ice would appear in early October around the fringes of the Laptev Sea, and that the freeze-up of its central part would be delayed until October 20. This is late in comparison to earlier years (Fig. 5). By careful planning, but also lucky coincidence, we began our expedition in Murmansk on October 1 and the KAPITAN DRANITSYN returned there on October 30 after visiting 75 ship stations and 64 helicopter stations in the Laptev Sea during the period of October 6 to 24, 1995 (Fig. 7, 8, 9). This was the first modern expedition which attempted to explore the Laptev Sea that late in the year. The first days of the expedition were very discouraging because freeze-up was delayed this year after an unusually warm summer and we only found an ice-free Laptev Sea with a somewhat peculiar oceanography.

To find ice in the first half of October, the KAPITAN DRANITSYN had to go to the NE coast of Bolshevik Island where in front of the multiyear ice of the Arctic Ocean, new ice was under formation and where flotillas of small icebergs (from the Severnaia Zemlia archipelago) crowded the horizon, while according to satellite imagery, the entire Laptev Sea was ice free. We did not encounter any icebergs further east and south in the Laptev Sea. Side-scan sonar records, however, show

that recent plough marks up to several meters in width cover nearly the entire Laptev Sea (Kassens, 1994; Lindemann, 1994; Benthien, 1994). At the same time we encountered unusual calm and relatively warm weather with no major storms during the beginning of October, preserving an undisturbed and shallow stratification of the water column. The members of the expedition had to wait until the second half of October to observe freeze-up close to the coast of Kotel'nyi, the northernmost of the Novosibirskie Islands. This late freeze-up of the Laptev Sea, is the latest in the last 40 years. During the second half of the expedition, however, temperatures dropped dramatically, we had to endure snow storms and freezing periods, which at times made our equipment useless because all mobile parts froze when touching the water surface. At the end of the expedition wide stretches of the Laptev Sea were covered by mostly thin, but sometimes up to several decimeters thick ice. A polynia, which is typical for the ice covered Laptev Sea and well known from satellite images, had begun to form separating the fast ice near land and the drifting ice cover of the open Laptev Sea.

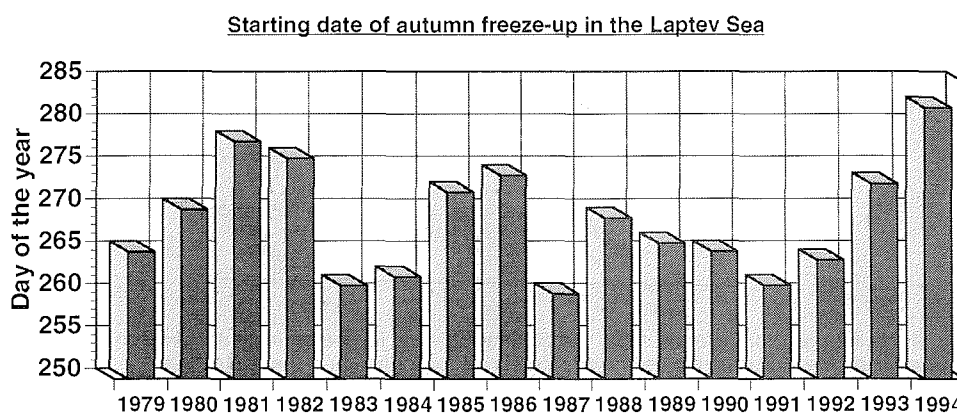


Fig 5: Starting date of autumn freeze-up derived from passive microwave satellite data (modified Eicken et al., 1997).

The expedition emphasized the eastern Laptev Sea and tracked areas of beginning freeze-up which we found off Kotel'nyi Island and off the Lena Delta (Fig. 9). Hydrographic measurements of the up to 40 m deep inner Laptev Sea showed a complicated layering of the water masses, consisting of a 7-10 m thick brackish, rapidly cooling (+1° to -1.3°C) water sheet overlying a warmer layer (+2° to +4°C) of increasing salinities at 10-20 m water depth, which overlaid a cold layer of normal marine salinities (Fig. 10). The source of this apparently unusual warm subsurface water was a subject of hot debate because we suggest that its advection to the surface and local upwelling under the prevailing easterly winds contributed to the late freeze-up of the Laptev Sea in 1995.

TRANSDRIFT III continued from the NE segment of the Laptev Sea to the South (Fig. 9) encountering various and hydrographically different surface waters of the river mouths of the Yana, Lena, Olenek and Khatanga. Differences in the suspended sediment load of these rivers, which were not in their peak draining season, could be detected in the various and very subtle colouring of the waters, whereas the surface waters and the newly formed sea ice of the open Laptev Sea

were clean. Wide stretches of turbid newly formed and dirty sea ice were found off the major deltas in the southern Laptev Sea (Yana, Lena and Olenek), but were lacking off of the Khatanga. The process of sediment entrainment remains unclear, but it is clear that it is linked to shallow waters and the presence of turbid fresh water off the deltas.

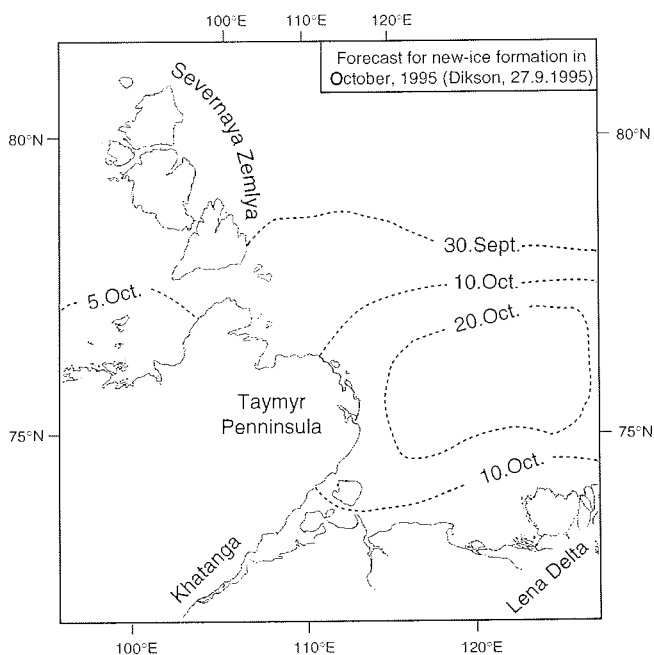


Fig. 6: Ice forecast for October, 1995 (Arctic and Antarctic Research Institute, Dickson, 27.9.1995). Dashed lines are indicating the estimated time of new ice formation in the Laptev Sea.

Off the Lena Delta, there was evidence for an intense fall plankton bloom discolouring the bottom of sea ice and surface waters. Endoscopic observations showed significant differences in ice characteristics between study sites. This method enables the observer to recognize small organisms as well as examine a panoramic view of the three-dimensional small-scale ice morphology which characterizes the habitat. The presence of organisms and the under-ice characteristics varied considerably between different new ice study sites with an ice thickness of about 20 cm. Off the Lena Delta high amounts of sediment particles as well as differently shaped bunch-like structures, probably of terrestrial origin, were included into the ice. In contrast, the ice floes east of the Taimyr Peninsula looked smooth and "clean".

Looking at the marine food web, we only occasionally observed fish, seals, birds and other members of higher trophic levels. On the other hand, benthic fauna was abundant but with little diversity. The megabenthos consisted mainly of brittle stars (Fig. 5) and isopods. Seafloor photography with a still camera and a TV-equipped ROV displayed intense bioturbation of the seafloor surface - an expression of a biologically productive shallow shelf sea. During the previous TRANSDRIFT-expeditions six benthic biocenoses were distinguished, inhabiting the zones of predominantly marine or fluvial influence. Most of the biocenoses sampled in autumn 1995 showed a decrease in abundance and biomass compared to the summer situations in 1993 and 1994.

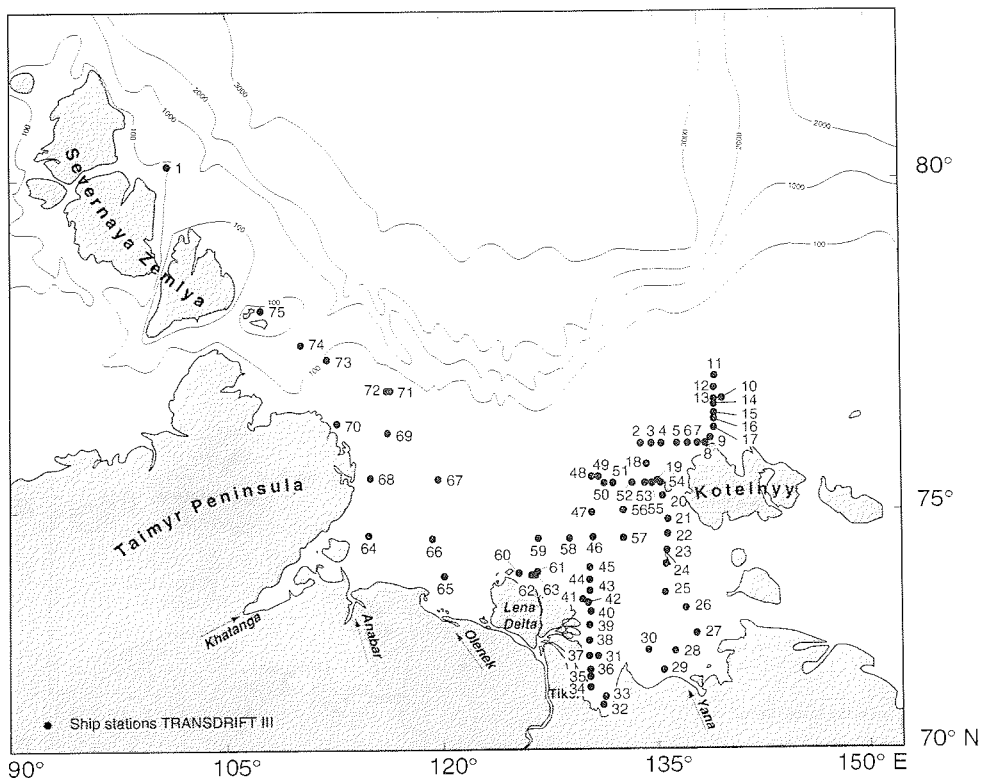


Fig. 7: Map of the Laptev Sea showing the ship stations of the TRANSDRIFT III expedition

The respiration rates as indicator of the metabolic activity of isopods were measured on board at in situ temperatures and different in situ salinities. Respiration rates were significantly higher at low salinities, indicating metabolic costs of osmotic stress. These findings lead to an energy budget model of benthos communities in the Laptev Sea.

TRANSDRIFT expeditions demonstrated the presence of submarine permafrost under a thin, soft and fine-grained cover of dominantly marine terrigenous sediments throughout the Laptev Sea (e.g. Kassens, 1995). This, in addition to inclement weather conditions and strong currents during ice formation prohibited long sediment core recovery in the western Laptev Sea. Nevertheless, 11 box cores and 3 vibro cores were recovered (Tab. A2, A6, A8), and significant changes were seen between the western and eastern Laptev Sea, as previously reported (Kassens, 1994; Dehn and Kassens, 1995; Dehn et al., 1995). In addition, we were able to show, that the opaque minerals in the western Laptev Sea are dominated by pyroxene, and the east by amphibol. Biogenic components of these sediments consisted of calcareous benthic foraminifers, mollusc (mainly bivalve) debris, few siliceous sponge spicules and diatom frustules, dinoflagellates, pollen and spores and a flood of organic fibers (probably plant debris delivered as part of the suspended river load). Older sediments (> 150 cm below surface) show high shear strength, with values reaching 30 kPa. This reflects over consolidated sediments, and could be explained by grounded ice masses compacting the sediments or by permafrost processes.

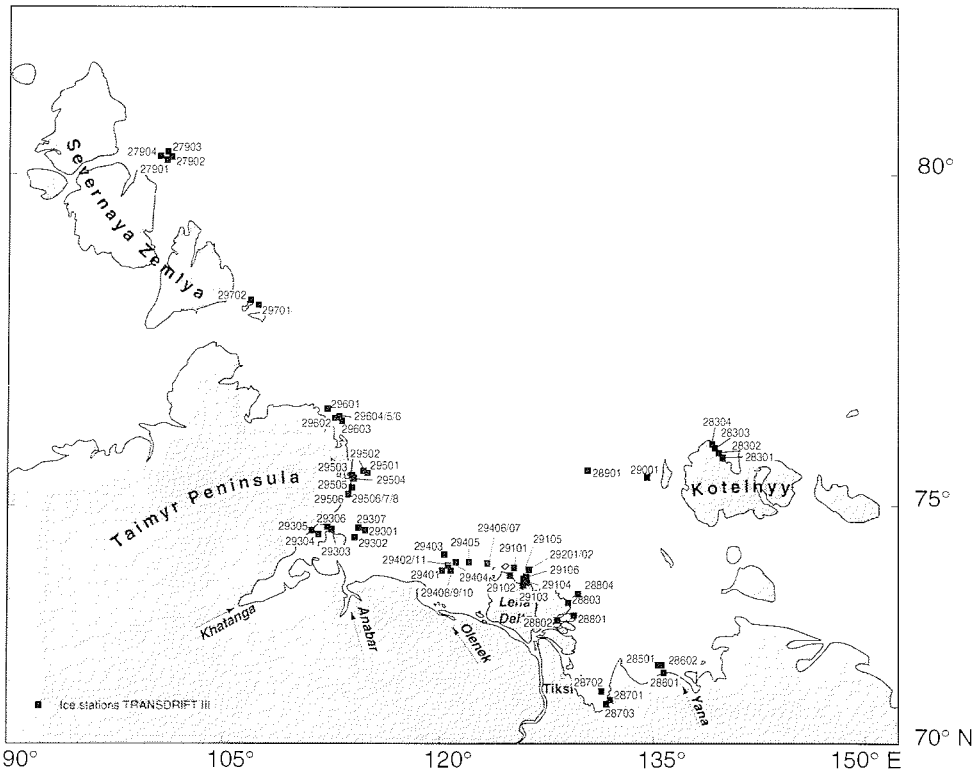


Fig. 8: Map of the Laptev Sea showing the helicopter stations of the TRANSDRIFT III expedition

October 1995, an anomaly?

Observations of the ice-free central Laptev Sea until late October 1995, where freeze-up usually occurs during late September/early October (Fig. 5), were surprising. According to the time series of measurements collected by Russian polar stations, this summer and fall were warmer than at any time during the past 40 years. We relate this anomalous situation to the extraordinary warm summer of 1995, the warm river run-off, the circulation mode in the Laptev Sea and the presence of the unusually warm subsurface layer in the central Laptev Sea (Fig. 10).

Hydrographic data and the nature of thermo- and haloclines above and below this water layer suggest that this is not Atlantic water drawn in from deeper parts of the Arctic Ocean, rather with a left-over from the years anomalously warm summer. However, this observation and many of the other data require further analysis because these unique data have never previously been collected in the Laptev Sea in any systematic fashion, and hence we do not know if the 1995 situation is anomalous or not. To identify the causal relationships of/for the global climate requires further efforts.

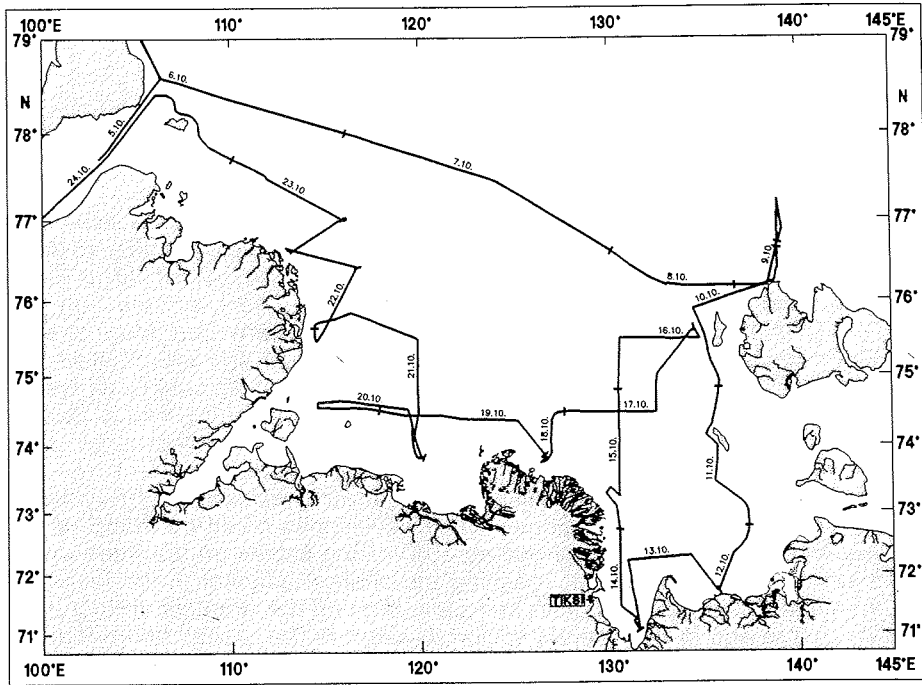


Fig. 9: Cruise track of the TRANSDRIFT III expedition

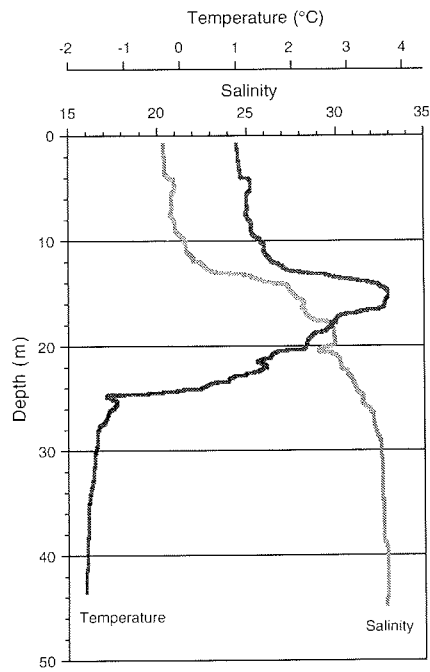


Fig 10: Temperature and salinity records of Station KD95 19 in the eastern Lena Valley (8.10.1995). Note the increase of temperature between 13 and 24 m water depth.

The KAPITAN DRANITSYN, Icebreaker Equipped for Research

O. I. Agafonov, J. Thiede*

Murmansk Shipping Company, Murmansk, Russia

*• GEOMAR Research Center for Marine Geosciences, Kiel, Germany

Based on a careful analysis of potentially available and affordable ships as well as considering the particularly difficult season of freeze-up studies in an area known to be prone to heavy ice conditions one of the potent large Russian icebreaker was chosen to conduct TRANSDRIFT III. The final selection fell on KAPITAN DRANITSYN of the Murmansk Shipping Company from Murmansk (Fig. 11). She is usually engaged in icebreaking duty. In 1994 she was refitted for her use as a base for touristic expeditions in Arctic and Antarctic waters as well as a base for scientific venues, but she has not been converted into a dedicated research icebreaker. Offering facilities and advantages of a rather large platform she also has some disadvantages when used as a research platform; specifically she is lacking proper winches, a seafloor penetrating echosounding system and labs for dry and wet analysis. Some of the deficiencies could be made up for by installing 4 lab containers and by putting 100 m long cables on the three available cranes which were sufficient for reaching the shallow seafloor in the investigated area. In addition company, captain and crew showed the greatest willingness and flexibility before and during the expedition to adapt to the wishes and needs of the scientific party.



Fig. 11: The Russian icebreaker KAPITAN DRANITSYN in the Laptev Sea.

The KAPITAN DRANITSYN (Fig. 11) has been built by the WÄRTSILA shipyard in Finland in 1980, and is a diesel-electrical icebreaker. The 4,100 t deadweight ship is 133 m long, 26.5 m broad, 48 m high and has a maximum draught of 8.5 m. Her total of 24,840 hp allows her to reach a maximum speed of 19 kn on 3 propellers,

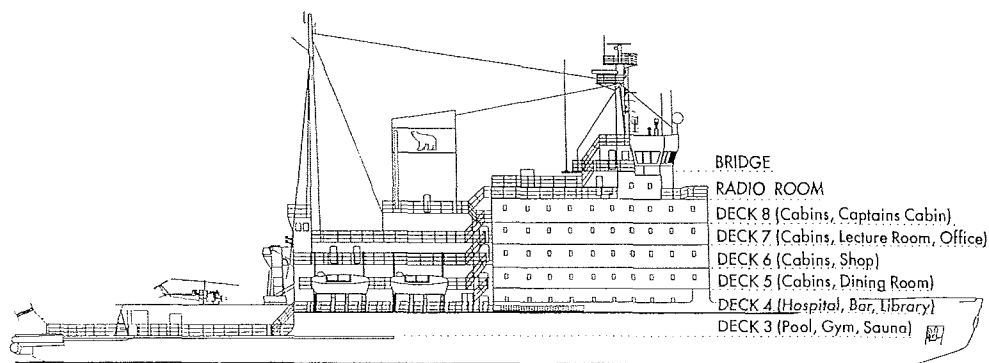
but she has no thrusters. Stations - if needed - were therefore carried out on anchor. Station work was carried out mainly from the bow and from the portside. A number of scientific groups had brought small winches which could be operated over the side. For heavy instruments cranes could be used for and aft. In particular the heavy geological gear required cranes. The grab and the box core were run from the bow, while the vibrocorer was installed on the heli-deck and run from the aft portside crane. The cranes had lifting capacities of up to 10 t. Running hot and cold fresh water as well as sea water was made available by the ship crew at various places.

Limited lab facilities which, however, satisfied the major needs of groups were available through lab containers (three installed on the bow; one installed on deck 6 just before the stack) and through a number of duty rooms as well as cabins inside the ship which were converted into labs (mainly located on decks 3, 4 and 6) (Fig. 12a, 12b). Satellite imagery was received on the bridge where we also were allowed to document positioning, necessary antennas being installed on the flying bridge. The library was converted into a computer room.

Work outside the ship or immediately at the water/ice surface was possible by 3 venues:

1. Two helicopters (double tourbines, up to 8 passengers) were available for station work on land and in areas with a minimum of 50% ice cover. They were also frequently used for ice reconnaissance.
2. Several zodiacs with outboarders which could be used in daylight and under favorable weather conditions.
3. The ships gangway which in quiet weather could be lowered to the water/ice surface. This was particularly important during the early days of "freeze-up" when the ice was not yet bearing. In addition, a mummy chair could be lowered to the ice surface on the bow either to the starboard or to the portside (Fig. 4).

In general it can be concluded that the KAPITAN DRANITSYN provided for a very suitable and highly dependable research platform for the particular needs of the TRANSDRIFT III expedition, visiting a shallow and probably freezing stormy shelf sea of the Arctic Ocean during fall and travelling to and from the investigated area through regions usually on the fringe of being navigable even for icebreakers during that season.



КАПИТАН ДРАНИЦЫН

КАПИТАН ДРАНИЦЫН

Fig. 12a: Deck plan of the KAPITAN DRANITSYN (provided by Murmansk Shipping Company).

DECK PLAN

I/B KAPITAN DRANITSYN

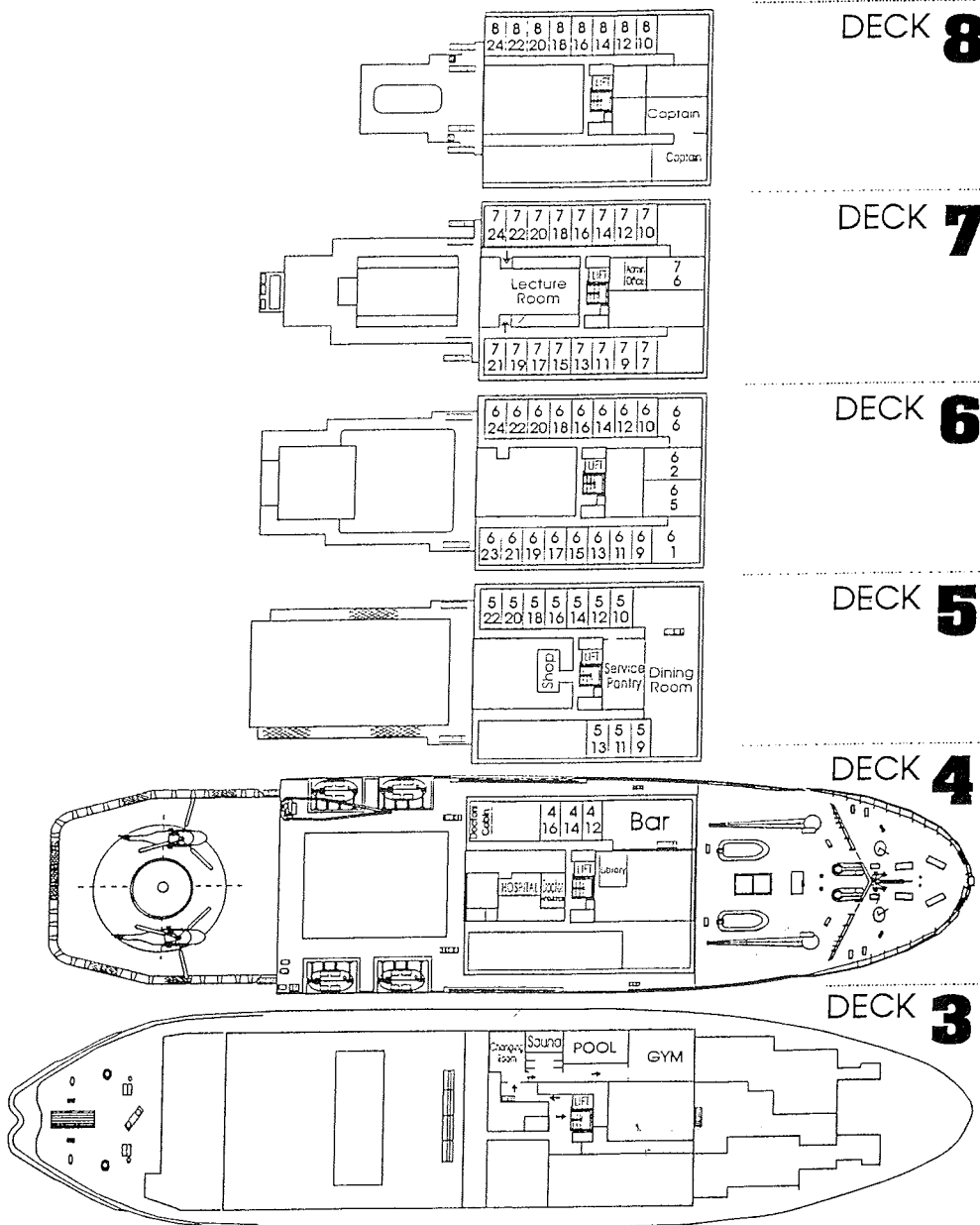


Fig. 12b: Deck plan of the KAPITAN DRANITSYN (provided by Murmansk Shipping Company).

SCIENTIFIC RESULTS

Sea-Ice Conditions during the TRANSDRIFT III Expedition

V. Aleksandrov, J. Kolatschek*

State Research Center - Arctic and Antarctic Research Institute, St. Petersburg, Russia

* Alfred-Wegener-Institut für Polar- und Meeresforschung, Bremerhaven, Germany

While the ship was traveling within ice-covered areas, an observation team (V. Aleksandrov, H. Cremer, A. Darovskikh, J. Freitag, J. Kolatschek, S. Kovalev, F. Lindemann, E. Reimnitz, M. Strakhov, K. Tyshko, F. Valero Delgado, A. Zachek) observed the ice conditions at regular 1- to 2-hour intervals from the bridge (Tab. A5).

Observations recorded routinely include standard parameters such as position, concentration and characteristics of the ice types observed. Even though the observations are somewhat subjective and valid only for a limited area, they could be used for validating remote sensing data obtained from helicopter and satellite.

The following section provides some general information on the ice conditions in the Laptev Sea as obtained from satellite data, helicopter reconnaissance flights and the regular sea-ice observations.

The first ice in form of frazil ice was observed at the passage of Vilkitskii Strait. The first ice station was east of the Red Army Strait near Severnaia Zemlia on October 6, 1995. Near the station, the ice concentration estimated was about 6-8/10 and the partial concentration of old ice was 4-5/10. New-ice types and nilas were also observed. The thickness of old ice was 40-60 cm. About 100 icebergs were observed in the area studied (Fig. 13), the maximum size of them reached 1 km.

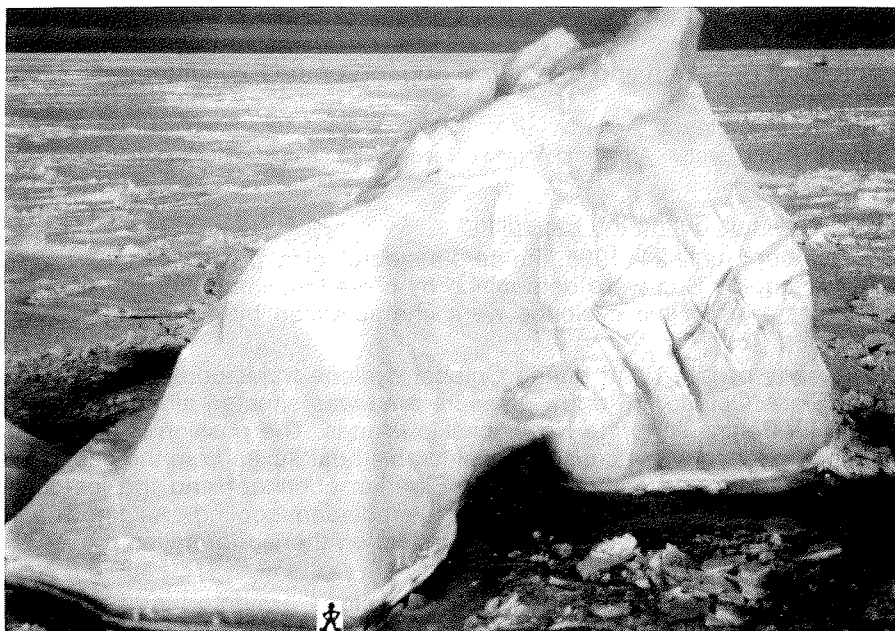


Fig 13: Iceberg near Severnaia Zemlia (6.10.1995). In this region more than 100 icebergs were observed (Photo - M. Kunz-Pirrung).

After finishing the first station, the ship proceeded through open water to the area of Kotel'nyi and Bel'kovskii Islands. Only in the Dragotsennaia Bay nilas was observed. Around October 12 shuga and grease ice were observed near the Lena mouth. The following two days, a stable ice formation began in the area of the Yana and Buorkhaya Bays. The ice concentration was estimated at 7-8/10 consisting of pancake ice, dark and light nilas. In this south-eastern part of the Laptev Sea, ice rafting has been observed but with varying spatial extension.

On the following transect along the 130 degree meridian ice concentrations varied from 3-4/10 to 9-10/10, but mainly compact ice was observed. Light nilas was the predominant ice type, although dark nilas, pancake and grease ice have also been observed. On October 16, the ship reached open water at 74°59'N, 130°29'E and entered the ice-covered zone again at 75°28'N, 130°41'E. After October 17, the ship turned to the west. There, ice concentrations varied considerably. Large areas of open water were met. In other areas nilas predominated. Light nilas, grey and pancake ice were also met. A huge polynya caused by south wind was observed on October 18 near the Lena mouth. From October 19 on the ship worked in young ice, predominantly nilas, but the amount of grey-white and white ice increased with time. The snow thickness on ice reached up to 5 cm.

The last ice station was carried out on October 24 near Mal'yi Taimyr Island. About 20 to 30 small icebergs have been observed there. The main ice types were nilas and grey ice with a concentration of 8-10/10.

It should be noted that in summer 1995 the ice-edge position differed widely from that of previous years: it was in an extreme northern position when the KAPITAN DRANITSYN left Murmansk (Fig. 14) and only in the western part the ice edge moved considerably to the south. New-ice formation started then at the northern ice edge and, as late as on October 12-14, on the southern shores of the Laptev Sea. On October 24, the ice concentration in the central Laptev Sea was still below 5/10.

Meteorological Research and Synoptical Support of the Expedition

A. Zachek, A. Korablev

State Research Center - Arctic and Antarctic Research Institute, St. Petersburg, Russia

Weather Conditions during the Expedition

From October 5 until 24, 1995, the aero-meteorological processes in the working areas of the Laptev Sea were determined by a predominant influence of cyclonic series. Trajectories of the cyclones were characterized by a highly pronounced zonal type (Fig. 15).

It can clearly be seen that during October cyclone trajectories approached the coastline. Since October 15 a low-pressure area was situated along the coastline from the Kola Peninsula to the Novosibirskie Islands. The position is explained by the presence of open water causing considerable heat fluxes from the ocean to the atmosphere. During the same time, the Siberian continent and the ice-covered southern Arctic Ocean were influenced by radiation cooling. As known, such weather conditions provide a considerable effect on the ice-formation processes in the Laptev Sea.

In the first half of the expedition the cyclone trajectories were located approximately along 60°N. Cyclones stayed to the south of Taimyr Peninsula, causing heat advection from south and south-west into the central and eastern

Laptev Sea. Therefore, the air temperature near the Novosibirskie Islands varied between -4° and -10°C , and the water heat storage was high. According to annual multi-year data, such a stable cyclone position usually leads to complete cyclone destruction. Nevertheless, in this case the cyclones regenerated and they then moved along the coastline to the East Siberian Sea. The tracks were modified by adding a meridional component from south to north (Fig. 15, tracks 1,2);

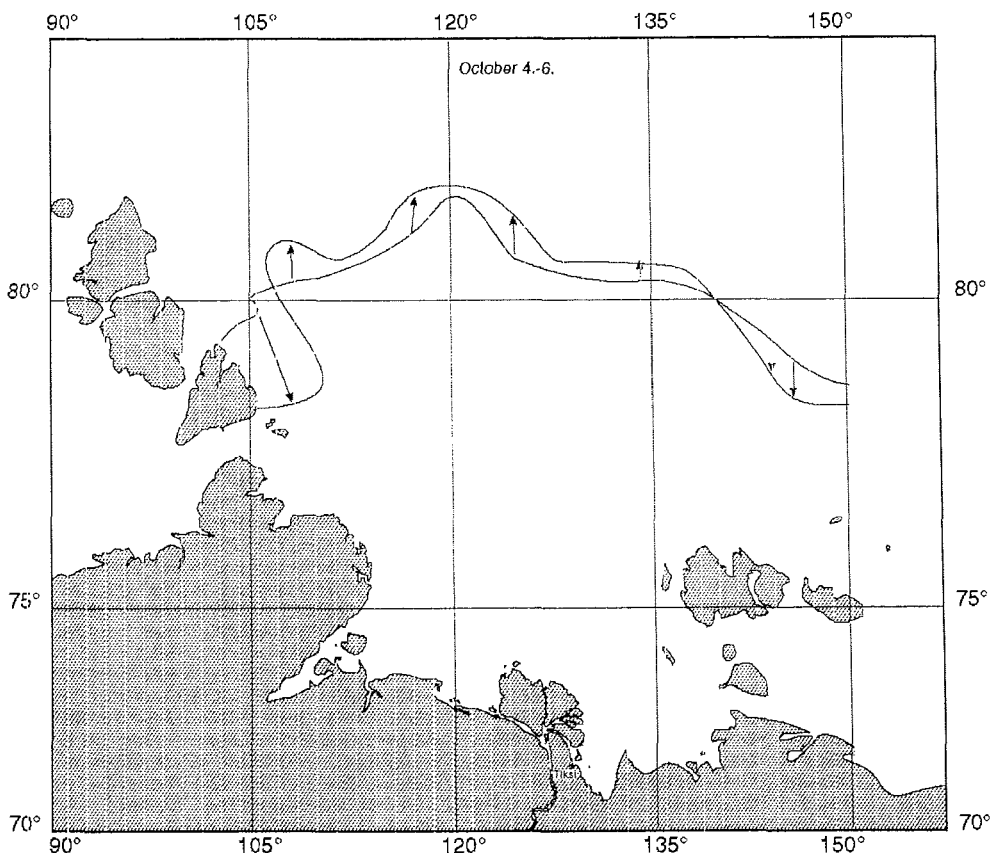


Fig. 14: Ice-edge position during the TRANSDRIFT III expedition in autumn 1995. The arrows indicate the movement of the ice edge.

On the other hand, during the entire period under study a high-pressure area formed until the middle of October in the central and eastern parts of the Polar Basin, moved to the Canadian Basin due to negative heat and radiation balance over pack ice (according to POLARSTERN expedition data).

The results issued from meteorological observations, ocean-atmosphere interaction parameters and aerosol particle measurements during the cruise are presented below.

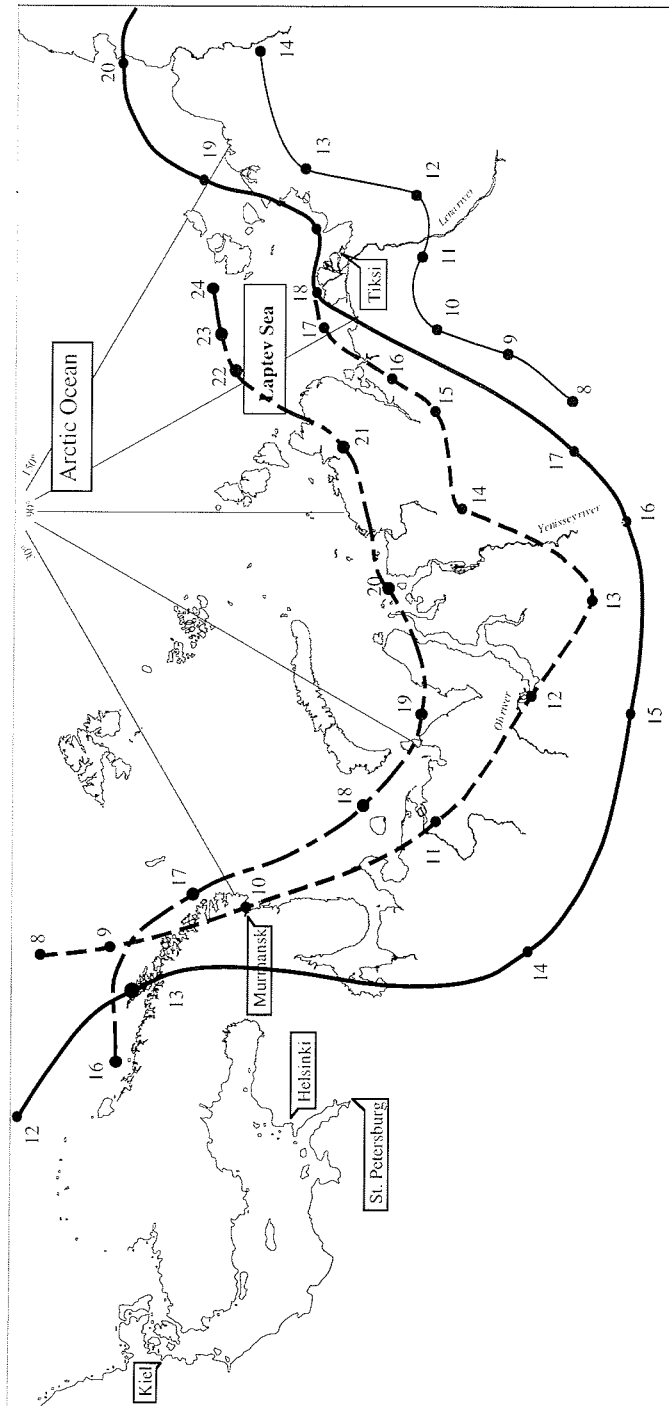


Fig. 15: Cyclone tracks in October, 1995.

Weather Forecasts

Information about future weather conditions was important for planning station work, ship navigation and helicopter flights. For this purpose the weather maps were received aboard through radio channels. Every day, the weather forecast was prepared at 6pm and reported to the chief scientists and the captain.

Meteorological Conditions in the Working Area

The temporal variability of the most important meteorological parameters measured during the cruise allows us to estimate the variability of the weather conditions (Fig. 16). The air temperature varied from 0°C to -14°C with a mean value of -6.2°C. Changes of the atmospheric pressure have shown that the cyclonic activity was particularly predominant in the second part of the cruise when cyclone tracks shifted to the north. Two local pressure minima on October 18 and 22 correspond to the passing of a cyclone center through the working area. At the first time, the total cloud amount decreased rapidly, wind diminished and intense northern lights were observed. South-east and south-west winds mostly predominated with an average speed of about 8.1 m/s (Fig. 16). 51% of the observations registered snowfall. Stratocumulus clouds prevailed in a low layer. In open-water areas cumulus and cumulonimbus clouds were observed. Nimbostratus clouds were noticed during warm front passages. As the calculations show, the strongest correlations exist between air temperature and atmospheric pressure (correlation coefficient 0.52) and atmospheric pressure and wind direction (-0.57). At the same time, the correlation between pressure and total cloud amount is near zero (0.07), which made cloud forecast difficult.

Meteorological Investigation Program (Tools and Methods)

Routine meteorological observations started on October 5, 1995, in the Vilkitskii Strait and finished on October 24, 1995, at the same ship position. Observations were made at 0, 3, 6, 9, 12, 15, 18 and 21 UTC time. Additional measurements included sea-surface radiation temperature and longwave radiation. Shortwave radiation was not measured due to insignificant values.

Routine observations consisted of:

- cloud observations (visual)
- precipitation (visual)
- visibility (visual)
- wind speed and direction
- air temperature
- humidity
- atmospheric pressure

The following equipment was used:

- remote meteorological station (air temperature, relative humidity, wind speed and direction)
- longwave pirgeometer Pâ-30 with a spectral range of 20 to 30 µm
- radiation thermometer KT4
- barometer-aneroid, barograph

Radiation measurements were registered at 2-minute intervals.

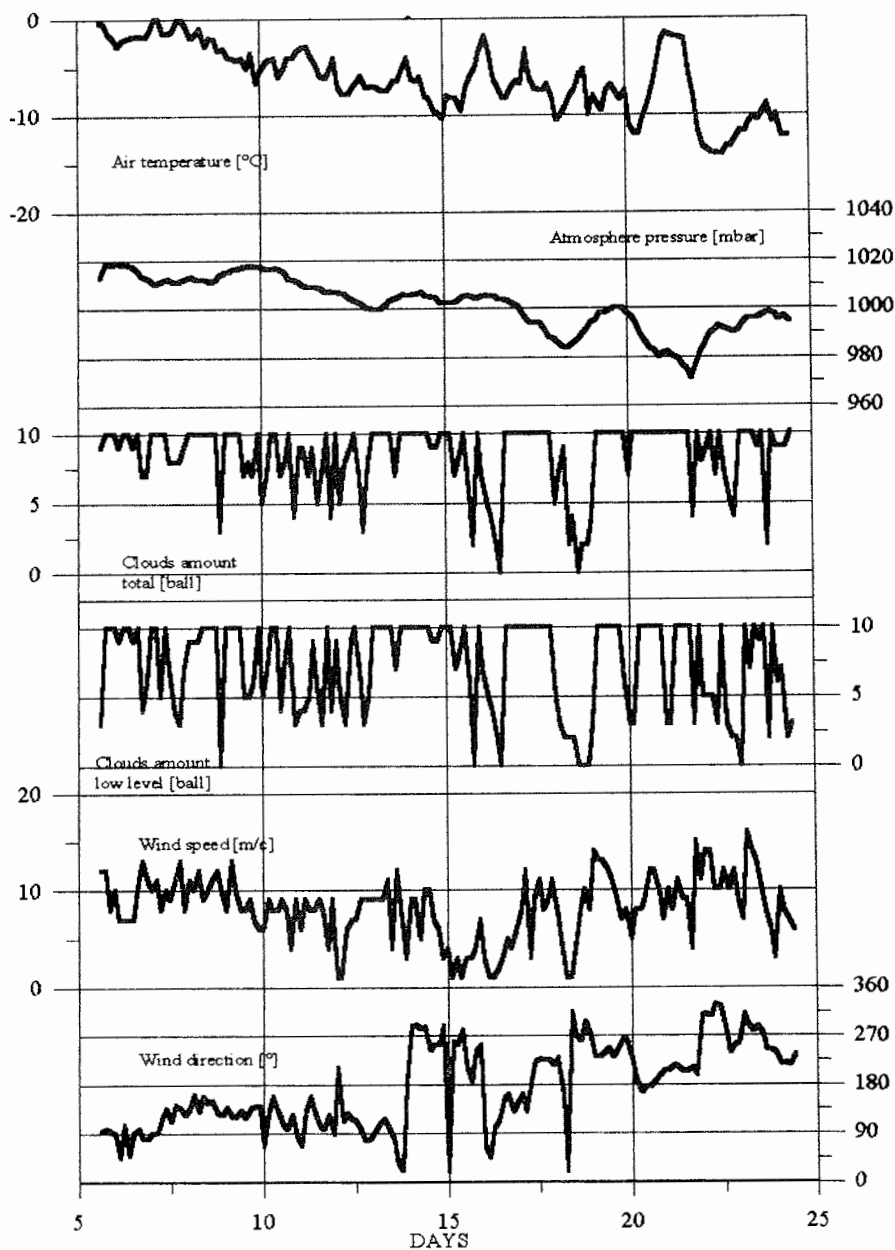


Fig. 16: Variability of meteorological parameters during the TRANSDRIFT III expedition (October 5. to 24,1995).

Data Sets

During the entire cruise the routine meteorological observations were entered in the weather log and then transferred to a PC in a format suitable for calculation. The stored information consists of eight meteorological observation data sets per day from October 5 to 24 and of radiation measurements at 2-minute intervals from October 9 to 23, 1995.

Ocean-Atmosphere Interaction Processes

A. Zachek, A. Korablev, A. Darovskikh

State Research Center - Arctic and Antarctic Research Institute, St. Petersburg, Russia

Heat exchange between the atmosphere and the ocean in the Laptev Sea was clearly anomalous during the expedition in comparison with previous years.

Due to features of atmospheric circulation in June-September a large part of the Laptev Sea was ice free up to 80°N. Therefore, a considerable radiation and turbulent heating was established between the upper layer of the Laptev Sea and the atmosphere. The heat storage played a main role in the development of ice formation :

- water temperature reached the freezing point with delay;
- radiation cooling decreased due to an intensive cloud cover from cyclonic activity.

The heat balance components (Fig. 17,18) were computed from radiation measurements and routine meteorological observations. The following heat components were estimated: B - radiation balance, H - turbulent heat flux, LE - latent heat and Q - heat balance; (where $Q=H+LE+B$).

The results obtained agree with the measurements made during the initial period of ice formation in the Barents Sea in December 1984. The heat components were as follows: $Q = 120 \text{ w/m}^2$, $B = 60 \text{ w/m}^2$, $H = 40 \text{ w/m}^2$, $LE = 30 \text{ w/m}^2$. The close correspondence between radiation balance and cloud amount is noteworthy (Fig. 17).

Aerosol Measurements

A. Zachek, A. Korablev

State Research Center - Arctic and Antarctic Research Institute, St. Petersburg, Russia

It has been traditionally assumed and is documented by observations that the Arctic atmosphere is exceptionally clean and transparent. Later, since the early 1950s, a large-scale inflow of aerosol masses into the lower and middle troposphere was discovered, leading to a decrease in the atmosphere's transparency. The effect that changes in the atmosphere radiation characteristics have on climate conditions is stronger in the Arctic than anywhere on the Earth. For this reason, aerosol measurements were included in the working plan of the autumn expedition in the Laptev Sea. The aerosol influence consists of two components, first, the influence on the radiation exchange in the atmosphere and, second, the strong effect on processes of clouds and haze nucleation in winter time.

Aerosol measurements aboard KAPITAN DRANITSYN were conducted by an aerosol particle photoelectric counter A3-5. Aerosol observations were made from October 6 to 21. The summary of the aerosol particle measurements during the POLARSTERN cruise and TRANSDRIFT III expedition in the Laptev Sea is presented in Table 1.

The results obtained allow us to conclude that mean aerosol concentrations for the entire range of particle sizes increased due to the reduction of liquid precipitations and fogs in autumn as compared with summer.

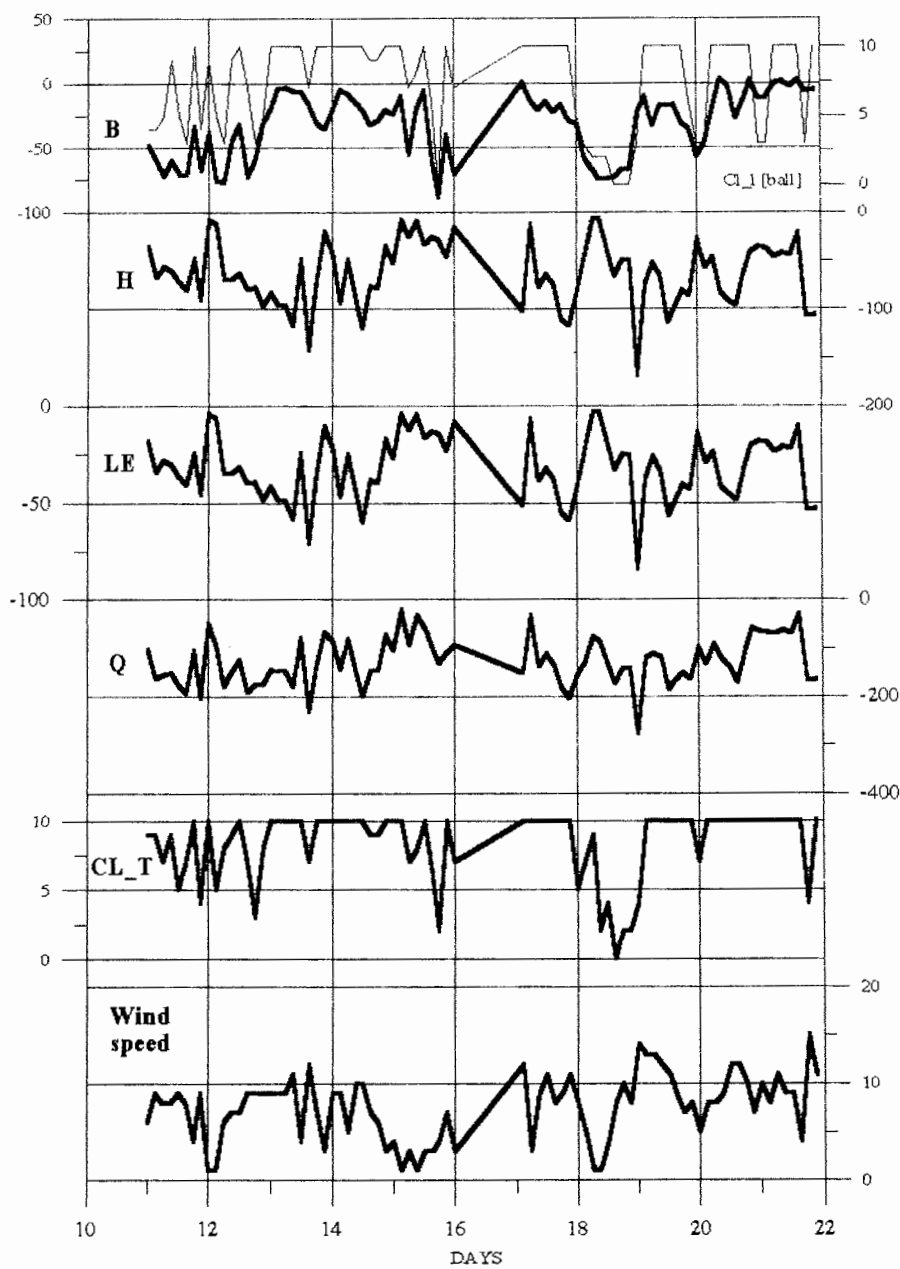


Fig. 17: Heat balance components (w/m^2) in the Laptev Sea during the TRANSDRIFT III expedition (October 11 to 21, 1995)

Tab. 1: Mean numbers of aerosol particles of different size (μm) measured in August and September during the POLARSTERN expedition as well as in October during the TRANSDRIFT III expedition in the Laptev Sea.

august-september 1995								
size:	0.4	0.5	0.6	0.7	0.8	0.9	1.0	1.5
mean	534	170	129	34	22	11	7	1
sigma	439	141	124	38	29	16	1	1
october 1995								
mean	848	514	171	74	39	37	24	20
sigma	384	333	168	78	37	46	25	22

HEAT BALANCE COMPONENTS 11-21,10.95 Laptev Sea

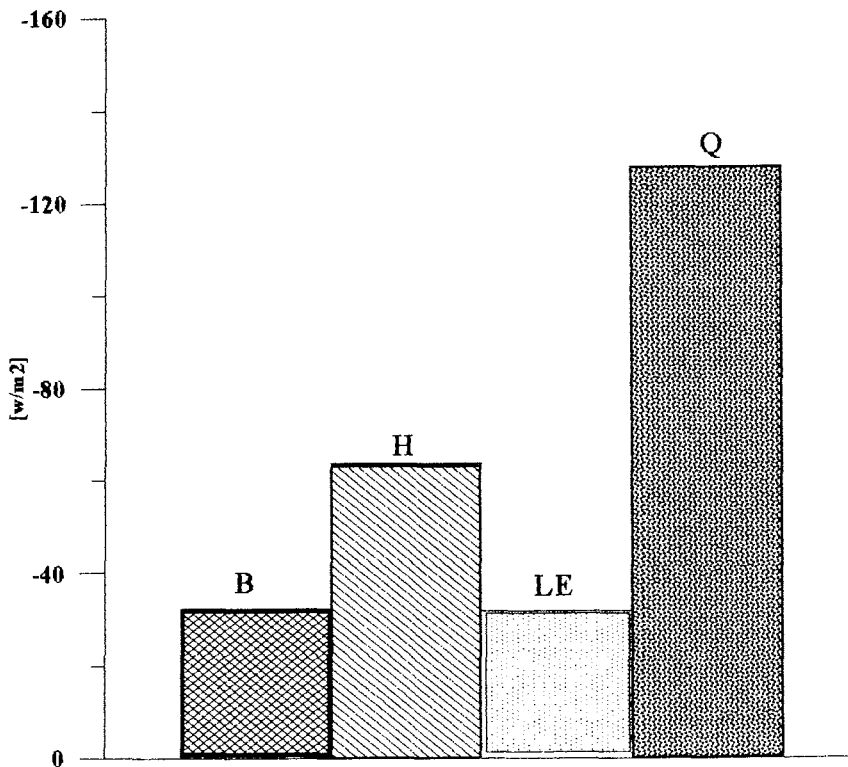


Fig. 18: Components of the heat balance in the Laptev Sea during the TRANSDRIFT III expedition (October 11 to 21, 1995).

Sea-Ice Remote Sensing

V. Aleksandrov, A. Darovskikh, J. Kolatschek*

State Research Center - Arctic and Antarctic Research Institute, St. Petersburg, Russia

* Alfred-Wegener-Institut für Polar- und Meeresforschung, Bremerhaven, Germany

Sea ice covers large areas in polar regions of the World Ocean and considerably influences the global climate and man's activities in these regions. Regular sea-ice monitoring there is necessary because of large seasonal variations of ice cover. For these reasons, weekly ice charts are prepared for the entire Arctic Ocean using data from all sources for that week. These charts are the main source of information for planning navigation, forecasting of ice conditions and for climatic research.

Remote sensing techniques are the main source of information for ice chart preparation. Active and passive sensors, operating in visual, infra-red (IR) and microwave spectral bands are used for sea-ice studies, and the most important sea-ice parameters are retrieved from these data. Subsatellite experiments are conducted for the improvement of interpretation techniques of remote sensing data.

Remote sensing studies have been conducted aboard KAPITAN DRANITSYN on the TRANSDRIFT III expedition. The program consisted both of large-scale studies using satellite data from "Okean" (radar and passive microwave images), NOAA and "Meteor" satellites and of a small-scale study by means of a side-looking helicopter-borne radar and aerial photosurvey.

The aims of the satellite observations were the following:

- to estimate radiation temperatures of the surface layer;
- to study the possibility of interpreting radar satellite images of young ice;
- to study the possibility of interpreting IR satellite images in the freeze-up period.

Satellite images have also been used for assessing sea-ice conditions in the Kara and Laptev Seas and for the purpose of meteorological forecasts.

Working Program.

For the realisation of the scientific program the following procedures have been carried out:

- receiving satellite images using a portable receiving station;
- processing and interpreting satellite images including the determination of sea-ice parameters and sea-surface temperatures, and for ice-chart preparation.

The routine work included the following procedures:

- preliminary calculation and choice of satellite trajectories over studied areas;
- receiving satellite images from "Okean", NOAA and "Meteor" satellites and their preliminary processing;
- interpretation of received images, sea-ice parameters, sea-surface temperature determination and ice-chart preparation.

The following equipment has been used for this work:

- 2 IBM PC/AT with a printer;
- 2 portable stations for the receiving of satellite images;
- oscillograph S1-94.

Preliminary Scientific Results

69 satellite images, including 42 NOAA and 27 Okean images have been

received aboard the KAPITAN DRANITSYN during the expedition. These images have been used for realising the scientific program, for the study of ice conditions in the Laptev Sea and for the purpose of expedition logistics. Ice charts have been prepared regularly on the base of "Okean" images. Visual air reconnaissance flights were carried out to estimate sea-ice parameters in areas covered by satellite images. Ice charts composed by means of these flights will be used for a comparison with charts issued from satellite images. Preliminary analyses have shown that, at the first ice station, areas of predominantly old ice and the ice-edge position have been quite accurately determined from "Okean" images. Decoding features of different young-ice types will be studied on the basis of the research conducted.

Our analysis has shown that a joint use of radar and passive microwave satellite images is more beneficial for sea-ice studies than was thought before, because areas with low ice concentrations or with new-ice types can be determined accurately, when both types of images are analysed.

Sea-surface temperatures (SST) were calculated from NOAA IR satellite images by using a program developed at the AARI. Real sea-surface temperatures have been measured by the meteorologists with the help of an IR radiometer (KT-4) and a thermometer. The accuracy of SST determination from NOAA IR images will be estimated after comparing it with these data.

Sea-ice conditions in the Laptev Sea were determined also by means of visible and IR NOAA satellite images. So, it can be stated that it is possible to determine some sea-ice parameters not only at low air temperatures but also, when the air temperature lies between 0 and -10°C.

Subsatellite experiments conducted helped to improve the techniques of satellite image interpretation. More concrete and broader results will be obtained after detailed home analysis.

Side-Looking Airborne Radar and Aerial Video Recording of Sea Ice

A. Darovskikh, J. Kolatschek*

State Research Center - Arctic and Antarctic Research Institute, St. Petersburg, Russia

* Alfred-Wegener-Institut für Polar- und Meeresforschung, Bremerhaven, Germany

Scientific Program

Over the past three decades, imaging radars have evolved into an important tool for monitoring surfaces of polar regions. The most important reason for using radars is their independence of clouds and the sun as a source of illumination. During the TRANSDRIFT III expedition the aims of radar investigations were:

- comparison of side-looking airborne radar images with radar images from satellites;
- calculation of backscattering coefficients of different ice surfaces and ice types;
- measurements of size and shape of ice floes;
- calculations of ice drift using repeated radar images;
- calculation of statistical characteristics of radar images.

Working Program

The working program included:

1. mounting of a radar system on helicopter MI-2;
2. carrying out radar flights. For comparison with the radar data and for the determination of ice characteristics (floe sizes, type of ice, etc.), radar measurements were carried out in combination with side-looking video recordings (SLVR).

Observations and Equipment

The radar looked to the right side along flight direction. The technical specifications of the system are shown below:

• Frequency	9.4 GHz
• Peak power	3 kW
• Pulse duration	100 ns
• Pulse repetition frequency	1 kHz
• Flight altitude	250 - 1500 m
• Swathwidth	(6 - 10)* flight altitude
• Horizontal beamwidth	0.5 deg.
• Polarization	H/H
• ADC digitation rate	20 MHz
• Range sampling	7.5 m
• Weight	85 kg
• Used power	9 A 27 V

Table 2 gives an overview of all radar flights. On most flights a constant speed of 150 km/h (above ground) and an altitude of 300 m was maintained. Geopositioning of radar data was achieved by a GPS receiver, logged continuously during each flight. For flights 5, 6, 8 and 9, absolute radar calibration flights were performed separately. Trihedral corner reflectors (100 m² backscattering cross-section) were deployed on the ice, and radar overflights were carried out at different angles of incidence.

Preliminary Results

1. The preliminary analysis of the radar images has shown that grease ice, nilas and grey ice can be distinguished through their characteristic backscattering and textural properties.

2. In general, the observed streaks of grease ice during ice formation were oriented parallel to the wind direction. In some cases an orientation perpendicular to the wind was observed. This phenomenon needs a more detailed investigation.

3. By comparing the ship's position determined by a ship-mounted GPS system with the position estimated from the geolocated radar images, an accuracy of 84 m was found. This allows us to estimate ice drift velocities using the helicopter-mounted radar system.

Tab. 2: Radar flights during the TRANSDRIFT III expedition

No.	Date	Time - min		Location	Remark
		Radar	SLVR		
1	06-10	33	-	Severnaya Zemlya	Open water, icebergs dark nilas, rafted ice (20 - 40 cm)
2	10-10	24	22	Kotelnyy	Open water, grease ice dark and light nilas (10-12 cm), rafted ice (thickness about 1 m)
3	12-10	15	29	Yana	Open water, grease ice, pancake ice, nilas
4	13-10	38	27	Yana	Open water, grease ice, pancake ice, nilas
5	18-10	38	27	Lena	Nilas, grey ice (18 cm), fast ice
6	20-10	18	7	Khatanga	Light nilas, grey ice (14 cm)
7	21-10	54	54	Olenek	Open water, grease ice, pancake ice, dark nilas (5 - 10 cm)
8	22-10	47	41	Taimyr	Grease ice, nilas, grey ice (18 cm)
9	24-10	13	8	Starakadomsky	Grease ice, grey ice (18 cm)

The ice thickness data are from direct measurements made by Thyshko et al.

Dirty Sea-Ice Studies

J. Freitag, F. Lindemann*, E. Reimnitz**

Alfred-Wegener-Institut für Polar- und Meeresforschung, Bremerhaven, Germany

* GEOMAR Research Center for Marine Geosciences, Kiel, Germany

** US Geological Survey, Menlo Park, USA

The Problem

Recent investigations in all parts of the major Arctic Ocean ice circulation systems and in different years have shown that drifting sea ice carries significant amounts of ice rafted debris (IRD). Knowledge of this polar transport process is important for five principal reasons:

- 1) The high rates of Arctic coastal retreat, and accompanying erosional adjustments of the continental shelf profile, require cross-shelf transport of shallow-water sediment to the deep Arctic basin. Because wave energy along the Arctic coast is low, and the open water season short, the action of sea ice is thought to be necessary to accomplish this removal of sediment from Arctic shelves.
- 2) Much of the ice in the Arctic Ocean is produced on shallow shelves, where it

commonly acquires a sediment load before moving off the shelf and entering the Transpolar Drift toward Fram Strait into the Norwegian Greenland Sea, where it melts and sediments are released. This process is thought to account for an important part of the Holocene sediment budget. Thus, knowledge of ice rafting is important for the total polar sediment budget from source to depocenter during the present interglacial.

- 3) An understanding of modern sea-ice rafting also is a key to unraveling the climatic and oceanographic sedimentary record of the Arctic Ocean basin.
- 4) Hazardous substances, e.g. radionuclides, may also be dispersed by sediment-laden ice and be released in the Norwegian Greenland Sea.
- 5) The darkening of ice through sediment entrainment increases its heat absorption, enhances melting, and causes thinning of sea ice. A reduced ice cover results in increased heat gain of the ocean. The sediment load of sea ice therefore may play a role in global change.

Studies of the mineralogy of IRD and of contained microfossils, as well as calculated backward trajectories for ice floes based on archives of drift buoy motions and pressure fields, increasingly point to the Laptev Sea as an important sediment source for the Siberian Branch of the Transpolar Drift. The setting of the Laptev Sea is ideal for sediment entrainment by suspension freezing, the principal mechanism for the incorporation of sediments. The mechanism requires shallow water depths, the maintenance of an ice-free surface by offshore advection of newly formed ice, strong, freezing winds producing turbulence, and slight supercooling of the water below its freezing point. Many of these requirements are favored by a seasonally recurring large flaw lead in shallow waters (~20-30 m) around the entire Laptev Sea.

Because of logistic and operational difficulties of studying sediment entrainment in darkness after full establishment of fast ice and the Laptev Sea flaw lead, the onset of freezing during the month of October was chosen for our studies.

Objectives

The list of principal objectives achievable within the practical constraints of TRANSDRIFT III includes the following:

- 1) Quantification of IRD and suspended particulate matter (SPM) in different types of new ice as a function of age, microstructure, and growth history.
- 2) Attempt to map regional patterns in IRD loads, and to relate these to environmental parameters like meteorological conditions, water depth, wave action, and river discharge.
- 3) Sedimentological characterisation of IRD and SPM.
- 4) Characterisation of the particulate organic matter (POM) in sea-ice sediments.
- 5) Search for clues on entrainment mechanisms from the mode of sediment occurrence in ice and from comparing ice microstructure to presence or absence of SPM.
- 6) Look for evidence in potential entrainment areas for the growth of anchor ice as a means to raise bottom sediments to the surface.
- 7) Attempt to gather data that may allow making IRD transport estimates.
- 8) Study the formation of fast ice and the Laptev Sea flaw lead.
- 9) Establish field experiments that will allow monitoring the seasonal behaviour of ice with different sediment loads, or the metamorphosis of an IRD/ice mixture.

- 10) Studies about the depth to which frazil ice occurs in the water column.
- 11) Incidental to actual freeze-up studies was an effort to develop a dendrochronological data base for Siberia by collecting driftwood samples. Dendrochronology may ultimately serve to pinpoint source regions for ice floes in all parts of the Arctic Ocean.

Methods of Investigation

Sample collection:

- a) drilling ice cores of the ice floe and taking water samples directly beneath the ice floe,
- b) sampling from the diving platform when ice adjacent to ship was too thin to stand on,
- c) helicopter landing on beach and wading into new ice too thin to walk on,
- d) hovering with the helicopter over thin ice and coring or water sampling,
- e) taking samples of slush ice using any of the above approaches,
- f) collection of driftwood samples.

Regional characterisation of ice types:

The broad view of variations in ice types is provided through several methods, either alone or in combinations:

- a) hourly ice observations while in transit,
- b) helicopter reconnaissance flights,
- c) side-looking airborne radar (SLAR) helicopter flights (see A. Darovskikh, this report),
- d) monitoring and recording of various satellite images aboard ship (AVHRR, Okean, etc.) (see V. Aleksandrov, this report).

Shipboard sample analyses:

- a) measured volumes of melted ice- and water samples were filtered through pre-weighed 0.4 μm filter papers. In a shore-based laboratory the filters will be re-weighed for quantifying the load of IRD and SPM,
- b) melted ice- and water samples were filtered through pre-weighed GF/F filters for quantifying and analysing POM,
- c) vertical variations in ice salinity, density and temperature were measured on most ice cores collected,
- d) sections were prepared of ice cores for the study of its microstructure,
- e) the porosity of slush ice samples was measured,
- f) sub-samples of ice cores were taken for later measurements of stable isotopes.

Monitoring the metamorphosis of ice with sediments:

Three 2x2m plots were prepared on new lagoonal fast ice of about 40 cm thickness, onto which different sediment types were spread evenly. Additionally, twenty five pebbles of different sizes, ranging from about 1 cm to 4.5 cm diameter, were placed in a 25 cm rectangular pattern on one of the 3 plots. Also, various amounts of sediments were placed into 5-cm-diameter holes drilled to various depths, in order to simulate the seasonal behaviour of cryoconite holes with various sediment types. Attempts will be made to re-visit this protected site during next year's POLARSTERN cruise and to document changes as summer melt has removed the upper 20-50 cm of this first-year ice.

Some Preliminary Observations

During the cruise TRANSDRIFT III, 64 ice stations were occupied by ship and helicopter (Fig. 8, Tab. A3, A4). At most of the ice stations, samples for biological, ice-physical and sedimentological investigations were taken (Tab. A7).

The onset of new-ice growth in the Laptev Sea in 1995 was about 2 weeks later than the latest recorded from analysis of satellite images and ice charts during the last decade. Not only was freeze-up unusually late, but it also was accompanied by rather mild and calm weather, as documented in the ship's meteorological records.

In spite of calm and mild conditions, we observed dirty ice to be widespread in some areas and on certain days. Thus, 50% of an area with 9/10 or more ice cover was observed to be dirty in a helicopter flight west of the Lena River Delta extending well over 100 km distance (Fig. 8, Ice Stations KD95 294). Because of prevailing offshore winds during TRANSDRIFT III, turbid or sediment-laden ice layers, however, were usually less than 10 cm thick. Noteworthy is the fact that turbid ice, or ice with rather evenly disseminated fine particles, always had a granular structure. Such granular turbid ice commonly was underlain by clean columnar ice. This observation indicates that sediment was entrained from the water column during a turbulent episode probably related to current or wave activity in shallow coastal waters, followed by ice growth under relatively quiet conditions.

We observed either a hard, ice-bonded substrate or actual anchor ice at all sites where shallow-water samples were taken by wading seaward from the beach. In one case a surface grab sample taken from the ship at over 10 m water depth also exhibited ice-bonded surficial sediments. Ice bonding, or cooling of the substrate to its freezing point, seems to be one of the requirements for the growth of anchor ice, an important factor for sediment entrainment into sea ice. Based on experiences from Alaska, the ultimate release of anchor ice occurs after establishment of a total ice cover, and had not occurred when our field work was terminated.

The sediment loads per unit area for the relatively thin ice observed in the Laptev Sea is estimated to be much lower than values reported per unit area in the Beaufort Sea, where turbid ice can be rather thick. We point out, however, that ice- and therefore sediment export from shallow water can continue all winter in the Laptev Sea because of the divergent nature of the ice cover and the maintenance of the flaw lead. Some data on ice drift is available from consecutive airborne radar flights during the fall expedition, and from navigational data while the ship was locked into ice during station work. Such data soon will be available to allow some quantification of sediment transport rates, and to assess the importance of freeze-up for sediment dynamics in the Laptev Sea.

Crystal Structure and Physical and Mechanical Properties of Laptev Sea Ice at the Initial Period of Ice Formation.

S. Kovalev, M. Strakhov, K. Tyshko

State Research Center - Arctic and Antarctic Research Institute, St. Petersburg, Russia

Scientific Program

Even though some data on the mechanisms of ice genesis and its physical and mechanical properties in the Laptev Sea are presently available, systematic investigations of sea ice are scarce. Variations of these properties may be dominated by different hydrometeorological factors in the period of ice formation and, first of all, by an intensive river-water outflow especially in the south-eastern

Laptev Sea.

Supercooling of both the surface layer (heat and conductive mechanism) and the pycnocline (concentration and contact mechanism based on the phenomenon of "double diffusion") appears in the flaw polynya and directly under the ice cover as a result of river-water spreading. Vast amounts of crystals of congelation ice and shuga are formed under these conditions. They can be transported for tens of kilometers from the source of their origin, thereby exerting significant influence on the crystalline structure of ice and its physical and mechanical properties. The thickness of congelation ice and shuga can vary, according to investigations in the neighbouring Barents and Kara Seas, from several centimeters under stable conditions of ice formation (fast ice) up to several meters in its most dynamic parts.

The presence of stable under-ice surface currents is another significant hydrological factor which determines some peculiarities of the ice structure, in particular, its spatial regularity and the anisotropy of the physical and mechanical properties. From this aspect, combined investigations of the surface currents and the crystalline structure of ice are of particular interest.

The opportunity to study the mechanical characteristics of ice at their original temperature is very rare. This is mostly due to peculiarities of the crystalline structure of ice hindering to a vast extent the complete parameterization of the physical and mechanical properties of ice for practical purposes. Ice-structure investigations at different stages of its development are also necessary for solving the problem of penetration mechanisms of sediment aggregates.

Hence, the main goals of these investigations are:

- to study the spatial variability of the ice structure and its physical and mechanical properties in order to reveal prevailing mechanisms of ice formation in different regions of the Laptev Sea;
- to investigate the spatial regularity of the ice structure and the anisotropy of its physical and mechanical properties caused by stable surface currents;
- to determine mean integral values of the physical and mechanical characteristics of ice of different structural-genetic types for different ice temperatures;
- to obtain comparative physical and mechanical characteristics of ice of different structural-genetic types with equal physical properties.

Working Program

Every ice station was chosen for different age types of ice (nilas, grey, grey-white ice, etc.). The work has been carried out in some distance of the icebreaker. Two ice cores were drilled for the determination of ice temperature and salinity. After determining the ice temperature for each layer of the core, a third ice core was drilled in order to determine the mechanical characteristics of ice for the same layers. Three other cores were taken for further investigations aboard the icebreaker, e.g. physical and mechanical properties of ice, its texture and structure.

All equipment and apparatus were installed in a warm laboratory aboard the icebreaker. Analyses of the samples collected for the determination of salinity, concentration of oxygen and silica have been carried out by hydrochemists.

Investigations of the ice texture and structure for different layers and comparative measurements of their mechanical characteristics were carried out under identical temperature and salinity conditions.

The following equipment was used during the expedition:

1. Grinding machine
2. Polarizable table

3. Hydraulic press HP-1
4. Circular drills
5. Glasses for samples
6. Device for salinity measurements
7. Device for ultrasound velocity measurements

Analysis of Crystal Structure, Physical and Mechanical Properties of Sea Ice

For the Laptev Sea as well as for some of the other Russian Arctic seas, October is a time of intensive ice formation (in October 1995, this process developed very slowly as a consequence of an exclusively warm summer). That is why the coexistence of old and new forms of ice is very typical of this period in the marginal ice zone at the northern part of the sea. The distribution of ice is characterised by alternations of small ice floes of pack ice, nilas, pancake, shuga and slush ice. Icebergs and growlers are also present here. Because of the coexistence of numerous age ice types mainly five types of crystal structure prevail in this zone: the metamorphic types D2 and D3 in pack ice, small-grained C7, C8 and different-crystalline structure C6 (Cherepanov, 1977) in new ice. The fact that in October all types of ice usually exist at average air temperatures not below -10°C may be of major importance to the formation of the physical and mechanical properties of ice. Thus, in small floes of second-year ice with thicknesses of 40-60 cm and a depth of snow cover of 10-12 cm at an air temperature of -2.35°C a negligible range of ice temperatures was observed. For example, the temperature of the lower surface of such an ice floe measured -1.75°C , the upper one -1.90°C while the temperature of the upper surface of snow was -2.30°C . For young ice with a thickness of 10-12 cm at an air temperature of -4.1°C the difference between these values was more clearly expressed: -1.60°C at the lower and -2.60°C at the upper surface of ice. With the air temperature decreasing to -10.8°C , the temperature difference measured for nilas reached 4°C : -1.65°C at the lower surface and -5.65°C at the upper one.

The vertical distribution of salinity in old forms of ice is rather homogeneous, and its absolute value in most layers is not above 0.5, excluding the upper layer where the value can achieve 1.5-2.0. In young ice forming at air temperatures from -5° to -10°C salinity is more variable and usually varies from 4 to 8. In near-shore regions where water salinity ranges between 2.0 and 24.7, ice salinity values decrease down to 2.0-3.5. For this period the drift of such ice floes to offshore regions was typical, especially from the mouth of the Lena River, where the temperature of the water surface was slightly above freezing. The maximum value of the remaining summer heat was about 0.2°C . Among the floes of young, rafted ice, layers of slush ice and shuga gradually accumulated. Not only is the thickness of such layers small (20-30 cm), ice concentrations in such layers are also low (20-30%).

The crystal structure and physics of old and new forms of ice determine the its mechanical characteristics and also the ultrasound velocity in ice. Thus, for young-ice types with average temperatures of -3 to -4°C and salinities of 6-7, the flexural strength of ice σ_{fl} measured in situ mostly ranged from 0.5 to 1.0 MPa. The vertical distribution of σ_{fl} can differ depending on the vertical distribution of the temperature, salinity and crystal structure of ice. If the crystal structure of ice is rather homogeneous, the most typical vertical distribution of σ_{fl} will be such as shown in Fig. 19a. In these cases the smaller values of σ_{fl} are observed in the upper and lower ice layers. This is caused by maximum values of ice salinity there (Fig. 20a). Besides, the least value of σ_{fl} more often occurs in the lower ice layer (Fig. 19b,c) as a consequence of its very high temperature that is near the freezing point of water

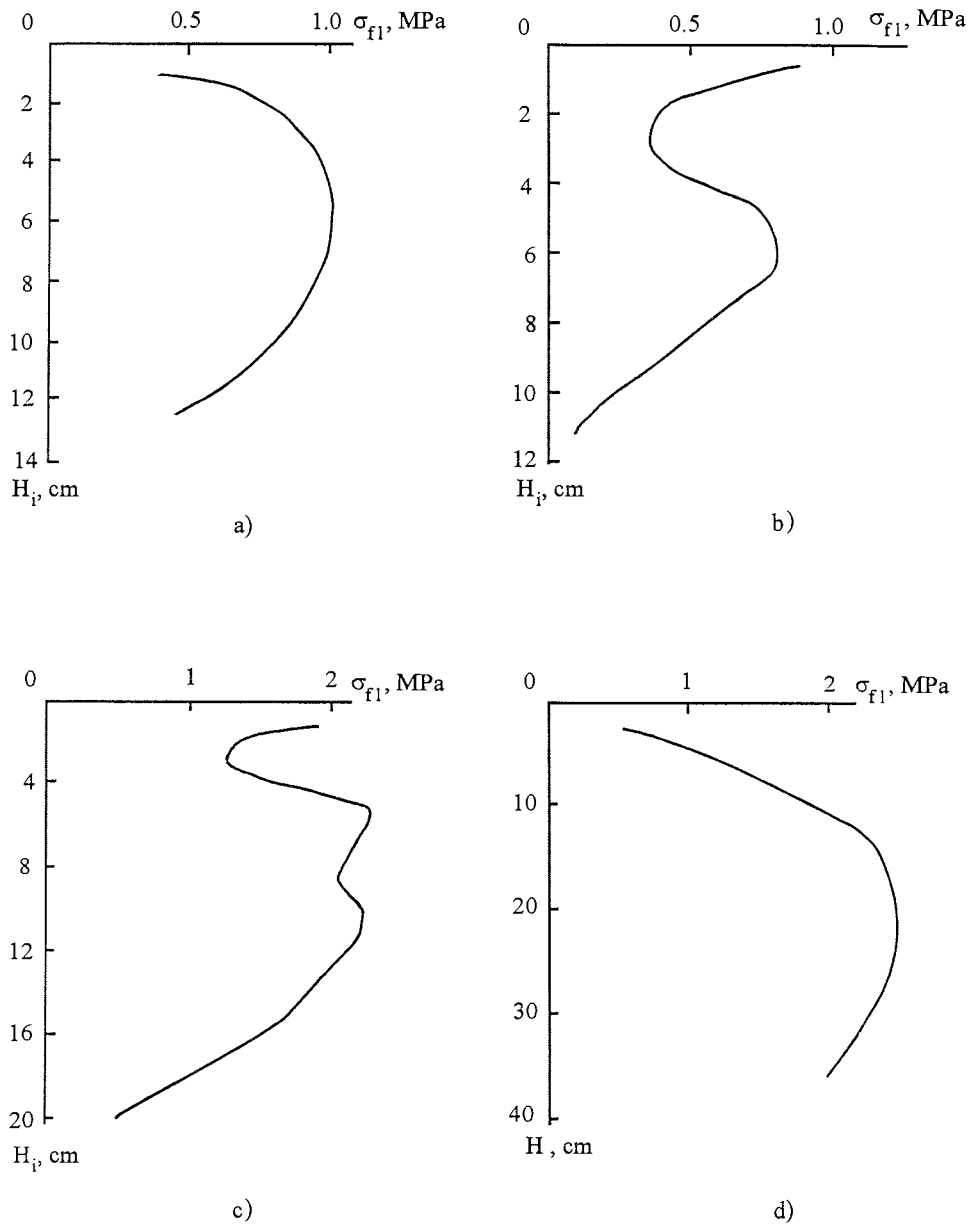


Fig. 19: Vertical distribution of flexural strength in: a) small-grained ice, b) layered ice, c) brackish different-crystalline ice, d) second-year ice

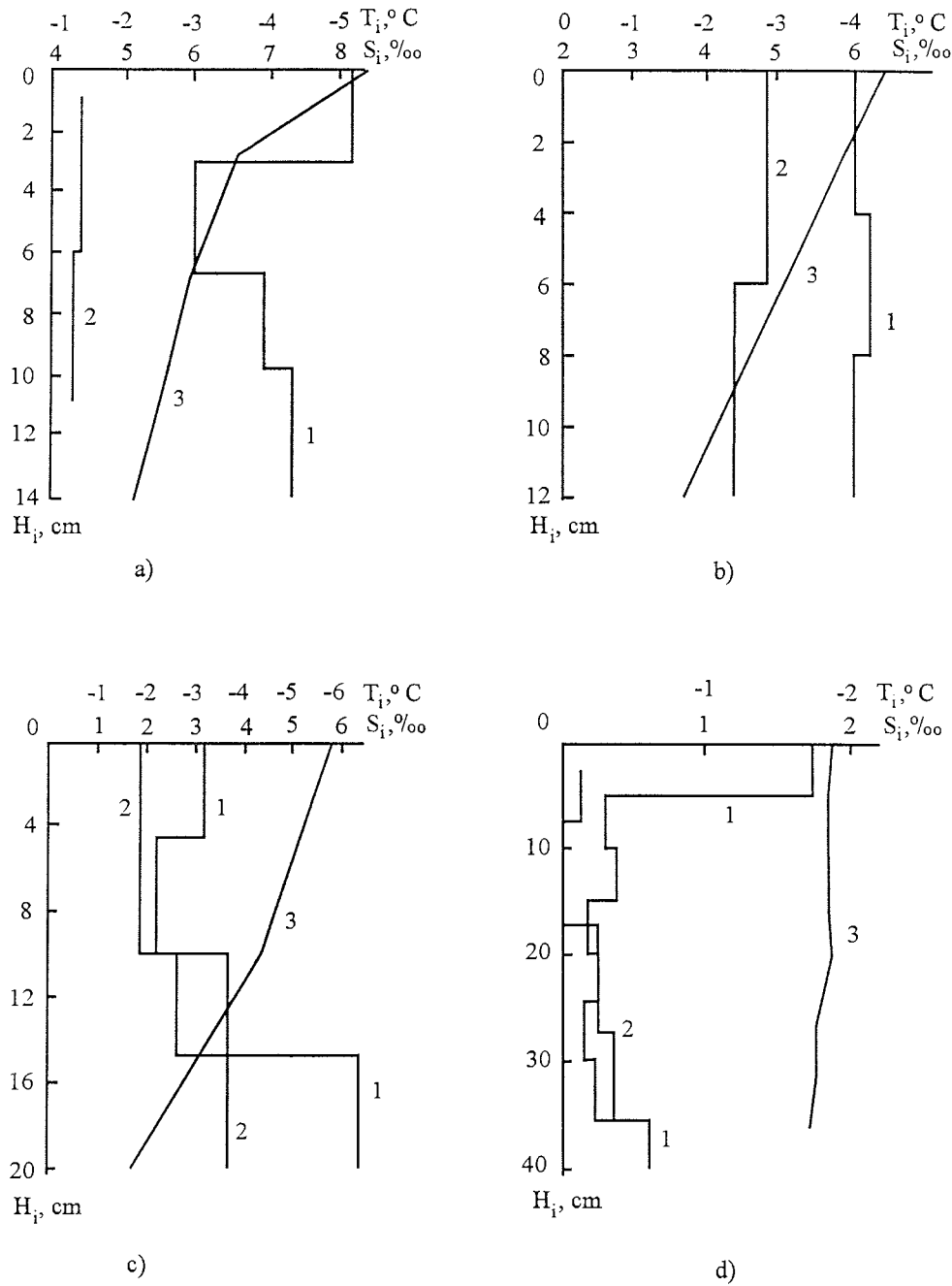


Fig. 20: Vertical distribution of ice salinity in situ (1), ice salinity when mechanical properties were measured (2), and ice temperature in situ (3) in: a) small-grained ice, b) layered ice, c) brackish different-crystalline ice, d) second-year ice

(Fig. 20b,c). The vertical distribution of flexural ice strength may have a more complicated form (Fig. 19b) if the ice cover has a layered crystal structure, i.e. one layer consists, for example, of parallel-fibrous crystals and another of small-grained ones (Fig. 21a). Here, the first maximum of σ_{fl} in the upper layer is explicable in the minimum ice temperature on its surface. As the ice temperature increases at rather constant salinity values (Fig. 20b), σ_{fl} decreases down to its first minimum. Then, in spite of a continuously increasing ice temperature σ_{fl} also starts to increase as a result of intensive growth and integration of fibrous ice crystals. This process interrupts at the transition from the fibrous to the small-grained layer, and from this moment a steady decrease of σ_{fl} is observed.

An increase of σ_{fl} values up to 1.5-2.5 MPa (Fig. 19c) was only registered in brackish ice with a salinity of less than 3 (Fig. 20c) and in second-year ice with a salinity of not more than 0.5 with the exception of the upper layer where it reached 1.7-1.9 (Fig. 20d). That is why another of vertical distribution of σ_{fl} occurred there with its clearly expressed minimum in the upper ice layer (Fig. 19d).

Measurements of ultrasound velocity and tests of uni-axial compression strength of ice are usually carried out after storing the ice samples in a refrigerator for some time. As a consequence of brine discharge from ice samples during this storage, their total salinity noticeably decreases and gradually becomes approximately equal in all ice layers (Fig. 20a). Most of the brine loss in such cases takes place in the lower layer, resulting in a large number of empty voids. This is unimportant for measurements of ultrasound velocity V_{us} in vertical direction when the average value has been measured through the whole ice core. But if such measurements are made parallel to the ice surface, this phenomenon may predetermine the decrease of V_{us} values in the lower ice layer by approximately 100-200 m/s (Fig. 22a). In a number of cases in young ice with a homogeneous isometric crystal structure (Fig. 21b,c) the values of ultrasound velocity, measured both parallel to the upper ice surface and normally, ranged from 3400 to 3600 m/s with their minimum in the lower ice layer (Fig. 22a). On the other hand, with a layered crystal structure (Fig. 21a) the vertical distribution of V_{us} measured parallel to the upper ice surface may have its maximum in the lower layer due to the predominant influence of this type of crystal structure (Fig. 22b). A noticeable difference of more than 200 m/s (Fig. 22c) in values of V_{us} measured normally and parallel to the ice surface appears at a test of congelation ice with parallel-fibrous structure (upper layer in Fig. 21a). Anisotropy of physical and mechanical properties is typical of this type of ice. With a decrease in salinity down to less than 3 the V_{us} values gradually increase and at last in second-year ice that contains only small amounts of brine (several g/kg), the ultrasound velocity is with 3750-3850 m/s through the entire ice core nearly the same as in fresh ice. Even the weakly pronounced anisotropy of physical properties in its lower layers that is typical of a metamorphic fibrous structure of ice (Fig. 23b) (type D2 according to Cherepanov's structural classification, 1977) does not disturb the homogeneous character of the vertical distribution of ultrasound velocity in ice samples directed both parallel to its upper surface and normally to it (Fig. 22d).

The anisotropy of the physical and mechanical properties of congelation ice with a parallel-fibrous structure was also clearly pronounced when measuring the uni-axial compression strength σ_c . Thus, the values of this parameter were by 1.5 to 4.0 times higher when the load was applied normally to the upper ice surface than if applied parallel to it (Fig. 24b). And, on the contrary, they were nearly the same for small-grained ice (Fig. 24a).

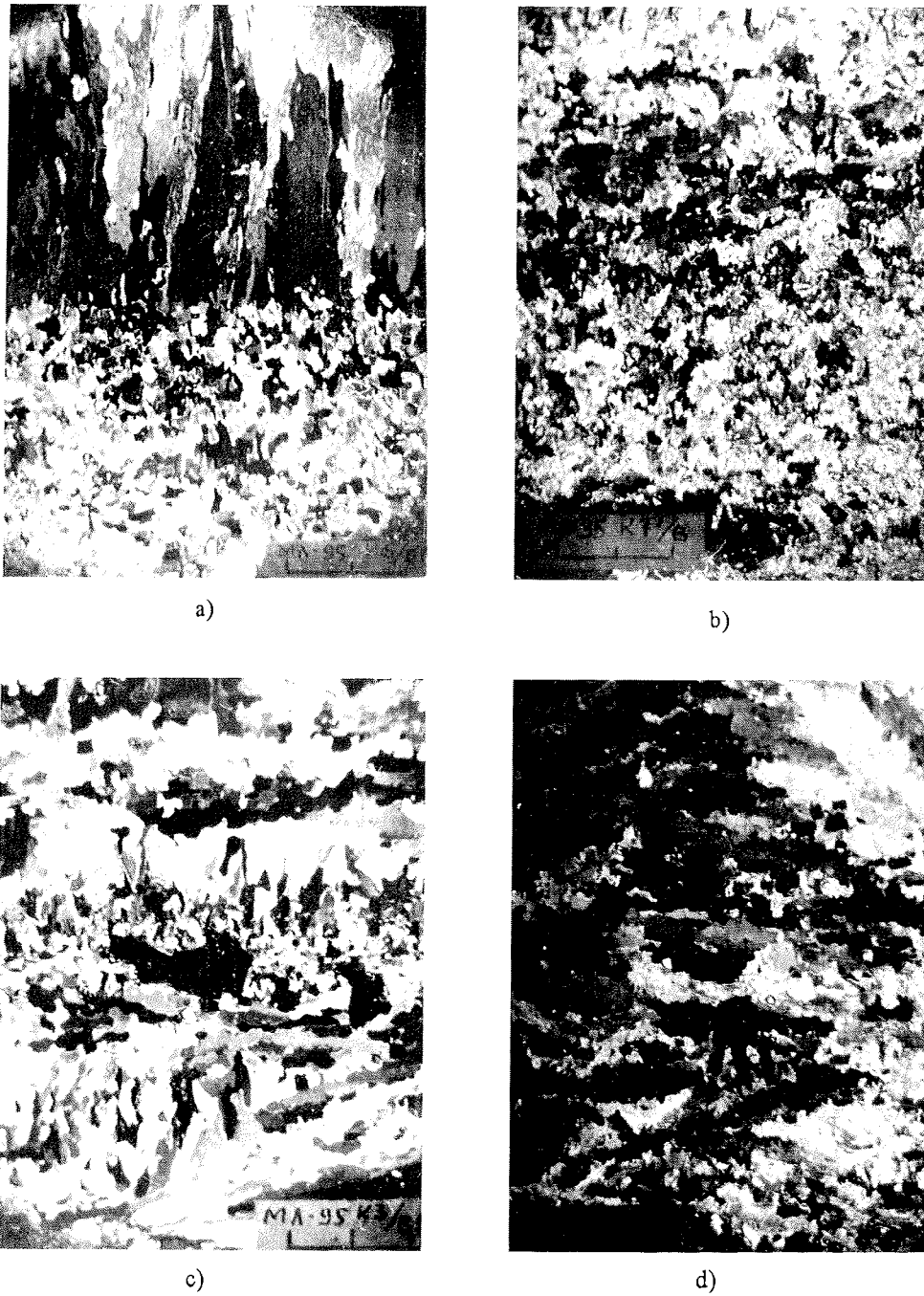


Fig. 21: Vertical thin cross section of: a) layered ice (upper layer has a parallel-fibrous crystal structure and the lower small-grained one); b) small-grained ice; c) different-crystalline ice; d) different-crystalline ice with horizontal alignment of the crystals and vertical orientation of C-axes. The scale marks in 1 cm.

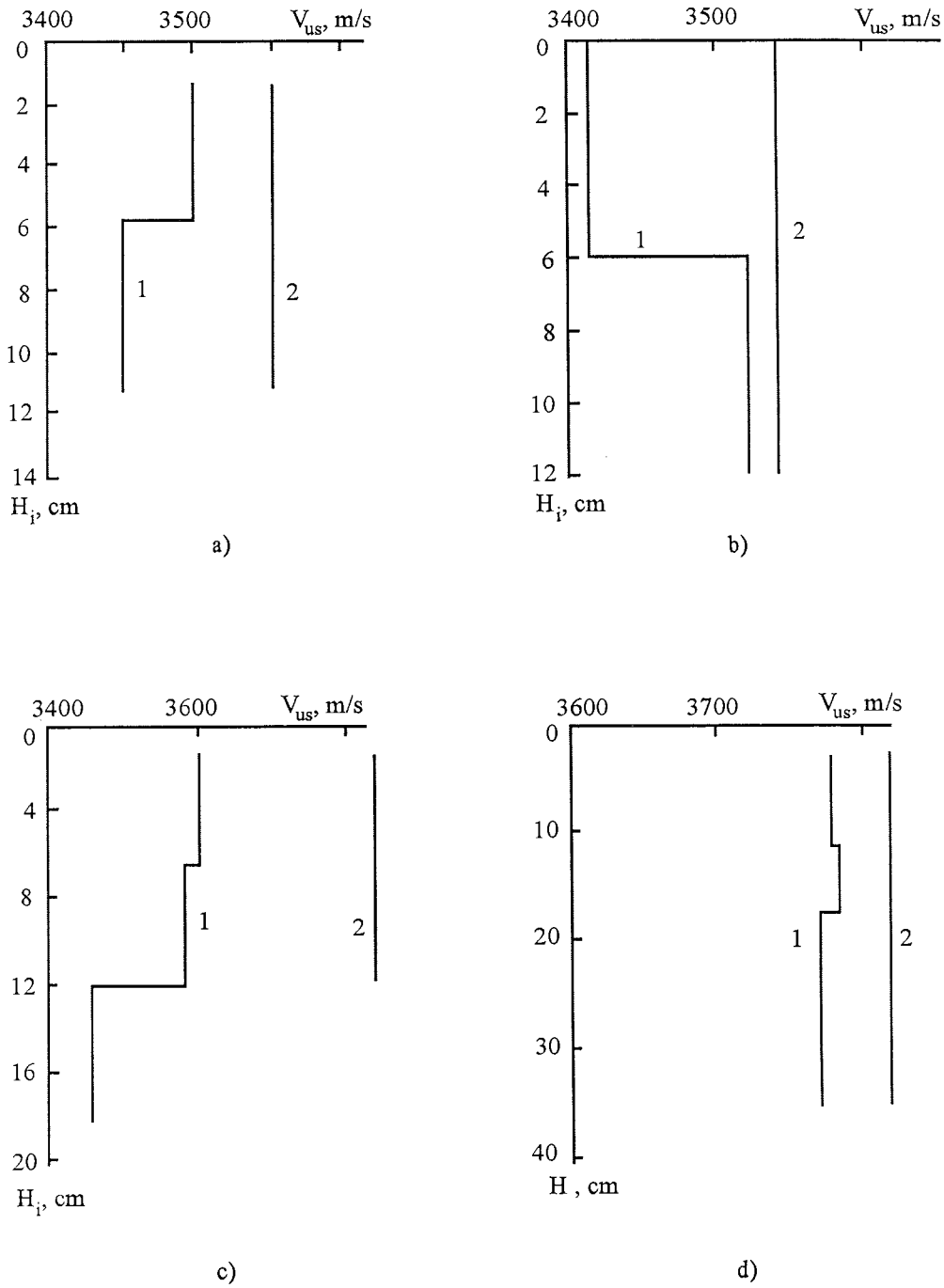
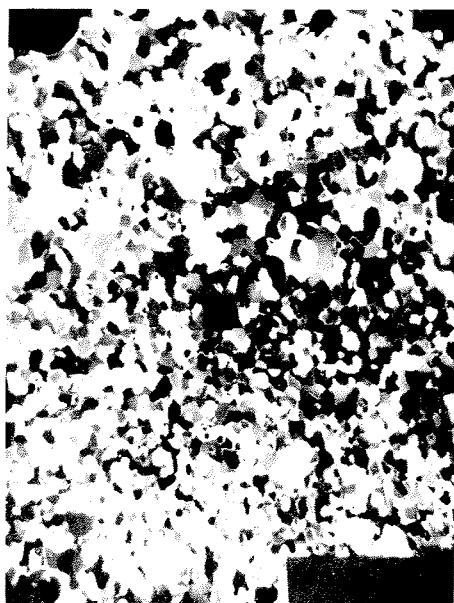


Fig. 22: Vertical distribution of ultrasound velocity in: a) small-grained ice, b) layered ice, c) congelation ice with parallel-fibrous crystals, d) second-year ice. Measurements were made parallel to the upper ice surface and, in addition, normal to it.



a)



b)

Fig. 23: Vertical thin cross sections of the upper (a) and lower (b) layer of second-year ice (scale marks in 1 cm). a) metamorphic grained structure (type D3), b) metamorphic fibrous structure (type D2, Cherepanov, 1977).

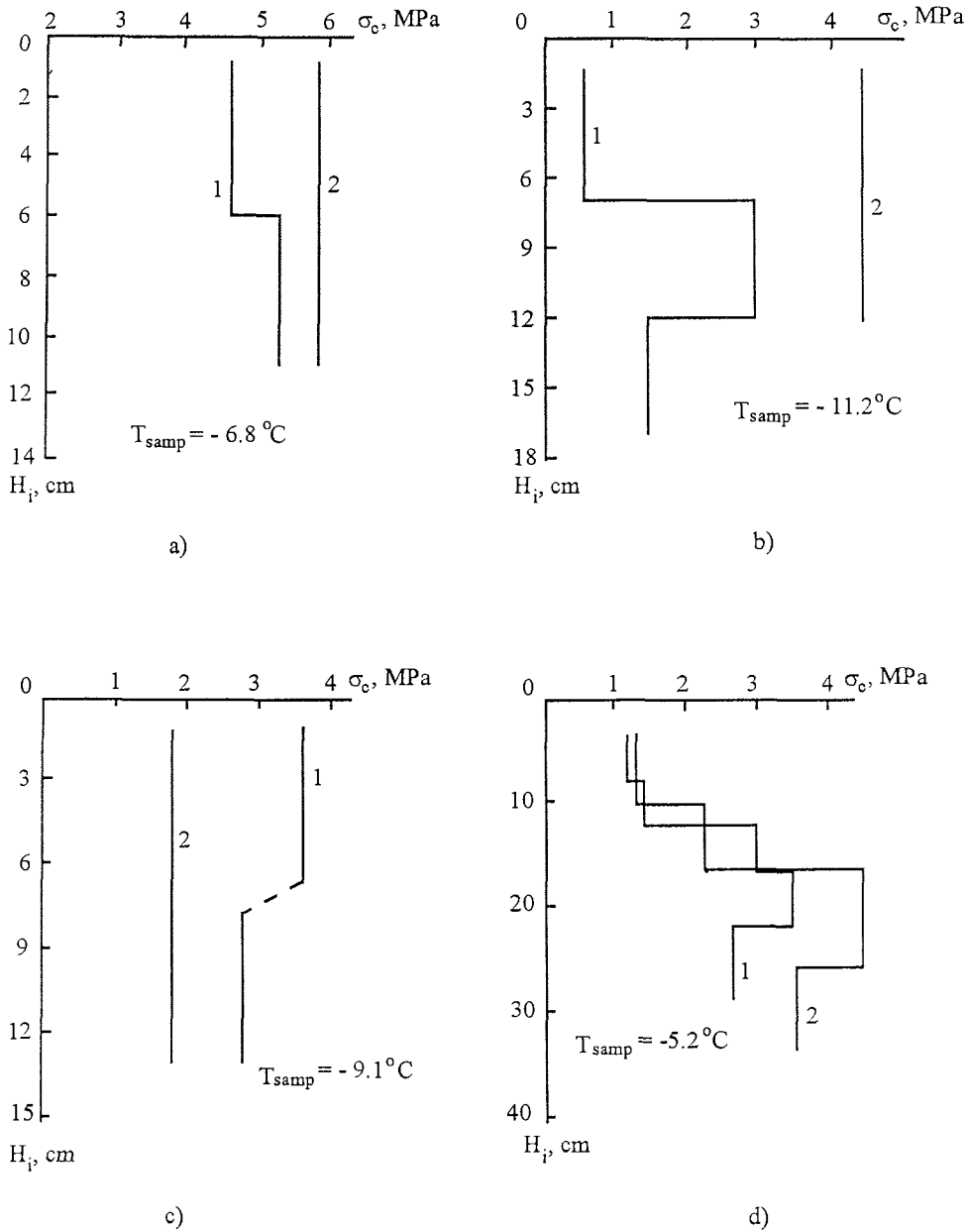


Fig. 24: Vertical distribution of uni-axial compression strength in a): small-grained ice, b) congelation ice with parallel-fibrous crystals, c) different-crystalline ice with horizontal alignment of the crystals and vertical orientation of C-axes, d) second-year ice. T_{samp} - temperature of ice samples at the moment of their mechanical tests. 1 - the load was applied parallel to the upper ice surface and 2 - normally to it.

Young types of ice like nilas with thicknesses of 10 to 15 cm usually have a small-grained isometric structure with grain sizes of 1-5 mm (types C7, C8; Fig.

21b). But in near-shore regions with a very complicated hydrological regime, where a large variety of physical and dynamic characteristics of the surface water layer is observed, a different-crystalline type C6 prevails in crystal structure of ice (Fig. 21c). Such ice is mainly characterised by ice crystals widely varying in shape and size, by air bubbles and brine inclusions (the ice types of the C-group are typical of the central and northern parts of the sea where water salinity is above 24.7. In near-shore regions, where water salinity ranges from 2.0 to 24.7, the ice belongs to group B which is similar to group C. The main difference between them is low salt content in group B). Ice type C6 is usually supposed to be isotropic in its physical and mechanical properties. But, in some cases, a very surprising horizontal alignment of crystals with vertical orientation of their C-axes is observed (Fig. 21d). Testing such ice shows that the anisotropy of its physical and mechanical properties is, like in parallel-fibrous ice, rather distinctly pronounced as well (Fig. 24c).

The vertical distribution of the uni-axial compression strength in second-year ice was determined mainly by a salinity maximum of 1.7 to 1.9 in its upper layer as compared to ice salinities in other layers that do not exceed 0.5 (Fig. 20d). The brine discharge from this layer and the appearance of high pore space cause a noticeable decrease in σ_c down to 1.2-1.3 MPa. This fact, as well as the isometric crystal structure of the upper ice layer and also partly of the middle layer, which mostly consists of metamorphic grained crystals (Fig. 23a), may be the reason for approximately equal values of σ_c when the load is applied both parallel to ice surface and normally to it. The lower layers of this core have a crystal structure D2, i. e. a metamorphic fibrous crystal structure was predominant (Fig. 23b). The weak anisotropy of physical and mechanical properties for such ice is typical. That is why the value of σ_c along the metamorphic fibrous crystals was a little bit higher than if measured normally to them (Fig. 24d).

The analysis of data obtained gives a good chance to point out the most typical features of crystal structure, physical and mechanical properties of old and new ice in the Laptev Sea in the period of initial ice formation. In combination with the data on the geographical distribution of different age types of ice these data can be used for the further schematic mapping of the main physical and mechanical properties of the Laptev Sea ice cover.

Oceanographic Processes in the Laptev Sea during Autumn

I. Dmitrenko, L. Timokhov, P. Golovin, N. Dmitriev

State Research Center - Arctic and Antarctic Research Institute, St. Petersburg, Russia

Oceanographic studies within the Russian-German research project "Laptev Sea System" were devoted to investigate the features of oceanographic processes which govern the hydrological situation in the Laptev Sea in summertime. In the course of the work performed, it was found that in the eastern Laptev Sea, most affected by the continental runoff, the outflow of river water was the deciding factor governing typical formation features of all the environmental components in the Laptev Sea.

The natural system formed in summer under the influence of different factors, primarily river runoff, obviously undergoes significant changes being transformed under the effect of autumn processes. The main transformation mechanisms in the field of oceanographic characteristics are known. However, they remain unknown in detail, especially with respect to the basins subjected to a strong influence of

freshwater runoff. The effect of autumn processes on other natural components, first of all, sedimentation processes including sediment incorporation into ice during freeze-up, is unstudied either.

Oceanographic studies in 1995 were aimed to investigate the evolution of the hydrological and hydrochemical structure of water in autumn. The main goals were:

- to study freeze-up processes as affected by hydrophysical environmental factors: runoff processes, wave-wind mixing, gravitational convection, hydrological structure of the subsurface layer;
- to study the structure of gravitational convection under ice covers of different thicknesses, the influence of convection and radiation cooling on the hydrological structure of the upper layer, the formation of locally mixed water layers in the seasonal pycnocline as well as the influence of these processes on the incorporation of passive mixture into sea ice.

Working Program

The working program entailed oceanographic observations aboard the icebreaker and on young ice of different thicknesses in regions both subjected to river runoff and beyond them. Shipborne observations were to be conducted in open water and during the onset of ice formation.

Scope of Observations and Equipment

As up to October 15 the central and southern Laptev Sea remained ice-free, the oceanographic observations performed can be divided into two stages according to the ice situation. In the first stage, observations in open water were carried out along oceanographic transects oriented mainly along and across the outflow zone of the Lena and Yana Rivers. Subsequently, in connection with the onset of intense ice formation and difficulties in conducting observations and sampling, the main emphasis was put on obtaining background information on the distribution of hydrological characteristics, chiefly in the central and eastern regions. The activities in the course of the second stage included observations from young drifting ice.

In total, 75 oceanographic stations were carried out, 46 of them at 5 oceanographic sections in the zone of river runoff (Fig. 25), as well as along three transects crossing the outflow zone. At 7 stations, observations from drifting ice were performed, including observations from drifting multi-year ice at one station at the traverse of the Shokal'skii Strait.

If there was an ice-cover, shipborne observations by means of a single sounding (less frequent by using 2 or 3 single soundings) were conducted in polynyas and, in some cases, in the channel broken by the icebreaker. Observations on ice were made using multiple soundings with an equal time interval varying at different stations from 2 to 30 minutes during 3-7 hours.

For observations aboard the icebreaker, a CTD system was installed on the foredeck so that the CTD sonde, when being submerged, was at a 4 to 5-meter distance from the board the underwater part of which did not exceed 3 m in this place.

Thus, the influence of the hull at the measurement point was insignificant. On the contrary, distortions of the data obtained during oceanographic observations were mostly considerable with an ice concentration of 10/10 when the measurements were done in the channel behind the icebreaker. Given a subsurface layer stratified they manifested themselves as numerous density inversions down to a depth of approximately 2H, where H is the icebreaker's draft (about 8 m). For observations

from the ice, the CTD system was placed at a distance of 30-80 m from the ship's board connected with the interface block and the computer by a cable.

For oceanographic observations, the sounding system OTS-1600 PROBE Serie 3 (ME Meerestechnik Elektronik GmbH, Germany) was used measuring temperature, electrical conductivity of sea water and pressure by means of sounding technique in combination with a PC AT 486. Main technical characteristics of the sensors are as follows:

- temperature: the measurement accuracy is 0.02°C, inertia 160 m/s;
- electrical conductivity: the measurement accuracy is 0.02 mC/cm, inertia 100 m/s;
- hydrostatic pressure: the measurement accuracy is 0.1%.

For determining the location of the ship during oceanographic stations, a satellite navigation system with the GPS receiver "Flightmate PRO GPS" (Trimble Navigation, USA) was used. The accuracy in locating the ship's position was 15 m.

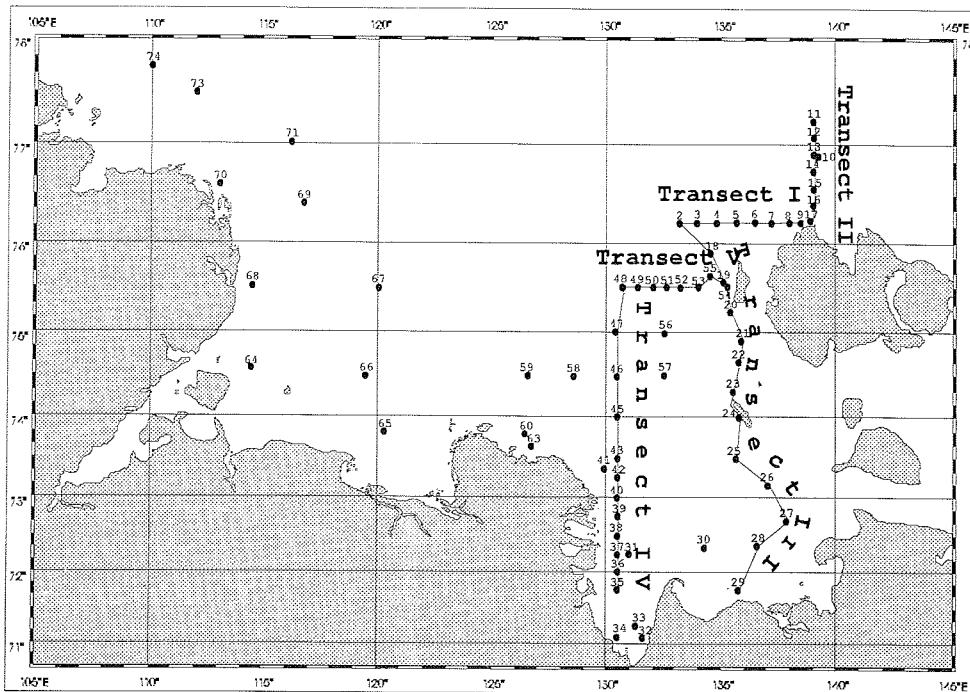


Fig. 25: Map of oceanographical stations during the TRANSDRIFT III expedition (October 6-24, 1995).

Preliminary Results

1. The hydrological situation in the eastern Laptev Sea in autumn and, probably, also in summer 1995, was governed by the north-eastward spreading of freshwater of the Lena and Yana Rivers so that the core of the outflow was located over the eastern slope of the relict submarine Yana River valley. However, as compared with 1993 and 1994 when the minimum salinity values at the outflow cores of the Lena River at 74° 00' N, 74° 30' N, 75° 30' N were 3, 7, and 12.5 in September 1993 (Kassens and Karpiy, 1994) and 9.5, 18.5, and 25.5 in September 1994 (Kassens,

1995), the corresponding values in October 1995 were 12.5, 14.9, and 16.0 (Fig. 26). Obviously, in 1993 the off-shore type of river-water spreading to the north was observed and in 1994 the on-shore type with attenuated indicators of the river-water outflow, whereas in 1995 it was the off-shore type with the general outflow direction of river water to the north-east from the Lena delta along Kotel'ny Island with a less sharp gradient at the outflow core. As in 1994, the Khatanga River runoff in the eastern part of the sea was practically not pronounced in the field of oceanographic values (as compared with 1993, the difference was 10 the north-east of Bol'shoi Begichev Island). The runoff of the Olenek River and the Olenek Branch of the Lena River is slightly more pronounced. It differs, however, in a similar value from 1993. However, since in 1995 the observations were carried out in October, river water flowing into the sea could be subjected to a transformation whose extent we are not able to estimate on the basis of the data available.

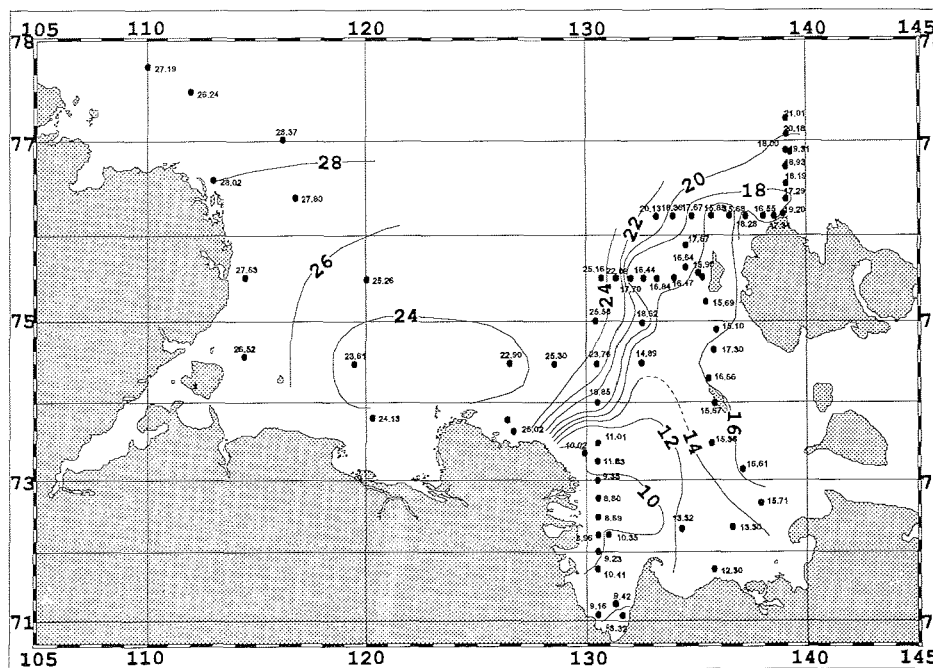


Fig. 26: Salinity distribution at the sea surface (October 6-24, 1995).

The surface distribution of water temperature (Fig. 27) reflects the freeze-up processes which began in the second half of October. Relating to the autumn-winter season it cannot be considered as a parameter characterizing the spreading of river runoff.

2. At the peripheries of the river-water outflow zone, as in 1993 and 1994 (Kassens and Karpiy, 1994; Kassens, 1995; Gribanov and Dmitrenko, 1994; Golovin et al., 1995), numerous isopycnic intrusions of warm and cold water were found resulting from the hydrodynamic instability of the runoff hydrofronts (Fig. 28). The measurements confirm the presumption made in 1994 that the runoff hydrofronts in Arctic seas have a two-layer structure (Golovin et al., 1995). The upper part of the hydrofront forms due to the outflow of freshwater of riverine origin and spreads down to the depth of river-water penetration (seasonal pycnocline),

being sharply baroclinic (Fedorov, 1983). The lower part of the hydrofront extends from the seasonal to the main pycnocline. It is formed as a result of isopycnic convergence at the runoff hydrofronts and has a sharp thermocline (Fedorov, 1983). The isopycnic warm and cold intrusions mentioned above are formed as a result of the instable thermocline front located at depths from 10 to 18-23 m.

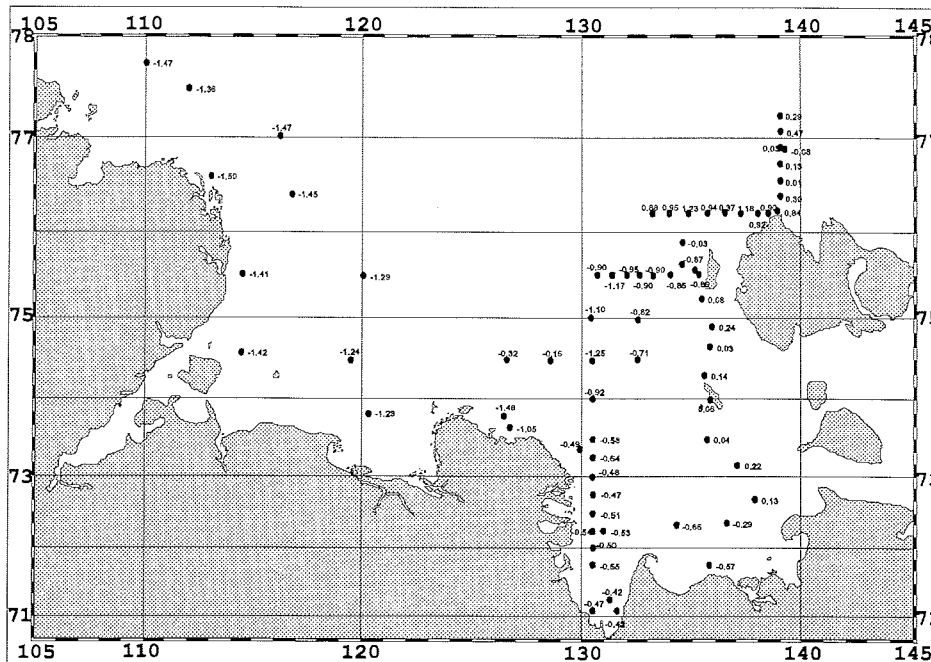


Fig. 27: Water temperature distribution ($^{\circ}\text{C}$) at the sea surface (October 6-24, 1995).

3. The suggestion based on the results of 1994 studies that there occurs a subfrontal convergence in the zones of runoff hydrofronts is confirmed (Golovin et al., 1995). As in 1994, the existence of water layers differing in the indicators of dissolved silica (Fig. 29) and oxygen (Figs. 30, 31, 32, 33, 34), close to surface water of non-riverine origin, is observed in the river-water outflow zone. The convergence of relatively warm surface water of non-riverine origin results in the formation of an anomalously warm water layer under the runoff lens, whose temperature differs little from surface water of riverine origin (Fig. 28). The seasonal thermocline is absent, and the surface quasi-thermal warm layer extends to 25-27 m in summertime (Kassens, 1995; Golovin et al., 1995).

4. It is found that the processes of storm mixing, typical of the autumn season, do not destroy the seasonal pycnocline (Fig. 35a/b, 36, 37a/b). Hence, at negative temperatures of ambient air, the surface layer is cooled down only to the seasonal pycnocline (Fig. 38, 39). On the other hand, in zones of spreading subfrontal convergence in the spring-summer season, warm surface water spreads down to a depth limited by the main pycnocline. As a result of the processes indicated, in the autumn season preceding freeze-up and after its onset, quite a thick anomalously warm water layer remains "buried" under the runoff lens at depths of 12-25 m (Fig. 35a, 38). Its temperature reaches 4°C , with a temperature of the surface layer close to the freezing point (Fig. 38). This layer forms due to radiation heating and

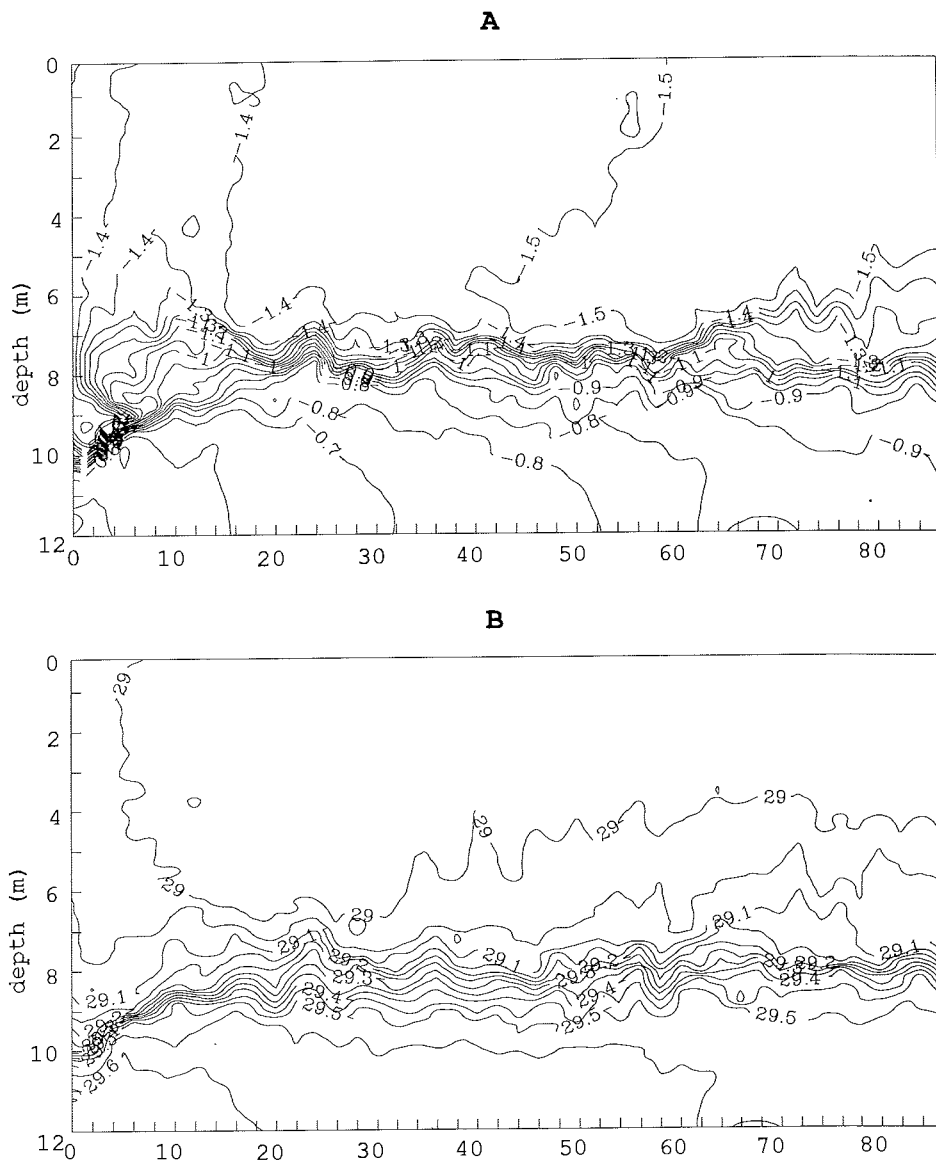


Fig. 28: Temporal variability of (A) temperature ($^{\circ}\text{C}$), (B) salinity at station KD9560 (October 18, 1995).

convergent processes at the runoff hydrofronts. In those regions that are not subjected to the river runoff, there are also observed intermediate residual layers of warm water which result only from summer radiation heating. As a rule, their thickness does not exceed 5 m and the temperature gradients at the upper boundary of the layer are by 1.5 to 2 times less than the corresponding gradients under the runoff lens (Fig. 39). The above conclusions are also confirmed by the results of hydrochemical observations.

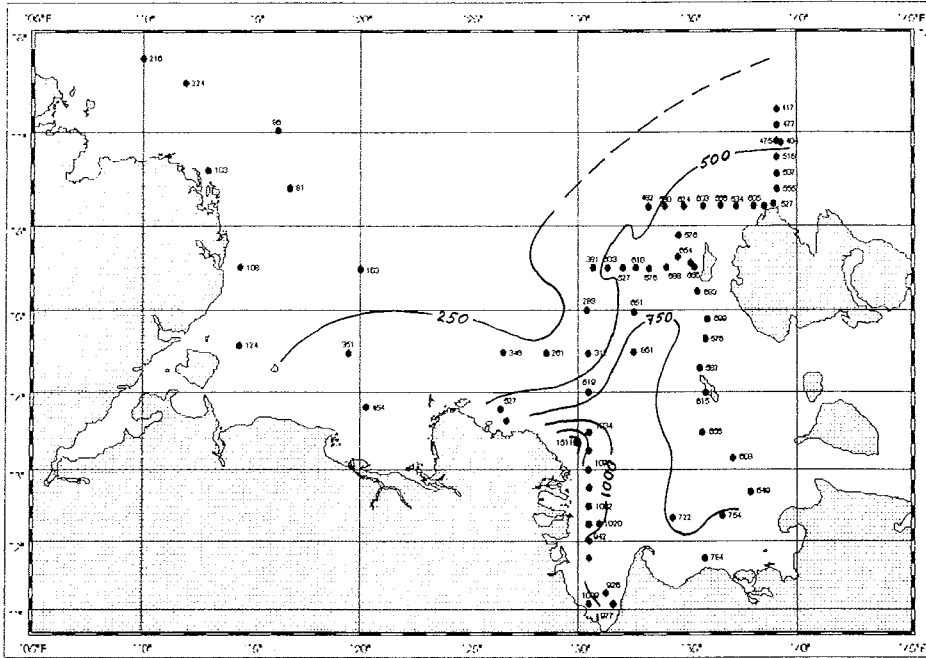


Fig. 29: Distribution of silica ($\mu\text{g/l}$) on the surface of the Laptev Sea in October 1995.

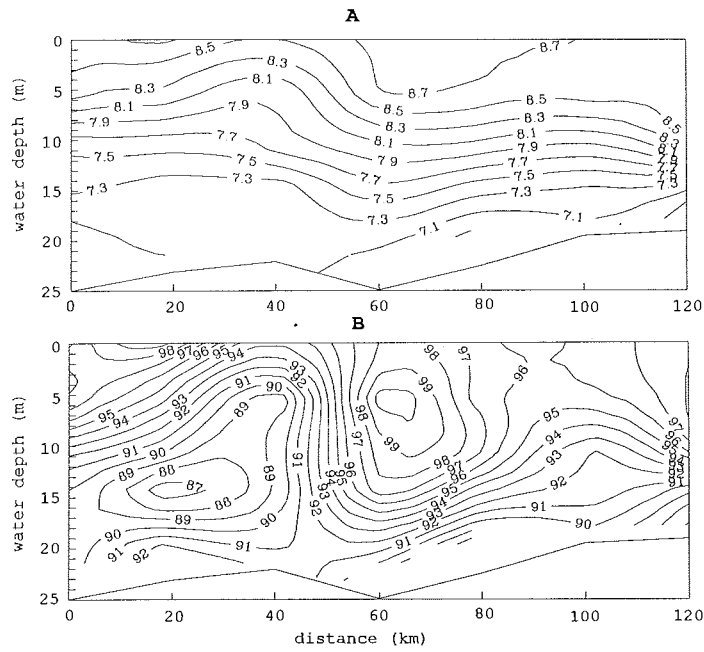


Fig. 31: Distribution of dissolved oxygen, (A) - ml/l, (B) - % along Transect II (October 9-10, 1995).

The fact that such thick well-heated water layers exist with young-ice thicknesses at the surface reaching 20 cm cardinaly changes our understanding of the thermal character of freeze-up and the dynamics of further ice growth in the wintertime. Obviously, heat will be transferred to the surface by convective processes for a long time, thus delaying the processes of young-ice growth. In addition, this phenomenon suggests that the existence of the Great Siberian Polynya, whose geographical position in the eastern Laptev Sea approximately coincides with the zones of the development of subfrontal convergences, is not only governed by synoptic-climatic factors. Probably, the convective heat transfer to the surface can also be considered as one of the mechanisms maintaining the existence of the polynya in winter.

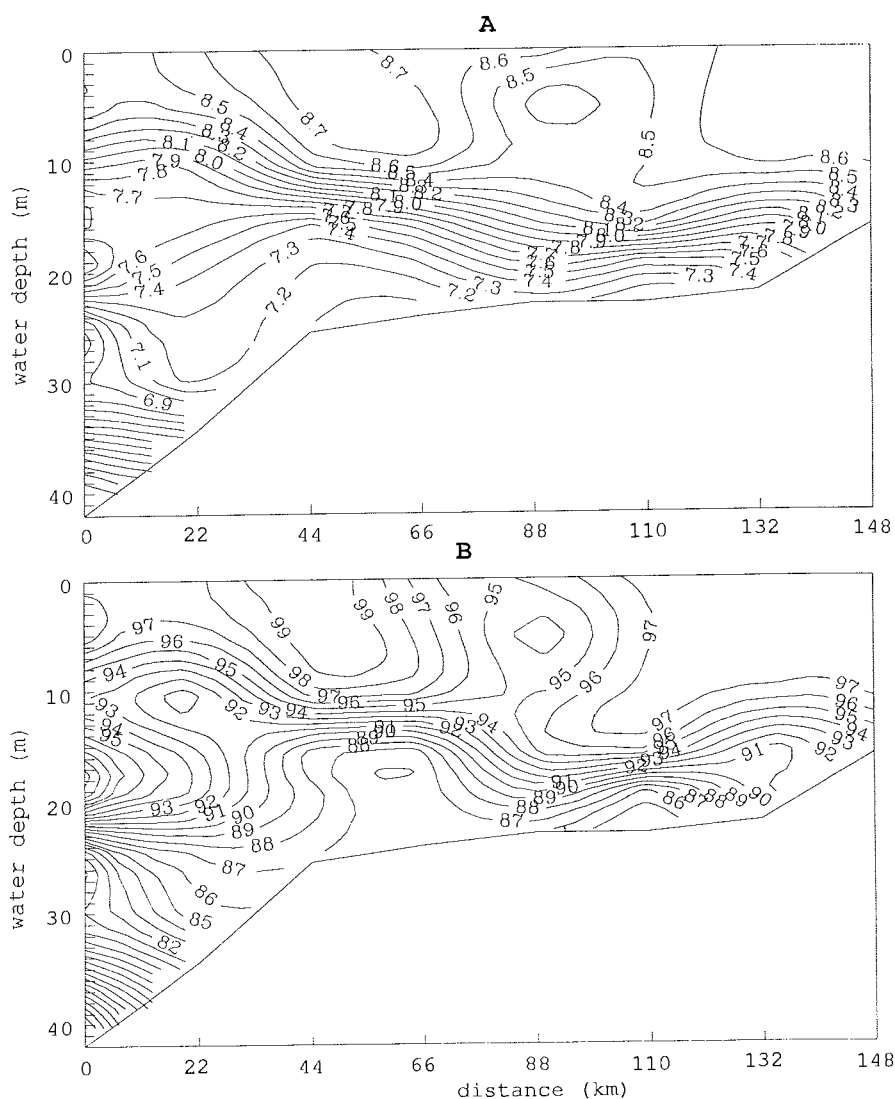


Fig. 30: Distribution of dissolved oxygen, (A) - ml/L, (B) - % along Transect I (October 8-9, 1995).

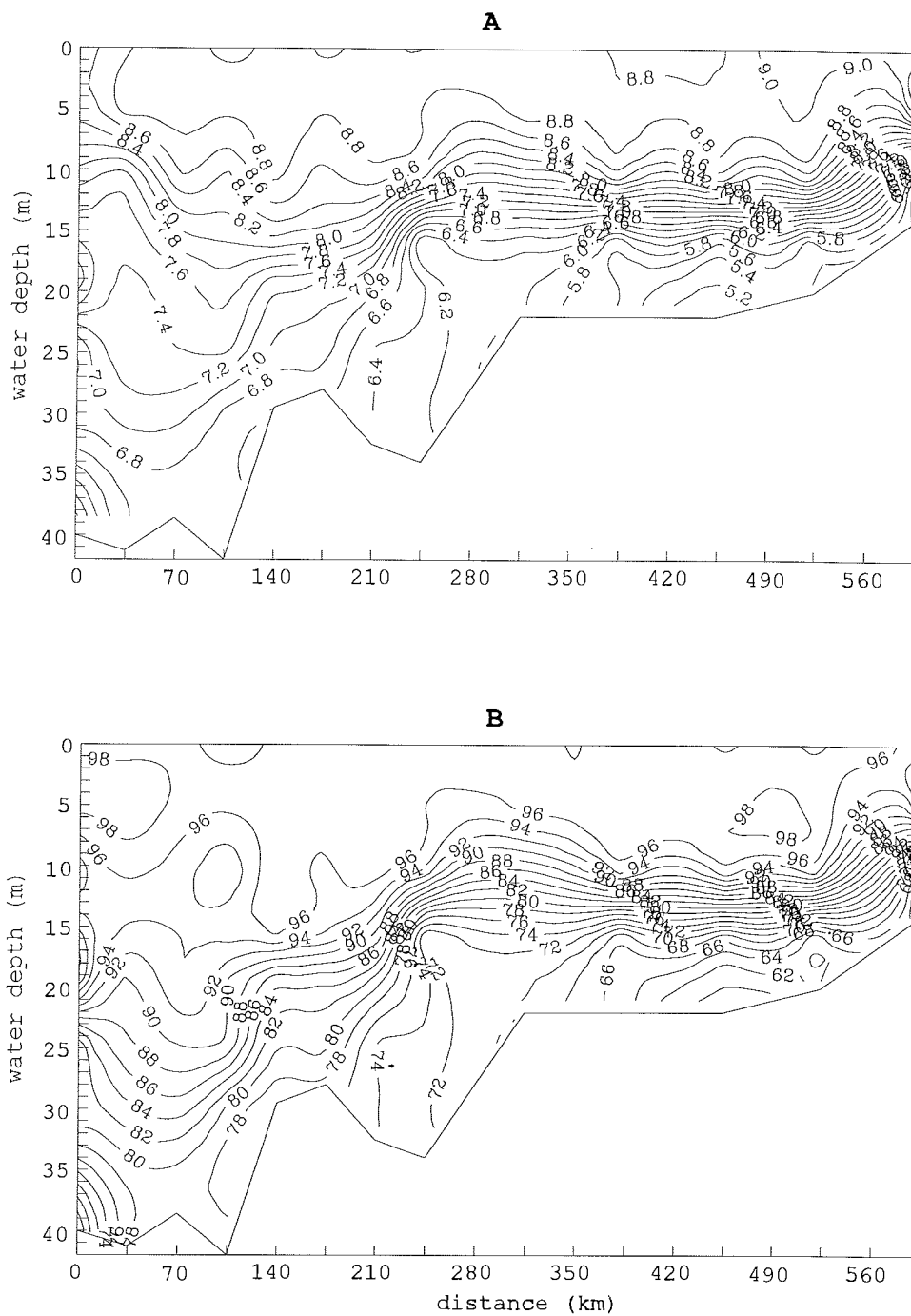


Fig. 32: Distribution of dissolved oxygen, (A) - ml/l, (B) - % along Transect III (October 10-12, 1995).

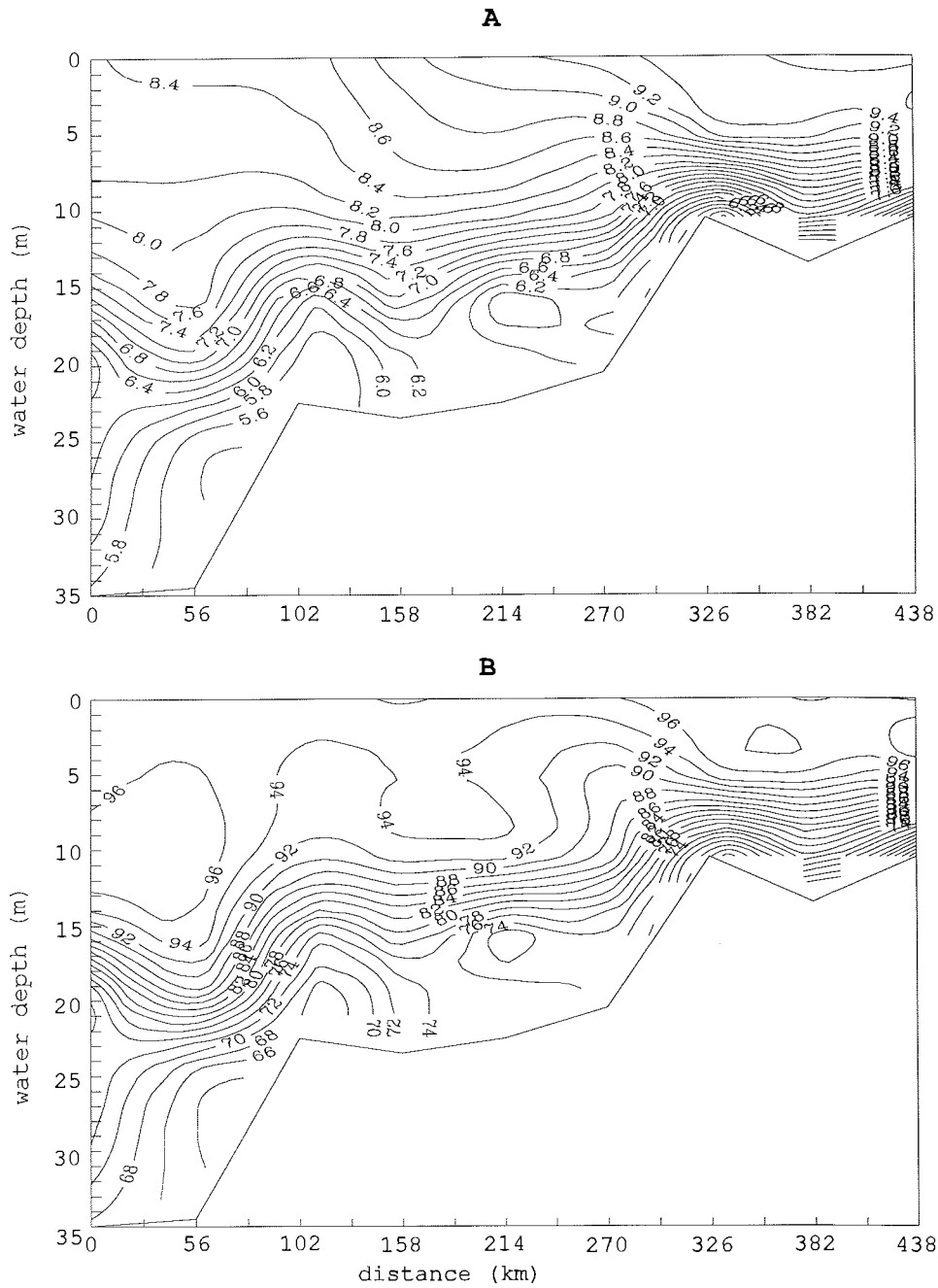


Fig. 33: Distribution of dissolved oxygen, (A) - m/l, (B) - % along Transect IV (October 14-16, 1995).

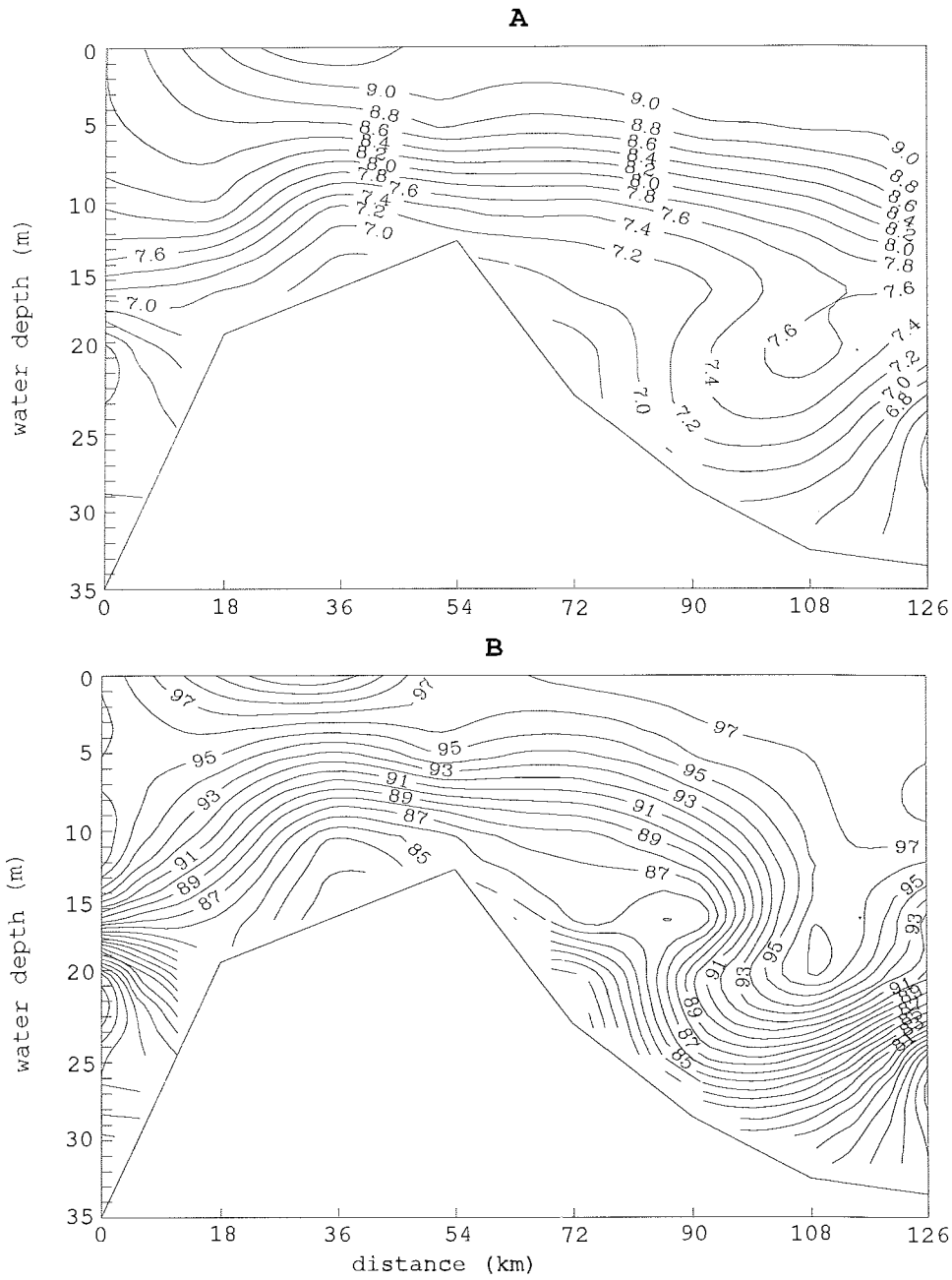


Fig. 34: Distribution of dissolved oxygen, (A) - ml/l, (B) - % along Transect V (October 16-17, 1995).

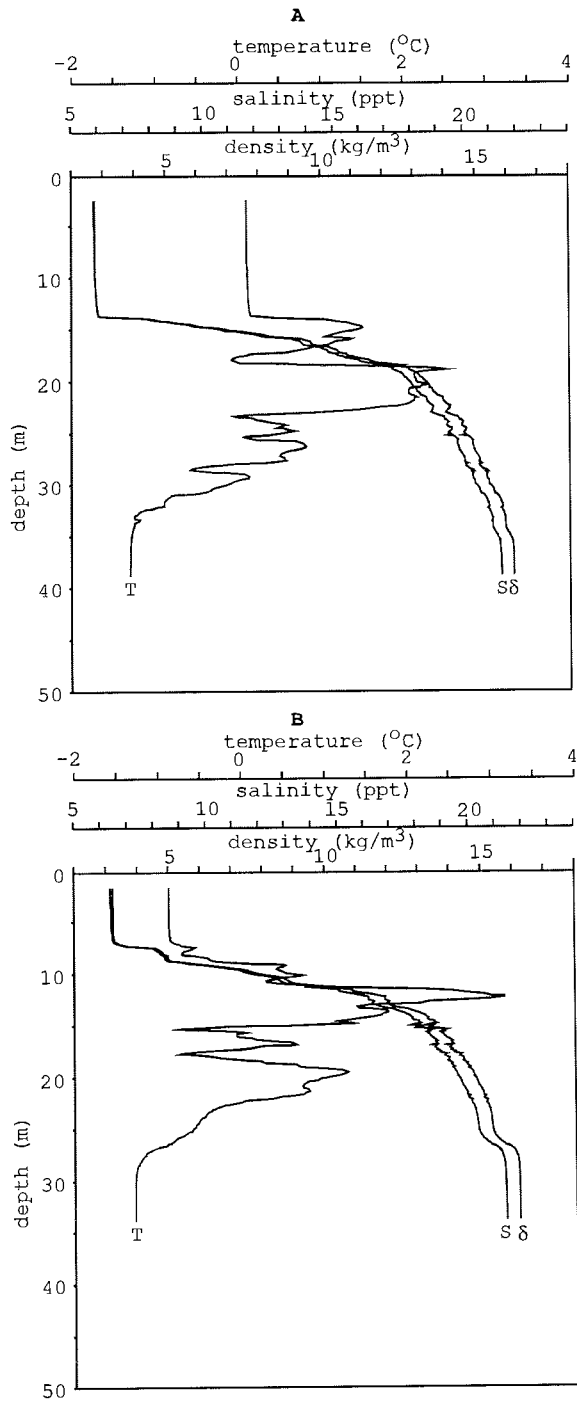


Fig. 35: Vertical distribution of temperature (°C), salinity and density (kg/m³) near run-off hydrofronts, (A) - station KD9519, (B) - station KD9553.

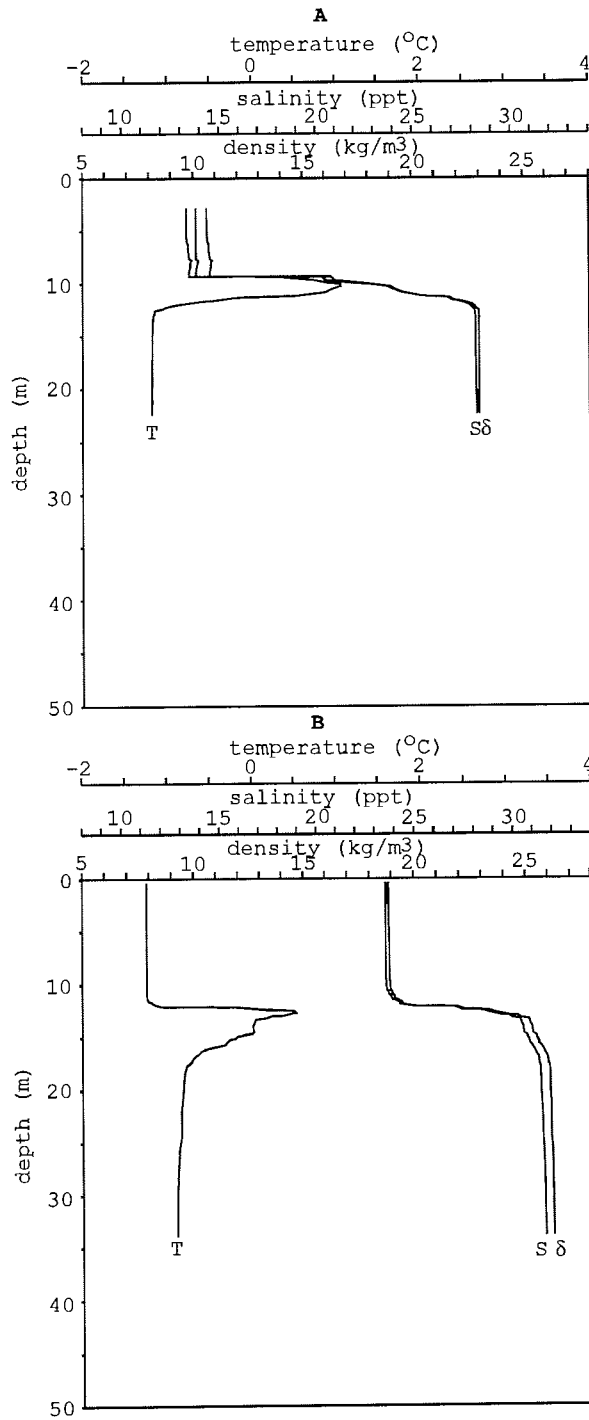


Fig. 36: Vertical distribution of temperature ($^{\circ}\text{C}$), salinity and density (kg/m^3), outside of river water, (A) - station KD9530, (B) - station KD9566.

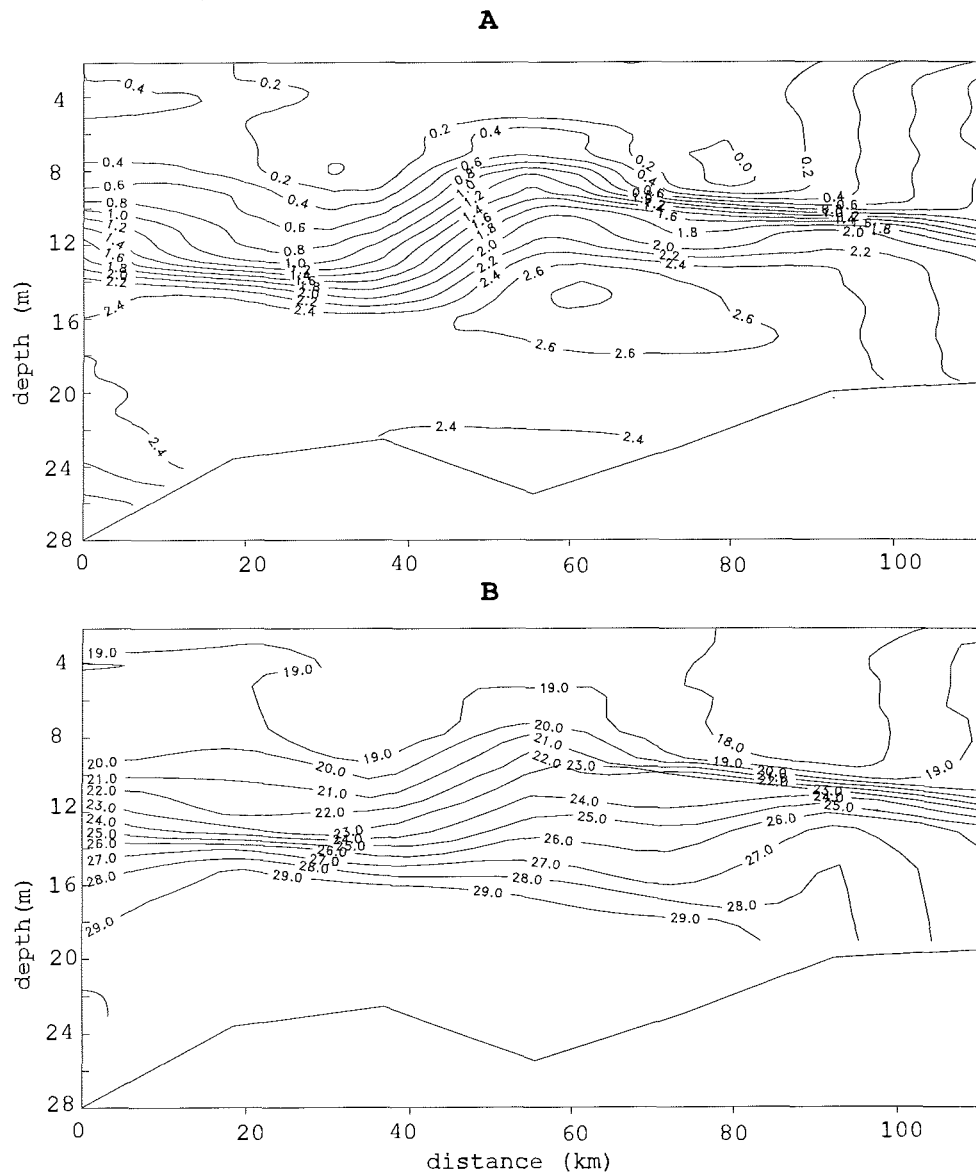


Fig. 37: Distribution of (A) temperature (°C) and (B) salinity along Transect II (October 9-10, 1995).

5. The series of oceanographic soundings from young drifting ice have shown that, at the high drift rates observed (up to 3 knots), studies of the development of gravitational convection under the ice are virtually impossible. Such studies require observations from fast ice, which has not yet been formed at that time of the year, or in fractures between multi-year ice obscuring the drift effects. Also, the high-frequency internal waves which were observed in high-gradient water layers (Fig. 40, 44), cannot unambiguously be considered as a result of natural processes since the influence of the ship hull even at a significant distance from the board can be quite large at such high drift rates.

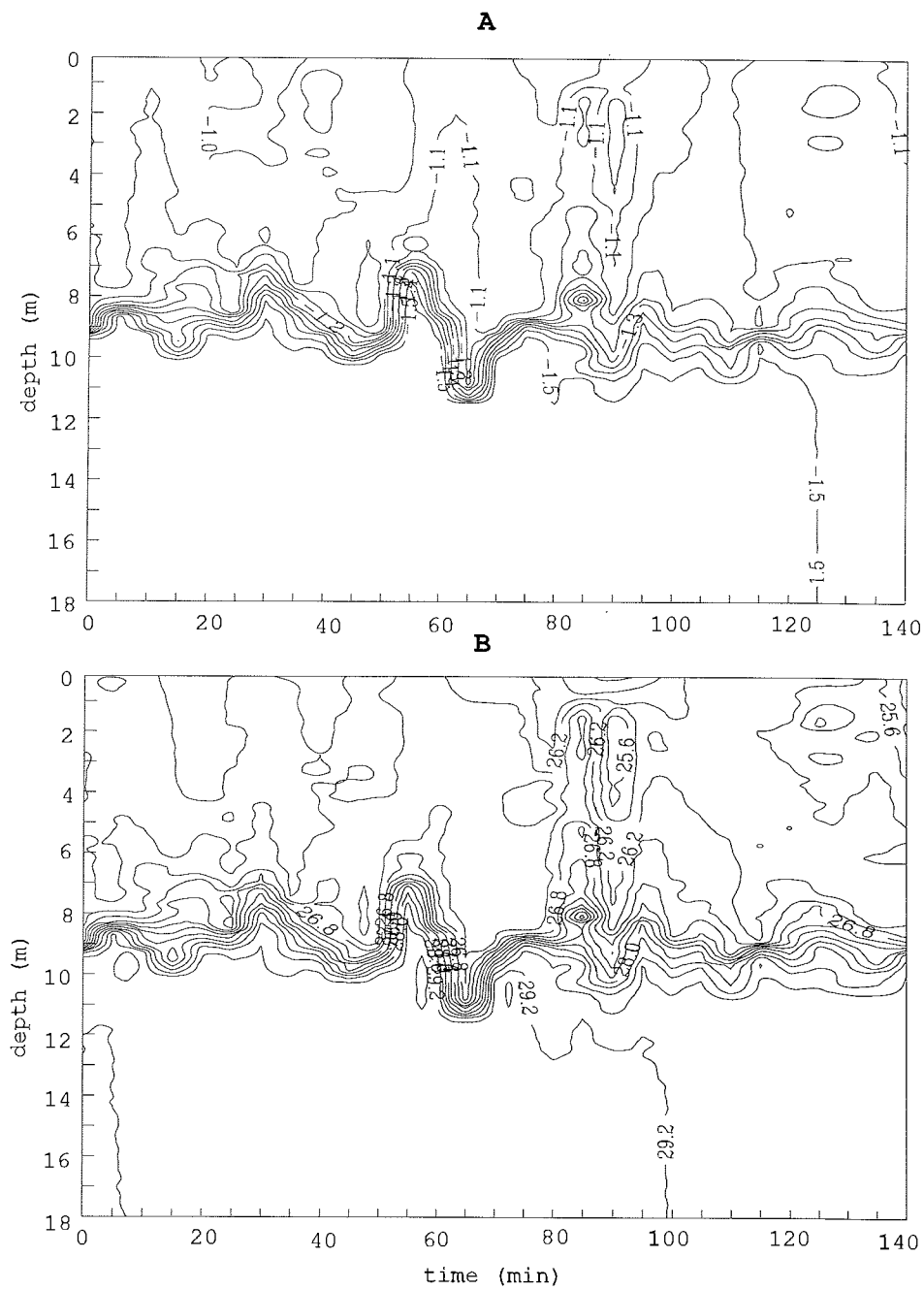


Fig. 38: Temporal variability of (A) temperature ($^{\circ}\text{C}$) and (B) salinity at station KD9563 (October 19, 1995).

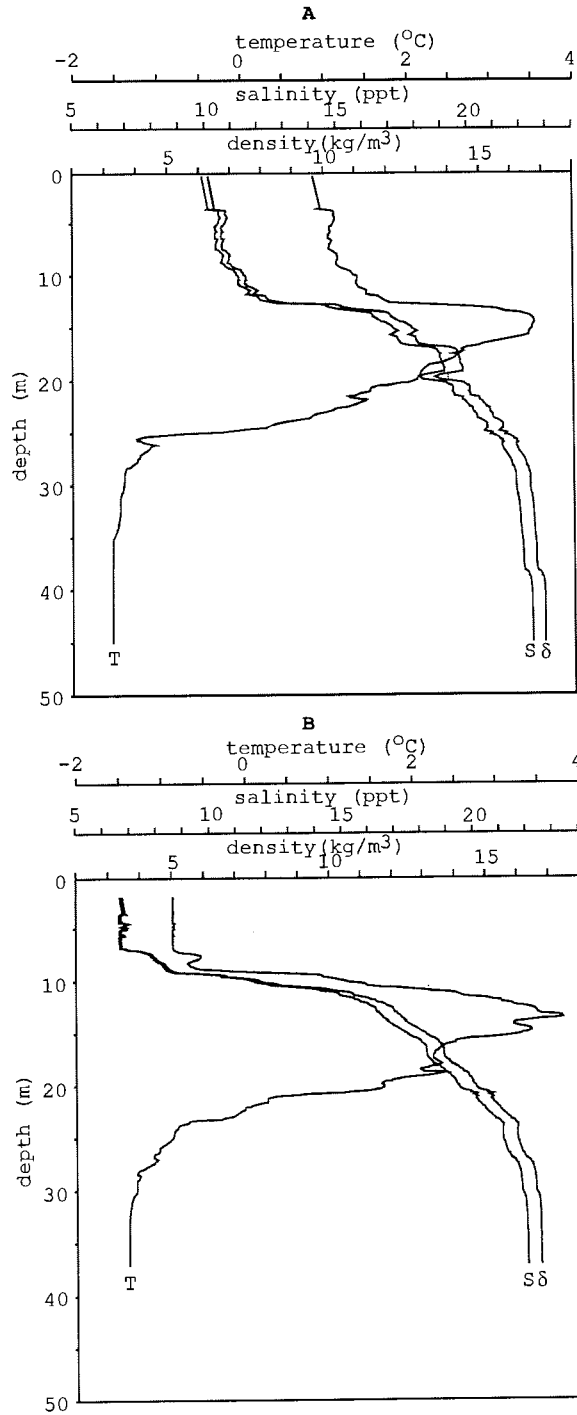


Fig. 39: Vertical distribution of temperature (°C), salinity and density (kg/m³) under river water, (A) - station KD9519, (B) - station KD9553.

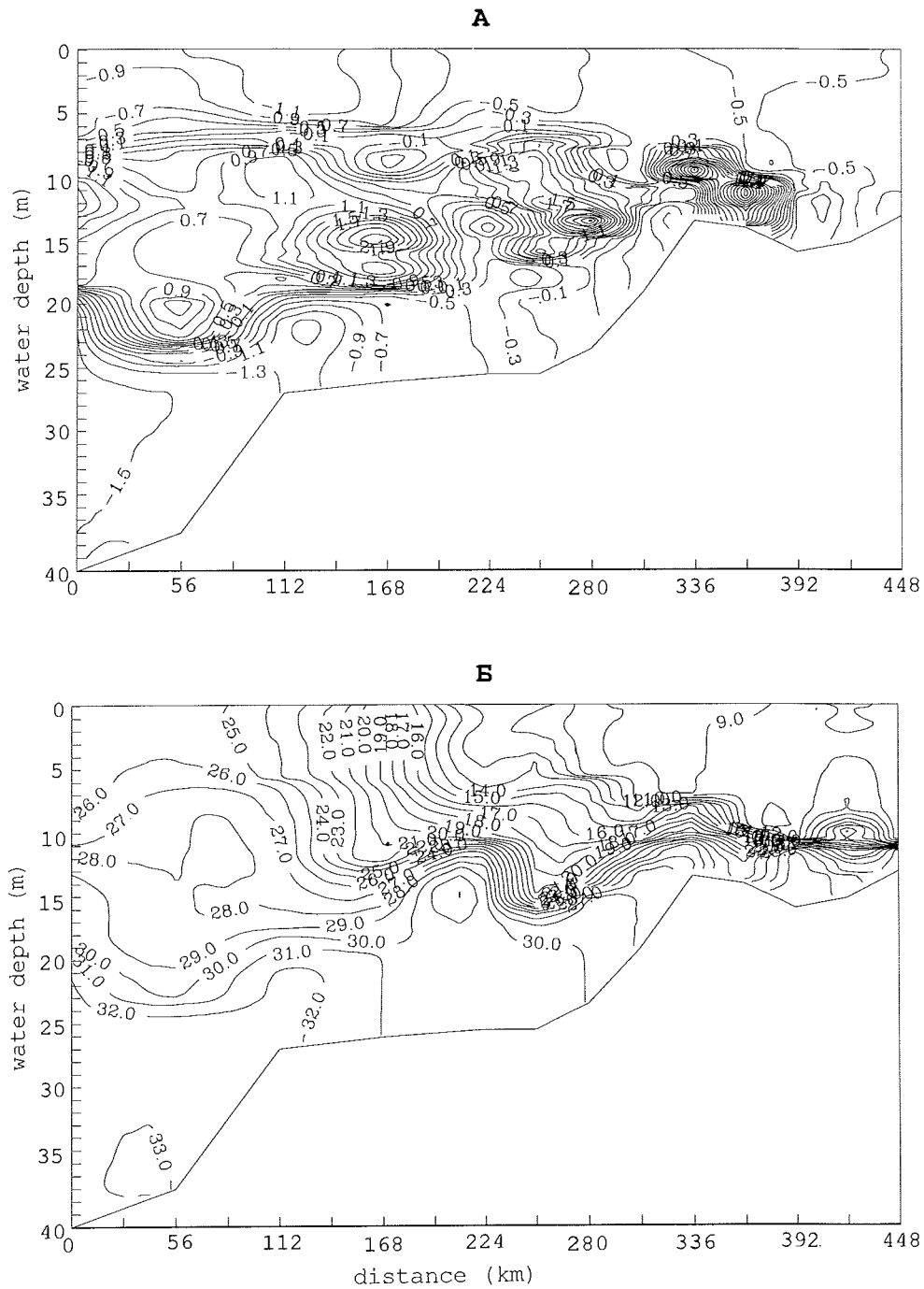


Fig. 40: Distribution of (A) temperature (°C) and (B) salinity along Transect IV (October 14-16, 1995).

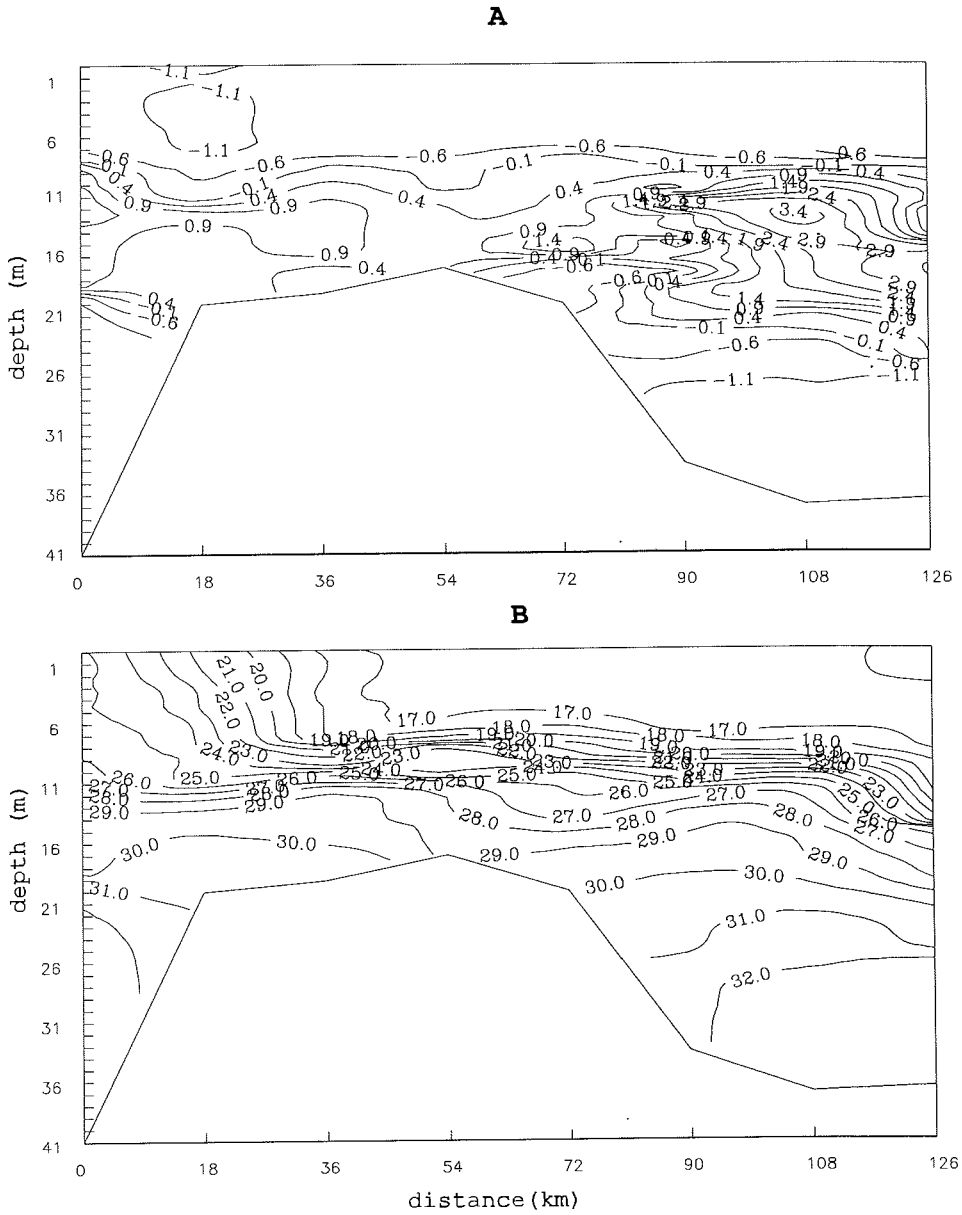


Fig. 41: Distribution of (A) temperature ($^{\circ}\text{C}$) and (B) salinity along Transect V (October 16-17, 1995).

The Distribution of Chlorophyll Fluorescence Intensity in the Laptev Sea: Results of Hydrooptical Measurements

A. Anoshkin

Krylov Shipbuilding Research Institute, St. Petersburg, Russia

Research Program

Hydrooptical studies during the expedition focussed on the spatial distribution of chlorophyll fluorescence intensity in autumn season continuing the studies of the TRANSDRIFT II expedition.

The substance transport in such a dynamic zone of the Laptev Sea as that of river/sea-water interaction is to a great extent governed by hydrophysical characteristics. Spatial and temporal variability scales can have a range of several meters and minutes respectively. Hence, for measuring properties of the medium strongly dependent on the hydrophysical characteristics, it is necessary to use methods which allow us to obtain data with a corresponding spatial-temporal resolution.

With regard to suspended matter, in particular to phytoplankton, different optical instruments are employed. Optical methods can be applied in order to investigate substance fluxes in seas because the substances suspended and dissolved in sea water are capable to affect the light rays propagating in the medium. The in situ measurements of this effect allow us to detect without sampling the presence of different substances in water and, in particular, to investigate the small- and meso-scale variability of their distribution.

Some substances as, for example, chlorophyll a, are able to emit light at a longer wave than the absorbed one, i.e. they are fluorescent. The fluorescence intensity in the water column depends on the concentration of these substances, thus allowing a quantitative analysis.

Studies during the expedition in 1994 have shown that in situ measurements of the chlorophyll fluorescence intensity allow us to study the variability of its distribution in the area of interaction of river runoff and marine environment (Kassens, 1995). Furthermore, they enable us to identify zones of influence of the latter with a sufficient spatial resolution. By comparing these results with the plankton and macrobenthos biomasses it is possible to delineate zones of elevated biological activity. The results of the previous year have defined the goals of the TRANSDRIFT III expedition:

- to study the influence of river runoff on the spatial distribution of chlorophyll fluorescence under autumn conditions and to delineate the zone of river-water spreading,
- to delineate the vertical variability of the chlorophyll a fluorescence intensity,
- to estimate the seasonal variability of the distribution by comparing the results of the measurements in summer during the TRANSDRIFT II expedition with the results of 1995.

The data obtained on chlorophyll fluorescence will allow us to assess the influence of river runoff on the environment.

Working Program

The impulse fluorimeter Variosens II was used for vertical soundings of the water column from the sea surface to the bottom. Soundings were performed aboard the icebreaker. As measurements were made in real time, continuous vertical profiles of

fluorescence intensity at all hydrochemical stations were obtained. On their basis, the distributions along hydrological transects were constructed.

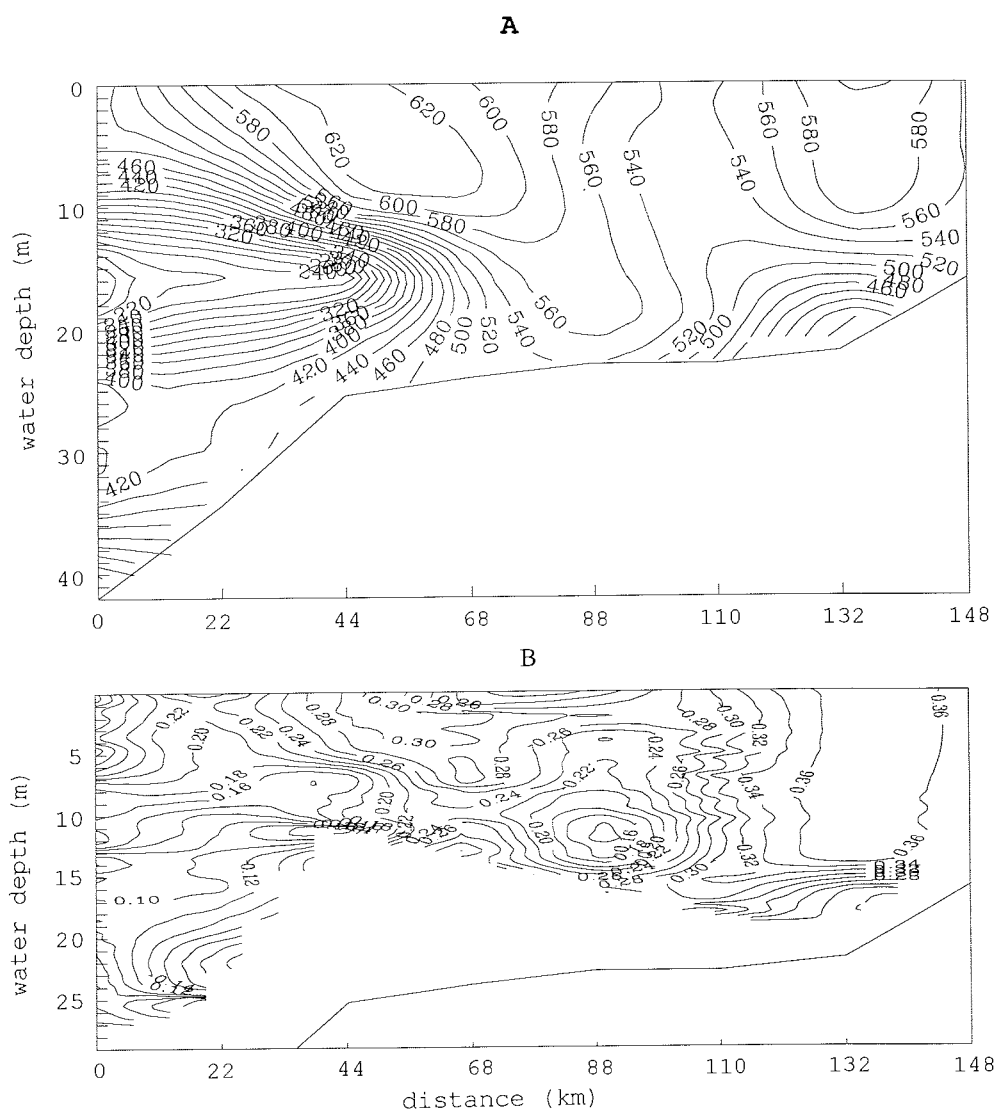


Fig. 42: Distribution of (A) silica ($\mu\text{g/l}$) and (B) chlorophyll a fluorescence intensity (c.u.m) along Transect I (October 8-9, 1995).

Preliminary Scientific Results

The analysis of the structure of fluorescence intensity distributions (Fig. 42, 43, 44, 45, 46) and its comparison with CTD data shows that zones of enhanced intensities (more than 0.25) correspond to zones of river-water spreading. The frontal zone of the sea/river-water boundary begins with station KD9543 where a fluorescence intensity typical of river water was observed. Then, the level gradually decreases to a level typical of a marine environment at station KD9546. To the north-east of this region at stations KD9549, KD9502 and KD9503 the data obtained do not display monotonic variations. But in view of the fact that east of it there were recorded values typical of the zones of river runoff influence, this area can be identified as a transient zone.

The comparison of data from transects IV and V with the corresponding last-year data shows that, in the river outflow zone, the fluorescence intensity in the 5-meter surface layer actually has the same values.

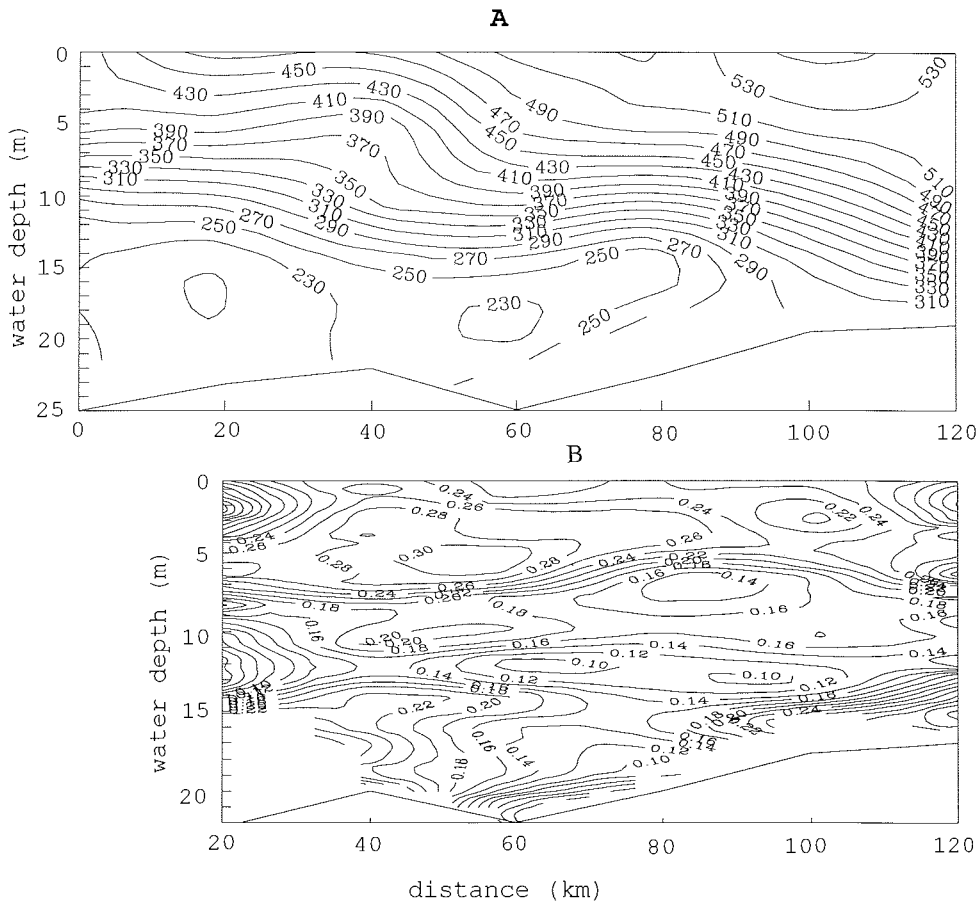


Fig. 43: Distribution of (A) silica (µg/l) and (B) chlorophyll a fluorescence intensity (c.u.m) along Transect II (October 9-10, 1995).

Vertical variations of profiles even in the zone with a strong influence of the Lena River runoff (transect IV) were of non-monotonic character which manifested itself in the presence of local maxima not only at the sea surface, but in the intermediate and the near-bottom layers. In summer 1994, only one-modal profiles with maxima at the surface were recorded here.

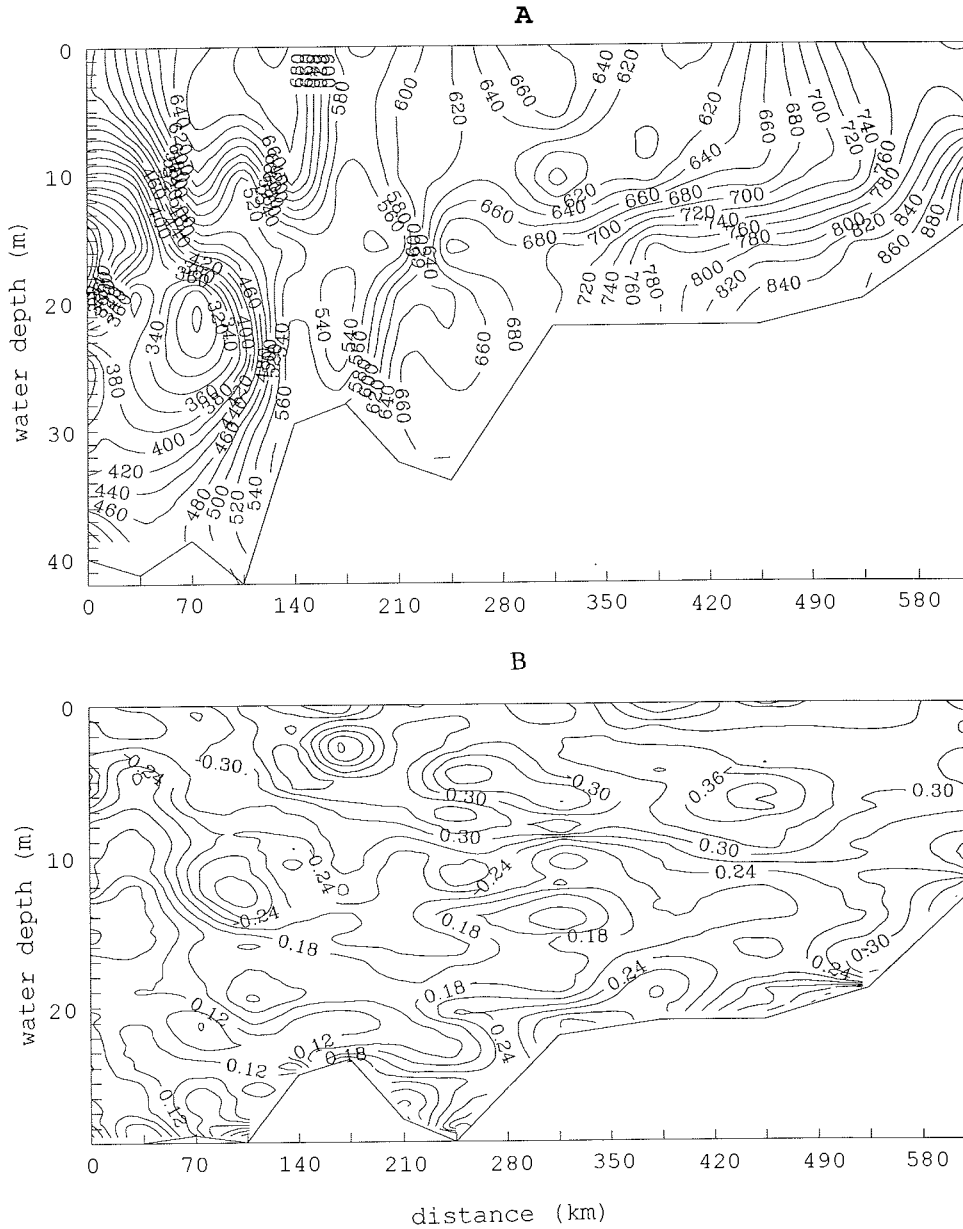


Fig. 44: Distribution of (A) silica ($\mu\text{g/l}$) and (B) chlorophyll a fluorescence intensity (c.u.m) along Transect III (October 10-12, 1995).

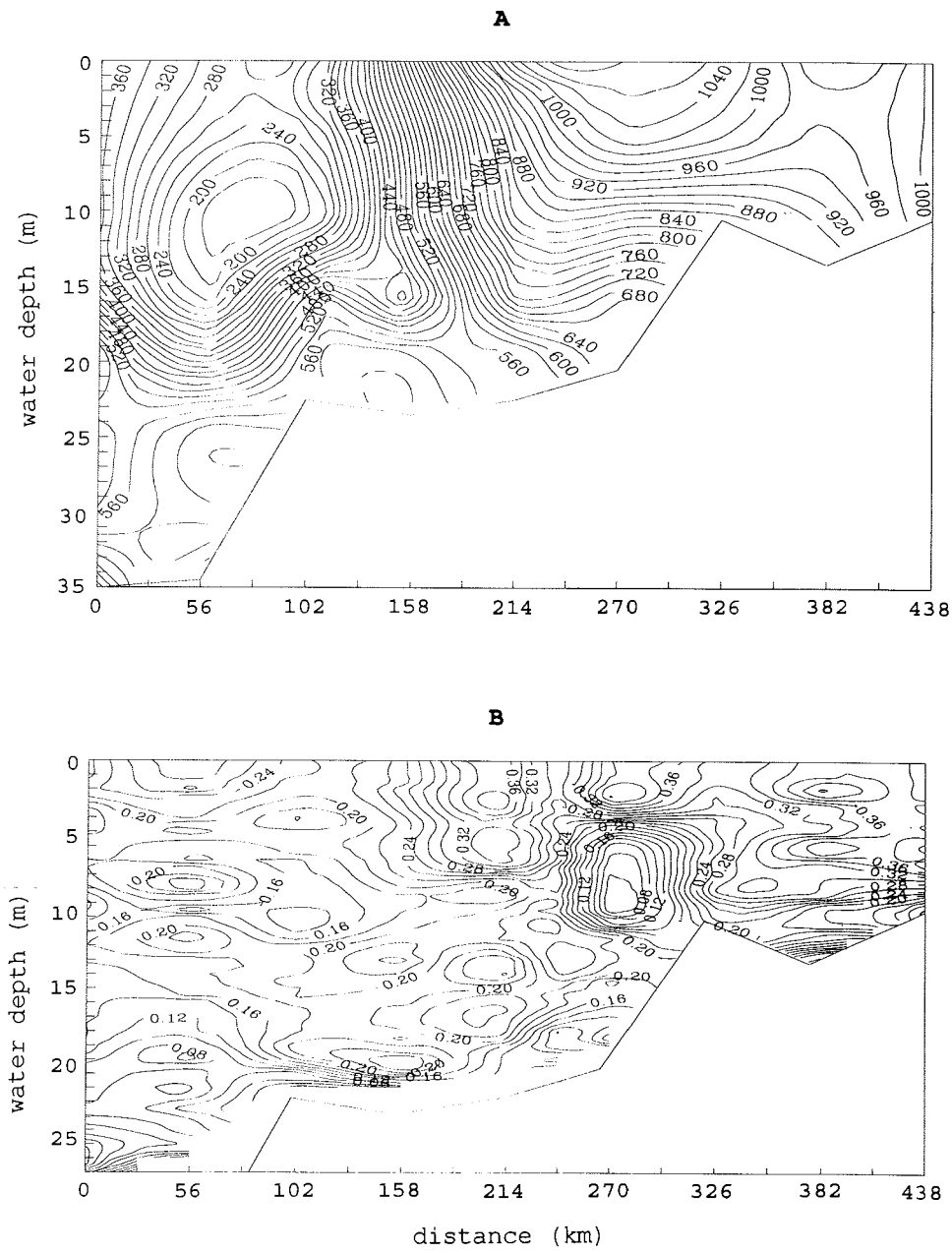


Fig. 45: Distribution of (A) silica ($\mu\text{g/l}$) and (B) chlorophyll a fluorescence intensity (c.u.m) along Transect IV (October 14-16, 1995).

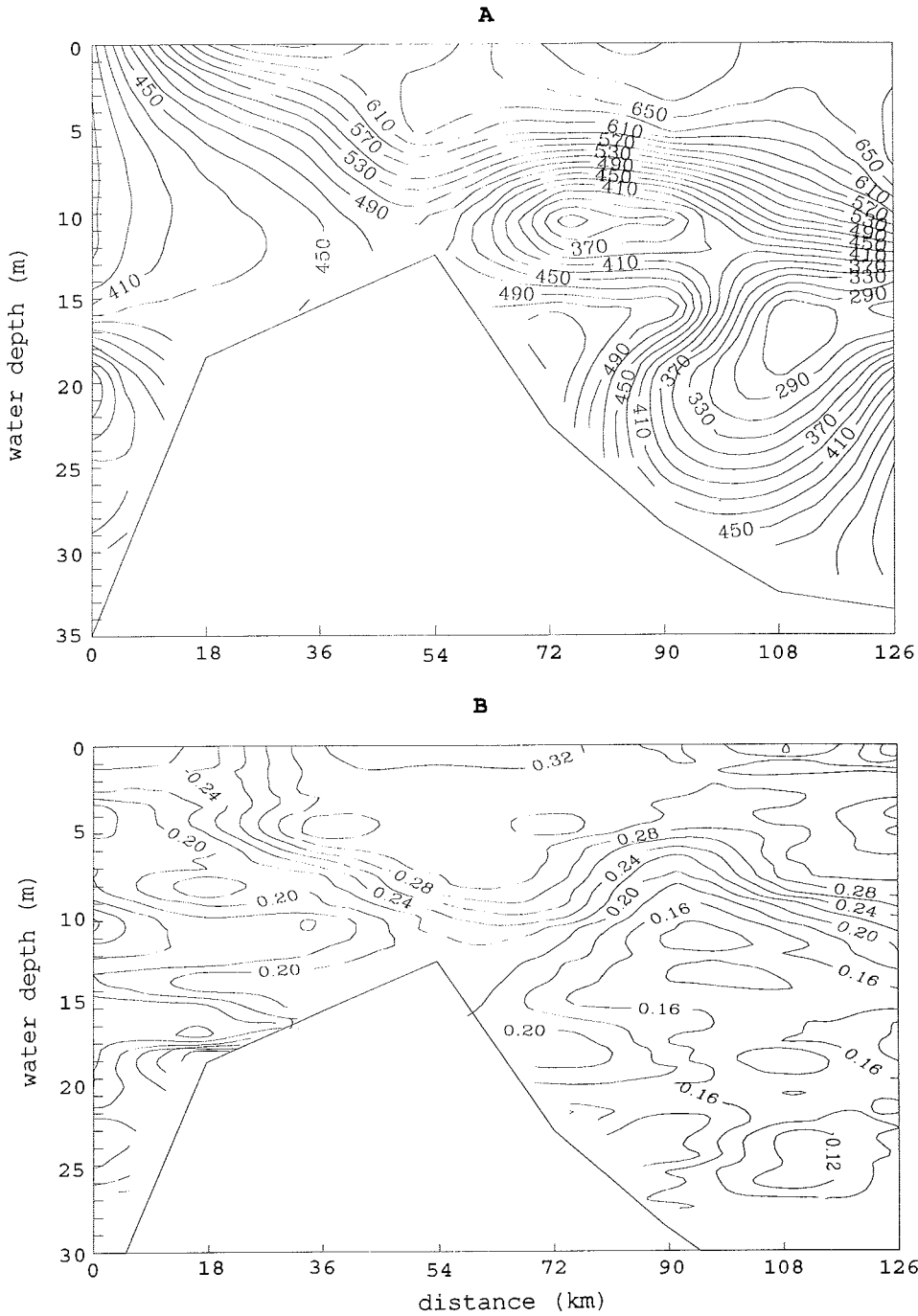


Fig. 46: Distribution of (A) silica ($\mu\text{g/l}$) and (B) chlorophyll a fluorescence intensity (c.u.m) along Transect V (October 16-17, 1995).

Hydrochemical Observations

S. Pivovarov, B.T. Rossak*, Iu. Sherbakov, V. Sviridov

State Research Center - Arctic and Antarctic Research Institute, St. Petersburg, Russia

* GEOMAR Research Center for Marine Geosciences, Kiel, Germany

Hydrochemical investigations were carried out in order to address the following scientific problems:

- to study the evolution of the vertical hydrochemical water structure in the layer beneath the ice during ice formation and the development of gravitational convection;
- to study the mineral nutrient concentration in sea ice;
- to study the alkalinity distribution in the water column;
- to determine the spatial distribution of dissolved inorganic carbon (DIC) as well as the $^{13}\text{C}/^{12}\text{C}$ stable isotope ratios during freeze-up;
- to measure the biogenic methane concentration in the water column of the Laptev Sea.

Working Program

Concentrations of dissolved oxygen and silica at oceanographic stations were determined at standard levels. Phosphate concentrations were determined at stations with hydrobiological observations. Sampling was carried out to measure the annual biochemical consumption of oxygen in the surface layer, in the main halocline and in the bottom layer. Silicate and phosphate were measured in samples of melted ice. For measurements of alkalinity, DIC, stable isotopes and methane, water samples were taken at 12 hydrochemical stations at different water depths (Tab. A2). To analyze alkalinity 250 ml of water were filled into small plastic bottles. 100 ml of the water sample were filled, without any air inclusions, into glass bottles and were then poisoned in order to determine DIC, stable isotopes and methane.

Observations and Equipment

The following work was done in the Laptev Sea from October 6 to 24, 1995:

- 461 measurements of dissolved oxygen concentration in sea water at 65 stations;
- 471 measurements of silica in sea water at 65 stations;
- 192 measurements of phosphate in sea water at 18 stations;
- 89 measurements of silica in sea-ice samples;
- 89 measurements of phosphate in sea-ice samples;
- 30 measurements of silica and 6 of phosphate in pore water at 3 stations;
- 32 samples were taken to determine the annual biochemical consumption at 11 stations.

The dissolved oxygen concentration was determined by means of the Winkler method (Manual, 1993) using the automatic electronic burette ABU 80. The oxygen phials and other calibrated bottles were verified in 1995. Silicate concentrations were measured by a colorimetric method using ascorbin acid for reducing the silicium-molybdenum complex (Manual, 1993). Phosphate concentrations were determined by the colorimetric method of Murphy and Riley (Manual, 1993). Colorimetric measurements were carried out by the photoelectrocolorimeter KFK-2.

Before starting the work, calibrating plots were constructed using sea water with low concentrations of phosphate and silica.

Alkalinity measurements will be carried out at the CTH-GU, Gothenburg (Sweden). Determinations of DIC and stable isotopes will be done at the CLK, Kiel (Germany). Methane analyses will be carried out at the USGS, Menlo Park (USA).

Preliminary Results

- The main features of the hydrochemical structure in autumn (October 1995) and in summer (September 1993 and 1994) are the same. There was a big difference between the western and the eastern parts of the Laptev Sea, especially in the silica distribution which indicates river influence. The maximum of silica (1500 mg/l) at the surface layer was found near the Lena Delta (Fig. 29).
- As a result of mixing and convection, the surface layer had a very low oxygen saturation ($96 \pm 2\%$) in October 1995. On the other hand, a lot of phosphate has been elevated to the surface by convection. The phosphate concentration in October 1995 was by three times higher than in September 1993 and September 1994.
- In the eastern part of the Laptev Sea, there was a multi-layered water structure in October 1995. An intermediate layer with a low silica concentration has been observed at almost all stations (Figs. 42, 43, 44, 45, 46).

Biological Investigations

K. v. Juterzenka, V. Petriashov*, D. Piepenburg, M.K. Schmid, K. Tuschling

Institut für Polarökologie der Universität Kiel (IPÖ), Germany

* Zoological Institute of the Russian Academy of Sciences St. Petersburg (ZIN RAS), Russia

Scientific Background

The ecology of the broad and shallow Laptev Sea shelf is shaped by a distinct coupling between sea ice, water column and seabed biota as well as by a strong seasonality of the terrestrial influence. As for almost all previous expeditions to the Laptev Sea, emphasis of the biological work during the cruises TRANSDRIFT I and II has been on an investigation of the "summer situation" characterized by lack of sea ice, high terrestrial influence and high biological productivity. It became evident that transformed river water channeled through submerged valleys had a pronounced effect on the distribution of benthic and pelagic communities. Some indicator species of the transformed runoff water penetrated far to the north ($75^\circ - 75^\circ 30'N$) along the river valleys.

Data on seasonal dynamics of Laptev Sea ecosystems were available only from the Tiksi region (Gukov, 1994), and faunistic samples during the fall freeze-up period were obtained only north of Kotel'nyi Island by the expeditions of the vessels "Zarya" (1901-1902) and "Sadko" (1937-1938). There was thus a clear need for further investigations in a later phase of the seasonal cycle (fall freeze-up situation) which is characterized by the development of "third marine biota" - the sea ice - as well as by less terrestrial influence and biological productivity.

Working Program and First Results

During TRANSDRIFT III, the biological studies extended the work of the previous TRANSDRIFT cruises (faunistic inventory of water column and seabed

communities, analysis of the distribution and composition of distinct biocenoses in relation to environmental parameters, determination of abundance and biomass). This time, additional emphasis was on the investigation of sea ice biota. For an adequate sampling of the different habitats (sea ice, water column, seabed), various sampling gears were employed (Tab. 3, A2). Furthermore, studies on the reproductional status, feeding ecology and respiration of dominant species were carried out.

Tab. 3: List of biological sampling tools

Sea Ice

Sub-ice net	Catch of sub-ice zooplankton
Video endoscope	Observation of sub-ice zooplankton

Water Column

Water sampler	Chlorophyll measurements
Secchi disc	Measurement of turbidity
Hand net	Catch of phytoplankton
Bongo net	Catch of zooplankton

Benthos

Dredge	Catch of macrobenthic organisms
Van Veen grab	Sampling of macro- and meiobenthos
Box corer	Sampling of macro-epibenthic organisms
Underwater photo probe	Observation of mega-epibenthos (photography)
Remotely Operated Vehicle (ROV)	Observation of mega-epibenthos (video)

Sea Ice

Biological sea-ice investigations focussed on the qualitative and quantitative determination of flora and fauna in relation to physical conditions of sea ice. For that purpose, frazil, slush and various new-ice types were sampled at 15 ice stations. Melted ice samples were prepared for Chlorophyll a analysis, some samples were fixed for further biological investigations. On three ice stations, a sub-ice net was lowered through a ten-centimeter-wide ice hole to get information on the sub-ice and ice-associated fauna. A video endoscope showed the small-scale structure of the ice-water interface as a habitat for ice-associated organisms, e.g. copepods and an amphipod at an ice floe that survived the last summer. As example for a different sub-ice environment, anorganic and organic enclosures of "dirty ice" could be observed in new ice off the Lena Delta.

Phytoplankton

In order to estimate phytoplankton biomass in relation to hydrographical measurements, vertical profiles of Chlorophyll a will be provided by water samples. The water samples were filtered and prepared for laboratory analysis in the Institute of Polar Ecology in Kiel. Quantitative analysis of phytoplankton populations will be carried out using the Utermöhl method. Additional phytoplankton samples for qualitative species composition were taken by means of a hand net (mesh size 20 µm).

Zooplankton

The species composition and biomass of zooplankton will be determined from Bongo net and hand net samples which were taken at 13 stations. Striking was the presence of large hyperiid amphipods east of Taimyr Peninsula, which seemed to have been caught near the ice-water interface of a new-ice floe. At 4 stations, phyto- and zooplankton nets were lowered through an ice hole. Following analysis, the qualitative and quantitative zooplankton composition will be compared with results from sub-ice net samples.

Benthos - Macrobenthic biocenoses

Qualitative benthos samples were taken at 15 stations applying the standard procedure of Golikov and Scarlato (1965). Macrobenthos was collected by means of a Van Veen grab (0.1 m²), meiobenthos with small vials (area 78.5 cm², height 3.5 cm). Thus, 38 macrobenthos and 28 meiobenthos samples were obtained. Meiobenthos samples were fixed for further laboratory processing. Macrobenthos samples were already analyzed aboard the vessel. Each organism was identified, if possible to species level, counted and weighed. Mean abundance and biomass were determined for each taxon at each station. Taxa dominating the bottom fauna by weight were used to characterize distinct biocenoses. The collected material will be further investigated in the laboratories of the ZIN RAS in St. Petersburg.

In the regions investigated during the TRANSDRIFT expeditions in the Laptev Sea, six widely distributed biocenoses were distinguished. Three (*Portlandia siliqua*, *Aglaophamus malmgreni*, *Tridonta borealis* + *Nicania montagui*) mark regions influenced by river water. The biocenosis characterized by *Tridonta borealis* indicates the marine zone. The other two biocenoses (*Myriotrochus rinkii*, *Leionucula bellotii*) are typical of the transitional region.

A decrease in abundance and biomass was found for most bottom biocenoses (*Portlandia siliqua*, *Aglaophamus malmgreni* + *Portlandia siliqua*, *Leionucula bellotii*; *Myriotrochus rinkii*) if we compare our fall data from 1995 to results from nearby stations sampled during the TRANSDRIFT expeditions in the summers of 1993 and 1994 (Fig. 47,48). This finding corresponds to the results reported by Gukov (1994) from the Tiksi region. The ratios of summer [Ns] to autumn [Na] densities ranged from 0.6 to 7.0 (for 50% of the stations from 1.2 - 2.7), the analogous biomass ratios [Bs/Ba] from 1.2 to 2.8 (Fig. 47, 48). But in the biocenosis characterized by *Tridonta borealis* + *Nicania montagui* these results were often contrary (Ns/Na: 0.8 - 3.3; Bs/Ba: 0.3 - 2.7).

The relationship between the macrobenthic biomass and the near-bottom water salinity and density found during summer (Petrjashev, 1994) was modified in autumn: Then, the biomass of most biocenoses decreased while the near-bottom water salinity and density increased. Furthermore, the minimum macrobenthic biomass was observed at a near-bottom water salinity of 30.4 and a density of 1.0245 whereas in summer this minimum was found at a salinity of 30.0 and a density of 1.0240.

Benthos - Megabenthic communities

A small dredge could be used to sample the epibenthic bottom fauna on some ice-free stations (KD9502, KD9523, KD9568). Generally, all samples were scarce but yielded typical faunal elements of the Laptev Sea. The most common species was *Saduria entomon* var. *sibirica*. At deeper locations with a clear affiliation to waters with higher salinities (> 25), brittle stars (*Ophiura sarsi*) could also be found as a second important faunal group in sizable numbers.

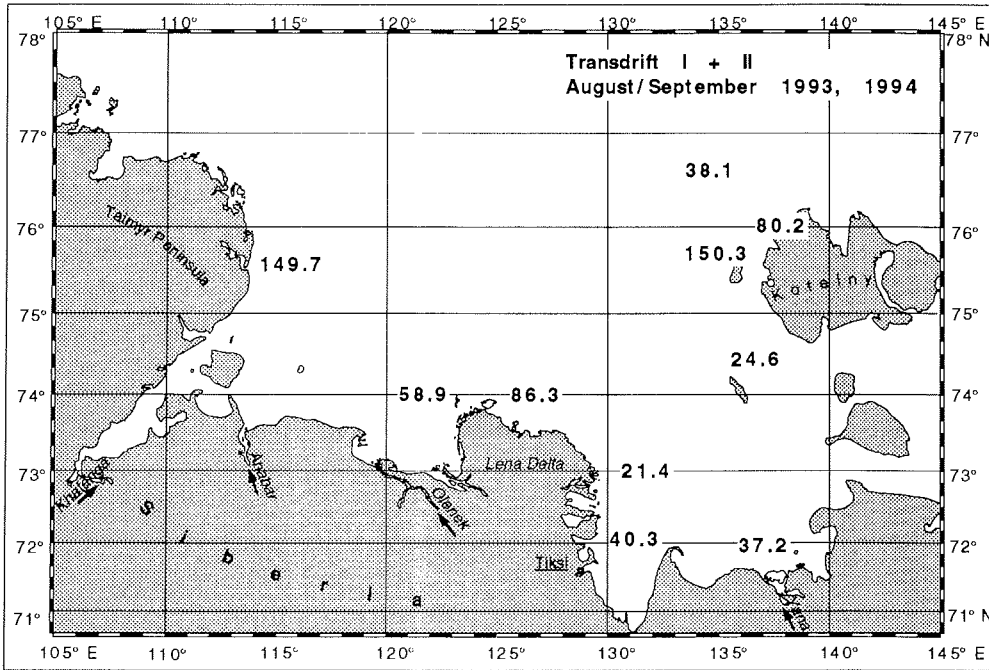


Fig. 47: Laptev Sea: Distribution of macrobenthic biomass (g wet weight m⁻²) in August-September 1993-1994.

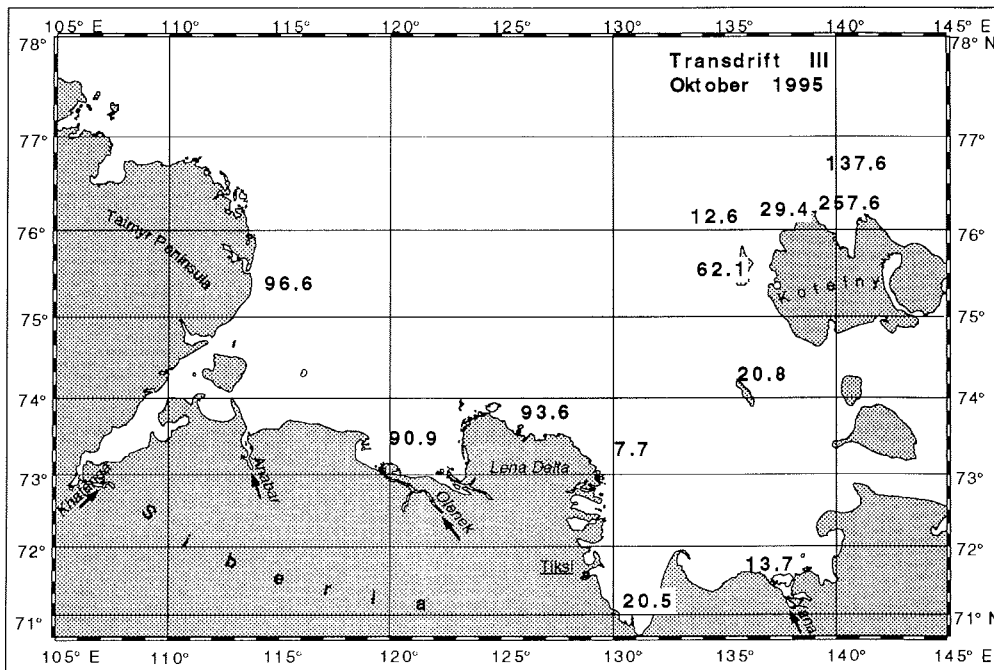


Fig. 48: Laptev Sea: Distribution of macrobenthic biomass (g wet weight m⁻²) in October 1995.

Seabed imaging by means of a underwater photo probe (UWP) at nine stations and a remotely operated vehicle (ROV) at four stations provided in situ views of undisturbed epibenthic habitats. The two imaging methods differed in seabed area covered and image resolution (UWP: photographs; ROV: video tapes). The seabed images will be analyzed in the home laboratory for absolute abundances of epibenthic species and their small scale dispersion patterns. In addition, tracks of iceberg scouring and anchor ice formation should be investigated. By combining the information on epibenthic abundance and mean respiration rates (see below), the population oxygen uptake of selected species will be estimated.

The UWP consists of a vertically oriented camera and an obliquely strobe. It was vertically lowered from the drifting ship and was triggered at a fixed distance from the seabed. Due to the generally high turbidity of the bottom water in the Laptev Sea (see also M. Antonow et al., this issue), this distance had to be chosen lower than in other Arctic regions (0.7 instead of 1.4 m). Thus, at each station sequences of 20 to 30 images, each picturing 0.25 m² of the seabed, were obtained along transects of approximately 300 m length. The color slides taken by the UWP will be developed and analyzed after the cruise in Kiel.

Due to the ice conditions and the generally strong currents, the ROV could provide video images from only four stations. Stations KD9523, KD9533 and KD9541 showed only few macrobenthic organisms, no fish, brittle stars or crustaceans could be seen. Only few *Saduria entomon* could be tracked on several hundred meter of seabed. Fine sediments predominated alternating with small consolidate and or frozen patches (Kassens and Karpiy, 1994). The scarcity of epibenthic life could be confirmed by the grab and box corer samples on these stations. A totally different situation has been found on station KD9548 in the Yana valley where a dense population of brittle stars (*Ophiura sarsi*) dominated the epibenthic community. A preliminary assessment gives numbers in the order of one hundred animals per m². Quite frequently *Saduria entomon* could be seen, too. A typical behaviour of these soft bottom scavengers seems to be digging in the mud with their heads, probably searching for food. Three behavioural patterns could be differentiated for the brittle stars. Although belonging to one species, some *Ophiura* were buried in the ground with only the armtips protruding into the overlying water. Those specimen are probably acting as filter feeders. Others were moving around searching the sediment surface, and the third group was elevating their disc from the sediment by "standing" on the armtips, egesting larger food particles (pers. comm. K.v. Juterzenka). Furthermore, the soft coral *Eunephtya*, usually living on hard bottom, was also observed.

Conclusion: The ROV is a good tool to provide a real view of the seafloor, its macro-epibenthic organisms and the sediment texture they are living on. The observation of behavioural mechanism of key groups, such as isopods or ophiuroids gives additional information of their role in the ecosystem.

Ecophysiological investigations

The second focus of the benthic programme was on autecological studies of selected key species. From dredge catches and box core samples (KD9548, KD9568) live specimens in good condition (Isopoda: *Saduria*; Ophiuroidea: *Ophiura sarsi*, *Ophiocten sericeum*) were collected and kept in aquaria for respiration measurements (both aboard and later in home laboratory) and analyses of population structures. The investigated species represented different life styles and feeding guilds. Growth and production will be interpreted in combination with the measurements of metabolic performances and will give information of the energetics of polar organisms.

The isopod *Saduria entomon* has been identified to play an important role in the ecosystem of the Laptev Sea. Therefore, the respiration measurements performed aboard focussed on this species. Animals of different size classes and weights were measured with an intermittent-flow respirometer. This method is a good means for long-term studies (several hours or days) of the oxygen uptake of an animal without creating oxygen deficiencies during the experimental phase. Additionally, the activity of the animals during the measurement has been monitored by video imaging.

The metabolic rate of an organism is a well known parameter to monitor the condition and ability of an animal under varying environmental conditions. In the investigation area this means strong currents with seasonally high sediment loads, high fluvial input and ice.

Figure 49 shows a typical plot of a respiration experiment. The concentration of oxygen in the seawater and the oxygen consumption of one animal is plotted against the time. The design of the experiment is such that the variation of the oxygen in the chamber can only vary by 5% (95%-90%). After such a period oxygenated seawater is flushed into the chamber and a new measurement interval starts. Thus, the animal is always under in situ oxygen conditions. The plot shows six intervals with an overall duration of the experiment of more than 20 hours. The variation of the oxygen consumption during the measurement can have various causes. The most important factor is the activity of the animal during the experiment. Therefore, this parameter is monitored separately and will be accounted for in later calculations of the weight and activity corrected oxygen consumption.

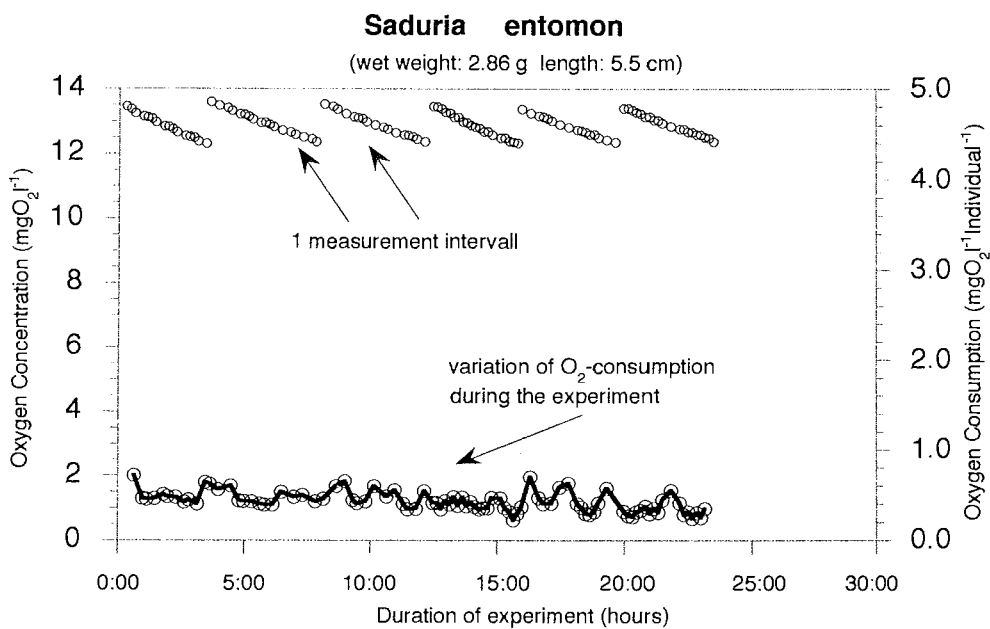


Fig. 49: *Saduria entomon* var. *sibirica*: Respiration rates during 20 h experiment.

Multiprobe Suspension and Current Speed Measurements: Aspects of Sediment Dynamics during Freeze-up Studies in the Laptev Sea

M. Antonow, B. Fürst, V. Haase**, C. Strobl*, R. Thiede

Technische Bergakademie Freiberg, Germany

* Heidelberger Akademie der Wissenschaft, Germany

** GEOMAR Research Center for Marine Geosciences, Kiel, Germany

During the Arctic summer the Laptev Sea is highly influenced by big river systems draining large parts of Siberia. High amounts of suspended matter are carried into the Laptev Sea. Part of the sediment remains where it settles or is resuspended by bottom currents. Later the intensity of the river run-off rapidly decreases. During freeze-up ice forms and the circulation pattern of shelf water masses seem to be rather variable in comparison to the ice-free summer situation. Due to this ice formation, sediment particles from the shallow shelf areas are incorporated into the sea ice and further transported and distributed via the Transpolar Drift into the Arctic Ocean. Investigations of sediment and current dynamics of the Laptev Sea shelf will provide basic parameters for nearly all research groups joining the expedition TRANSDRIFT III.

The main scientific goals are:

- characterization of the present current regime,
- estimation of the near-bottom sediment transport during freeze-up,
- evaluation of sediment-dynamic shelf processes.

The application and combination of a set of sedimentological and oceanographic methods was carried out to answer questions regarding small-scale surficial circulation patterns and bottom current regimes as well as suspended matter content in the water column under Arctic autumn and winter conditions.

Working Program

For the interpretation of sediment dynamics it was necessary to record the hydrographic parameters during freeze-up. Important background features like temperature and salinity have been determined by means of a CTD probe (together with AARI). Simultaneously, measurements of the amount of suspended matter was carried out using an "optical backscatter" nephelometer (OBS). This was complemented by measurements of current velocities, directions, and turbulence in the still ice-free and/ or ice-covered water column.

A specialized probe was designed in order to measure the properties of the water column. This probe (MUM = "Modulares Umweltmeßsystem" built by ADM Elektronik GmbH, Warnau, Germany) combines up to 11 individual sensor units in one housing. Energy is supplied by 9 LR20 1.5V batteries in a water- and pressure-resistant housing together with the electronic CPU (central processing unit). The CPU carries 3 memory chips: one 64 kb program EPROM, one 8 kb RAM for individual batch commands and one 248 kb RAM as a static data store for up to 124,000 data. The CPU allows individual programming of measuring intervals and an additional variety of sub- and burst cycles within one measuring interval. The MUM is armed with a V4A steel cage to shield it from damage.

The following sensors are fixed to the CPU housing: a piezoresistive pressure-gauge, a Pt 100 temperature sensor, a 7 pin conductivity cell, an AANDERAA INSTRUMENTS compass, and a piezoelectrical ultrasonic oscillator device for measurements of the current velocity in X, Y and Z directions. The following individual sensors can be placed wherever it is necessary (i.e. on the CPU housing,

the cage or even the cable depending on the length of the data cable): one calorimetric thermistor for current velocity measurements, and three optical backscatter systems to measure the amount of suspended matter in the water column. These latter four devices are connected with the CPU via data cables and plugs. After each deployment data are recovered via a laptop. The data are given in ASCII format (integer values between 0 and 60,000) and need to be parsed, calibrated and statistically treated before any further interpretation.

The geologic samples gained (in accordance with the activities of GEOMAR, see appendix) will provide detailed sedimentologic parameters including settling velocity analyses, fine fraction granulometry (especially of the silt size fraction which is most sensitive to current energy fluctuations), and X-ray diffraction analyses of the clay and silt fractions by home-lab investigations.

The main investigation was devoted to areas off the Lena Delta as well as to the submarine valleys of Yana, Lena, Olenek and Khatanga. A total of 62 stations were measured. Continuous measurements were performed along 7 transects throughout the inner shelf of the Laptev Sea (Fig. 50). Most of the measurements were hooked on oceanographic transects taken by the Russian scientific party allowing combination of the data to yield a thorough insight into the Laptev Sea system by means of oceanographic and in situ sedimentological studies.

Preliminary Results

All data obtained require some additional treatment (absolute values may vary after calibration). Figure 51 shows seven stations belonging to Transect III across the Yana valley as an example. The water column is composed of two water masses clearly separated by a thermocline at 5-12 m above sea floor. Salinity and temperature changes with water depth appear to be in good accordance thus producing a stable water-mass stratification. Since at various locations the water temperature beneath the pycnocline tends to slightly exceed surface water temperatures, an instable stratification of the water column could never be excluded.

It can be inferred that the uppermost water layer is cooled by ice formation within the freshwater of the Yana and (probably) Lena Rivers whereas the lowermost layer represents normal brackish-marine conditions which are comparable to other epicontinental seas. Decreasing surface temperatures and salinities combined with an increasing thickness of the transitional layer (see temperature values between 10 and 20 m water depth at our example) can therefore be explained as a consequence of the cooling of the surface water which then sinks into the transitional layer until it reaches a stable level with regard to temperature and salinity. The bottom water mass mostly appeared to be clearly separated by higher salinities and lower temperatures.

The absolute amount of suspended matter cannot yet be given since a set of calibration measurements is required to transform OBS (optical backscatter system) raw data into quantitative suspension data. However, data given in Figure 51 provide an image of the relative distribution of suspended particles within the water column. As shown in the example, the amount of suspended matter in the upper half of the water column is very low. Backscatter values then increase until the bottom of the transitional layer is reached. At the beginning of this pycnocline backscatter values rise, indicating an increased suspension load within the lowermost water layer. This is a common feature for nearly all investigated stations. Vertical profile optical backscatter data yield uni- to trimodal distributions of suspended matter. A very small maximum could often be measured from 0 to 3 m water depth; another maximum was mostly below 10 m. Highest amounts of

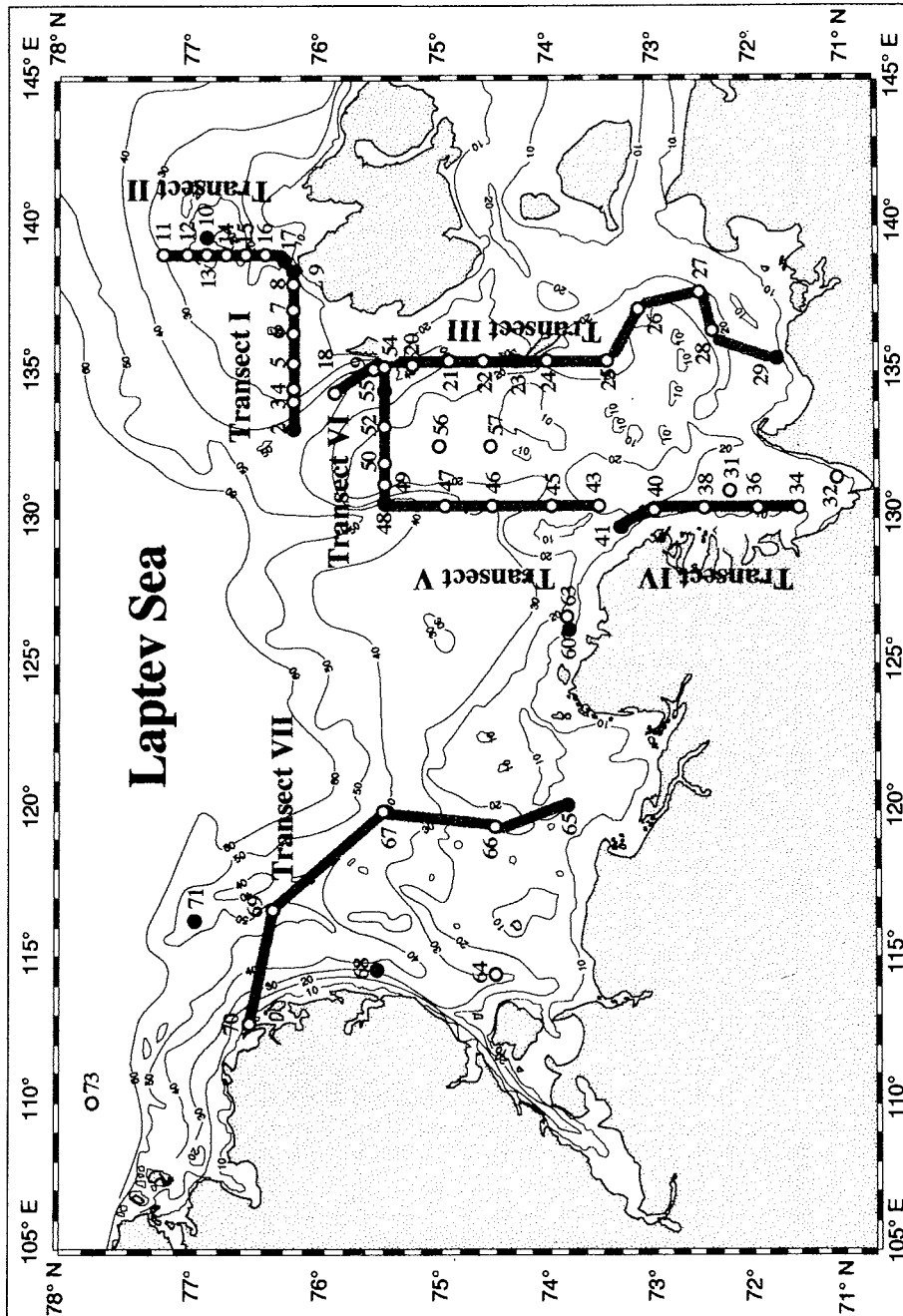


Fig. 50: Multiprobe suspension and current speed measurements carried out during the TRANSDRIFT III expedition.

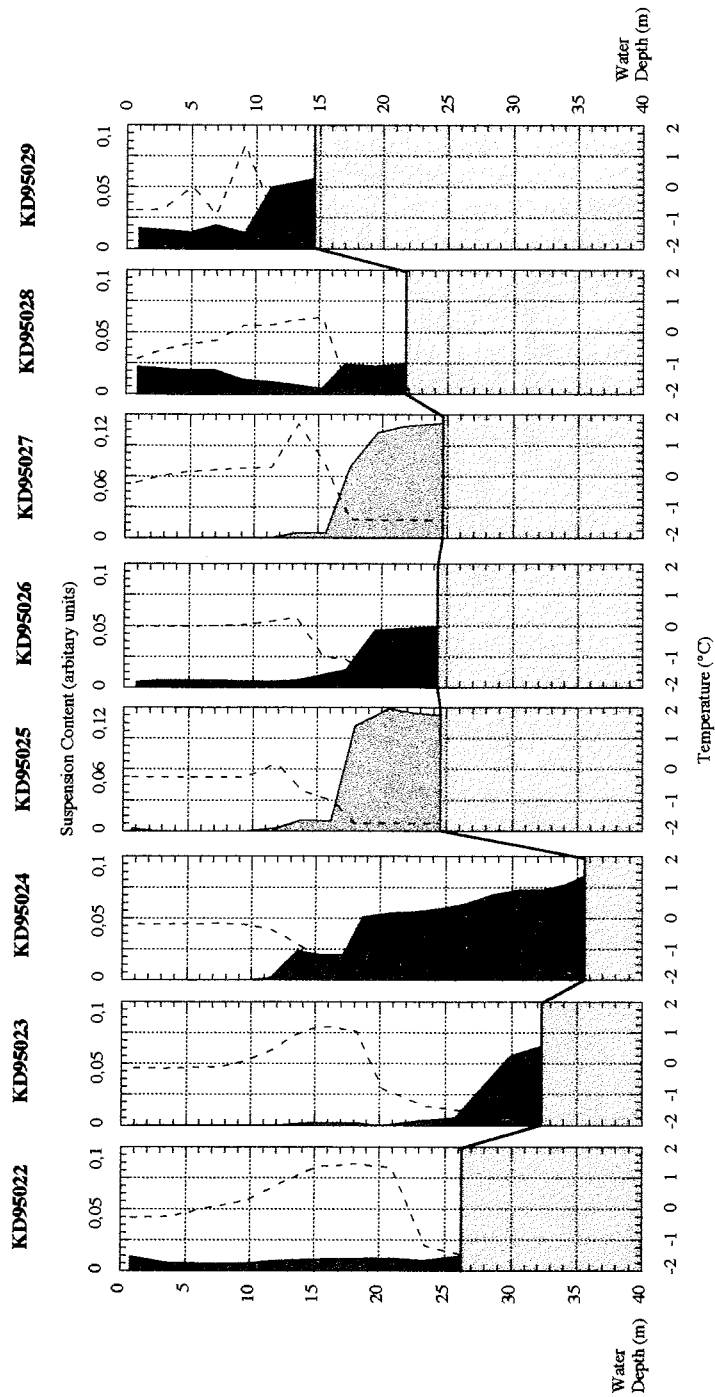


Fig 51: Suspension and temperature data of the southern part of transect III along the Yana Valley.

suspended matter are suggested by a strong increase beginning at 5 to 1 m over the seafloor. The upper 2 OBS maxima are thought to be at least partly of biogenic origin (phytoplankton) whereas the deep maximum is likely to reflect benthic boundary layer conditions (see also A. Anoshkin, this volume). Total amounts of suspended matter do not change significantly between the eastern and western Laptev Sea. However, there are some differences between single locations which need further interpretation.

Current velocities also show increased values. Whether increasing current speed is responsible for the increase of the suspension load cannot yet be substantiated. It is also possible that the suspension load supplied by riverine waters precipitates after slight mixing with higher salinity waters. Higher amounts of suspended matter in the lowermost water layer (up to the pycnocline) may be caused by a mixture of turbulent resuspension of particles in the near-bottom zone (which cannot surmount the lower pycnocline) and particles incoming from surficial and transitional water layers. The current direction at some stations extremely varies with depth, but in most cases directions do not change significantly throughout the water column. For interpretation of the in situ current speed and direction data the meteorological data set has to be involved.

Current velocities appear to be slightly higher in the eastern Laptev Sea. Irregular changes in current velocity and current direction throughout the water column were observed at various stations.

The Laptev Sea is a sensitive estuarine system composed of surficial freshwater originating from large streams such as the Lena River and bottom waters of various origin (e.g. the Arctic Ocean). As far as the data obtained during the TRANSDRIFT III expedition could be evaluated, the following preliminary conclusions can be drawn for the period of the expedition.

Preliminary data of the multisensor MUM probe show features which provide together with other investigations a thorough insight into the Laptev Sea system. Further processing of the MUM data will enable us to describe and interpret in situ sedimentary processes (e.g. sediment transport in different water layers) and their relation to water mass properties and oceanographic features of the Laptev Sea.

The Depositional Environment of the Laptev Sea

D. Nürnberg**, H. Kassens, V. Haase, M. Kunz-Pirrung, V.A. Kosheleva*, E.E. Musatov*, B. Peregovich, M. Siebold**, R. Thiede***, J. Thiede

GEOMAR Research Center for Marine Geosciences, Kiel, Germany

* VNIIOkeangeologia, St. Petersburg, Russia

** Alfred-Wegener-Institut für Polar- und Meeresforschung, Bremerhaven, Germany

*** Technische Bergakademie Freiberg, Germany

Modern investigations in the Arctic Ocean emphasize the importance of the broad Siberian shelves for shelf-to-basin sediment transport processes, in particular for the formation of "dirty" sea ice. The Laptev Sea, which belongs to the world's largest and shallowest shelf areas, acts as an important source area for fine-grained sediments transported to the deep Arctic Ocean (e.g. Wollenburg, 1993; Nürnberg et al., 1994; Kassens, 1995). The Laptev Sea is north of East Siberia between the Taimyr Peninsula and the Novosibirskie Islands (Fig. 1). A major controlling factor of the modern depositional environment of the Laptev Sea is river run-off of the large Siberian river systems, such as the Yana, Lena, Olenek,

Anabar and Khatanga Rivers (Fig. 3) (e.g. Rossak, 1995). However, little is known in detail about the environmental history of the Laptev Sea because the shallow permafrost level made recovery of long sediment cores difficult during the TRANSDRIFT I and II expeditions (e.g. Dehn and Kassens, 1995). The specific task of TRANSDRIFT III was to differentiate the sediments and variability of the rivers feeding the Laptev Sea and thus to recover long sediment cores.

Working Program

The sedimentological working program was conducted at 11 stations in the eastern Laptev Sea (Fig. 52, Tab. A2, A6). Near-surface sediments were recovered with a Van Veen grab and a spade box core (penetration weight 700 kg, 50*50*60 cm). Long sediment cores were recovered with a vibro corer (rectangular cross-section of 10*10 cm, core barrel length max. 5m) at 3 stations in the ice-free area of the Lena Valley. This was possible only during the first part of the expedition. Later, after several unsuccessful attempts, heavy ice conditions and strong currents below the new ice made deployment of the vibro corer (Dehn and Kassens, 1995) impossible.

The sediment cores obtained were routinely photographed, described in detail and graphically displayed (Tab. A8). Sediment colors were classified by a Minolta CM 2002 scanner, thus eliminating bias due to conditions or lighting.

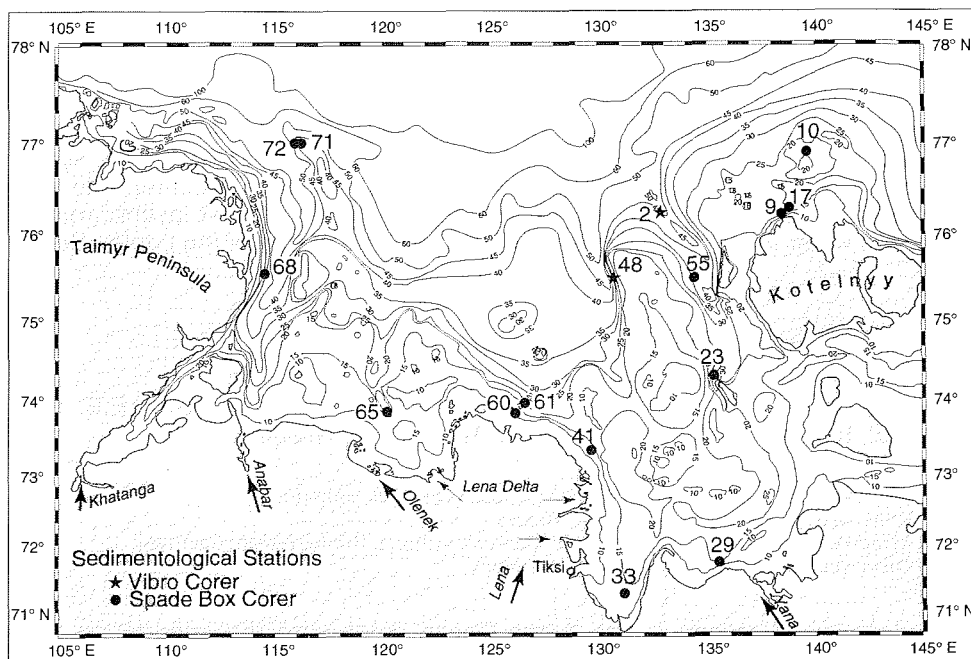


Fig. 52: Map showing the sedimentological stations of the TRANSDRIFT III expedition.

Smear slide investigations

The investigation of smear slides provides a first evaluation of the grain size distribution and the composition of the sediments. In the course of the cruise, smear

slides of about 90 samples were prepared and investigated with a polarizable microscope. In order to minimize considerable personal bias when estimating grain sizes and sediment composition, the smear slide analysis was consistently carried out by one scientist. The results (Tab. 4) were cross-checked and up-dated with data derived from the coarse fraction analysis (percentage of the coarse fraction, > 63 μm , in relation to the fine fraction, < 63 μm).

Grain sizes were differentiated into sand (> 63 μm), silt (2 μm to 63 μm) and clay (< 63 μm) according to the classification scheme of Shepard (1954). The first lithological description was corrected accordingly. Sediment components were classified into biogenic and terrigenous (detrital) components. Biogenic particles were differentiated into benthic foraminifers, diatoms and diatom fragments, silicoflagellates and radiolarians, sponge spicules, plant fragments including spores and pollen, and unknown biogenic components. Terrigenous particles comprise quartz (angular and rounded), feldspar, mica (biotite, muscovite, and chlorite), opaque minerals (heavy minerals), clay minerals, and unidentified particles. Heavy minerals could further be distinguished into the most prominent specimens amphibole, pyroxene, epidote, granate, and titanite. Due to their minor occurrence and the time-consuming mineralogical identification, we only differentiated between rare and abundant occurrences (marked by crosses in Tab. 4).

Coarse fraction analysis

For all surface sediments and for selected cores, a coarse fraction analysis was carried out. The bulk sediment was weighed before and after drying at ca. 105°C to derive an estimation of the water content. The coarse fraction was extracted by sieving through a 63 μm sieve, and subsequently investigated by microscopic techniques. The quantification of single sediment components was consistently done by one scientist, in order to minimize considerable personal bias (Tab. 5). The results were compared and cross-checked with the smear slide investigations. Similar to the smear slide investigations, biogenic and terrigenous components were differentiated. Both the coarse fraction analysis and the smear slide investigations lead to comparable results.

Results of the Sedimentological Study

Surface and surface-near sediments

All sediment surfaces consist of olive-gray - and sometimes dark brownish - mud, the dominant size fraction of which is silt. Only at a few sites, sandy lithology appears. Terrigenous grains (mainly quartz, feldspar, opaque minerals and clay minerals) predominate. Quartz is mostly transparent and angular-shaped. Only at a few sites within the Olenek and the Yana Valleys, as well as near the Lena Delta, rounded quartz appears in higher amounts. Accessory minerals include opaque minerals, epidote, amphiboles, granate, cirkon, and mica. Authigenic minerals comprise glaukonite, pyrite, markasite, and iron hydroxides. A few dropstones were found in the direct vicinity of the Taimyr Peninsula in the western Laptev Sea - not only on the sediment surface, but also down to 25 cm core depth. Further east, ice-rafted detritus is lacking.

Biogenic components are of minor importance, though diatoms, benthic foraminifers, bivalve fragments and plant remains are always present (Fig. 53). The density of the benthic populations changes considerably from site to site. Most abundant are ophiuredeans and polychaets. Bivalves are always common. Sponges were not observed, though a few sponge spicules were found in the

smear slides. In general, the sediment surfaces are often disturbed by animal traces underlying the importance of benthic life in this environment.

Tab. 4: Results of the smear slide analysis.

SMEAR SLIDE DATA										BIOGENIC COMPONENTS (%)										TERRIGENEOUS COMPONENTS (%)																													
TRANSDRIFT III										KAPITAN DRANITSYN										QUARTZ										OPAQUE MINERALS										CLAY									
SITE	DEPTH (cm)	LATITUDE (N)	LONGITUDE (E)	WATER DEPTH	LITHOLOGY	SAND	SILT	CLAY	BENTH.FORAM.	SPONGE SPC.	DIATOMS	RADIOL.SILICOFL.	BLACK SPHERES	PLANT REMAINS	ANGULAR	ROUNDED	FELDSPAR	MICA	IN GENERAL	AMPHIBOLE	PYROXENE	TITANITE	CLAY MINERALS	TOTAL (%)																									
KD95 48-17 VC	105	75°27,857	130°41,004	43	Silt	5	80	15			2		3	3	55		5	2	10	xxxx			20	100																									
KD95 48-17 VC	110	75°27,857	130°41,004	43	Sandy silt	30	60	10			1		5	5	55		9	10	xxxx				15	100																									
KD95 48-17 VC	115	75°27,857	130°41,004	43	Silt	5	90	5			2		8	6	60		3	2	10	xxxx			10	100																									
KD95 48-17 VC	120	75°27,857	130°41,004	43	(Clayey) silt	5	75	20					5	5	55		4	1	10	XX	x	x	15	95																									
KD95 48-17 VC	130	75°27,857	130°41,004	43	Silt	5	80	15			1		10	4	60		3	2	5				15	100																									
KD95 48-17 VC	140	75°27,857	130°41,004	43	Silt	5	80	15			2		10	7	60		2	1	8	XX	x		10	100																									
KD95 48-17 VC	150	75°27,857	130°41,004	43	Silt	5	80	15			1		8	4	60		5	2	10				10	100																									
KD95 48-17 VC	160	75°27,857	130°41,004	43	Silt	5	80	15					5	5	60		8	2	10		XX		10	100																									
KD95 48-17 VC	170	75°27,857	130°41,004	43	Silt	5	80	15			1			3	60		4	2	15				15	100																									
KD95 48-17 VC	180	75°27,857	130°41,004	43	Silt	2	80	18						5	60		10	10			XX		15	100																									
KD95 48-17 VC	190	75°27,857	130°41,004	43	Silt	5	80	15						3	60		4	3	15				15	100																									
KD95 48-17 VC	200	75°27,857	130°41,004	43	Silt	5	80	15						3	60		10	2	10				15	100																									
KD95 48-17 VC	205	75°27,857	130°41,004	43	(Clayey) silt	5	75	20						3	50		7	5	20	xxx			15	100																									
KD95 48-17 VC	210	75°27,857	130°41,004	43	Silt	5	80	15						3	60		4	3	15				15	100																									
KD95 48-17 VC	215	75°27,857	130°41,004	43	Silt	8	90	2						2	60		8	5	10				15	100																									
KD95 48-17 VC	220	75°27,857	130°41,004	43	Silt	2	80	18						6	60		10	5	10		X		15	100																									
KD95 55-10 GKG	0	75°36,060	134°31,341	36	Sandy silt	30	60	10	1	1	1			2	60		10	5	10	xx			10	100																									
KD95 55-10 GKG	5	75°36,060	134°31,341	36	Sandy silt	20	70	10			2			3	60	x	10	5	10	xx			10	100																									
KD95 55-10 GKG	20	75°36,060	134°31,341	36	Sandy silt	20	70	10						6	60		8	7	10				15	100																									
KD95 55-10 GKG	36	75°36,060	134°31,341	36	Sandy silt	20	70	10						6	60		8	7	10				15	100																									
KD95 61-3 GKG	0	73°54,180	126°54,868	23	Clayey silt	5	70	25			2			5	60		3	2	8	xxx			10	90																									
KD95 61-3 GKG	50	73°54,180	126°54,868	23	Clayey silt	5	60	35			2			5	60		3	2	8				10	90																									
KD95 61-4 GKG	0	73°54,374	126°56,172	23	Clayey silt	15	70	15			2			5	60		3	2	8				10	90																									
KD95 65-8 BG	0	73°50,84	120°18,07	26	Silty sand	60	30	10						2	70	xxxx	8	5	5		xxx		10	100																									
KD95 65-11 GKG	0	73°50,76	120°19,00	21	Sandy silt	45	50	5			8	2		5	60	xxxx	10	5			xxx		10	100																									
KD95 65-12 GKG	0	73°50,954	120°20,852	21	Silty sand	50	45	5			1			1	60	xxxx	10	8	15		xxxx		5	100																									
KD95 65-12 GKG	32	73°50,954	120°20,852	21	Silty sand	60	30	10						2	65	xxx	8	5	15		xxxx		5	100																									
KD95 68-7 GKG	0	75°29,100	114°28,902	34	Sandy silt	35	60	5			7			3	70		3	2	5	X	XX	X	10	100																									
KD95 68-7 GKG	20	75°29,100	114°28,902	34	(Sandy) clayey silt	20	60	20			5			5	60		3	2	5		XX		20	100																									
KD95 68-7 GKG	40	75°29,100	114°28,902	34	(Sandy) clayey silt	20	60	20			5			5	60		3	2	5		XX	X	20	100																									
KD95 68-8 GKG	0	75°29,040	114°29,754	34	Sandy silt	40	55	5			1	10		5	70		4	5	5	X	XX	X	5	100																									
KD95 72-1 GKG	0	77°01,457	116°03,150	50.5	Sandy silt	30	60	10			1	6		3	55	10	5	5	5		XX	X	10	100																									
KD95 72-1 GKG	10	77°01,457	116°03,150	50.5	Sandy silt	20	65	15			5			5	55	10	3	2	5		X	X	15	100																									
KD95 72-1 GKG	20	77°01,457	116°03,150	50.5	Clayey silt	15	65	20			3			2	55	15	2	3	5		X	X	15	100																									
KD95 72-1 GKG	30	77°01,457	116°03,150	50.5	Clayey silt	15	65	20			3			2	55	15	2	3	5		X		15	100																									
KD95 72-1 GKG	40	77°01,457	116°03,150	50.5	Clayey silt	15	65	10			2			3	55	15	2	3	5				15	100																									

Tab. 5: Results of the coarse fraction analysis.

Sample	Water content (%)	Bulk sediment (%)	Fraction >63µm (%)	Fraction <63µm (%)	TERRIGENEOUS COMPONENTS (%)								BIOGENIC COMPONENTS (%)				AUTH. COMP.
					Quartz								Beath. foraminifers	Ostracodes	shell fragments	Plant remains	Oxide (%)
					Total	Rounded	Angular	Feldspar	Mica	Rock fragments	Opaque minerals						
1 KD95 02-14 VC 11-12cm	36.5	63.5	7.2	92.8	91	25	66	1	2	2	2				*	2	
2 KD95 02-14 VC 31-32cm	35.4	64.6	0.8	99.2	75	25	50	3	3	2	3	3	1	5	1	4	
3 KD95 02-14 VC 51-52cm	36.0	64.0	0.3	99.7	83	30	54	3	2	2	4	2	*		1	3	
4 KD95 02-14 VC 71-72cm	35.1	64.9	9.1	90.9	82	30	52	4	4	2	5				1	2	
5 KD95 02-14 VC 91-92cm	35.6	64.4	1.0	99.0	80	30	50	4	2	1	3	1	1	2	1	5	
6 KD95 02-14 VC 111-112cm	35.9	64.1	0.5	99.5	80	45	35	2	3	1	5	3		2	1	3	
7 KD95 02-14 VC 131-132cm	38.6	61.4	0.6	99.4	73	28	45	2	2	1	3	1	*	15	1	2	
8 KD95 02-14 VC 151-152cm	36.0	64.0	0.7	99.3	87	30	57	2	2	1	2	1		1	1	3	
9 KD95 02-14 VC 171-172cm	37.6	62.4	0.4	99.6	77	30	47	2	2	1	1	5	*	1	1	10	
10 KD95 02-14 VC 191-192cm	40.9	59.1	0.2	99.8	79	25	54	1	1	1	1	7			*	10	
11 KD95 02-14 VC 211-212cm	38.2	61.8	0.6	99.4	73	20	53	2	1	1	1	7	1	3	1	10	
12 KD95 09-6 BG	20.2	79.8	73.1	26.9	69	20	49	4	2	10	7	*	*	5	1	1	
13 KD95 10-3 BG	21.0	79.0	95.3	4.7	92	25	67	4	1	1	2	*			*		
14 KD95 17-3 BG	29.0	71.0	49.3	50.7	85	20	65	4	1	5	3			1	*	1	
15 KD95 19-11 BG	5.8	94.2	16.7	83.3	80	20	60	3	2	1	10		*		1	3	
16 KD95 29-12 GKG Surface	48.8	51.2	9.2	90.8	79	29	50	3	2	1	10	*	*	*	1	2	
17 KD95 33-10 GKG Surface	27.3	72.7	82.3	17.7	54	25	25	3	1	1	30				*	10	
18 KD95 41-12 GKG Surface	51.5	48.5	35.2	64.8	80	35	45	3	1	1	10	1			2	2	
19 KD95 41-15 GKG Surface	47.0	53.0	52.1	47.9	83	40	43	3	2	1	8	*	*	*	*	1	
20 KD95 48-17 VC 19-20cm	42.5	57.5	5.4	94.6	82	20	62	3	1		3	1		2	5	3	
21 KD95 48-17 VC 29-30cm	44.9	55.1	0.4	99.6	84	25	59	3	1		7	*			*	4	
22 KD95 48-17 VC 39-40cm	39.4	60.6	17.1	82.9	66	20	46	3	1	1	1	1			7	20	
23 KD95 48-17 VC 49-50cm	41.1	58.9	7.4	92.6	79	25	54	4	2	1	4	1	*		5		
24 KD95 48-17 VC 59-60cm	39.4	60.6	4.3	95.7	82	30	52	3	1	1	3	*	*		6	4	
25 KD95 48-17 VC 69-70cm	33.3	66.7	4.4	95.6	37	15	22	3	1		3	1		30	20	5	
26 KD95 48-17 VC 79-80cm	30.8	69.2	0.7	99.3	71	20	51	3	1		3	1		1	15	5	
27 KD95 48-17 VC 89-90cm	34.2	65.8	0.7	99.3	50	15	35	2	4	1	2	1		*	35	5	
28 KD95 48-17 VC 99-100cm	31.6	68.4	0.7	99.3	29	10	19	2	4	1	1	1			30	12	
29 KD95 48-17 VC 109-110cm	28.4	71.6	0.5	99.5	24	12	12	2	2	1	1	1	*		65	1	
30 KD95 48-17 VC 119-120cm	34.5	65.5	1.2	98.8	29	10	19	2	5	1	1	1			60	1	
31 KD95 48-17 VC 129-130cm	32.2	67.8	0.8	99.2	48	20	28	1	2	1	1	*	*	3	45		
32 KD95 48-17 VC 139-140cm	31.2	68.8	0.6	99.4	39	10	29	2	1	1	1	1			35	20	
33 KD95 48-17 VC 159-160cm	30.7	69.3	0.6	99.4	33	13	20	2	3	1	1	1		*	45	15	
34 KD95 48-17 VC 169-170cm	32.7	67.3	0.5	99.5	58	25	33	2	1	1	2	1	1	*	15	20	
35 KD95 48-17 VC 179-180cm	33.2	66.8	0.9	99.1	25	10	15	2	3		1	*		4	50	15	
36 KD95 48-17 VC 189-190cm	33.3	66.7	0.7	99.3	56	20	36	2	1		10	1	*	3	2	25	
37 KD95 48-17 VC 199-200cm	33.2	66.8	0.9	99.1	52	20	32	2	2	1	5	1	*	2	25	10	
38 KD95 48-17 VC 209-210cm	32.9	67.1	0.8	99.2	60	25	15	1	1	1	2	*	*		20	14	
39 KD95 61-4 GKG Surface	70.4	29.6	1.4	98.6	85	30	55	2	2	1	3	5	*	*	*	2	

The uppermost dark brown to olive-gray (oxic) lithological unit of the sediment cores ranges from 1-14 cm in thickness. This strongly bioturbated unit resembles the sediment surface in the box cores and apparently reflects the depth of oxygenation. Below, the sediment color is gradually darkening due to Fe and Mn precipitations. When exposed to the atmosphere for a sufficient time, the dark sediment color changes again to olive-greenish colors. Bioturbation by living organisms (bivalves and polychaets) homogenizing the sediment column was observed down to ca. 25 cm core depth. The sediment contains high amounts of organic matter, the main component of which is terrigenous in origin (plant fibres). In general, the sediment becomes very stiff in only a few centimeters core depth. The pore water is apparently reducing, and shear strength increases significantly, obviously causing difficulties when penetrating with our coring devices.

All long sediment cores (to about 2.3 m sediment depth) except core KD9548-17 exhibit monotonous sedimentary sequences with minor changes in grain size and

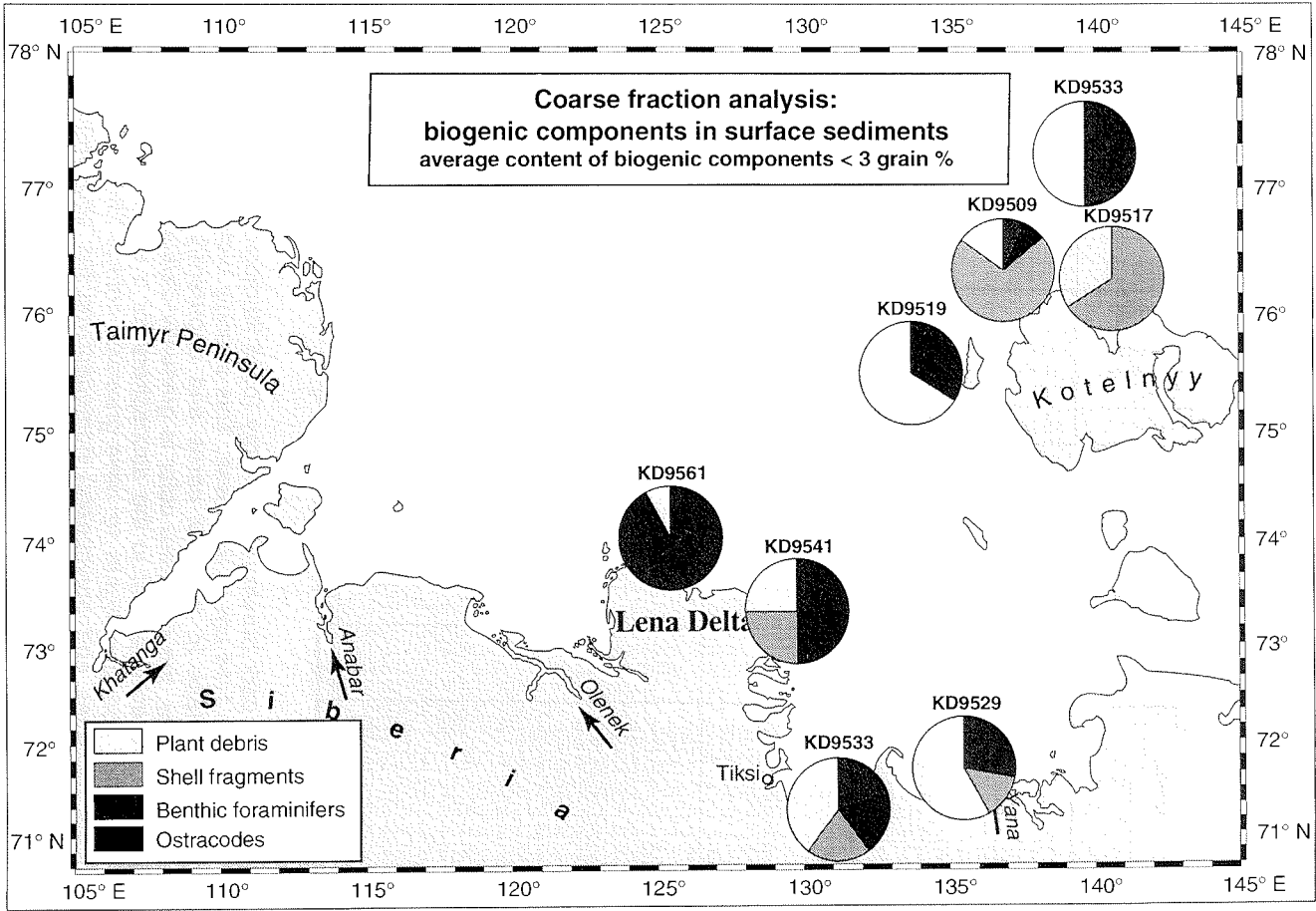


Fig. 53: Distribution of biogenic components in the coarse fraction (> 63 µm) of surface sediments.

sediment composition. Terrigenous components dominate over biogenic particles, though the portion of terrestrial plant fragments is high in selected core sequences. Well-preserved bivalve shells (*Tridonta borealis*, *Macoma calcarea*, *Kiatella arctica*) and fragments are present in all the cores down to about 2 m core depth. Mixing of sediment is extremely strong and prevents any stratification. Core KD9548-17 from the eastern Lena Valley, in this respect, is anomalous.

Sediment core KD9548-17 VC from the eastern Laptev Sea

Figures 54, 55, 56 summarize most important results for core KD9548-17 VC located within the outer eastern Lena Valley 30 miles west of Bel'kovskii Island. The core is 2.2 m in length and comprises - in contrast to all other cores recovered during the expedition - various lithological units, which can clearly be differentiated by color. The uppermost unit of ca. 100 cm consists of olive-gray sandy silt, which darkens gradually downcore due to Fe, Mn-precipitations and gradually becomes stiffer. Only the uppermost 14 cm show oxic, brownish colors. The nearly black sequence is interrupted by an olive-gray sandy layer of about 10 cm (101-110 cm core depth) subsequently followed by ca. 30 cm of silt, also characterized by light, olive-gray colors. Below ca. 142 cm to the end of the core, a very dark clayey silt dominates, which stiffens drastically at the core bottom. The gradual stiffening of the uppermost and the lowermost lithological units is clearly reflected in the shear strength.

Though the sediment dominantly consists of terrigenous material, distinct changes in sediment composition were recognized (Fig. 54). The uppermost sequence has a considerably higher sand content, mainly composed of quartz. The coarse fraction, however, decreases below ca. 70 cm, and silt dominates the lithology. Accordingly, quartz shifts from the sand to the silt fraction (Fig. 55). Rounded quartz is present in considerable amounts. Opaque minerals are present all over the core, but do not show significant variations. Amphibole dominates over pyroxene. A few grains of granate and epidote are present.

Biogenic components are of minor importance, though benthic foraminifers, diatoms (and diatom fragments), pollen and spores occur throughout the entire core (Fig. 56). Abundances of diatoms decrease downcore. Remains of terrigenous plants, instead, play an important role within the coarse fraction. Especially within the middle, olive-gray silt section, plant debris increases to about 60 % in the coarse fraction. This section is also characterized by the occurrence of small (ca. 10 μm in diameter), opaque, black spheres, the origin of which is not clear yet.

Depositional environment

During the previous expeditions to the inner (ESARE '92, TRANSDRIFT I and II) and to the outer Laptev Sea shelf (POLARSTERN cruise ARK IX-4), we already received a well substantiated impression about the Laptev Sea depositional environment and its sediment dynamics (Kassens and Karpiy, 1994; Kassens, 1995; Nürnberg et al., 1995). Nevertheless, the TRANSDRIFT III expedition added valuable material especially from areas, where no samples or no long cores were recovered before in the frame of the joint Russian-German cooperation.

In principle, the Laptev Sea shelf is characterized by a strong supply of terrigenous material from the continent to the Laptev Sea shelf edge, which is then transported downslope into the deep-sea basins. The main sediment components comprise minerals, which originate from nearby sources and/or Siberian hinterland igneous provinces. A first evaluation of the amphibole vs. pyroxene concentration supports the study of Lapina et al. (1965) and Ibanova et al. (in press), who defines

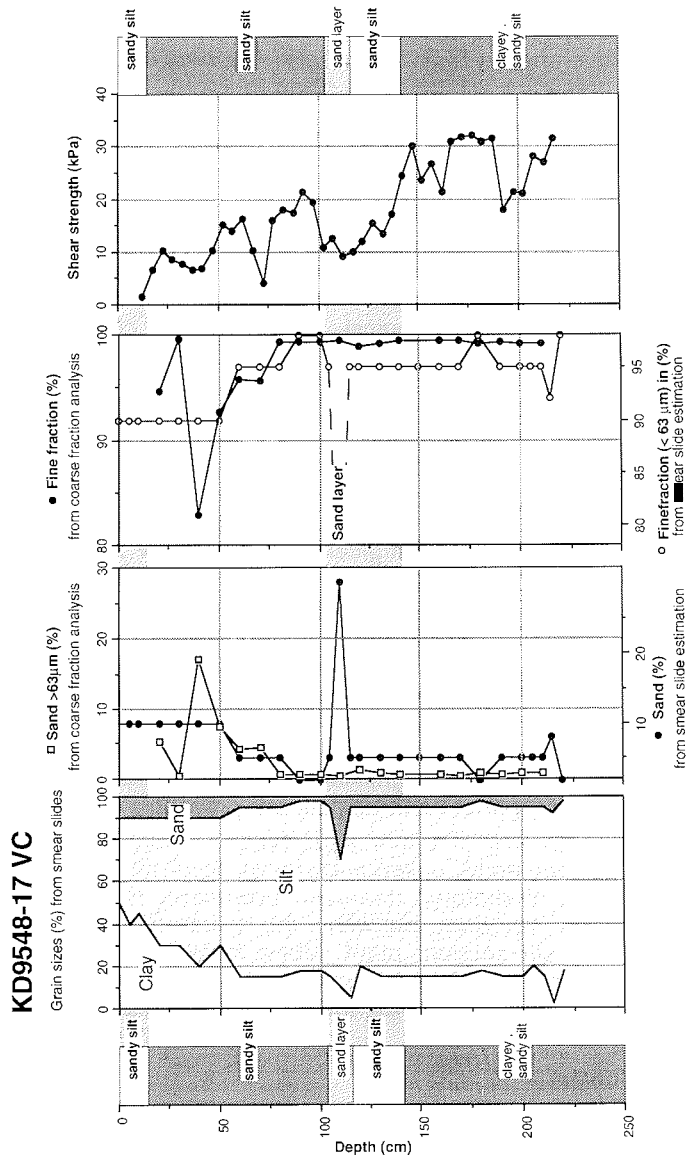


Fig. 54: Downcore variations of grain sizes in core KG9548-17 recovered from the eastern Lena Valley 30 mls west of Bel'kovskii Island. Comparative studies by smear slide and coarse fraction analyses reveal similar trends, though absolute values may differ. The shear strength record reflects the downcore gradual stiffening of the sediments.

a pyroxene-dominated western Laptev Sea and an amphibole-dominated eastern shelf area. Such differentiation into a western and an eastern province is also apparent from clay minerals (Rossak, 1995; Wahsner and Shelekhova, 1994), grain size studies (Lindemann, 1994), and echosoundings (Benthien, 1994). It is, however, not possible from our few sites to support the findings of Lindemann

(1994) that the western shelf area is more sandy than the eastern and southeastern Laptev Sea. Sandy sediments (sandy silts) do occur in the western part near Taimyr Peninsula, but are most likely restricted to the valleys of the Siberian rivers dewatering into the Laptev Sea (station KD9565 in the Olenek Valley, KD9548 in the eastern Lena Valley, KD9502 and KD9555 in the Yana Valley). Due to the enhanced outflow current speeds within the valleys, the fine fraction is apparently winnowed. At the same time, the portion of rounded quartz grains significantly increases (station KD9555 in the Yana Valley, station KD9565 in the Olenek Valley, and station KD9541 near the Lena main outflow). Further sandy sediments with partly rounded quartz grains were recovered near the coast of Kotel'nyi Island and the Siberian mainland.

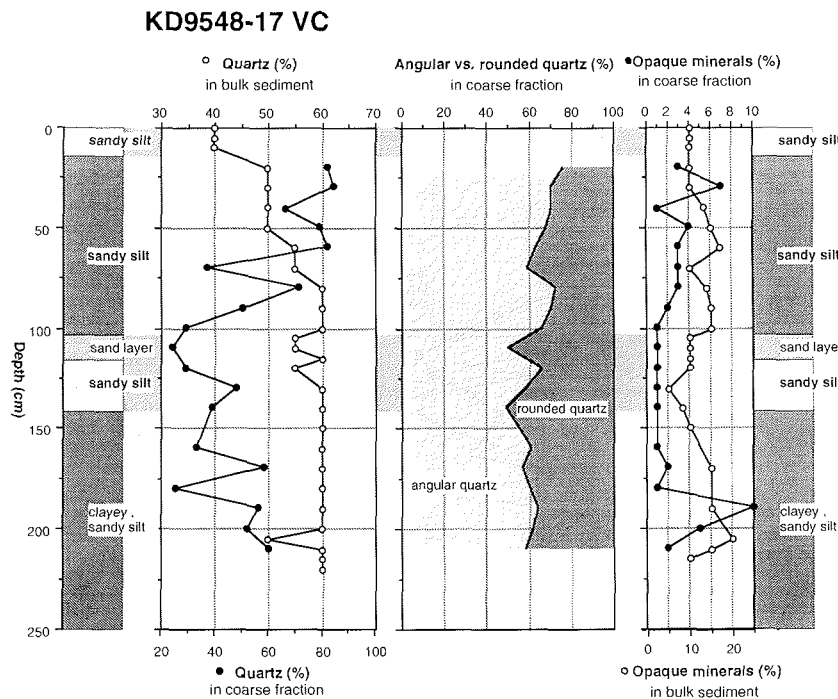


Fig. 55: Downcore distribution of quartz and opaque minerals in core KD9548-17.

The occurrence of dropstones, which is limited to a few sites in the vicinity of Taimyr Peninsula, traces the tracks of icebergs, which originate from Severnaia Zemlia and are transported via the southerly directed Taimyr surface current into the Laptev Sea. Benthien (1994) observed high numbers of ice gouges in the area of the Khatanga and Anabar outflows. In the eastern Laptev Sea, ice-rafted coarse detritus was no longer observed, most probably released during the eastward directed pathways of icebergs. Also, outer shelf and slope sediments only contain minor portions of coarse sand and gravel, suggesting that iceberg transport is a minor process in these areas (Nürnberg et al., 1995).

As could be shown by Stein and Nürnberg (in press), the Laptev Sea shelf and slope sediments contain high amounts of organic matter (max. 2%), the main component of which is terrigenous in origin. Especially for the slope sediments, free hydrogen sulphide formation is typical, pointing to the decay of organic matter by the activity of sulphate-reducing bacteria under reducing conditions. Formation of

hydrogen sulphide gas was not observed in our cores, however, the typical black spots and streaks coloring the subsurface sediments dark gray to black originate from iron and manganese precipitations, which must be attributed to the decay of marine organic matter. Accompanied by the strong anaerobic bacterial activity (in: Fütterer, 1994), this process indicates a rapid burial of high amounts of marine organic matter before a sufficient oxidation from seawater could take place.

Dehn and Kassens (1995) established a preliminary facies zonation for the Laptev Sea shelf sediment cores comprising four facies types. Due to our limited sediment recovery, this facies zonation cannot be transferred completely. However, it seems that our surface-near sediments consisting of dark brown to olive-gray clayey to sandy silts best fit into Facies 1.

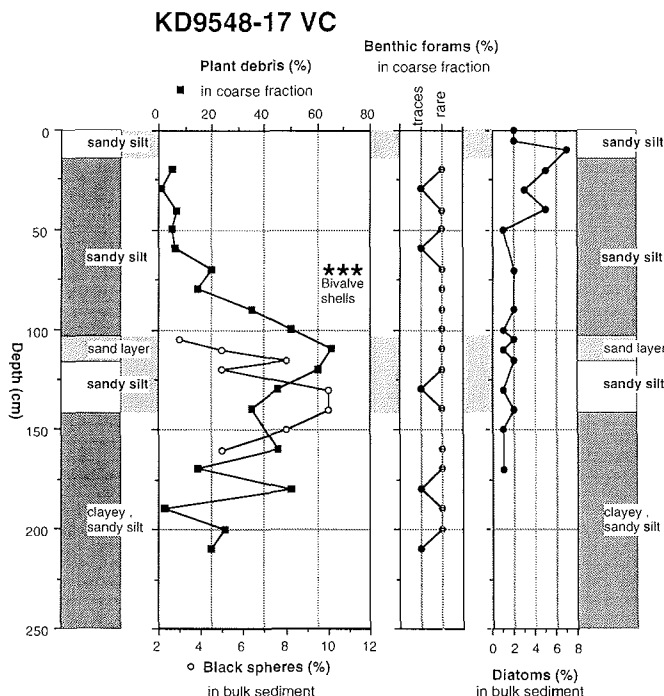


Fig. 56: Downcore variation of biogenic components in core KD9548-17. Note the occurrence of black spheres, the origin or formation of which is still unknown

Facies 4, which consists of dark greenish gray silty deposits characterized by dominant quartz and clay mineral portions, and a depletion in opaque minerals, was found in the western Lena Valley during TRANSDRIFT II, but could not be traced further east. This year's recovery of core KD9548-17 in the eastern Lena Valley just north of the site sampled during TRANSDRIFT II, however, revealed olive-gray silty sediments of mainly quartz and clay composition in between very stiff and black clayey silts (ca. 100 - 140 cm core depth), which we attribute to Facies 4. The portion of opaque minerals seems to be slightly reduced (Fig. 55), whereas the portion of terrestrial plant debris is drastically enhanced. Also, this core section shows high concentrations of opaque, black spheres, which do not occur below and above this section. Up to now, we can only speculate about their origin and/or generation. Volcanic or cosmic origin, authigenic formation, or the generation of eolian ashes during wide-spread forest fires may be possible

explanations. It should, at least, be noted that the temporally restricted occurrence of the black spheres may provide a powerful time-marker for stratigraphical investigations.

The facies zonation previously described by Dehn and Kassens (1995) in addition to the slight lithological changes observed in core KD9548-17 indicate changing environments through time. Since we - up to now - have no reliable high resolution age control on the shelf deposits, a detailed reconstruction of the paleoenvironment still remains open. However, from the only minor changes in lithology (Yashin and Kosheleva, 1994) and in the reflexion geometry of echosoundings (Nürnberg et al., 1995), we suspect that the - in parts very thick - deposits are entirely of Holocene age. Nevertheless, distinct changes in the environment did happen during the Holocene, most probably changing sediment sources for the shelf deposits, changing influence of various water masses, and changing sea level, hence shaping the environment from active delta to estuarine and shallow marine.

Micropaleontological Studies

H. Cremer and M. Kunz-Pirrung

GEOMAR Research Center for Marine Geosciences, Kiel, Germany

Scientific Goals

The results of microfloral investigations of the material collected on the TRANSDRIFT I and II expeditions clearly show that the distribution of the microflora of the Laptev Sea is obviously water-mass dependent. Especially the distribution patterns of organic-walled microfossils (dinoflagellate cysts, acritarchs, green algae, protozoans) and of siliceous algae (diatoms and silicoflagellates) can be linked to a distinct water-mass situation. The influence of freshwater as well as of Atlantic water, Pacific water and Arctic water can be characterized by these microfossils.

Besides the mapping of the general distribution of microfloral assemblages in the water column, the sea ice and the sediment, the main objective of our studies is the identification of freshwater and its temporal variability. The characterization of river-transported sediments and typical limnic algae in long sediment cores gives evidence for the evolution of freshwater influence in present and past. For this purpose diatoms which exhibit a wide ecological range (freshwater to brackish to marine) and which are quite abundant in the Laptev Sea are excellent tracers. The chlorophyte microplankton (such as *Pediastrum* spp.) is another useful tool for monitoring the freshwater input by the large rivers discharging into the Laptev Sea. Marine dinoflagellates are a probate means for a paleoecological and paleoclimatological interpretation as their cysts consist of very stable organic substance. During diagenesis the cysts remain unaltered. Based on their good preservational mode dinoflagellate cysts are most important for interpreting Holocene climatic variabilities in long sediment cores.

Furthermore, ostracods and foraminifers are used to obtain more informations on water-mass parameters by applying trace element analyses (mg/Ca - ratio) and oxygen and carbon stable isotope analyses.

Investigations of spores and pollen contained in Laptev Sea sediment samples will contribute to a better understanding of the temporal variability and the post-glacial evolution of Siberia's boreal vegetation.

Working Program

The investigation of surface sediment samples as well as long sediment cores will complete our knowledge about microplankton assemblages in time and space in the Laptev Sea. Although this expedition was dedicated to the study of sea-ice formation processes, we were able to recover valuable sediment cores by the spade box corer and by the vibrocorer. A total of 14 sediment cores were gained (Tab. A2).

Sea ice investigations were carried out in order to get a general view on the quality and quantity of the microflora in different ice types. These investigations will mainly focus on the determination of abundance and composition of sea-ice diatom and dinoflagellate assemblages in relation to physical properties of ice. For this purpose, ice cores and ice samples as well as sub-ice water samples from slush ice, pancake ice, anchor ice and fast ice were taken during helicopter flights and during ice stations realized with a "mummy chair" from the KAPITAN DRANITSYN. A total of 80 samples had been collected, were then melted and fixed for further microfloral investigations (Tab. A6). Important was the sampling of sediment-laden sea ice. Sediments which get incorporated into sea ice during ice-formation processes are believed to be a vehicle for incorporation of microalgae into sea ice. Furthermore, of particular interest is the so-called "green ice" which is mainly found in the western part of the Laptev Sea. The strong green color of this ice and sub-ice water probably derived from diatoms eventually indicating a late autumn bloom.

In addition to the ice-sampling program, phytoplankton samples were taken in open-water areas (so-called polynyas) for investigations of the species composition of the microflora. For this purpose, a 20 μ mesh size phytoplankton net was used.

Physical Properties of Near-Surface Sediments in the Laptev Sea

A. Benthien, H. Kassens, E. Musatov*

GEOMAR Research Center for Marine Geosciences, Kiel, Germany
• VNIIOkeangeologia, St. Petersburg, Russia

The physical properties (e.g. shear strength, porosity) in Holocene near-surface sediments of the Laptev Sea (upper 0.5 m) are controlled by sediment composition (Benthien, 1994). Surficial sediments are overconsolidated only in some coastal areas, such as in front of the Yana Delta (Benthien, 1994; Kassens und Benthien, 1994). This would normally be the result of a much greater level of loading in the past than under the existing overburden. However, in these Holocene surface sediments, freeze/thaw processes are suggested as a major cause of this overconsolidation.

So far, physical property data of long sediment cores are restricted to 5 sites in the eastern Laptev Sea (Benthien, 1994; Dehn and Kassens, 1995), although physical properties are an important database for (i) paleoceanographic reconstructions, (ii) offshore developments, and (iii) permafrost studies. To fill this gap, physical property measurements were carried out on 11 short and 2 long sediment cores (Tab. A6).

Methods

Wet bulk density, water content and porosity:

Mass physical property measurements were made on spade box cores (GKG) and on long sediment cores recovered with a vibrocorer (VC). The sampling interval

ranged from 2 cm (GKG) to 5 cm (VC). Physical properties measured on board included water content and wet bulk density. From these index properties sediment phase relations as dry density, void ratio and porosity can be derived. The index properties can be determined from the direct measurement of the total (wet) mass of the sample (M_t), the dry mass (M_d), and the total volume of the saturated sample (V_t). A constant volume sample tube of 10 ccm was used. The tube was carefully pushed into the sediment, then cut out, trimmed, and weighed. To compensate for the ships motion, mass was determined using a technique of differential counterbalancing on twin top loading electronic balances which is described by Childress and Mickel (1980). The computerized precision electronic balance system used during the cruise was kindly provided by GEOMAR Technologie GmbH, Kiel.

After determining the total mass (M_t), most of the samples were dried aboard at a temperature of 105°C and weighed again. The other samples were stored for later drying in the home laboratory.

Water content (w) is reported as a percent ratio of water (M_w) to dry mass (M_d):

$$w = M_w/M_d * 100 \text{ (wt \%)}.$$

Wet bulk density (wbd) is the density of the total sample, including pore fluid:

$$wbd = M_t/V_t \text{ (g/ccm)}$$

$$M_t = \text{total mass, } V_t = \text{total volume (10 ccm).}$$

Porosity (n) is determined after Richards (1962):

$$n = e/(1+e)*100 \text{ (\%)}$$

$$e = (d_s*d_w*V_t/M_d) - 1$$

The specific weight (d_s) of near-surface sediment of the Laptev Sea (2.74 g/ccm) was determined from the average of 119 samples of the TRANSDRIFT I expedition (Benthien, 1994). Density of seawater (d_w) was assumed with 1.025 g/ccm.

Shear strength:

A vane shear instrument (HAAKE viscometer, RV 3) was used to measure undrained shear strength of undisturbed box cores and long sediment cores. The sampling interval ranged from 2 cm (GKG) to 5 cm (VC). At each interval 2 to 4 measurements were made in order to determine inhomogenities caused for instance by bioturbation or ice-transported material. A 10 x 8.8 mm vane was inserted perpendicularly 1 cm deep into the sediment and rotated at a speed of 4 rotations per minute. At peak failure the shear strength was measured. With this method the undrained shear strength of fine-grained and water-saturated sediments could be determined. The investigations did not include sandy sediments. All values are reported in kPa.

First results

In near-surface sediments of the Laptev Sea (average for the upper 50 cm) the values of wet bulk density vary between 1.48 (KD9548-17) and 1.86 g/ccm (KD9533-11). Low wet bulk density values ($\rho < 1.6$ g/ccm) were found in regions which are dominated by clayey sediments such as along the Yana and Lena Valley, high values ($\rho > 1.7$ g/ccm) were found in coastal areas with more silty and sandy sediments (Fig. 57). In general, the values do not increase with depth suggesting high sedimentation rates (Fig. 58).

The average shear strength for the upper 50 cm varies between 8.57 kPa (KD9565-11) and 12.41 kPa (KD9541-13). Most of the sediment cores show shear strength values increasing with depth which can be explained by an increasing

overburden pressure.

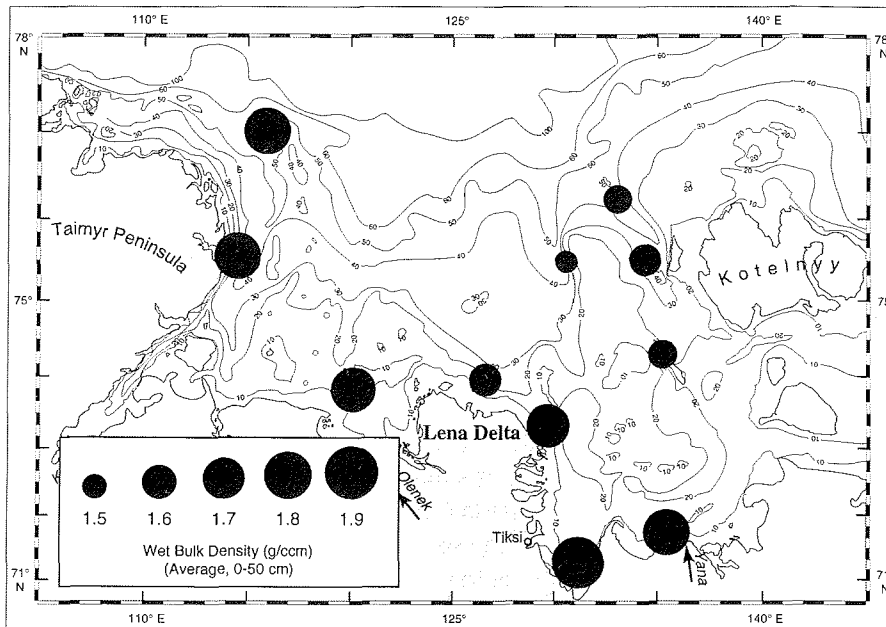


Fig. 57: Average distribution of wet bulk density in surficial sediments of the Laptev Sea. High values are typical of coastal areas.

In the core KD9548-17VC (Fig. 59) taken at the eastern slope of the upper Lena Valley the wet bulk density increases in the upper 80 cm from 1.4 to 1.7 g/ccm due to a decrease of the clay fraction. From 0.8 m to the end of the core (2.2 m) the values stay quite constant between 1.6 and 1.7 g/ccm corresponding to a silty-dominated sediment. The average shear strength of this core is 17.6 kPa, and the values generally increase with depth. The low values at 0.7 m, from 1.6 to 1.7 m and from 1.9 to 2.1 m core depth are caused by bioturbation or bivalve fragments (Tab. A8). Changes in lithology between 1 m and 1.4 m are considered to be responsible for the low shear strength in this interval. Between 1.6 and 2 m core depth the values reach about 30 kPa reflecting an overconsolidated sediment (Fig. 59). Such abnormally high values in a shallow depth below sea floor can either be explained by grounded ice masses compacting the sediments or by permafrost processes (Reimnitz et al., 1980; Lee and Winters, 1985). Previous investigations during the TRANSDRIFT I expedition have shown a high density of ice gouges in this region (Benthien, 1994) so that ice masses grounding with their keels in shallower regions are suggested to be responsible for these high shear strength values.

In sediment core KD9502-14 recovered at the upper Yana Valley the physical properties hardly vary with depth reflecting a very homogeneous lithology and high sedimentation rates. Wet bulk density values are about 1.6 g/ccm (Fig. 60).

Our investigations have shown that the near-surface sediments of the Laptev Sea generally are normal to underconsolidated. Changes in physical properties correspond to lithologic changes. High sedimentation rates are suggested because

of little trend with core depth. In regions where drifting ice masses ground on the sea floor the interaction between ice and sediment could be responsible for over consolidated sediments. These results correspond well to previous investigations carried out in the Laptev Sea (Benthien, 1994; Kassens and Karpiy, 1994).

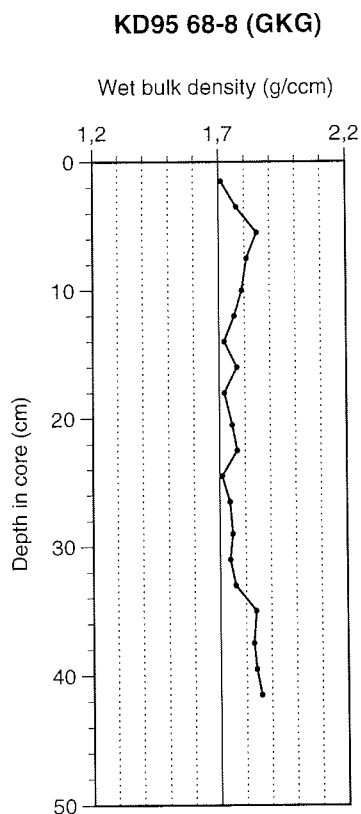


Fig. 58: Vertical distribution of wet bulk density in sediment core KD9568-8 from the Khatanga Valley.

Geochemical Pathways

- J. Hölemann, M. Schirmacher*, S. Schultz**, C. Strobl***
 GEOMAR Research Center for Marine Geosciences, Kiel, Germany
 * GKSS Research Center Geesthacht, Germany
 ** Institute for Marine Research University of Kiel, Germany
 *** Heidelberg Academy of Sciences, Germany

One of the most remarkable findings during the TRANSDRIFT III expedition is the occurrence of "dirty" sea ice near the Lena River Delta. Extensive areas of the shallow (< 20m) south-eastern Laptev Sea were covered with brown-coloured young ice. Preliminary investigations have shown that in most cases this phenomenon is caused by high concentrations of mineral particles embedded in the ice.

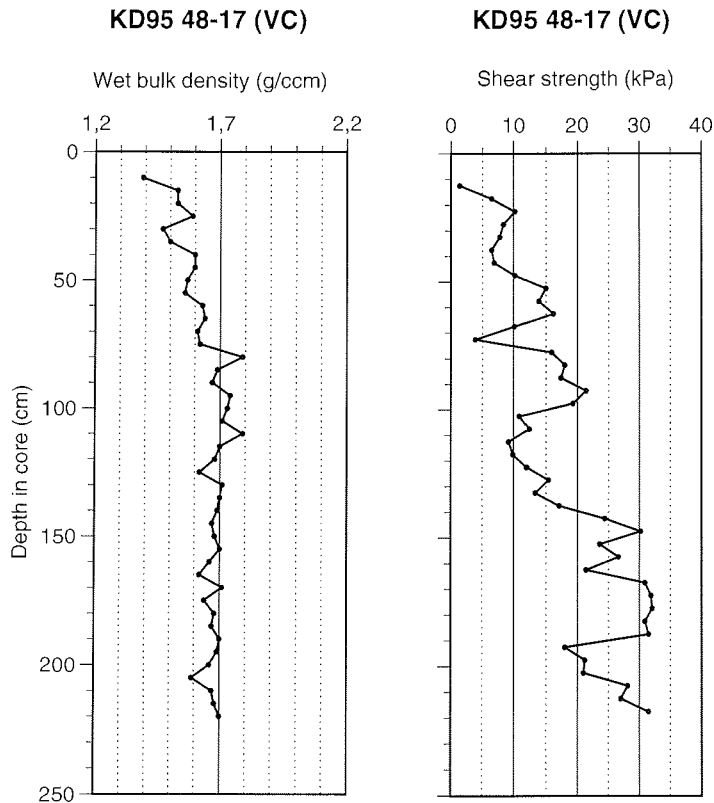


Fig. 59: Wet bulk density and shear strength profiles of sediment core KD9548-17 from the northern Lena Valley.

Incorporation of mineral and biogenic particles into newly formed ice has a dramatic effect on the geochemical pathways of anorganic and organic compounds that were carried to the Laptev Sea by the large Siberian rivers. In particular, surface (particle) reactive substances like metals and organics such as polychlorinated biphenyls (PCB) can be scavenged by particles. During the summer period these particles were deposited within the sediments of the shallow Laptev Sea. In the late autumn and winter season, strong currents and wind-induced turbulence, concurrent with the formation of ice crystals in the water column, are able to resuspend sediments and further incorporate the particles into the new ice. This process continuously delivers sediment-laden sea ice to the Siberian branch of the Transpolar Drift. The geochemical signature of these ice-bound particles and adsorbed substances can be used as a tracer for the dynamic of the Arctic sea-ice cover.

On the basis of the scientific sampling program of the TRANSDRIFT III expedition we are able to compare the trace element and PCB spectrum of the water column and the surface sediments with that of ice-bound particles from the same region. This will lead to a better understanding of the cycling and transport processes of geogenic and anthropogenic substances in the Arctic environment.

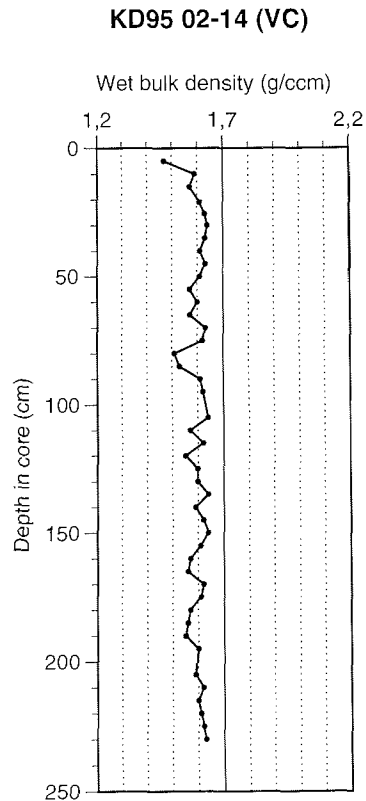


Fig. 60: Wet bulk density profil of sediment core KD95 02-14.

Another important particle-reactive element is Beryllium-10. The geochemical pathway of this cosmogenic element, which is used as a dating tool for sediments of high northern latitudes, can be studied in the area of the Laptev Shelf in more detail. Our investigations will give a key for the understanding of the geochemical behavior of Beryllium-10 in the water column, sediments and sea ice. Based on this work, the dating of sediment cores of the Arctic Ocean with Beryllium-10 will become a more precise stratigraphic tool. During the TRANSDRIFT III expedition main attention was given to the riverine fluxes of Beryllium (e.g. Lena), the sedimentary fluxes and the export flux by dirty sea ice.

Working Program

Trace Elements

The TRANSDRIFT III expedition is the third expedition to the Laptev Sea in which we have had the chance to study the trace element composition of different geochemical compartments. The main scientific and technical goal for our geochemical working group was the contamination-"free" sampling of the young sea-ice cover. These ice-related studies were completed by investigations of the water column and surface sediments.

Most sampling sites are situated in coastal areas near the outlets of the major river systems (Lena, Yana, Olenek, Khatanga). Detailed positions and sampling lists are given in Tabel A2, A6. 30 young-ice samples were collected in order to investigate the geochemical composition of the dissolved and particulate phases (Tab. A7). 28 water/suspended matter and 10 surface sediment samples from the the same regions complete the sampling program. Additional filters at 0, 5, 10, 15, 20 and 30 m were taken at about 20 stations in order to determine the concentration and bulk particle composition of suspended matter (SPM).

Slush-ice samples were taken with clean nets (1 mm mesh size). Ice cores were hand-drilled with conventional drilling equipment and cleaned with a ceramic knife.

The ice was melted on board the vessel and immediately filtered through pre-cleaned Nuclepore filters (0,4 μm poresize; N-pressure filtration) in a transportable class 100 clean air cabinet. Water samples were taken using teflon water samplers (Hydro-Bios).

The final analysis was performed at the Research Center Geesthacht including salt-matrix separation and pre-concentration of the water samples followed by analyses with Total Reflection X-Ray Fluorescence (TXRF). Measurements using Atomic Absorption Spectroscopy (AAS) and Inductively Coupled Plasma Mass Spectrometrie (ICP-MS) complete these investigations. Elements measured in sea water include V, Mn, Fe, Ni, Cu, Zn, Se, Mo, Cd, U and Pb. In the sediments (< 20 μm fraction) and the suspended particulate matter, about 30 elements including the REE can be measured.

The determination of suspended matter concentrations and scanning electron microscopy in combination with EDAX was carried out at GEOMAR in Kiel.

Chlorinated Biphenyls

Chlorobiphenyls (CB) are a series of chemically similar compounds with a large range of physico-chemical properties. Their environmental levels and the compositions of CB mixtures can be used to identify water bodies and different source areas for CB in Arctic sea ice. To study the present PCB (polychlorinated biphenyls) concentration in new ice of the Laptev Sea, 9 ice samples were taken at 8 stations (Tab. A6). About 30 l of ice were sampled with the help of pre-cleaned steel instruments and were then immediately transferred to a closed steel container. After the ice was melted within the container, it was filtered through glassfibre filters (N-pressure filtration). Filters were stored frozen at -20° C.

Surface sediments for the analysis of PCB were taken at 8 stations, especially near the mouth of the Lena and Yana Rivers .

Beryllium-10

Sediments recovered during the expeditions TRANSDRIFT I, II and III will enable us to determine the evaluation of Beryllium-10 fluxes during the last one hundred years. Furthermore, 26 water samples (30 l) with different salinities were taken (Tab. A6). On the base of these samples we can estimate the residence time of Beryllium-10 in the water column in this area.

8 samples were filtered through 0,45 μm Nuclepore filters. Filtered and unfiltered water samples were acidified with 25% HCl to pH 3. Iron 3+ (100 - 200mg) and 1ml Beryllium-9 were added to the samples. After one day the iron was precipitated with NH₄OH and the samples could be reduced from 30 l to 2 l. After the chemical preparation of the water samples and sediments at the HAW, Beryllium-10 will be measured via accelerator mass spectrometry (AMS) at the tandem facility of the ETH Zürich.

Dirty ice-cores were also collected which will be analyzed for Beryllium-10 (Tab. A7). These samples should yield some information about the export flux of Beryllium-10 from the Laptev Shelf via sea-ice. Ice and water samples will be prepared in the same way for the analysis of Beryllium-10.

Pore-Water Geochemistry

C. Langner

Alfred-Wegener-Institut für Polar- und Meeresforschung, Bremerhaven, Germany

Marine particulate matter is either preserved in the sediments or subject to degradation. In case of degradation it will be mineralized to CO₂ and metabolites and subsequently returned to the bottom water. During this process, oxygen is respired, which is available in dissolved form within the sediments. When the oxygen is consumed, it starts to react with various electron acceptors in the overlying sediment layers (e.g. manganese and iron). The reaction rates influence the benthic fluxes through the sediment/bottom water interface, which play an important role in the global biogeochemical cycles in the ocean. The main objective of this program is the quantification of benthic fluxes of recycled organic carbon. Here, the difference between the autumn/winter situation and the summer is of interest.

Working Program

The samples for these investigations were taken from a box corer at 10 stations (Fig. 61). In the surface sediments, the dissolved oxygen was determined directly after the sampling to derive the oxygen gradients across the sediment/water interface. These measurements were carried out with specific microelectrodes (type 737 Clark style Micro oxygen electrode, Diamont General, Ann Arbor, USA). Sea water directly overlying the sediment surface was taken for the calibration of oxygen measurements by Winkler titration, carried out by S. Pivovarov (AARI).

The extraction of pore water was performed on 1 - 1.5 cm sediment slides with a gaspress (N₂-gas, 3 - 4 bar). Pore water was filtered through 0.45 µm cellulose acetate filters. The remaining solid phases were packed airtight. Thus, it was possible to separately investigate pore water and solid phase from the same intervals. All the samples were stored at 4°C aboard the ship.

To assess the influence of river water in the sediments, the salinity of pore water was measured at fixed intervals (1, 2, and 9 cm) with an optical salinometer (refractometer).

The investigations of nutrients, manganese and iron will be carried out at the laboratory of the AWI Bremerhaven.

Preliminary Results

Gradients of dissolved oxygen in the surface sediments show a relatively similar trend. In general, the oxic layer of the sediments is very thin. The thickness ranges from about 3 mm (KD9572) to 11 mm (KD9533). This is a typical character of shelf sediments from shallow water. These results are in contrast to those gained from slope and deep-sea sediments north of the Laptev Sea, in which the oxic layer extends some centimeters (Fütterer, 1994). On the shallow shelf of the Laptev Sea, a high rate of degradation of the organic matter must exist. Figure 61 shows the

distribution of the thicknesses of the oxic layer in surface sediments recovered during October 1995. The low thickness is connected with a steep oxygen gradient across the sediment/water interface. Only minor differences were observed in the various regions the Laptev Sea. West of the Lena Delta and near the outflows of the Yana and Olenek Rivers into the Laptev Sea, the oxic layers are slightly thicker than in the other sediment cores investigated.

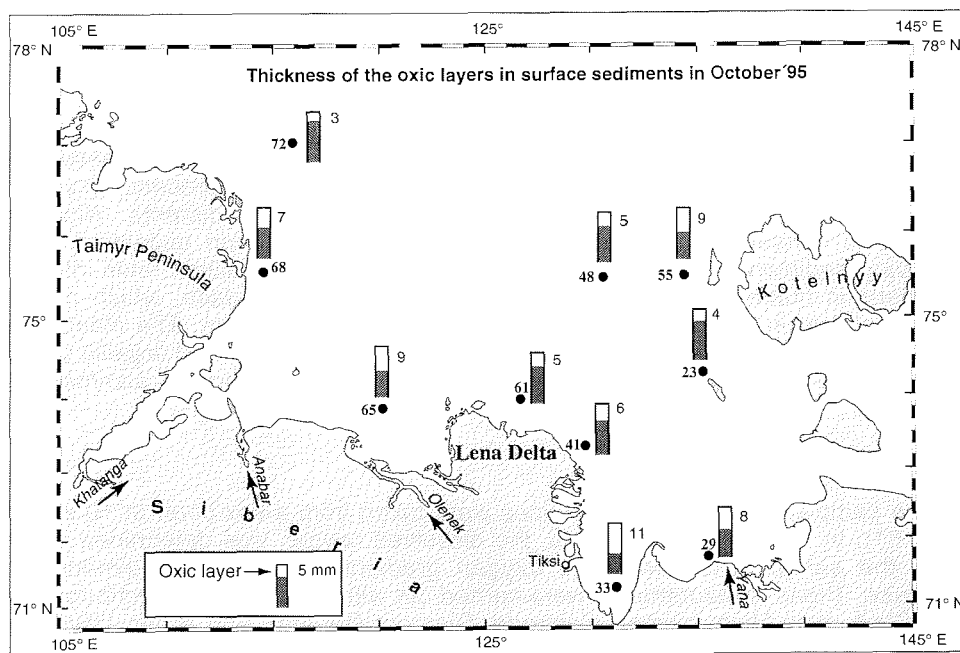


Fig. 61: Thickness of the oxic layers in surface sediments of the Laptev Sea in October 1995.

REFERENCES

- Benthien, A. (1994): Echographiekartierung und physikalische Eigenschaften der oberflächennahen Sedimente in der Laptevsee. Unpubl. Master Thesis, University of Kiel, 80 pp.
- Cherepanov, N.V. (1977): Ice Classification of Natural Basins. Proc. of AARI, 331, 77-99, (in Russian).
- Childress, J.J. and Mickel, T.J. (1980): A Motion Compensated Shipboard Precision Balance System. Deep Sea Res., 27, 965-970.
- Dehn, J. and Kassens, H. (1995): Temporal and Regional Changes in the Sedimentary Environment of the Laptev Sea. In: H. Kassens (ed.), Laptev Sea System: Expeditions in 1994. Ber. Polarforsch., 182, 87-97.
- Dehn, J., Kassens, H., and TRANSDRIFT II Shipboard Scientific Party (1995): Regional and Temporal Changes in the Sediments of the Laptev Sea: First Results of the TRANSDRIFT Expeditions. In: H. Kassens, D. Piepenburg, J. Thiede, L. Timokhov, H.-W. Hubberten, and S. Priamikov (eds.), Russian-German Cooperation: Laptev Sea System. Ber. Polarforsch., 176, 314-323.
- Dethleff, D., Nürnberg, D., Reimnitz, E., Saarloos, M. and Savchenko, Y.P. (1993) East Siberian Arctic Region Expedition '92: The Laptev Sea - its Significance for Arctic Sea Ice Formation and Transpolar Sediment Flux. Ber. Polarforsch., 120, 3-37.
- Eicken, H., Reimnitz, E., Alexandrov, V., Martin, T., Kassens, H. and Viehoff, T. (1997): Sea-Ice Processes in the Laptev Sea and their Importance for Sediment Export. Continental Shelf Research, 17/2, 205-233.
- Fedorov, K.N. (1983): Physical Nature and Structure of Oceanic Fronts. Leningrad, Gidrometeoizdat, 296 pp.
- Fütterer, D.K. (ed.) (1994): The Expedition ARCTIC '93. Leg ARK-IX/4 of RV "Polarstern" 1993. Ber. Polarforsch., 149, 244 pp.
- Golikov, A.N. and Scarlato, O.A. (1965): Hydrobiological Investigations in the Posiet Bay Using Diving Technique (in Russian). Investigations of the Fauna of the Seas, 3(11), 5-21.
- Golovin, P.N., Gribanov, V.A., and Dmitrenko, I.A. (1995): Macro- and Mesoscale Hydrophysical Structure of the Outflow Zone of the Lena River Water to the Laptev Sea. In: H. Kassens, D. Piepenburg, J. Thiede, L. Timokhov, H.-W. Hubberten, and S. Priamikov (eds.), Russian-German Cooperation: Laptev Sea System. Ber. Polarforsch., 176, 99-106.
- Gribanov, V.A. and Dmitrenko, I.A. (1994): Types and Features of Vertical Distribution of Thermohaline Characteristics in the Laptev Sea in Summer of 1993. In: Scientific Results of the LAPEX-93 Expedition. St. Petersburg, Gidrometeoizdat, 76-82.
- Gukov, A.Yu. (1994): Biotsenozy bukhty Tiksi i ikh sezonnaia dinamika. Avtoreferat dissertatsii, St. Petersburg, 23 pp.
- Ibanova, A.M., Kosheleva, V.A., and Neizvestnov, Iu.V. (in press): Atlas of Russian Outer and Inner Seas. (in Russian).
- Kassens, H. and Benthien, A. (1994): Physical Properties of Near-Surface Sediments in the Laptev Sea. In: H. Kassens and V. Karpiy (eds.), Russian-German Cooperation: The Transdrift I Expedition to the Laptev Sea. Ber. Polarforsch., 151, 73-77.
- Kassens, H. and Karpiy, V. (eds.) (1994): Russian-German Cooperation: The Transdrift I Expedition to the Laptev Sea. Ber. Polarforsch., 151, 168 pp.
- Kassens, H. and the TRANSDRIFT I Shipboard Scientific Party (1994): Along the Northern Sea Route into the Ice Factory of the Arctic Ocean. The Nansen Icebreaker, 6, 4-6.

- Kassens, H. (ed.) (1995): Laptev Sea System: Expeditions in 1994. Ber. Polarforsch., 182, 195 pp.
- Lapina, N.N., Kulikov, N.N., and Semenov, V.P. (1965): Bottom Sediments of the Arctic Ocean. Regional Geology 17. Leningrad 1972 (in Russian).
- Lee, H.J. and Winters, W.J. (1985): Strength and Consolidation Properties of Stiff Beaufort Sea Sediment. In: Proceedings of the Arctic Energy Technologies Workshop November 1984, U.S. Department of Energy, Morgantown, West Virginia.
- Lindemann, F. (1994): Sonographische und sedimentologische Untersuchungen in der Laptevsee, sibirische Arktis. Unpubl. Master Thesis, University of Kiel, 75 pp.
- Manual on Chemical Analysis of Sea Waters (1993): St. Petersburg, Gidrometeoizdat, 264 pp.
- Nürnberg, D., Wollenburg, I., Dethleff, D., Eicken, H., Kassens, H., Letzig, T., Reimnitz, E. and Thiede, J. (1994): Sediments in Arctic Sea Ice - Implications for Entrainment, Transport and Release. Marine Geology, 119, 185-214.
- Nürnberg, D., Fütterer, D.K., Niessen, F., Nørgaard-Pedersen, N., Schubert, C.J., Spielhagen, R.F., and Wahsner, M. (1995): The Depositional Environment of the Laptev Sea Continental Margin: Preliminary Results from the R/V Polarstern ARK IX-4 Cruise. Polar Research, 14 (1), 43-53.
- Petrjashev, V. (1994): Hydrobiological investigations in the Laptev Sea. In: H. Kassens and V. Karpuy (eds.), Russian-German Cooperation: The Transdrift I Expedition to the Laptev Sea. Ber. Polarforsch., 151, 54-59.
- Pfirman, S., Lange, M.A., Wollenburg, I. and Schlosser P. (1990): Sea Ice Characteristics and the Role of Sediment Inclusions in Deep-Sea Deposition: Arctic-Antarctic Comparisons. In: U. Bleil and J. Thiede (eds.), Geological History of the Polar Oceans: Arctic versus Antarctic. Kluwer Academic Publishers, Dordrecht, pp. 187-211.
- Rachor, E. (ed.) (1997) Scientific Cruise Report of the Arctic Expedition ARK-XI/1 of RV "Polarstern" in 1995 (German-Russian Project LADI: Laptev Sea - Arctic Deep Basin Interrelations). Ber. Polarforsch., 226, 157 pp. + App.
- Reimnitz, E., Kempena, E., Ross, R., and Minkler, P. (1980): Overconsolidated Surficial Deposits on the Beaufort Sea Shelf. Open-File Report, 80-2010, U.S. Geological Survey, Menlo Park, 37 pp.
- Reimnitz, E., Dethleff, D. and Nürnberg, D. (1994): Contrasts in Arctic Shelf Sea-Ice Regimes and Some Implications: Beaufort Sea and Laptev Sea. Marine Geology, 119, 215-225.
- Richards, A.F. (1962): Investigations of Deep-Sea Sediment Cores, Part II: Mass Physical Properties. Technical Report, 106, U.S. Navy Hydrographic Office, Washington D.C., 145 pp.
- Rosak, B. (1995): Untersuchungen zur Tonmineralverteilung und Sedimentzusammensetzung an Oberflächensedimenten der Laptevsee, sibirische Arktis. Unpubl. Master Thesis, University of Würzburg, 68 pp.
- Stein, R. and Nürnberg, D. (1995): Productivity Proxies: Organic Carbon and Biogenic Opal in Surface Sediments from the Laptev Sea and the Adjacent Continental Slope. In: H. Kassens, D. Piepenburg, J. Thiede, L. Timokhov, H.-W. Hubberten, and S. Priamikov (eds.), Russian-German Cooperation: Laptev Sea System. Ber. Polarforsch., 176, 286-296.
- Wahsner, M. and Shelekhova, E.S. (1994): Clay Mineral Distribution in Arctic Deep-Sea and Shelf Surface Sediments. In: Greifswalder Geologische Beiträge A (2), p. 234 (abstract).
- Wollenburg, I. (1993): Sedimenttransport durch das arktische Meereis: die rezente lithogene und biogene Materialfracht. Ber. Polarforsch., 127, 1-159.

Yashin, D.S. and Kosheleva, V.A. (1994): Main Features of Holocene Sedimentation on the Laptev and Eastsiberian Sea Shelf. In: Scientific Results of the LAPEX-93 Expedition. St. Petersburg, 257-265, (in Russian).

ACKNOWLEDGEMENTS

The TRANSDRIFT III expedition, a major operation of the Russian-German research project 'System Laptev Sea' was supported by many authorities and institutions. We would like to thank various Russian authorities in Murmansk, St. Petersburg, and Moscow who granted the necessary permissions to carry out scientific work in the Laptev Sea as well as to transfer our equipment (six 20ft containers) to Russia. The Russian and the German embassies in Bonn and Moscow as well as the General Consulate in Hamburg have been very helpful in obtaining all the necessary documents and to clarify a number of questions related to the expedition.

The expedition was funded by the German Ministry of Science and Technology (FZK 52503G0517) and the Russian Ministry of Science and Technical Policy (LAPEX-95). We wish to thank these organizations for their financial and logistic support. B.I. Imerekov (Russian Ministry of Science and Technical Policy), K. Heyckendorf (German Ministry of Science and Technology, Warnemünde) and S. Müller (German Ministry of Science and Technology, Bonn) provided invaluable assistance before, during and after the expedition. We would like to thank our colleagues at GEOMAR, AARI, and AWI for their support, especially H. Heyn of GEOMAR, who was invaluable during negotiations in Murmansk. The English manuscripts of this cruise report were kindly improved by B. Rohr.

The Murmansk Shipping Company made available one of its powerful conventional icebreakers the KAPTIAN DRANITSYN for the expedition. In addition to being very gracious in accommodating the special needs of the expedition, and transforming the icebreaker into an efficient research platform, they have been especially helpful in arranging the transportation of the laboratory and cargo containers to Murmansk and Kiel.

Finally, the members of the expedition would like to express their appreciation to the Captain Agafonov and his crew for their tireless efforts above and beyond their duties. Though all of us have had extensive experience at sea, we all agreed that we were never better received than on board the KAPITAN DRANITSYN. The helicopter pilots provided tremendous support as well as aeronautic excellence.

APPENDIX

- Tab. A1: Participants aboard the KAPITAN DRANITSYN for TRANSDRIFT III
- Tab. A2: Station list of the TRANSDRIFT III expedition
- Tab. A3: Ice stations occupied by ship and helicopter during the TRANSDRIFT III expedition
- Tab. A4: Helicopter flights during the TRANSDRIFT III expedition
- Tab. A5: Ice Observations aboard KAPITAN DRANITSYN (5 - 24 Oct., 1995)
- Tab. A6: List of water and sea floor samples taken during the TRANSDRIFT III expedition
- Tab. A7: List of ice samples taken during the TRANSDRIFT III expedition
- Tab. A8: Description of sediment cores taken during the TRANSDRIFT III expedition

Tab. A1: Participants aboard the KAPITAN DRANITSYN for TRANSDRIFT III

Scientific Party:

Aleksandrov	Vitaliy	AARI	Sea-ice studies
Anoshkin	Andrey	KSRI	Hydrooptics
Antonow	Martin	BAF	Paleoceanography
Benthien	Albert	GEOMAR	Paleoceanography
Berger	Andreas	NDR	Journalist
Burmeister	Karl-Heinz	NDR	Journalist
Cremer	Holger	GEOMAR	Paleoceanography
Darovskikh	Andrey	AARI	Sea-ice studies
Dmitrenko	Igor	AARI	Co-chief Scientist, Oceanography
Dmitriev	Nikolay	AARI	Oceanography
Freitag	Johannes	AWI	Sea-ice studies
Fürst	Bernhard	BAF	Paleoceanography
Golovin	Pavel	AARI	Oceanography
Haase	Veit	GEOMAR	Paleoceanography
Hölemann	Jens	GEOMAR	Geochemistry
Ipatov	Aleksandr	AARI	Oceanography
Kassens	Heidemarie	GEOMAR	Co-chief Scientist, Paleoceanography
Kirndörfer	Jürgen G.	NDR	Journalist
Kolatschek	Josef	AWI	Sea-ice studies
Korablev	Aleksandr	AARI	Meteorology
Kosheleva	Vera	VNIIO	Paleoceanography
Kovalev	Sergey	AARI	Sea-ice studies
Kunz-Pirrung	Martina	GEOMAR	Paleoceanography
Langner	Constanze	AWI	Paleoceanography
Lindemann	Frank	GEOMAR	Sea-ice studies
Musatov	Evgeniy	VNIIO	Paleoceanography
Neufeld	Sergej	GTG	Technician
Nürnberg	Dirk	AWI	Paleoceanography
Peregovich	Bernhard	GEOMAR	Paleoceanography
Petryashov	Viktor	ZISP	Biology
Piepenburg	Dieter	IPÖ	Biology
Pivovarov	Sergey	AARI	Marine chemistry
Reimnitz	Erk	USGS	Sea-ice studies
Rohr	Bettina	GEOMAR	Interpreter
Rossak	Bettina	GEOMAR	Marine chemistry
Schirmacher	Martina	GKSS	Marine chemistry
Schmid	Michael	IPÖ	Biology
Schultz	Stefanie	IFM	Marine chemistry
Sherbakov	Yuriy	AARI	Marine chemistry
Siebold	Martina	AWI	Paleoceanography
Strakhov	Mikhail	AARI	Sea-ice studies
Strobl	Christopher	HAW	Marine chemistry
Sviridov	Viktor	AARI	Marine chemistry
Thiede	Jörn	GEOMAR	Coordinator, Paleocceanography
Thiede	Rasmus	BAF	Paleoceanography
Timokhov	Leonid	AARI	Coordinator, Oceanography
Tuschling	Kirsten	IPÖ	Biology
Tyshko	Konstantin	AARI	Sea-ice studies
Valero Delgado	Fernando	AWI	Sea-ice studies
von Juterzenka	Karen	IPÖ	Biology

Zachek	Andrey	AARI	Meteorology
Zakharchuk	Evgeniy	AARI	Marine chemistry

Ships Crew:

Agafonov	Oleg	MSC	Captain
Antonov	Aleksandr	MSC	Chief Mate
Afanas'ev	Sergey	MSC	Chief Mate
Bakhvalov	Sergey	MSC	2nd Officer
Semenchenko	Vladimir	MSC	3rd Officer
Bazarnyy	Dmitriy	MSC	4th Officer
Ivanov	Valeriy	MSC	Radio Officer
Talanov	Aleksander	MSC	Engineer for Navigational Instruments
Gladin	Mikhail	MSC	Chief Engineer
Baranov	Sergey	MSC	2nd Engineer
Ivanov	Aleksey	MSC	2nd Engineer
Lepinin	Aleksey	MSC	3rd Engineer
Firsov	Ruslan	MSC	4th Engineer
Savoley	Sergey	MSC	Chief Electrical Engineer
Beyzel	Vladimir	MSC	2nd Electrical Engineer
Ryzhenkov	Sergey	MSC	2nd Electrical Engineer
Voronov	Andrey	MSC	3rd Electrical Engineer
Ivanov	Aleksandr	MSC	4th Electrical Engineer
Rumyantsev	Nikolay	MSC	Passenger Officer
Zaykov	Sergey	MSC	Administrator
Spasov	Vladimir	MSC	Administrative Assistant
Magadov	Gasan	MSC	Boatswain
Kroshin	Vladimir	MSC	Deck-hand
Losev	Aleksandr	MSC	Deck-hand
Grushevskiy	Mikhail	MSC	Deck-hand
Lozhenitsyn	Yuriy	MSC	Deck-hand
Burakov	Aleskey	MSC	Deck-hand
Kuchaev	Boris	MSC	Deck-hand
Fomin	Sergey	MSC	Deck-hand
Moshnikov	Viktor	MSC	Engine Mechanic
Kuzmichev	Andrey	MSC	Engine Mechanic
Fedorov	Boris	MSC	Engine Mechanic
Marakhovets	Peter	MSC	Engine Mechanic
Gromyko	Evgeniy	MSC	Engine Mechanic
Mashedo	Nikolay	MSC	Engine Mechanic
Kokoulin	Vasiliy	MSC	Engine Mechanic
Polezhaev	Vladimir	MSC	Engine Mechanic
Nikitkov	Dmitriy	MSC	Engine Mechanic
Gal'yanov	Oleg	MSC	Engine Mechanic
Kudryashov	Vladimir	MSC	Engine Mechanic
Bitsutin	Gennadiy	MSC	Lathe-operator
Kukushkin	Roman	MSC	Welder
Bykov	Yuriy	MSC	Electrician
Dorofeev	Viktor	MSC	Electrician
Val'shin	Artur	MSC	Electrician
Degtyarev	Nikolay	MSC	Electrician
Polovinkin	Sergey	MSC	Electrician
Oskirko	Elena	MSC	Cleaning Woman
Bakhurinskiy	Aleksandr	MSC	Steward

Kolpakov	Mikhail	MSC	Steward
Latifullin	Rais	MSC	Steward
Petrova	Liliya	MSC	Stewardess
Korshikova	Lyudmila	MSC	Stewardess
Koptyaeva	Oksana	MSC	Stewardess
Filatov	Viktor	MSC	Cook
Mitrokhova	Irina	MSC	Cook
Uvarov	Igor	MSC	Cook
Bashkin	Oleg	MSC	Cook
Eremenko	Violetta	MSC	Buffet Assistant
Osipova	Elena	MSC	Buffet Assistant
Chuyko	Valentina	MSC	Laundrywoman
Zubareva	Zhanna	MSC	Laundrywoman
Kulakova	Galina	MSC	Cleaning Woman
Valickaya	Tat'yana	MSC	Cleaning Woman
Brodnikova	Tat'yana	MSC	Cleaning Woman
Sedlin	Igor	MSC	Cleaner
Brezinskiy	Oleg	MSC	First Pilot
Malinovskiy	Aleksandr	MSC	2nd Pilot
Pryamikov	Nikolay	MSC	Aircraft Mechanic
Dezhurov	Aleksandr	MSC	Aircraft Mechanic
Shikov	Sergey	MSC	Physician
Seikov	Boris	MSC	Hunter

AARI	Arctic and Antarctic Research Institute, 38 ul. Beringa, 199337 St. Petersburg, Russia
AWI	Alfred-Wegener-Institut für Polar- und Meeresforschung, Postfach 120161, D-27515 Bremerhaven
BAF	TU Bergakademie Freiberg, Institut für Geologie, Bernd-von-Cotta-Str. 2, D-09596 Freiberg
GEOMA R	Forschungszentrum für marine Geowissenschaften, Wischhofstr. 1-3, D-24148 Kiel
GKSS	Forschungszentrum Geesthacht GmbH, Postfach 1160, D-21494 Geesthacht
GTG	GEOMAR Technologie GmbH, Wischhofstr. 1-3, D-24148 Kiel
HAW	Heidelberger Akademie der Wissenschaften, INF 366, D-69120 Heidelberg
IFM	Institut für Meereskunde, Düsternbrooker Weg 20, D-24105 Kiel
IPO	Institut für Polarökologie, Wischhofstr. 1-3, D-24148 Kiel
KSRI	Krylov Shipbuilding Research Institute, 20 Moskovskoye chaus., 196158 St. Petersburg, Russia
MSC	Murmansk Shipping Company, 15 ul. Kominterna, 183636 Murmansk, Russia
NDR	Norddeutscher Rundfunk, Landesfunkhaus Schleswig-Holstein, Eggerstedtstraße 16, D-24103 Kiel
USGS	US Geological Survey, 345 Middlefield Road, MS 999 Menlo Park, CA 94025, U.S.A.
VNIIO	VNIIOkeangeologia, All-Russia Research Institute for Geology and Mineral Resources of the World Ocean, 1 Angliyskiy Per., 190121 St. Petersburg, Russia
ZISP	Zoological Institute, Russian Academy of Sciences, 1 Universitetskaya nab., 199034 St. Petersburg, Russia

Tab. A 2: Station list of the TRANSDRIFT III expedition

Station #	Date	Time (Moscow)	Latitude (° N)	Longitude (° E)	Depth (m)	Activity	
KD9501	06.10.	04:45	80°10.01'	102°30.75'	86	begin of station	
	R/1	06.10.	05:00	80°09.97'	102°29.96'	86	CTD
	R/2	06.10.	07:39	80°09.95'	102°29.52'	86	CTD
	R/3	06.10.	7:39-8:00	80°09.95'	102°29.52'	86	Sil,Oxy,Ph; FI
	R/4	06.10.	08:02	80°09.96'	102°28.88'	86	CTD
	R/5	06.10.	08:31	80°09.92'	102°28.61'	86	CTD
	R/6	06.10.	09:05	80°09.97'	102°28.17'	86	CTD
	R/7	06.10.	09:31	80°10.01'	102°27.83'	86	CTD
	R/8	06.10.	10:19	80°10.07'	102°27.17'	86	CTD
	R/9	06.10.	10:31	80°10.02'	102°26.73'	86	CTD
-1	06.10.	06:10-12:30	80°10.02'	102°29.52'	86	Ice sampling	
-2	06.10.	11:10-12:23	80°10.02'	102°29.52'	down to 70	MUM	
-3	06.10.	11:30-11:40	80°10.02'	102°29.52'	5 + 10	WS (equipment test)	
KD9502	08.10.	04:16	76°11.52'	133°06.99'	46	begin of station	
	R/1	08.10.	4:40-5:00	76°11.48'	133°07.01'	45	Sil,Oxy,Ph;FI
	R/2	08.10.	7:30-8:00	76°11.63'	133°06.80'	43	Sil,Oxy,Ph;FI
	R/3	08.10.	11:10-12:30	76°11.62'	133°06.90'	44	Sil,Oxy,Ph;FI
	R/4	08.10.	14:50-15:30	76°11.62'	133°06.96'	44	Sil,Oxy,Ph;FI
	-1	08.10.	05:17-05:27	76°11.52'	133°06.99'	2, 43	WST
	-2	08.10.	05:57-07:16	76°11.52'	133°06.99'	2, 5, 10, 15, 20, 25, 30, 35, 40	SPM, C-13/O-18/Methane, Chl, SACT
	-3	08.10.	05:58-07:18	76°11.52'	133°06.99'	46	MUM
	-4	08.10.	06:13-06:30	76°11.52'	133°06.99'	10	PN
	-5	08.10.	07:25-07:42	76°11.52'	133°06.99'		WSB (unsuccessfully, stopped)
	-6	08.10.	08:00-08:29	76°11.52'	133°06.99'	36	BN
	-7	08.10.	08:32-08:41	76°11.52'	133°06.99'		WSB (unsuccessfully, stopped)
	-8	08.10.	08:48-08:51	76°11.52'	133°06.99'	5	WSB (30 l)
	-9	08.10.	09:00-09:44	76°11.52'	133°06.99'	46	UWP
	-10	08.10.	10:00-10:10	76°11.52'	133°06.99'	46	BG (unsuccessfully, stopped)
	-11	08.10.	10:20-10:30	76°11.52'	133°06.99'	46	Bio: 3 x BG
	-12	08.10.	10:48-10:54	76°11.52'	133°06.99'	46	Geo: BG (recovery:10 cm)
-13	08.10.	11:32-12:43	76°11.52'	133°06.99'		PC	
-14	08.10.	11:58-12:25	76°11.52'	133°06.99'	46	VC (recovery: 230 cm)	
-15	08.10.	13:25-13:40	76°11.52'	133°06.99'	46	VC (unsuccessfully, stopped)	
-16	08.10.	16:44-17:00	76°11.52'	133°06.99'	46	Dredge	
KD9503	R/1	08.10.	18:33	76°10.97'	133°59.79'	35	CTD
	R/2	08.10.	18:40-19:10	76°10.97'	133°59.79'	35-26	Sil,Oxy;FI
	-1	08.10.	18:38-18:55	76°10.58'	133°59.47'	34	MUM
KD9504	R/1	08.10.	20:27	76°10.99'	134°49.97'	23	CTD
	R/2	08.10.	20:30-21:00	76°10.99'	134°49.97'	23	Sil,Oxy;FI
	-1	08.10.	20:27-20:49	76°10.58'	134°49.48'	22	MUM
KD9505	R/1	08.10.	22:07	76°10.95'	135°39.90'	25	CTD
	R/2	08.10.	22:10-22:40	76°10.95'	135°39.90'	25	Sil,Oxy;FI
	-1	08.10.	22:02-22:24	76°11.02'	135°39.52'	22	MUM
KD9506	R/1	08.10.	23:46	76°10.94'	136°30.24'	22	CTD
	R/2	08.10.	23:46	76°10.94'	136°30.24'	22	Sil,Oxy;FI
	-1	08.10.	23:43-00:06	76°10.57'	136°30.10'	22	MUM
KD9507	R/1	09.10.	01:08	76°10.99'	137°09.85'	24	CTD
	R/2	09.10.	1:10-1:40	76°10.99'	137°09.85'	24.	Sil,Oxy;FI
	-1	09.10.	01:08-01:27	76°11.02'	137°09.15'	22	MUM
KD9508	R/1	09.10.	02:38	76°10.83'	138°00.60'	23	CTD
	R/2	09.10.	2:40-3:00	76°10.83'	138°00.60'	23	Sil,Oxy;FI
	-1	09.10.	02:41-02:56	76°11.01'	137°59.52'	21	MUM

Station #	Date	Time (Moscow)	Latitude (° N)	Longitude (° E)	Depth (m)	Activity
KD9509	R/1	09.10. 11:15	76°11.13'	138°27.42'	15	CTD
	R/2	09.10. 11:15-11:30	76°11.13'	138°27.42'	12.	Sil,Oxy;FI
	-1	09.10. 07:00-08:00	76°11.11'	138°31.32'	16	ROV
	-2	09.10. 08:33-08:41	76°11.10'	138°27.50'	16	Bio: BG
	-3	09.10. 08:45-08:47	76°11.10'	138°27.50'	16	Bio: BG
	-4	09.10. 08:48-08:51	76°11.10'	138°27.50'	16	Bio: BG
	-5	09.10. 08:53-08:55	76°11.10'	138°27.50'	16	Bio: BG
	-6	09.10. 08:57-08:59	76°11.14'	138°27.54'	16	Geo: BG (recovery 10 cm)
-7	09.10. 11:17-11:38	76°11.12'	138°27.60'	16	MUM	
KD9510		09.10. 15:01	76°53.06'	139°14.77'	20	begin of station
	R/1	09.10. 15:17	76°53.11'	139°14.92'	20	CTD
	R/2	09.10. 15:17-15:50	76°53.11'	139°14.92'	20	Sil,Oxy
	-1	09.10. 15:25-15:40	76°53.05'	139°14.77'	2	MUM
	-2	09.10. 15:40-15:45	76°53.04'	139°14.85'	20	Bio: BG
	-3	09.10. 15:58-16:00	76°53.03'	139°14.71'	20	Geo: 2 x BG (recovery 2 x 10 cm)
-4	09.10. 16:11-16:58	76°53.03'	139°14.75'	20	ROV	
KD9511	R/1	09.10. 19:31	77°14.02'	139°00.69'	28	CTD
	R/2	09.10. 19:35-20:00	77°14.02'	139°00.69'	28	Sil,Oxy
	-1	09.10. 19:36-20:00	77°13.86'	138°59.89'	27	MUM
	-2	09.10. 19:40-19:55	77°13.86'	138°59.89'	2, 20	WST
KD9512	R/1	09.10. 21:00	77°04.14'	138°59.93'	21	CTD
	R/2	09.10. 21:00-21:40	77°04.14'	138°59.93'	21	Sil,Oxy;FI
	2	09.10. 21:03	77°04.17'	138°59.41'	21	CTD
	-1	09.10. 20:57-21:11	77°04.15'	138°59.09'	20	MUM
KD9513	R/1	09.10. 22:18	76°54.17'	138°58.83'	20	CTD
	R/2	09.10. 22:20-23:00	76°54.17'	138°58.83'	20	Sil,Oxy;FI
	R/3	09.10. 22:15	76°54.19'	138°58.90'	20	CTD
	-1	09.10. 22:14-22:26	76°54.16'	138°59.01'	21	MUM
KD9514	R/1	09.10. 23:33	76°44.35'	138°59.54'	22	CTD
	R/2	09.10. 23:40	76°44.35'	138°59.54'	22	Sil,Oxy;FI
	-1	09.10. 23:25-23:35	76°44.20'	138°59.30'	21	MUM
KD9515	R/1	10.10. 00:44	76°34.00'	138°59.00'	24	CTD
	R/2	10.10. 00:50-01:20	76°34.00'	138°59.00'	24	Sil,Oxy;FI
	-1	10.10. 00:40-00:53	76°34.19'	138°59.61'	22	MUM
KD9516	R/1	10.10. 02:00	76°24.21'	139°28.00'	20	CTD
	R/2	10.10. 2:00-2:25	76°24.21'	139°28.00'	20	Sil,Oxy;FI
	-1	10.10. 01:57-02:08	76°24.21'	138°59.69'	20	MUM
KD9517		10.10.	76°14.29'	138°50.10'	18	begin of station
	R/1	10.10. 03:10	76°14.23'	138°49.11'	21	CTD
	R/2	10.10. 3:10-3:40	76°14.23'	138°49.11'	21	Sil,Oxy;Ph;FI
	-1	10.10.	76°14.29'	138°50.10'		Ice sampling
	-2	10.10. 04:55-04:58	76°14.29'	138°50.10'	18	Bio: BG
	-3	10.10. 05:00-05:04	76°14.29'	138°50.10'	18	Bio/Geo: BG (recovery 10 cm)
	-4	10.10. 05:50-06:02	76°14.29'	138°50.10'	18	UWP
	-5	10.10. 10:00-10:35	76°14.29'	138°50.10'	18	MUM
	-6	10.10. 09:43-09:47	76°14.29'	138°50.10'	2, 5, 10, 15	SPM, C-13/O-18/Methane, Chl, SACT
	-7	10.10. 10:15	76°14.29'	138°50.10'	1	WSB
-8	10.10. 10:25	76°14.29'	138°50.10'	1	WSB	
-9	10.10. 10:50	76°14.29'	138°50.10'	10	PN	
KD9518	R/1	10.10. 17:30	75°53.28'	134°31.33'	44	CTD

Station #	Date	Time (Moscow)	Latitude (° N)	Longitude (° E)	Depth (m)	Activity	
	R/2	10.10	17:30-18:05	75°53.28'	134°31.33'	44	Sil,Oxy;FI
	R/3	10.10	17:40	75°53.13'	134°31.99'	44	CTD
	R/4	10.10	17:48	75°53.16'	134°32.33'	46	CTD
	-1	10.10.	17:24-17:39	75°53.12'	134°31.79'	44	MUM
KD9519	R/1	10.10	19:26	75°35.20'	135°04.14'	39	CTD
	R/2	10.10	19:30-20:00	75°35.20'	135°04.14'	38	Sil,Oxy;FI
	-1	10.10.	19:29-19:48	75°35.05'	135°04.48'	37	MUM
KD9520	R/1	10.10	21:24	75°15.30'	135°21.40'	40	CTD
	R/2	10.10	21:30-22:05	75°15.30'	135°21.40'	40	Sil,Oxy;FI
	-1	10.10.	21:31-21:53	75°15.00'	135°21.07'	47	MUM
	-2	10.10.	21:30	75°15.00'	135°21.07'	2, 43	WST
KD9521	R/1	10.10	23:30	74°55.44'	135°53.60'	30	CTD
	R/2	10.10	23:30-23:59	74°55.44'	135°53.60'	30	Sil,Oxy;FI
	-1	10.10.	23:28-23:44	74°55.37'	135°53.31'	29	MUM
	-2	10.10.	23:28-23:40	74°55.37'	135°53.31'	2, 20	WST
KD9522	R/1	11.10	01:05	74°39.69'	135°45.44'	27	CTD
	R/2	11.10	1:05-1:45	74°39.69'	135°45.44'	27	Sil,Oxy;FI
	-1	11.10.	01:08-01:25	74°39.47'	135°45.95'	27	MUM
KD9523		11.10.	03:30	74°18.46'	135°27.61'	32	begin of station
	R/1	11.10	03:10	74°18.46'	135°27.44'	36	CTD
	R/2	11.10	3:10-3:30	74°18.46'	135°27.44'	36	Sil,Oxy;Ph;FI
	-1	11.10.	03:34-04:06	74°18.46'	135°27.61'	2, 5, 10, 15, 20, 25	SPM, C-13/O-18/Methane, Chl, SACT
	-2	11.10.	03:42-03:51	74°18.47'	135°26.98'	10	PN
	-3	11.10.	04:06-04:11	74°18.49'	135°26.90'	22	BN
	-4	11.10.	04:12-04:52	74°18.42'	135°26.99'		WSB
	-5	11.10.	05:01-05:24	74°18.45'	135°27.01'	32	Bio: BG
	-6	11.10.	05:25-05:35	74°18.46'	135°27.61'	32	Bio: BG (equipment lost)
	-7	11.10.	06:56-07:34	74°18.43'	135°26.98'	32	GKG (recovery: 46 cm)
	-8	11.10.	07:50-08:02	74°18.42'	135°26.91'	32	GKG (recovery: 47 cm)
	-9	11.10.	09:49-10:17	74°18.45'	135°27.00'	32	VC (no recovery)
	-10	11.10.	10:25-11:09	74°18.45'	135°27.00'		PC (test)
	-11	11.10.	10:56-11:18	74°18.44'	135°26.61'	32	VC (unsuccessfully, stopped)
	-12	11.10.	11:34-13:07	74°18.44'	135°26.41'	32	ROV
	-13	11.10.	14:16-14:40	74°18.42'	135°26.54'	32	MUM
	-14	11.10.	14:16-14:40	74°18.42'	135°26.54'	32	UWP
	-15	11.10.	15:24-15:56	74°18.31'	135°25.70'	32	Dredge
KD9524	R/1	11.10	17:51	74°00.11'	135°45.67'	36	CTD
	R/2	11.10	17:51-18:20	74°00.11'	135°45.67'	36	Sil,Oxy;FI
	-1	11.10.	17:53-18:13	74°00.06'	135°45.47'	37	MUM
KD9525	R/1	11.10	20:32	73°29.00'	135°37.04'	24	CTD
	R/2	11.10	20:32-21:00	73°29.00'	135°37.04'	24	Sil,Oxy;FI
	-1	11.10.	20:31-20:49	73°28.89'	135°37.07'	24	MUM
KD9526	R/1	11.10	23:16	73°00.08'	137°07.86'	24	CTD
	R/2	11.10	23:20-23:50	73°00.08'	137°07.86'	24	Sil,Oxy;FI
	-1	11.10.	23:13-23:52	73°09.03'	137°08.20'	16,5	MUM
KD9527	R/1	12.10	01:45	72°42.00'	137°49.81'	26	CTD
	R/2	12.10	1:45-2:20	72°42.00'	137°49.81'	26	Sil,Oxy;FI
	-1	12.10.	02:45-02:57	72°41.88'	137°50.00'	24	MUM
	-2	12.10.	02:50-03:00	72°41.88'	137°50.00'	2, 17	WST

Station #	Date	Time (Moscow)	Latitude (° N)	Longitude (° E)	Depth (m)	Activity	
KD9528	R/1	12:10	04:31	72°22.15'	136°33.13'	23	CTD
	R/2	12:10	4:35-5:00	72°22.15'	136°33.13'	23	Sil,Oxy,Fl
	R/3	12:10	04:36	72°22.18'	136°32.91'	23	CTD
	-1	12.10.	04:20-04:35	72°22.53'	136°33.11'	2, 2, 15	WST
	-2	12.10.	04:22-04:34	72°22.53'	136°33.11'	22	MUM
KD9529		12.10.	07:35	71°45.37'	135°44.93'	15	begin of station
	R/1	12.10.	08:27	71°45.16'	135°44.12'	16	CTD
	R/2	12.10.	8:30-9:00	71°45.16'	135°44.12'	16	Sil,Oxy,Ph,Fl
	R/3	13.10.	06:09-06:30	71°45.18'	135°44.19'	15	CTD
	-1	12.10.	08:00	71°45.17'	135°44.15'		Observation flight
	-2	12.10.	07:35-07:52	71°45.37'	135°44.93'		WST
	-3	12.10.	07:40-07:52	71°45.30'	135°44.87'	15	MUM
	-4	12.10.	08:33-08:41	71°45.15'	135°44.25'	10	PN
	-5	12.10.	08:38-08:44	71°45.15'	135°44.17'	2, 5, 10	SPM, C-13/O-18/Methane, Chl, SACT
	-6	12.10.	08:57-09:08	71°45.14'	135°44.19'	10	200 µ hand net
	-7	12.10.	09:00-09:09	71°45.14'	135°44.19'		WSB
	-8	12.10.	11:35-12:05	71°45.14'	135°44.19'		Ice sampling
	-9	12.10.	12:24-12:46	71°45.14'	135°44.19'		Ice sampling
	-10	13.10.	05:14	71°45.18'	135°44.19'	15	Bio: 4 x BG
	-11	13.10.	05:26	71°45.18'	135°44.19'	15	Geo: BG (recovery 10 cm)
	-12	13.10.	06:52-06:57	71°45.18'	135°44.19'		GKG (recovery 18 cm)
	-13	13.10.	07:10-07:17	71°45.18'	135°44.19'	15	GKG (recovery 15 cm)
	-14	13.10.	08:00	71°38.06'	135°22.15'		Ice sampling
	-15	13.10.	09:02-09:22	71°45.16'	135°44.17'	10, 13	PN, 200 µ handnet
-16	13.10.	09:08-09:20	71°45.14'	135°44.12'		WSB	
-17	13.10.	10:45-10:50	71°45.14'	135°44.12'	15	UWP	
-18	13.10.	10:55-11:10	71°45.14'	135°44.12'		PC	
-19	13.10.	11:12-11:16	71°44.61'	135°40.54'	2	Ice sampling	
KD9530	R/1	13.10.	14:44	72°20.13'	134°16.33'	21	CTD
	R/2	13.10.	14:45-15:20	72°20.13'	134°16.33'	21	Sil,Oxy,Fl
	-1		14:42-14:56	72°20'	134°15'	21	MUM
KD9531	R/1	13.10.	19:14	72°15.04'	130°55.12'	16	CTD
	R/2	13.10.	19:14	72°15.04'	130°55.12'	16	Sil,Oxy,Fl
	-1	13.10.	19:18-19:39	72°14.93'	130°55.12'	15	MUM
	-2	13.10.	19:25-19:30	72°14.93'	130°55.12'	2	WSB
KD9532	R/1	14.10.	03:09	71°05.18'	131°31.50'	14	CTD
	R/2	14.10.	3:10-3:25	71°05.18'	131°31.50'	14	SIL,Oxy,Ph
	R/3	14.10.	03:28	71°05.22'	131°31.57'	14	CTD
	-1	14.10.	03:30-03:40	71°05.20'	131°31.38'	2, 10	WST
	-2	14.10.	03:36-03:46	71°05.20'	131°31.38'	2, 5, 10	SPM, C-13/O-18/Methane, Chl, SACT
	-3	14.10.	03:04-03:20	71°05.20'	131°31.38'	14	MUM
KD9533		14.10.	05:30	71°14.45'	131°14.07'	14,5	begin of station
	R/1	14.10.	05:39	71°14.81'	131°14.48'	15	CTD
	R/2	14.10.	5:40-5:55	71°14.81'	131°14.48'	15	Sil,Oxy,Ph,Fl
	-1	14.10.	05:32-05:38	71°14.66'	131°14.07'	2, 12	WST
	-2	14.10.	05:38-05:52	71°14.81'	131°14.63'	14,5	MUM
	-3	14.10.	05:40-05:56	71°14.84'	131°14.73'	10	PN
	-4	14.10.	05:46-06:00	71°14.81'	131°14.86'	2, 5, 10	SPM, C-13/O-18/Methane, Chl, SACT
	-5	14.10.	06:01-06:06	71°14.91'	131°15.38'		WSB
	-6	14.10.	06:16-06:23	71°14.76'	131°15.37'	14,5	Bio: 5 x BG
	-7	14.10.	06:34-06:48	71°14.56'	131°15.36'	14,5	Geo: BG (recovery 10 cm)
-8	14.10.	08:25-08:29	71°13.91'	131°20.15'	14,5	GKG (no recovery)	
-9	14.10.	08:42-08:50	71°14.02'	131°20.64'		WSB	

Station #	Date	Time (Moscow)	Latitude (° N)	Longitude (° E)	Depth (m)	Activity
-10	14.10.	08:37-08:41	71°14.02'	131°20.64'	14,5	GKG (recovery 20 cm)
-11	14.10.	08:55-08:58	71°13.90'	131°20.79'	14,5	GKG (recovery 31 cm)
-12	14.10.	09:29-09:57	71°14.48'	131°21.89'		Ice sampling
-13	14.10.	10:08-10:36	71°14.50'	131°23.24'		Ice sampling
-14	14.10.	10:36-11:19	71°14.51'	131°24.19'		Ice sampling
-15	14.10.	11:24-11:40	71°14.56'	131°26.02'		Ice sampling
-16	14.10.	11:55-12:10	71°14.48'	131°26.76'		Ice sampling
-17	14.10.	12:15-12:20	71°14.52'	131°27.47'		Ice sampling
-18	14.10.	12:40-13:15			14,5	ROV
-19	14.10.	13:20-13:35	71°14.68'	131°30.37'	14,5	UWP
-20	14.10.					Ice sampling
<hr/>						
KD9534	R/1	14.10. 16:15	71°30.11'	130°30.10'	12	CTD
	R/2	14.10. 16:15-16:35	71°30.11'	130°30.10'	12	Sil,Oxy,FI
	-1	14.10. 16:17-16:29	72°30.13'	130°25.84'	12	MUM
<hr/>						
KD9535	R/1	14.10. 17:59	71°45.20'	130°30.62'	14	CTD
<hr/>						
KD9536	R/1	14.10. 19:19	72°00.00'	130°29.90'	15	CTD
	R/2	14.10. 19:20-19:40	72°00.00'	130°29.90'	15	Sil,Oxy,FI
	-1	14.10. 19:20-19:35	71°59.96'	130°30.04'	15	MUM
<hr/>						
KD9537	R/1	14.10. 21:01	72°15.17'	130°29.72'	14	CTD
<hr/>						
KD9538	R/1	14.10. 22:34	72°29.43'	130°30.13'	13	CTD
	R/2	14.10. 22:35-22:50	72°29.43'	130°30.13'	13	Sil,Oxy,FI
	-1	14.10. 22:36-22:40	72°29.53'	130°30.08'	12	MUM
<hr/>						
KD9539	R/1	15.10. 00:06	72°44.83'	130°29.66'	18	CTD
<hr/>						
KD9540	R/1	15.10. 01:41	73°01.28'	130°28.48'	23	CTD
	R/2	15.10. 1:45-2:05	73°01.28'	130°28.48'	23	Sil,Oxy,FI
	R/3	15.10. 01:50	73°01.29'	130°28.33'	24	CTD
	R/4	15.10. 01:58	73°01.17'	130°28.38'	23	CTD
	-1	15.10. 01:39-01:50	73°01.29'	130°28.63'	20,5	MUM
<hr/>						
KD9541		15.10. 03:30	73°18.42'	129°49.47'	22	begin of station
	R/1	15.10. 08:41	73°22.54'	129°56.70'	23	CTD
	R/2	15.10. 8:45-9:05	73°22.54'	129°56.70'	23	Sil,Oxy,Ph,FI
	-1	15.10. 03:44	73°18.42'	129°49.47'		Ice sampling
	-2	15.10. 03:44-04:07	73°18.42'	129°49.47'	2, 17	WST
	-3	15.10. 03:54-04:07	73°18.42'	129°49.47'	22	MUM
	-4	15.10. 04:10-04:30	73°18.42'	129°49.47'	2, 5, 10, 18	SPM, C-13/O-18/Methane, Chl, SACT
	-5	15.10. 04:22-04:44	73°19.07'	129°52.41'	10	PN, 200 µ handnet
	-6	15.10. 04:58-05:12	73°19.12'	129°52.78'		WSB
	-7	15.10. 05:40-06:10	73°20.91'	129°54.60'		Ice sampling
	-8	15.10. 06:13-06:30	73°20.54'	129°55.00'		Ice sampling
	-9	15.10. 06:32-06:44	73°20.70'	129°55.34'		Ice sampling
	-10	15.10. 06:45-07:06	73°20.84'	129°55.63'		Ice sampling
	-11	15.10. 08:31-08:40	73°22.58'	129°56.43'	22	Bio: 3 x BG
	-12	15.10. 08:41-08:44	73°22.66'	129°56.45'	22	Geo: BG (recovery 10 cm)
	-13	15.10. 08:51-08:59	73°22.80'	129°56.57'	22	GKG (recovery: 34 cm)
	-14	15.10. 08:50-09:05	73°22.80'	129°56.57'		WSB
	-15	15.10. 09:18-09:22	73°22.94'	129°57.27'	22	GKG (recovery: 32 cm)
	-16	15.10. 10:28-10:45	73°23.40'	129°59.04'	22	VC (no recovery)
	-17	15.10. 11:36-12:10	73°23.49'	130°01.19'	22	ROV
	-18	15.10. 12:15-12:35	73°23.49'	130°01.46'	22	UWP
<hr/>						
KD9542	R/1	15.10. 14:37	73°15.45'	130°31.32'	16	CTD
	R/2	15.10. 14:40-15:00	73°15.45'	130°31.32'	16	Sil,Oxy,FI

Station #	Date	Time (Moscow)	Latitude (° N)	Longitude (° E)	Depth (m)	Activity
KD9543	R/1	15.10. 16:10	73°29.80'	130°30.10'	26	CTD
	R/2	15.10. 16:10-16:35	73°29.80'	130°30.10'	26	Sil,Oxy;FI
	-1	15.10. 16:09	73°29.80'	130°30.10'	27	MUM
KD9544	15.10.	17:35	73°45.25'	130°29.95'	?	no measurements
KD9545	R/1	15.10. 19:04	74°00.00'	130°29.90'	24	CTD
	R/2	15.10. 19:05-19:30	74°00.00'	130°29.90'	24	Sil,Oxy;FI
KD9546	R/1	15.10. 22:11	74°30.10'	130°29.35'	25	CTD
	R/2	15.10. 22:15-22:40	74°30.10'	130°29.35'	25	Sil,Oxy;FI
	-1	15.10. 22:07-22:15	74°30.17'	130°30.10'	25	MUM
KD9547	R/1	16.10. 01:30	74°59.71'	130°28.68'	39	CTD
	R/2	16.10. 1:30-2:00	74°59.71'	130°28.68'	39	Sil,Oxy;FI
	-1	16.10. 01:00-01:19	74°59.89'	130°29.57'	38	MUM
KD9548		16.10. 03:50	75°29.71'	130°41.37'	39	begin of station
	R/1	16.10. 14:32	75°28.46'	130°41.22'	42	CTD
	R/2	16.10. 14:35-15:00	75°28.46'	130°41.22'	42	Sil,Oxy,Ph;FI
	-1	16.10. 03:55-04:15	75°29.79'	130°41.40'	2, 35	WST
	-2	16.10. 03:58-04:17	75°29.79'	130°41.40'	39	MUM
	-3	16.10. 04:38-04:44	75°29.70'	130°41.22'	2, 5, 10, 15, 20, 30	SPM, C-13/O-18/Methane, Chl, SACT
	-4	16.10. 04:44-05:04	75°29.67'	130°41.35'		Ice sampling
	-5	16.10. 04:30-04:44	75°29.67'	130°41.35'	10	PN, 200 µ handnet
	-6	16.10. 05:13-05:19	75°29.54'	130°41.53'		Ice sampling
	-7	16.10. 05:29-05:44	75°29.47'	130°41.65'	ca. 25	WSB
	-8	16.10. 05:55-06:15	75°29.16'	130°41.58'	20	BN
	-9	16.10. 06:23-06:33	75°29.11'	130°41.60'	39	UWP
	-10	16.10. 06:39	75°28.96'	130°41.66'	39	Bio: 3 x BG
	-11	16.10. 07:08-07:16	75°28.72'	130°41.74'	39	GKG (recovery: 37 cm)
	-12	16.10. 07:08-07:29	75°28.72'	130°41.74'		Ice sampling
	-13	16.10. 07:58-08:05	75°28.20'	130°41.62'	39	GKG (recovery: 40 cm)
	-14	16.10. 10:08-10:41	75°27.83'	130°41.22'		PC
-15	16.10. 09:50-11:00	75°27.83'	130°41.22'	39	ROV	
-16	16.10. 11:44-12:05	75°27.85'	130°41.19'	39	VC (recovery 160 cm)	
-17	16.10. 12:34-13:50	75°27.92'	130°41.00'	39	VC (recovery 220 cm)	
KD9549	R/1	16.10. 15:40	75°30.40'	131°17.07'	21	CTD
	R/2	16.10. 15:40-16:00	75°30.40'	131°17.07'	21	Sil,Oxy;FI
KD9550	R/1	16.10. 17:26	75°30.15'	131°59.37'	16	CTD
	R/2	16.10. 17:30-17:45	75°30.15'	131°59.37'	16	Sil,Oxy;FI
	-1	16.10. 17:23-17:33	75°30.27'	131°59.95'	17,5	MUM
KD9551	R/1	16.10. 19:05	75°29.98'	132°38.54'	15	CTD
	R/2	16.10. 19:05-19:20	75°29.98'	132°38.54'	15	Sil,Oxy;FI
KD9552	R/1	16.10. 20:53	75°29.66'	133°16.06'	24	CTD
	R/2	16.10. 20:55-21:20	75°29.66'	133°16.06'	24	Sil,Oxy;FI
	-1	16.10. 20:55-21:12	75°29.79'	133°15.71'	21,5	MUM
KD9553	R/1	16.10. 22:34	75°30.23'	133°00.19'	32	CTD
	R/2	16.10. 22:35-23:05	75°30.23'	133°00.19'	32	Sil,Oxy;FI
KD9554	R/1	17.10. 00:49	75°30.11'	135°14.50'	37	CTD
	R/2	17.10. 0:50-1:20	75°30.11'	135°14.50'	37	Sil,Oxy;FI
	R/3	17.10. 01:00	75°30.07'	135°14.53'	37	CTD

Station #	Date	Time (Moscow)	Latitude (° N)	Longitude (° E)	Depth (m)	Activity	
-1	17.10.	00:49-01:08	75°30.12'	135°14.49'	28,5	MUM	
KD9555	17.10.	02:35	75°31.92'	134°34.59'	36	begin of station	
R/1	17.10.	03:06-08:45	75°32.24'	134°04.06'	35	CTD	
R/2	17.10.	3:10-3:35	75°32.24'	134°04.06'	35	Sil,Oxy,Ph;Fl	
-1	17.10.	02:40-03:00	75°31.92'	134°34.59'	36	MUM	
-2	17.10.	04:06-04:21	75°33.22'	134°33.02'	2, 5, 10, 15, 20, 30	SPM, C-13/O-18/Methane, Chl, SACT	
-3	17.10.	04:15-04:35	75°33.22'	134°33.02'	10	PN	
-4	17.10.	04:30-04:52	75°34.16'	134°32.67'		Ice sampling	
-5	17.10.	04:52-05:28	75°34.16'	134°32.48'	36	UWP	
-6	17.10.	04:55-05:07	75°34.16'	134°32.48'		Ice sampling	
-7	17.10.	05:08-05:20	75°34.51'	134°32.19'		Ice sampling	
-8	17.10.	05:21-05:40	75°34.82'	134°31.90'		Ice sampling	
-9	17.10.	06:05	75°35.74'	134°31.40'	36	Bio: 4 x BG	
-10	17.10.	06:19-07:41	75°36.06'	134°31.34'	36	GKG (recovery: 38 cm)	
KD9556	R/1	17.10.	13:41	74°59.69'	132°30.04'	13	CTD
	R/2	17.10.	13:41-13:55	74°59.69'	132°30.04'	13	Sil,Oxy;Fl
	-1	17.10.	13:38-13:48	75°01.17'	132°29.97'		MUM
KD9557	R/1	17.10.	16:44	74°30.16'	132°30.59'	13	CTD
	R/2	17.10.	16:45-17:00	74°30.16'	132°30.59'	13	Sil,Oxy;Fl
	-1	17.10.	16:45-16:57	74°30.07'	132°31.74'	15	MUM
KD9558	R/1	17.10.	22:24	74°30.09'	128°29.76'	36	CTD
	R/2	17.10.	22:25-22:50	74°30.09'	128°29.76'	36	Sil,Oxy;Fl
KD9559	R/1	18.10.	01:47	74°30.06'	126°30.90'	36	CTD
	R/2	18.10.	1:50-2:15	74°30.06'	126°30.90'	36	Sil,Oxy;Fl
KD9560		18.10.	05:10	73°49.07'	126°20.21'	13	begin of station
	R/1	18.10.	07:35-10:18	73°47.55'	126°17.92'	12	CTD
	R/2	18.10.	7:35-7:50	73°47.55'	126°17.92'	12	Sil,Oxy,Ph;Fl
	-1	18.10.	05:28-05:40	73°48.62'	126°17.81'	2, 10	WST
	-2	18.10.	06:44-06:55	73°48.05'	126°16.86'	13	MUM
	-3	18.10.	07:10	73°47.93'	126°17.05'	13	Bio: 4 x BG
	-4	18.10.	07:25-12:00	73°47.93'	126°17.05'		Ice sampling
	-5	18.10.	07:31-07:35	73°47.77'	126°17.60'	13	Geo: BG (recovery:10 cm)
	-6	18.10.	09:24-09:45	73°47.02'	126°19.09'	13	MUM
	-7	18.10.	11:40-11:45	73°47.01'	126°19.09'	2, 5, 10	SPM, C-13/O-18/Methane, Chl, SACT
	-8	18.10.					Ice sampling
KD9561		18.10.	13:00	73°53.55'	126°50.81'	23	begin of station
	-1	18.10.	13:20	73°53.55'	126°50.81'		WSB
	-2	18.10.	13:25-13:45	73°53.80'	126°52.40'	23	UWP
	-3	18.10.	15:10-15:35	73°54.18'	126°54.86'	23	GKG (recovery: 54 cm)
	-4	18.10.	15:51-15:55	73°54.37'	126°56.17'	23	GKG (recovery: 38 cm)
KD9562	-1	19.10.	03:10-04:00	73°46.70'	126°48.70'	17	Ice sampling
	-2	19.10.	03:52-03:53	73°46.32'	126°56.49'	4	WST
KD9563		19.10.	06:04	73°51.24'	126°31.59'	15	begin of station
	R/1	19.10.	07:30-11:40	73°50.62'	126°39.19'	17	CTD
	-1	19.10.	06:14-11:30	73°51.24'	126°31.59'		Ice sampling
	-2	19.10.	10:18-10:50	73°49.31'	126°54.22'	10	PN, 200 μ handnet
	-3	19.10.	11:05-11:20	73°49.01'	126°58.18'	15	MUM
KD9564		20.10.	04:22	74°30.05'	114°35.28'	39	begin of station
	R/1	20.10.	11:53	74°36.97'	114°28.54'	35	CTD

Station #	Date	Time (Moscow)	Latitude (° N)	Longitude (° E)	Depth (m)	Activity	
R/2	20.10.	11:55-12:20	74°36.97'	114°28.54'	35	Sil,Oxy,Ph;FI	
R/3	20.10.	11:57	74°36.01'	114°28.59'	35	CTD	
-1	20.10.	07:31-10:46	74°32.97'	114°27.61'		Ice sampling	
-2	20.10.	09:30-09:33	74°33.99'	114°26.87'	10	PN, 200µ handnet	
-3	20.10.	09:45-10:13	74°34.31'	114°26.89'	39	MUM	
-4	20.10.	11:50-12:19	74°36.05'	114°28.52'		WSB	
-5	20.10.	12:45-13:15	74°36.80'	114°29.68'	39	UWP	
KD9565	21.10.	02:19	73°50.78'	120°11.31'	26	begin of station	
R/1	21.10.	06:01	73°50.85'	120°18.12'	23	CTD	
R/2	21.10.	6:05-6:25	73°50.85'	120°18.12'	23	Sil,Oxy,Ph;FI	
-1	21.10.	03:10	73°50.78'	120°11.31'		Ice sampling	
-2	21.10.	03:15-03:58	73°50.73'	120°13.59'		Ice sampling	
-3	21.10.	03:53-04:00	73°50.72'	120°14.92'	5, 10, 15, 20	SPM, C-13/O-18/Methane, Chl, SACT	
-4	21.10.	04:00-04:14	73°50.72'	120°15.25'		Ice sampling	
-5	21.10.	04:15-04:30	73°50.69'	120°15.65'		Ice sampling	
-6	21.10.	06:35-06:45	73°50.84'	120°18.07'	21	UWP	
-7	21.10.	06:50	73°50.84'	120°18.07'	21	PN, 200µ handnet	
-8	21.10.	06:55-07:40	73°50.84'	120°18.07'	21	Bio: BG	
-9	21.10.	07:25-08:45	73°50.84'	120°18.07'		Ice sampling	
-10	21.10.	07:30-07:40	73°50.84'	120°18.07'	2	Ice sampling	
-11	21.10.	07:50-07:55	73°50.76'	120°19.00'	21	GKG (recovery: 44 cm)	
-12	21.10.	08:12-08:20	73°50.95'	120°20.85'	21	GKG (recovery: 32 cm)	
-13	21.10.	08:40-08:52	73°50.96'	120°21.36'	21	MUM	
KD9566	R/1	21.10.	13:22	74°29.38'	119°59.88'	34	CTD
	R/2	21.10.	13:22-14:00	74°29.38'	119°59.88'	34	Sil,Oxy;FI
	-1	21.10.	13:35-13:58	74°29.53'	119°59.33'	22	MUM
KD9567	R/1	21.10.	18:20	75°29.66'	120°00.35'	43	CTD
	R/2	21.10.	18:20-18:50	75°29.66'	120°00.35'	43	Sil,Oxy;FI
	-1	21.10.	18:20	75°29.75'	120°00.17'	42	MUM
KD9568		22.10.	04:45	75°36.72'	114°31.83'	34	begin of station
	R/1	22.10.	05:41-06:41	75°32.30'	114°30.07'	22	CTD
	R/2	22.10.	7:15-7:35	75°32.30'	114°30.07'	22	Sil,Oxy,Ph;FI
	-1	22.10.	04:48	75°36.72'	114°31.83'		Ice sampling
	-2	22.10.	04:10	75°36.72'	114°31.83'		Ice sampling
	-3	22.10.	04:15	75°36.18'	114°31.85'	34	MUM
	-4	22.10.	05:22-05:53	75°34.39'	114°31.19'	10, 25	PN, 200 µ handnet
	-5	22.10.	05:55-06:20	75°33.55'	114°30.87'	34	MUM
	-6	22.10.	11:21-11:30	75°29.10'	114°27.63'	34	Bio: 3 x BG
	-7	22.10.	11:48-12:03	75°29.10'	114°28.90'	34	GKG (recovery: 40 cm)
	-8	22.10.	12:15-12:25	75°29.04'	114°29.75'	34	GKG (recovery: 38 cm)
	-9	22.10.	12:58-13:10	75°29.38'	114°30.41'		WSB
	-10	22.10.	12:58-13:07	75°29.38'	114°30.41'	34	UWP
	-11	22.10.	13:36-14:25	75°29.59'	114°32.52'	34	Dredge
KD9569	R/1	22.10.	19:44	76°24.53'	116°44.37'	53	CTD
	R/2	22.10.	19:45-20:25	76°24.53'	116°44.37'	53	Sil,Oxy,Ph;FI
	-1	22.10.	19:50-20:19	76°24.51'	116°45.22'	48	MUM
KD9570		23.10.	05:15	76°38.36'	112°53.39'	20	begin of station
	R/1	23.10.	07:21	76°36.64'	112°58.67'	22	CTD
	R/2	23.10.	7:25-7:50	76°36.64'	112°58.67'	22	Sil,Oxy,Ph;FI
	-1	23.10.	04:55-05:55				Ice sampling
	-2	23.10.	06:01-06:40	76°37.65'	112°55.45'		Ice sampling
	-3	23.10.	06:50-07:41	76°37.65'	112°55.45'		Ice sampling
	-4	23.10.	07:08-07:33	76°36.82'	112°57.91'	20	MUM
	-5	23.10.	08:00-08:23	76°36.82'	112°57.91'		Ice sampling

Station #	Date	Time (Moscow)	Latitude (° N)	Longitude (° E)	Depth (m)	Activity	
-6	23.10.	09:00-09:15	76°36.52'	113°09.11'	22	2 x PN: 20µm net lost	
-7	23.10.	09:28-09:33	76°36.52'	113°12.42'	2, 5, 10, 15	SPM, C-13/O-18/Methane, Chl, SACT	
KD9571	23.10.	13:38	77°01.66'	116°11.70'	42	begin of station	
R/1	23.10.	13:54	77°01.35'	116°12.48'	47	CTD	
R/2	23.10.	13:55-14:25	77°01.35'	116°12.48'	47	Sil,Oxy,Ph,Fl	
-1	23.10.	13:40-14:23	77°01.59'	116°11.96'	42	MUM	
-2	23.10.	13:48-14:07	77°01.59'	116°11.96'	42	Bio: 4 x BG	
-3	23.10.	14:04-14:12	77°00.98'	116°12.97'	42	Geo: BG (no recovery)	
-4	23.10.	14:15	77°00.83'	116°13.16'	5, 15, 25, 35	10-Be	
KD9572	23.10.	15:00	77°01.51'	116°03.15'	50	begin of station	
-1	23.10.	15:03-15:10	77°01.46'	116°03.08'	50	GKG (recovery: 42 cm)	
-2	23.10.	15:28-15:34	77°01.19'	116°02.13'	51	GKG (recovery: 10 cm)	
-3	23.10.	15:58-16:15	77°00.78'	116°00.13'	51	UWP	
KD9573	R/1	23.10.	21:33	77°30.95'	112°01.05'	60	CTD
	R/2	23.10.	21:35-22:10	77°30.95'	112°01.05'	60	Sil,Oxy,Fl
		23.10.	21:23-21:42	77°30.98'	112°01.11'	50	MUM (no measurements)
KD9574	R/1	24.10.	00:44	77°44.19'	110°05.51'	270	CTD
	R/2	24.10.	0:45-1:40	77°44.19'	110°05.51'	270	Sil,Oxy,Fl
KD9575	R/1	24.10.	08:07	78°15.16'	107°05.26'	30	CTD
	-1	24.10.	05:43	78°15.10'	107°05.14'		Ice sampling
	-2	24.10.	06:35	78°15.09'	107°05.14'		Ice sampling
	-3	24.10.	09:15-09:35	78°15.12'	107°05.13'	31	MUM

Abbreviations:

OC: Oceanographical measurements

CTD: Conductivity, Temperature, Depth

MUM: Modulares Umwelt Meßsystem

PC: Particle camera

HCh: Hydrochemistry

Oxy: Oxygen

Sil: Silicate

Ph: Phosphates

Fl: Fluorescence

Geo: Geology

GKG: Spade box corer

VC: Vibro corer

BG: Geological Greifer/Snapper

WS: Water sampling

SPM: Suspended matter

WST: Water sampling-trace elements

WSB: Water sampling-Beryllium

SACT: Salinity, Alkalinity, Chlorinity, TOC

C-13/O-18: Stable isotopes

Methane: Methane measurement

Chl: Chlorophyll measurements

BIO: Biological sampling

200 µ handnet: Zooplankton sampling

BN: Bongonet: Zooplankton sampling

UWP: Under Water Photography

ROV: Remotely Operated Vehicle

Dredge: Zoobenthos sampling

PN: Phytoplankton net

BG: Snapper

Tab. A 3: Ice stations occupied by ship and helicopter during the TRANSDRIFT III expedition

No	Date	Ship Station	Ice Station	Latitude [°N]	Longitude [°E]	Ship/Heli
1	06.10.1995	KD9501-01	KD9527901	80°10.01'	102°30.75'	S
2			KD9527902	80° 11,98'	102° 50,56'	H
3			KD9527903	80° 16,81'	102° 20,36'	H
4			KD9527904	80° 10,02'	101°59,79'	H
5	10.10.1995	KD9517-01	KD9528301	75° 56,0'	140° 00,0'	H
6			KD9528302	75° 59,3'	139° 35,1'	H
7			KD9528303	76° 03,1'	139° 25,5'	H
8			KD9528304	76° 09,8'	139° 02,1'	H
9	12.10.1995	KD9529-08	KD9528501	71°45.37'	135°44.93'	S
10	13.10.1995	KD9529-14	KD9528601	71° 38.06'	135° 22.15'	H
11		KD9529-19	KD9528602	71°44.61'	135°40.54'	S
12	14.10.1995	KD9533-20	KD9528701	70° 52.90'	131° 37.24'	H
13		KD9533-16	KD9528702	71°14.48'	131°26.76'	S
14			KD9528703	70° 52.05'	131° 38.32'	H
15	15.10.1995	KD9541-01	KD9528801	72° 48.41'	129° 18.64'	H
16			KD9528802	72° 45.04'	128° 07.74'	H
17			KD9528803	73° 07.34'	129° 09.92'	H
18		KD9541-09	KD9528804	73°20.70'	129°55.34'	S
21	16.10.1995	KD9548-04	KD9528901	75°29.67'	130°41.35'	S
22	17.10.1995	KD9555-07	KD9529001	75°34.51'	134°32.19'	S
23	18.10.1995	KD9560-04	KD9529101	73°47.93'	126°17.05'	S
24		KD9560-08	KD9529102	73°41.01'	125°59.16'	H
25			KD9529103	73°30.41'	126°26.68'	H
26			KD9529104	73°31.48'	126°28.18'	H
27			KD9529105	73°36.13'	126°24.91'	H
28			KD9529106	73°37.93'	126°25.14'	H
29	19.10.1995	KD9562-01	KD9529201	73°46.7'	126°51.82'	S
30		KD9563-01	KD9529202	73°51.24'	126°31.59'	S
31	20.10.1995	KD9564-01	KD9529301	74°32.97'	114°27.61'	S
32			KD9529302	74°26.93'	113°59.48'	H
33			KD9529303	74°32.01'	112°56.88'	H
34			KD9529304	74°34.07'	111°58.87'	H
35			KD9529305	74°35.51'	111°13.11'	H
36			KD9529306	74°40.19'	112°29.59'	H

No	Date	Ship Station	Ice Station	Latitude [°N]	Longitude [°E]	Ship/Heli
37			KD9529307	74°32.73'	114°03.90'	H
38	21.10.1995	KD9565-09	KD9529401	73°50.84'	120°18.07'	S
39		KD9565-01	KD9529402	73°55.15'	120°56.30'	H
40			KD9529403	74°03.55'	120°31.94'	H
41			KD9529404	73°57.04'	121°166.0'	H
42			KD9529405	73°57.32'	122°40.85'	H
43			KD9529406	73°55.43'	123°15.86'	H
44			KD9529407	73°56.70'	123°15.48'	H
45			KD9529408	73°51.58'	120°30.76'	H
46			KD9529409	73°51.65'	120°34.74'	H
47			KD9529410	73°52.17'	120°38.56'	H
48			KD9529411	73°52.40'	120°58.62'	H
49	22.10.1995	KD9568-02	KD9529501	75°36.72'	114°31.83'	S
50		KD9568-01	KD9529502	75°38.80'	114°07.23'	H
51			KD9529503	75°31.21'	113°33.85'	H
52			KD9529504	75°30.68'	113°41.79'	H
53			KD9529505	75°18.68'	114°31.59'	H
54			KD9529506	75°17.50'	114°04.75'	H
55			KD9529507	75°14.26'	114°06.38'	H
56			KD9529508	75°12.29'	114°08.50'	H
57	23.10.1995	KD9570-02	KD9529601	76°38.36'	112°53.39'	S
58		KD9570-01	KD9529602	76°28.01'	112°59.53'	H
59			KD9529603	76°27.99'	113°02.28'	H
60			KD9529604	76°30.27'	112°43.89'	H
61			KD9529605	76°31.73'	112°41.41'	H
62			KD9529606	76°32.42'	112°39.30'	H
63	24.10.1995	KD9575-02	KD9529701	78°15.1'	107°05.14	S
64		KD9575-01	KD9529702	79°21.98'	106°39.60'	H

Tab. A 4: Helicopter flights during the TRANSDRIFT III expedition

Date / Station	Flight No.	Ice Station	Landing Position	Departure Arrival	Participants	Comments
09.10.1995 KD9509	JD 282	KD9528201	76°18.0' N 140°19.9' E	9:00 10:55	Kolatschek Reimnitz Nürnberg Alexandrov Kassens Rohr	Reconnaissance Flight
	JD 282b		75°45.9' N 137°16.1' E	13:15 14:25	Thiede Kunz-Pirrung Kirndörfer Burmeister Tyshko Seikov	Reconnaissance Flight Coastal Processes
10.10.1995 KD9517	JD 283			6:10 7:30	Reimnitz Freitag Kolatschek Darovsky	Reconnaissance Flight SLAR
	JD 283b	KD9528301	75°65.0' N 140°00.0' E	8:15 8:45	Reimnitz Tyshko Kovalov Freitag Seikov	Shuttle Flight, Coastal Processes
			75°65.0' N 140°00.0' E	8:45 9:15	Juterzenka Tuschling	Shuttle Flight, Coastal Processes
			75°65.0' N 140°00.0' E	9:15 9:45	Schirmacher Cremer Burmeister Delgado Schulz	Shuttle Flight, Coastal Processes
				12:00 12:30	Hölemann Lindemann Cremer Schirmacher Tyshko Kovalov Delgado	Shuttle Flight
				12:30 13:00	Juterzenka Tuschling Schirmacher Burmeister Schulz	Shuttle Flight
	JD 283c	KD9528302	75°59.3' N 139°35.1' E	13:00 13:05	Reimnitz Freitag Hölemann Seikov Lindemann	Ice Station: Coastal Processes
	JD 283c	KD9528303	76°03.1' N 139°25.5' E	13:30 13:35	Reimnitz Freitag Hölemann Seikov Lindemann	Ice Station: Coastal Processes

Date / Station	Flight No.	Ice Station	Landing Position	Departure Arrival	Participants	Comments
	JD 283c	KD9528304	76°09.8' N 139°02.1' E	13:55 14:00	Reimnitz Freitag	Ice Station: Coastal Processes
	JD 283c			14:20 14:30	Hölemann Seikov Lindemann Reimnitz Freitag Hölemann Seikov Lindemann	Shuttel Flight
11.10.1995 KD9523	JD 284			9:10 9:57	Reimnitz Dimitrenko Freitag Lindemann	Reconnassaince Flight Stolbovoy-Island
12.10.1995 KD9529	JD 285		71°38.0' N 135°37.5' E	13:15 14:08	Reimnitz Alexandrov Kolatschek Lindemann Freitag Darovskikh	Reconnassaince Flight SLAR-Flight
	JD 285b			14:15 14:30	Burmeister Schmidt Piepenburg Kunz-Pirrung Schulz	
13.10.1995 KD9529	JD 286	KD9528601	71°38.0' N 135°37.5' E	8:29 8:36	Reimnitz Freitag Kovalov Seikov Lindemann	Shuttle Flight
	JD 286b		71°38.0' N 135°37.5' E	8:49 8:56	Tischkov Darovskikh Kirndörfer Burmeister Berger	Shuttle Flight
	JD 286c		71°38.0' N 135°37.5' E	9:00 9:35 9:40 9:48	Kolatschek Darovskikh Kolatschek Darovskikh Kovalov Tischkov	SLAR-Flight Shuttle Flight Refueling
			71°38.0' N 135°37.5' E	10:48 10:55 11:35 11:43	Kirndörfer Burmeister Berger	Shuttle Flight
	JD 286d			12:00 12:10 12:10 12:20	Reimnitz Freitag Kolatschek Lindemann Seikov Burmeister	Shuttle Flight
14.10.1995 KD9533	JD 287			8:30 9:04	Reimnitz Freitag Alexandrov Kolatschek Strachov	Reconnassaince

Date / Station	Flight No.	Ice Station	Landing Position	Departure Arrival	Participants	Comments
	JD 287b	KD9528701	70°52.9' N 131.37.2' E	10:10 12:22	Tischko Lindemann Reimnitz Freitag	Reconnaissance Flight
	JD 287c			14:35 15:20	Alexandrov Kolatschek Strachov Tischko Lindemann Darovskikh Kolatschek Benthien Haase Peregovich	SLAR-Flight
15.10.1995 KD9541	JD 288	KD9528801	72°48.4' N	9:35	Lindemann	Reconnaissance Flight
		KD9528802	129°18.6' E	13:21	Reimnitz	Delta Processes
			72°45.0' N		Freitag	
			128°07.7' E		Alexandrov	
		KD9528803	73°07.3' N		Cremer	
			129°09.9' E		Burmeister	
17.10.1995 KD9555	JD290			8:30 9:45	Reimnitz Lindemann Kolatschek Freitag Thiede, R. Alexandrov	Reconnaissance Flight Stolbovoy Island
18.10.1995 KD9560	JD 291	KD9529102	73°41.0' N	10:45	Reimnitz	Reconnaissance Flight
			125°59.1' E		Freitag	Ice Stations
		KD9529193	73°30.4' N		Seikov	
			126°26.6' E		Alexandrov	
		KD9529104	73°31.4' N		Lindemann	Hovering
			126°28.1' E		Peregovich	
		KD9529105	73°36.1' N			Hovering
			126°24.9' E			
		KD9529106	73°37.9' N			Hovering
			126°25.1' E			
	JD291b				Freitag Darovskikh Langner Siebold Rossak	SLAR and Video Flight
19.10.1995 KD9562	JD292			8:25 8:54	Tyschko Lindemann	Reconnaissance Flight
20.10.1995 KD9564	JD293	KD9529302	74°26.9' N	9:10	Reimnitz	Ice Sampling
			113°59.4' E	11:15	Freitag	
		KD9529303	74°32.0' N		Lindemann	
			112°56.8' E		Berger	
		KD9529304	74°34.0' N			
			111°58.8' E			
		KD9529305	74°35.5' N			
			111°13.1' E			
		KD9529306	74°40.1' N			
			112°29.5' E			
		KD9529307	74°32.7' N			
			114°03.9' E			
	JD293b			11:45 12:15	Kirndörfer Burmeister Dimitrenko Fürst / Strobel	Reconnaissance Flight

Date / Station	Flight No.	Ice Station	Landing Position	Departure Arrival	Participants	Comments
	JD293c			12:15 13:45	Alexandrov Darovsky Kolatschek Piepenburg Schmidt	SLAR-Flight Reconnaissance Flight (Green Ice)
21.10.1995 KD9565	JD294	KD9529402	73°55.1' N 120°56.3' E	6:15 8:45	Reimnitz Freitag Lindemann	Ice Sampling
		KD9529403	74°03.5' N 120°31.9' E			
		KD9529404	73°57.0' N 121°16.6' E			
		KD9529405	73°57.3' N 122°40.8' E			
		KD9529406	73°55.4' N 123°15.8' E			
		KD9529407	73°56.7' N 123°15.4' E			
	JD294b			9:15 10:30	Darovskikh Alexandrov Kolatschek Rohr	SLAR-Flight
	JD294c	KD9529408	73°51.5' N 120°30.7' E	11:30 12:16	Juterzenker Antonow Schmidt Piepenburg Tuschling Cremer	Ice Sampling
		KD9529409	73°51.6' N 120°34.7' E			
		KD9529410	73°52.2' N 120°38.5' E			
		KD9529411	73°52.4' N 120°58.6' E			
22.10.1995 KD9568	JD295	KD9529502	75°38.8' N 114°07.2' E	6:48 8:20	Lindemann Reimnitz Freitag Alexandrov	Ice Sampling
		KD9529503	75°31.2' N 113°33.8' E			
		KD9529504	75°30.6' N 113°41.7' E			
		KD9529505	75°18.6' N 114°31.5' E			
		KD9529506	75°17.5' N 114°04.7' E			
	JD295b			9:20 10:40	Darovskikh Kolatschek Schirmacher Hölemann Schulz	SLAR-Flight
	JD295c	KD9529507	75°14.2' N 114°06.3' E	11:20 12:30	Juterzenka Tuschling Cremer Lindemann	Ice Sampling
		KD9529508	75°12.2' N 114°08.5' E			
23.10.1995 KD9570	JD296	KD9529602	76°28.0' N 112°59.5' E	6:55 7:55	Reimnitz Freitag Lindemann Alexandrov	Ice Sampling
		KD9529603	76°27.9' N 113°02.2' E			
		KD9529604	76°30.2' N 112°43.8' E			
		KD9529605	76°31.7' N 112°41.4' E			
		KD9529606	76°32.4' N 112°39.3' E			

Date / Station	Flight No.	Ice Station	Landing Position	Departure Arrival	Participants	Comments
24.10.1995 KD9575	JD297	KD9529702	79°21.9' N 106°39.6' E	5:43	Freitag	Shuttle Flight
				11:45	Reimnitz Kolatschek Seikov Langner Lindemann	
	JD297b				Kirndörfer Berger Burmeister Kunz-Pirrung Schirmacher	
	JD297c			10:15 11:25	Alexanddrov Darovskikh Kolatschek Fürst	SLAR-Flight

Tab. A 5: Ice Observations aboard KAPITAN DRANITSYN (5 - 24 Oct., 1995)

Key:

Time	UTC
Code for floe size	0 Pancake
	1 Brash
	2 Ice cake
	3 Small floe (20-100 m)
	4 Medium floe (100-500 m)
	5 Big floe (500-2000 m)
	6 Vast floe (2-10 km)
	7 Giant floe (>10 km)
	8 Fast ice
Code for type of dirty ice	1 Sediments only at surface
	2 Sediments only in the interior
	3 Sediments at surface and interior

Observers: V. Alexandrov, H. Cremer, A. Darovskikh, J. Freitag, J. Kolatschek, S. Kovalev, F. Lindemann, E. Reimnitz, M. Strakhov, K. Tyshko, F. Valero Delgado, A. Zachek

Date	13. Oct 13:19	13. Oct 16:18	13. Oct 18:00	13. Oct 20:00	13. Oct 22:00	14. Oct 8:09	14. Oct 9:00	14. Oct 11:00	14. Oct 12:00
Lat. [DD MM]	72 18	72 15	71 55	71 26	71 05	71 14	71 13	71 15	71 30
Lon. [DD MM]	133 09	130 55	131 05	131 21	131 31	131 25	131 27	131 29	130 31
Bright/Dark	D	D	D	D	B	B	D	D	D
Total Ice Cover	0	3	8	8	10	8	8	10	1-3
Grease/Slush	-	3	3	3	-	-	-	-	-
Pancake Ice	-	-	5	-	-	-	-	-	1-2
Dark Nilas	-	-	-	5	-	4	3	-	1-2
Light Nilas	-	-	-	-	10	4	5	-	-
Grey/Grey-White	-	-	-	-	-	-	-	10	-
White	-	-	-	-	-	-	-	-	-
Brash Ice	-	-	-	-	-	-	-	-	-
Maximal Level Ice Thickness	-	-	0.5	0.1	0.06	0.15	0.1	0.3	0.1
Snow Thickness	-	-	-	0.05	0.05	0.03	0.02	0.05	-
Average Floe Size (see codes)	-	-	2	2-3	3	3	3	4	3
Maximum Floe Size (see codes)	-	-	2	3	4	3	3	5	3
Percent of Total Ice Dirty	-	-	-	-	-	30	-	-	-
Type of Dirty Ice (see codes)	-	-	-	-	-	3	-	-	-

Date Time	18. Oct 3:00	18. Oct 9:00	18. Oct 19:00	18. Oct 20:30	18. Oct 22:00	18. Oct 23:00	19. Oct 0:00	19. Oct 5:00	19. Oct 9:00
Lat. [DD MM]	73 48	73 82	73 57	73 58	73 58	73 48	73 47	73 50	73 50
Lon. [DD MM]	126 16	126 47	127 11	127 15	127 17	126 58	126 51	126 41	126 59
Bright/Dark	B	D	D	D	D	B	B	B	D
Total Ice Cover	6	8-9	9-10	3	3	5	9	10	10
Grease/Slush	2	-	-	-	-	-	-	-	-
Pancake Ice	-	4	-	-	-	-	-	2	-
Dark Nilas	-	5	4	-	-	5	9	3	3
Light Nilas	2	-	-	1	2	-	-	5	-
Grey/Grey-White	2	-	5	2	1	-	-	-	7
White	-	-	-	-	-	-	-	-	-
Brash Ice	-	-	-	-	-	-	-	-	-
Maximal Level Ice Thickness	0.2	0.15	0.2	0.15	0.15	0.08	0.05	0.15	0.15
Snow Thickness	0.05	0.02	0.05	0.03	0.03	0.01	-	0.05	0.05
Average Floe Size (see codes)	3	2	3	2	2	3	3	3	4
Maximum Floe Size (see codes)	3	2	3	2	5	4	4	4	4
Percent of Total Ice Dirty	-	-	-	-	-	-	100	40	-
Type of Dirty Ice (see codes)	-	-	-	-	-	-	3	3	-

	20. Oct		20. Oct		20. Oct		20. Oct		20. Oct		20. Oct		21. Oct	
	12:00	13:00	14:15	15:00	16:00	18:00	20:00	20:00	20:00	20:00	21:00	21:00	21:00	8:00
Lat. [DD MM]	74 39	74 39	74 37	74 35	74 33	74 34	74 32	74 32	74 32	74 20	74 20	74 00	74 00	
Lon. [DD MM]	115 40	116 36	117 41	118 23	119 10	119 21	119 29	119 29	119 35	119 35	119 35	119 58	119 58	
Bright/Dark	D	D	D	D	D	D	D	D	D	D	D	B	B	
Total Ice Cover	9	10	9	6	8	10	10	10	10	10	10	10	10	
Grease/Slush	?	-	-	-	-	-	-	-	-	-	-	-	-	
Pancake Ice	?	-	-	-	-	-	-	-	-	-	-	-	-	
Dark Nilas	?	-	3	4	6	6	-	-	-	-	-	4	4	
Light Nilas	?	10	4	2	2	4	6	6	10	10	10	5	5	
Grey/Grey-White	?	-	2	-	-	-	4	4	-	-	-	1	1	
White	?	-	-	-	-	-	-	-	-	-	-	-	-	
Brash Ice	?	-	-	-	-	-	-	-	-	-	-	-	-	
Maximal Level Ice Thickness	?	0.1	0.15	0.15	0.1	0.10	0.15	0.15	0.2	0.2	0.2	0.12	0.12	
Snow Thickness	?	0.03	0.03	0.03	0.03	0.03	0.05	0.05	0.07	0.07	0.07	0.02	0.02	
Average Floe Size (see codes)	?	4	4	4	4	4	4	4	4	4	4	4	4	
Maximum Floe Size (see codes)	?	4	4	4	4	4	4	4	4	4	4	4	4	
Percent of Total Ice Dirty	?	-	-	-	-	-	-	-	-	-	-	-	-	
Type of Dirty Ice (see codes)	?	-	-	-	-	-	-	-	-	-	-	-	-	

Date Time	24. Oct 10:00	24. Oct 12:00	24. Oct 13:00	24. Oct 14:00	24. Oct 15:15	24. Oct 18:10	24. Oct 21:00
Lat. [DD MM]	78 15	77 52	77 41	77 35	77 16	76 59	76 13
Lon. [DD MM]	105 20	103 48	103 05	102 37	101 02	99 44	92 32
Bright/Dark	-	-	-	D	D	-	B
Total Ice Cover	8	6	8-9	9	9-10	8-9	9
Grease/Slush	-	-	-	-	-	-	-
Pancake Ice	-	-	-	-	-	-	-
Dark Nilas	4	-	4-5	3	-	-	8
Light Nilas	3	2	4	6	2	3	1
Grey/Grey-White	1	4	-	-	7	6	-
White	-	-	-	-	-	-	-
Brash Ice	-	-	-	-	-	-	-
Maximal Level Ice Thickness	0.15	0.3	0.2	0.2	0.3	0.3	0.1
Snow Thickness	0.03	0.03	0.03	0.03	0.04	0.04	0.01
Average Floe Size (see codes)	3	2	2	3	3	2	3
Maximum Floe Size (see codes)	4	3	3	4	4	3	3
Percent of Total Ice Dirty	-	-	-	-	-	-	-
Type of Dirty Ice (see codes)	-	-	-	-	-	-	-

Tab. A 7: List of ice samples taken during the TRANSDRIFT III expedition

Ice station	Equipment	Sea-ice sediments	Heavy minerals	Micropaleontology	SPM	Particulate organic matter	Sub-ice zooplankton	Obs. of sub-ice zooplankton	Chlorophyll a	Trace elements	PCB	Nutrients	Salinity	Porosity	Isotopes (O-18)	Crystal structure	Temperature	Ice thickness	Density	Driftwood
KD95-279-01	Ship	X		X			X	X	X			X	X		X	X	X	X	X	
KD95-279-02	Heli	X								X										
KD95-279-03	Heli	X																		
KD95-279-04	Heli	X																		
KD95-282-01	Heli																			X
KD95-283-01	Heli	X	X	X				X	X	X	X	X	X		X	X	X	X	X	X
KD95-283-02	Heli	X	X									X	X		X					X
KD95-283-03	Heli	X										X	X		X					
KD95-283-04	Heli	X										X	X	X	X					
KD95-285-01	Ship	X		X				X	X	X		X			X	X		X		
KD95-286-01	Heli	X	X	X				X					X		X	X				
KD95-286-02	Ship	X			X			X							X	X				
KD95-287-01	Heli	X	X	X					X			X	X		X	X		X		
KD95-287-02	Ship	X		X	X	X		X	X	X	X	X	X		X	X	X	X		
KD95-287-03	Heli																			X
KD95-288-01	Heli	X	X	X								X	X		X	X	X	X		
KD95-288-02	Heli	X	X		X	X														
KD95-288-03	Heli	X	X	X								X	X		X	X	X	X		
KD95-288-04	Ship	X			X	X		X	X	X										
KD95-289-01	Ship	X		X	X	X		X				X	X		X	X		X		
KD95-290-01	Ship	X		X	X	X		X	X	X	X	X	X		X	X	X	X		
KD95-291-01	Ship	X		X		X	X	X	X	X	X	X	X		X	X	X	X	X	
KD95-291-02	Heli	X										X			X	X		X		
KD95-291-03	Heli	X													X		X	X		X
KD95-291-04	Heli											X			X	X		X		
KD95-291-05	Heli											X			X	X		X		
KD95-291-06	Heli											X			X	X		X		
KD95-292-01	Ship	X		X			X	X	X	X	X	X	X		X	X		X		
KD95-292-02	Ship	X		X	X	X	X	X	X	X										
KD95-293-01	Ship	X		X		X	X	X	X			X	X		X	X	X	X	X	
KD95-293-02	Heli	X										X			X	X		X		
KD95-293-03	Heli	X										X			X	X		X		
KD95-293-04	Heli	X										X			X	X		X		
KD95-293-05	Heli	X										X			X	X		X		
KD95-293-06	Heli	X										X			X	X		X		
KD95-293-07	Heli	X																		
KD95-294-01	Ship	X		X	X	X		X	X	X	X	X	X		X	X		X		
KD95-294-02	Heli	X		X								X			X	X		X		
KD95-294-03	Heli	X		X								X			X	X		X		
KD95-294-04	Heli	X	X	X	X	X						X	X		X	X		X		

Ice station	Equipment	Sea-ice sediments	Heavy minerals	Micropaleontology	SPM	Particulate organic matter	Sub-ice zooplankton	Obs. of sub-ice zooplankton	Chlorophyll a	Trace elements	PCB	Nutrients	Salinity	Porosity	Isotopes (O-18)	Crystal structure	Temperature	Ice thickness	Density	Driftwood
KD95-294-05	Heli							X												
KD95-294-06	Heli	X		X								X	X		X	X		X		
KD95-294-07	Heli	X	X																	
KD95-294-08	Heli			X				X												
KD95-294-09	Heli			X				X												
KD95-294-10	Heli							X												
KD95-294-11	Heli							X												
KD95-295-01	Ship	X	X					X				X	X		X	X	X	X	X	X
KD95-295-02	Heli	X	X						X			X			X	X		X		
KD95-295-03	Heli	X										X			X	X		X		
KD95-295-04	Heli	X										X			X	X		X		
KD95-295-05	Heli	X										X			X	X		X		
KD95-295-06	Heli	X										X			X	X		X		
KD95-295-07	Heli			X																
KD95-295-08	Heli			X																
KD95-295-09	Heli			X																
KD95-296-01	Ship	X	X			X		X				X	X		X	X	X	X	X	X
KD95-296-02	Heli	X	X						X			X			X	X		X		
KD95-296-03	Heli							X												
KD95-296-04	Heli							X												
KD95-296-05	Heli	X	X																X	
KD95-296-06	Heli	X	X									X			X	X		X		
KD95-297-01	Ship			X			X	X	X											
KD95-297-02	Heli								X							X				

Tab. A 8: Description of sediment cores taken during the TRANSDRIFT III expedition

KD9502-12 BG

Loc.: Yana Valley

TRANSDRIFT III

Recovery: 0,10 m

76°11.520'N 133°06.990'E

Water depth: 46 m

Surface		Clayey silt, olive-gray, smooth surface (Clayey Quartz Mud)			T= °C
Color :					
Lithology	Grain size	Texture	Color	Description	ss
				Clayey silt, olive-gray, smooth surface	
				Clayey silt, black, homogenous, few polychaet tubes, small crustaceans common (Clayey Quartz Mud)	
EOC 10 cm					
Depth in core (cm)					
0					
10					
20					
30					
40					
50					

KD9502-14 VC

LOC.: Yana Valley

TRANSDRIFT III

Recovery: 2,3 m

76°11.520' N 133°06.990' E

Water depth: 46 m

(m)	Lithology	Grain size	Texture	Color	Description	SS
0.0				10YR3/2	(Clayey) sandy silt, olive-gray, bioturbated, one isopod (<i>Saduria</i> sp.) in the uppermost sediment layer (Clayey Quartz Mud)	4cm
0.1						50 cm
0.2						50 cm
0.3						50 cm
0.4						50 cm
0.5						50 cm
0.6						50 cm
0.7						50 cm
0.8						50 cm
0.9						50 cm
1.0						100 cm

KD9502-14 VC

LOC.: Yana Valley

TRANSDRIFT III

Recovery: 2,30 m

76°11.520' N 133°06.990' E

Water depth: 46 m

(m)	Lithology	Grain size	Texture	Color	Description	SS
1.0						
1.1						
1.2				10YR3/2 2.5Y2/N2	(Clayey) sandy silt as above, increasingly darkening downcore due to Mn and Fe precipitates, bioturbated, bivalve fragments all over the core, large shell (1 cm in diameter) at 138 cm (Clayey Quartz Mud)	
1.3						
1.4						
1.5						150 cm
1.6						
1.7						
1.8						
1.9						
2.0						200 cm

KD9502-14 VC

LOC.: Yana Valley

TRANSDRIFT III

Recovery: 2,30 m

76°11.520' N 133°06.990' E

Water depth: 46 m

(m)	Lithology	Grain size	Texture	Color	Description	SS
2.0				10YR3/2	Clayey sandy silt as above, increasingly darkening downcore due to Mn and Fe precipitates, bioturbated (Clayey Quartz Mud)	230 cm
2.1				2.5Y2/N2		
2.2						
2.3	EOC 2,3 m					
2.4						
2.5						
2.6						
2.7						
2.8						
2.9						
3.0						

KD9509-6 BG

Loc.: off Kotelnny Island

TRANSDRIFT III

Recovery: 0,10 m

76°11.140'N 138°27.540'E

Water depth: 16.4m

Surface	Gravel in sandy silty matrix, olive-gray, pebbles up to 5 cm in diameter, surface disturbed due to sampling procedure (Clayey Quartz Mud with Gravel)	T= °C
Color :		

Lithology	Grain size	Texture	Color	Description	ss
0				Gravel in sandy silty matrix, olive-gray, increasingly darkening downcore, pebbles up to 5 cm in diameter (Clayey Quartz Mud with Gravel)	
EOC 10 cm					
10					
20					
30					
40					
50					

KD9510-3 BG

Loc.: northernmost location **TRANSDRIFT III**
off Kotelnýy Island

Recovery: 0,10 m

76°53.035 N 139°14.719 E

Water depth: 19.6 m

Surface	Fine sand, well-sorted, flat surface with few ophiuredians and holothuroideans, small pebbles (< 1 cm in diameter) common (Quartz Mud)	T=	°C
Color :			

Depth in core (cm)	Lithology	Grain size	Texture	Color	Description	ss
	0					Fine sand, well-sorted, flat surface with few ophiuredian sand holothuroideans, small pebbles (< 1 cm in diameter) common (Quartz Mud)
10	EOC 10 cm					
20						
30						
40						
50						

KD9519-11 BG

Loc.: west of Kotelnny Island **TRANSDRIFT III**

Recovery: 0,10 m

75°35.059`N 135°04.487`E

Water depth: 37.0 m

Surface	Sandy clayey silt, uneven surface, bivalve fragments common, oxic colors (Quartz Mud)	T= °C
Color :		

Lithology	Grain size	Texture	Color	Description	ss
0				Sandy clayey silt, uneven surface, bivalve fragments common, oxic colors (Quartz Mud)	0 cm
EOC 10 cm					
10					
20					
30					
40					
50					

KD9523-7 GKG

Loc.: north of Stolbovoy

TRANSDRIFT III

Recovery: 0,46 m

74°18.439 N 135°26.980 E

Water depth: 32.0 m

Surface	Clayey silt, homogeneous, bioturbated, smooth surface, bivalves and bivalve fragments common (<i>Yoldia amygdalea</i>), isopods, surface probably contaminated by metal flitters	T= -1.6 °C
Color :	1.3Y 2.6/1.0 L: 27.20 a: 2.99 b: 6.63	
	(Clayey Quartz Mud)	

Lithology	Grain size	Texture	Color	Description	ss
			L: 27.20 a: 2.99 b: 6.63	Clayey silt as above, oxic colors	0 cm
					3 cm
			6.1GY 3.8/0.3 L: 38.91 a: -0.73 b: -1.22	Clayey silt, homogeneous, bioturbated, color darkening downcore, black streaks and mottles, bivalve fragments at 11 cm, 19 cm (Clayey Quartz Mud)	20 cm
			7.6GY 3.0/0.4 L: 31.18 a: -1.06 b: 1.08		40 cm
EOC 46 cm					

KD9523-8 GKG

Loc.: north of Stolbovoy

TRANSDRIFT III

Recovery: 0,47 m

74°18.423 N 135°26.912 E

Water depth: 32.0 m

Surface	Silty clay, homogeneous, bioturbated, smooth surface, bivalves and bivalve fragments common, isopods (<i>Saduria</i> sp.)	T= °C
(Clayey Quartz Mud)		
Color :	1.5Y 2.2/ 0.9 L: 23.52 a: 2.66 b: 5.83	

Lithology	Grain size	Texture	Color	Description	ss
			L: 23.52 a: 2.66 b: 5.83	Silty clay as on surface, oxic colors	0 cm
			6.2GY 3.3/0.4 L: 33.91 a: -1.01 b: 1.56	Silty clay, homogeneous, bioturbated, color darkening downcore, black streaks and mottles, bivalve fragments, worm burrows (- 1 cm in diameter) (Clayey Quartz Mud)	
EOC 47 cm			8.0GY 3.3/0.4 L: 33.78 a: -1.13 b: 1.08		

KD9529-12 GKG

Loc.: north of Yana Delta

TRANSDRIFT III

Recovery: 0,18 m

71°45.181 N 135°44.208 E

Water depth: 15.0 m

Surface	Silt, uneven, wavy surface, stones (-0.5 cm in diameter) common, bivalve fragments (<i>Portlandia silligna</i> , estuarine species) and polychaet tubes common	T= -0.7 °C
Color :	3.2Y 2.8/1.2	L: 29.17 a: 2.66 b: 8.15
(Quartz Mud with Clay)		

Depth in core (cm)	Lithology	Grain size	Texture	Color	Description	ss
	0					
10				3.2Y 2.8/1.2 L: 29.17 a: 2.66 b: 8.15	(Sandy) silt, homogeneous, stones (-0.5 cm in diameter) common, bivalve fragments and polychaet tubes common (Quartz Mud with Clay)	10 cm
18					Silt, changing to black color, very stiff (overconsolidated?)	18 cm
20	EOC 18 cm					
30						
40						
50						

KD9541-12 BG

Loc.: off Lena Delta

TRANSDRIFT III

Recovery: 0,10 m

73°22.663 N 129°56.457 E

Water depth: 22.0 m

Surface	Sandy silt, flat surface, polychaet burrows, tubes, small pebbles, and bivalve fragments common (Clayey Quartz Mud)	T= °C
Color :		

Depth in core (cm)	Lithology	Grain size	Texture	Color	Description	ss
	0					Sandy silt, flat surface, polychaet burrows, tubes, small pebbles, and bivalve fragments common (Clayey Quartz Mud)
10	EOC 10 cm					
20						
30						
40						
50						

KD9548-13 GKG

Loc.: 30 mls west of
Belkovsky Island

TRANSDRIFT III

Recovery: 0,41 m

75°28.200 N 130°41.622 E

Water depth: 39.0 m

Surface	Sandy silt, flat surface, rich benthic life: many ophiuredeans, bivalves, polychaets, isopods (<i>Saduria sp.</i>), worm tubes sticking out of sediment surface	T = - 1.7 °C
Color :	2.5Y 3/2 Munsell Color Chart	

Depth in core (cm)	Lithology	Grain size	Texture	Color	Description	ss
	0				2.5Y 3/2	Sandy silt, homogeneous, bioturbated, oxic colors
10				2.5Y 3/2	Sandy silt, homogeneous, bioturbated, polychaet burrows and bivalve fragments common, darkening downcore, appears nearly black due to black streaks and mottles, downcore increasing stiffness due to overconsolidation, but not as hard as core KD9541-13	10 cm
20				2.5Y 2/N2		30 cm
30						
40						
EOC 41 cm						
50						

KD9548-16 VC

LOC.: 30 mls west of Belkovsky

TRANSDRIFT III

Recovery: 1.21 m

75°27.857 N 130°41.194 E

Water depth: 43 m

(m)	Lithology	Grain size	Texture	Color	Description	SS
0				2.5Y3/2	Sandy silt, oxic colors, homogeneous, bioturbated (very dark grayish brown)	0 cm
.1				2.5Y3/2	Sandy silt, oxic colors, homogeneous, bioturbated (very dark grayish brown) (Clayey Quartz Mud)	10 cm
.2				2.5Y3/2	From 10-40 cm gradual change to black color	20 cm
.3				2.5Y3/2		30 cm
.4				2.5Y2/N2	Below 40 cm: Sandy silt, homogeneous, bioturbated, dominantly black colors, black streaks and mottles, H ₂ S-odor (Clayey Quartz Mud)	40 cm
.5				2.5Y2/N2		50 cm
.6				2.5Y2/N2		60 cm
.7				2.5Y2/N2		70 cm
.8				2.5Y2/N2		80 cm
.9				2.5Y2/N2		90 cm
1.0				2.5Y2/N2		100 cm

KD9548-16 VC

LOC.: 30 mls west of Belkovsky

TRANSDRIFT III

Recovery: 1.21 m

75°27.857 N 130°41.194 E

Water depth: 43 m

(m)	Lithology	Grain size	Texture	Color	Description	SS
1.0				2.5Y2/N2	Sandy silt, homogeneous, bioturbated, dominantly black colors, black streaks and mottles, H ₂ S-odor (Clayey Quartz Mud)	110 cm
1.1						120 cm
1.2	EOC 121 cm					
1.3						
1.4						
1.5						
1.6						
1.7						
1.8						
1.9						
2.0						

KD9548-17 VC

LOC.: 30 mls west of Belkovsky

TRANSDRIFT III

Recovery: 2.20 m

75°27.925 N 130°41.004 E

Water depth: 43 m

(m)	Lithology	Grain size	Texture	Color	Description	SS
0.0						0 cm
0.1				7.2Y 3.6/0.5 L: 36.99 a: 0.47 b: 3.26	Silty clay to clayey silt, oxic colors, soft, homogeneous, bioturbated, bivalve fragments, polychaet tubes, core-top destroyed (Clayey Quartz Mud)	10 cm
0.2					Below 14 cm gradually darkening of sediment, black streaks and mottles (Clayey Quartz Mud)	20 cm
0.3					Clayey silt, homogeneous, bioturbated, bivalve fragments, polychaet tubes (Clayey Quartz Mud)	
0.4						40 cm
0.5				6.9GY 3.4/0.1 L: 94.87 a: -0.18 b: -0.17	at 52 cm: accumulation of bivalve fragments	
0.6						60 cm
0.7					Silt, homogeneous, bioturbated, bivalve fragments, polychaet tubes (Clayey Quartz Mud) at 69-74 cm: accumulation of bivalve fragments	
0.8					Silt, homogeneous, bioturbated, bivalve fragments, polychaet tubes (Clayey Quartz Mud)	80 cm
0.9				9.0PB 3.0/0.2 L: 30.73 a: 0.09 b: -0.79		100 cm
1.0						

KD9548-17 VC

LOC.: 30 mls west of Belkovsky

TRANSDRIFT III

Recovery: 2.20 m

75°27.925 N 130°41.004 E

Water depth: 43 m

(m)	Lithology	Grain size	Texture	Color	Description	SS
1.0				1.0P 3.4/0.2 L: 29.26 a: 0.13 b: -0.28	Silt as above Sandy silt layer, homogenous (Clayey Quartz Mud)	105 cm
1.1						110 cm
1.15						115 cm
1.2				2.8YR 3.5/0.2 L: 35.72 a: 1.04 b: 1.00	Sandy silt to (clayey) sandy silt to silt, homogenous, bioturbated, oxic colors, bivalve fragments (Clayey Quartz Mud)	120 cm
1.3						130 cm
1.4						140 cm
1.5					(Clayey sandy) silt, strongly bioturbated, plant fragments, nearly black	150 cm
1.6					(Clayey Quartz Mud)	160 cm
1.7					Below 170 cm: Sediment becomes increasingly stiff due to dewatering and consolidation	170 cm
1.8				0.7P 3.4/0.4 L: 34.49 a: 0.43 b: -1.92		180 cm
1.9						190 cm
2.0						200 cm

KD9548-17 VC

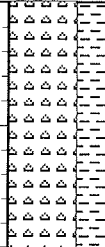


LOC.: 30 mls west off Belkovsky

TRANSDRIFT III

Recovery: 2,20 m

75°27.925 N 130°41.004 E

Water depth: 43 m

(m)	Lithology	Grain size	Texture	Color	Description	SS
2.0					(Clayey) silt, strongly bioturbated, plant fragments, nearly black, increasingly stiff due to dewatering and consolidation (Clayey Quartz Mud)	205 cm
2.1						210 cm
2.15						215 cm
2.2						220 cm
2.2	EOC 2,2 m					
2.3						
2.4						
2.5						
2.6						
2.7						
2.8						
2.9						
3.0						

KD9555-10 GKG

Loc.: off Belkovsky

TRANSDRIFT III

Recovery: 0.38 m

75°31.92 N 134°34.59 E

Water depth: 36.0 m

Surface	Sandy silt, uneven surface, bivalve fragments (<i>Leionucula belottii</i>), polychaets (<i>Glycera</i> sp.) and burrows (1 cm in diameter), 1 bryozoa (<i>Alcyonidium</i> sp.), isopods (<i>Saduria subini</i>)	T = - 1.6 °C
Color :	2.5Y 3/2 Munsell Color Chart	(Clayey Quartz Mud)

Lithology	Grain size	Texture	Color	Description	ss
				Sandy silt, oxic color, more sandy than below 4 cm (Clayey Quartz Mud)	0 cm
				7.8GY 3.6/0.1 L: 36.91 a: -0.28 b: 0.20	5 cm
				6.3P 2.9/0.6 L: 30.18 a: 2.12 b: -1.89	20 cm
				Clayey sandy silt, shell fragments, gradually darkening downcore, homogeneous, bioturbated (Clayey Quartz Mud)	36 cm
				6.2P 2.7/1.0 L: 27.51 a: 3.46 b: 3.10	EOC 38 cm
					50 cm

KD9560-5 BG

Loc.: north of Lena Delta

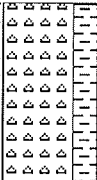
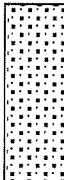
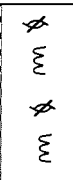
TRANSDRIFT III

Recovery: 0,10 m

73°47.770 N 126°17.663 E

Water depth: 13.0 m

Surface	Silty sand, uneven surface, bivalve fragments common, oxic colors (Clayey Quartz Mud)	T=	°C
Color :			

Lithology	Grain size	Texture	Color	Description	ss
0				Silty sand, uneven surface, bivalve fragments common, oxic colors (Clayey Quartz Mud)	0 cm
EOC 10 cm					
10					
20					
30					
40					
50					

KD9561-3 GKG

Loc.: off Lena Delta

TRANSDRIFT III

Recovery: 0.54 m

73°54.180 N 126°54.868 E

Water depth: 23.0 m

Surface	Clayey silt, flat and soupy surface, polychaets (<i>Glycera</i> sp.) and burrows (-1 cm in diameter), few ophiuredeans, sediment pile destroyed during sampling (Clayey Quartz Mud)	T= -0.4 °C
Color :	4.2YR 3.6/0.7 L: 37.15 a: 3.24 b: 4.04	

Lithology	Grain size	Texture	Color	Description	ss
			3.2YR 3.4/0.9 L: 36.06 a: 4.68 b: 5.30	Clayey silt as above, oxic color	0 cm
			3.4RP 3.5/0.5 L: 33.89 a: 2.96 b: 0.37	(Sandy) clayey silt, gradually darkening downcore, homogeneous, bioturbated (active bioturbation down to ca. 30 cm), polychaet burrows (-1 cm in diameter), sediment is very soft, sediment pile destroyed during sampling (Clayey Quartz Mud)	
			4.3P 3.6/0.6 L: 37.00 a: 1.25 b: -2.01		

EOC 54 cm

KD9568-8 GKG

Loc.: east of Taimyr

TRANSDRIFT III

Recovery: 0.38 m

75°29.040 N 114°29.754 E

Water depth: 34.0 m

Surface	Sandy silt, flat and even surface, abundant dropstones (- 7 cm in diameter), rich in small ophiuredeans (-3 cm in diameter), polychaets and tubes sticking out of the sediment surface, bivalve fragments (<i>Tridonta</i> sp.) common (Quartz Mud)	T= - 1.5 °C
Color :	5.1YR 3.9 /0.7	L: 40.29 a: 3.24 b: 4.47

Lithology	Grain size	Texture	Color	Description	SS
				As above, brownish color	0 cm
			3.9RP 4.0/0.3 L: 41.37 a: 1.08 b: 0.19	Sandy silt, homogenous, bioturbated, olive-gray, shell fragments all over the core (Quartz Mud)	
			4.1RP 3.7/0.5 L: 38.48 a: 2.50 b: 0.17	Sandy silt, gradually darkening downcore, black mottles and streaks due to strong bioturbation, polychaet burrows, bivalve fragments all over the core (Quartz Mud)	
			6.5P 3.7/0.6 L: 37.77 a: 1.75 b: -1.59		
EOC 38 cm					

KD9565-11 GKG

Loc.: Olenek channel

TRANSDRIFT III

Recovery: 0.44 m

73°50.760 N 126°19.000 E

Water depth: 21.0 m

Surface	Sandy silt, flat and even surface, polychaets and tubes sticking out of the sediment surface, bivalve fragments common, surficial enrichments of heavy minerals, brownish colors (Clayey Quartz Mud)	T = - 1.1 °C
Color :	3.9YR 3.7 0.7	L: 38.24 a: 3.54 b:4.25

Lithology	Grain size	Texture	Color	Description	ss
				As above, brownish color	0 cm
			0.1YR 3.8/0.3 L: 39.68 a: 1.32 b: 1.30	Sandy silt, homogenous, bioturbated, olive-gray, bivalve fragments common At ca. 7 cm: large plant fragment (ca. 15 cm in length, 3 cm in diameter)	
				Sandy silt, gradually darkening downcore, black mottles due to strong bioturbation, polychaet burrows (Clayey Quartz Mud)	
			3.2P 3.3/0.5 L: 33.97 a: 1.06 b: -2.05		
				Clayey silty sand, slightly finer than above, gradually darkening downcore, black streaks due to strong bioturbation, polychaet burrows and bivalve fragments common (Clayey Quartz Mud)	
			6.5P 3.1/0.9 L: 32.37 a: 3.07 b: -2.56		
EOC 44 cm					
					50

KD9568-7 GKG

Loc.: east of Taimyr

TRANSDRIFT III

Recovery: 0.40 m

75°29.100 N 114°28.209 E

Water depth: 34.0 m

Surface	Sandy silt, flat and even surface, abundant dropstones (-3 cm in diameter), rich in small ophiuredeans (-3 cm in diameter), polychaets and tubes sticking out of the sediment surface, bivalve fragments (<i>Tridonta</i> sp.) common, 1 snail (Clayey Quartz Mud)	T= - 1.3 °C
Color :	3.1YR 3.7 /0.6	L: 38.27 a: 3.16 b: 3.66

Lithology	Grain size	Texture	Color	Description	SS
				As above, brownish color	0 cm
			7.9R 3.6/0.4 L: 37.82 a: 2.58 b: 1.89	Sandy silt, homogenous, bioturbated, olive-gray, shell fragments all over the core (Clayey Quartz Mud)	
			0.6R 3.6/0.5 L: 37.07 a: 2.54 b: 1.15	Sandy silt, gradually darkening downcore, black mottles and streaks due to strong bioturbation, polychaet burrows (at ca. 20 cm: large burrow, 3 cm in diameter), bivalve fragments all over the core (Clayey Quartz Mud)	20 cm
			L: 38.89 a: 0.67 b: -2.63		40 cm
EOC 40 cm					
					50 cm

KD9565-8 BG

Loc.: Olenek channel

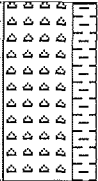
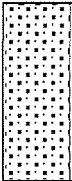
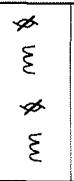
TRANSDRIFT III

Recovery: 0,10 m

73°N 50.840 120°18.070 E

Water depth: 26.0 m

Surface	Silty sand, uneven surface, bivalve fragments and polychaet tubes common, oxic brownish colors (Clayey Quartz Mud)	T= °C
Color :		

Depth in core (cm)	Lithology	Grain size	Texture	Color	Description	SS
	0					Silty sand, homogenous, bioturbated, bivalve fragments and polychaet tubes common, oxic brownish colors (Clayey Quartz Mud)
10	EOC 10 cm					
20						
30						
40						
50						

KD9568-8 GKG

Loc.: east of Taimyr

TRANSDRIFT III

Recovery: 0.38 m

75°29.040 N 114°29.754 E

Water depth: 34.0 m

Surface	Sandy silt, flat and even surface, abundant dropstones (- 7 cm in diameter), rich in small ophiuredeans (-3 cm in diameter), polychaets and tubes sticking out of the sediment surface, bivalve fragments (<i>Tridonta</i> sp.) common (Quartz Mud)	T = - 1.5 °C
Color :	5.1YR 3.9 /0.7	L: 40.29 a: 3.24 b: 4.47

Lithology	Grain size	Texture	Color	Description	ss
0				As above, brownish color	0 cm
0-10		?	3.9RP 4.0/0.3 L: 41.37 a: 1.08 b: 0.19	Sandy silt, homogenous, bioturbated, olive-gray, shell fragments all over the core (Quartz Mud)	
10-20		M			
20-30		?	4.1RP 3.7/0.5 L: 39.48 a: 2.50 b: 0.17	Sandy silt, gradually darkening downcore, black mottles and streaks due to strong bioturbation, polychaet burrows, bivalve fragments all over the core (Quartz Mud)	
30-40			6.5P 3.7/0.6 L: 37.77 a: 1.75 b: -1.59		
40	EOC 38 cm				
50					

KD9572-1 GKG

Loc.: east of Taimyr

TRANSDRIFT III

Recovery: 0.40 m

77°01.457 N 116°03.150 E

Water depth: 50.5 m

Surface	Sandy silt, flat and even surface, polychaets and tubes sticking out of the sediment surface, bivalve fragments (<i>Tridonta</i> sp., <i>Macoma calcarea</i>) common (Clayey Quartz Mud)	T = - 1.6 °C
Color :	3.5R 4.0 / 0.6	L: 41.05 a: 2.05 b: 2.01

Lithology	Grain size	Texture	Color	Description	ss
				As above, brownish color	0 cm
			7.1R 3.7/0.4 L: 38.70 a: 2.05 b: 1.51	Sandy clayey silt, homogenous, bioturbated, olive-gray with increasing dark streaks downcore, shell fragments all over the core (Clayey Quartz Mud)	10 cm
			9.4P 3.9/0.4 L: 39.91 a: 1.58 b: -0.66		20 cm
			9.6P 3.5/0.5 L: 36.02 a: 1.92 b: -0.79		30 cm
					40 cm
EOC 40 cm					
					50 cm

Symbols used in graphical core descriptions

Lithology



quartz



clay



silt



sand



silty clay



sandy silty clay



sandy silt

Texture

———— sharp boundary

- - - - boundary (2 cm)

----- fuzzy boundary (4 cm)

==== stratification

.....?..... gradational boundary

==== lamination

△ fining upwards

▽ fining downwards

○
○
○ soupy disturbance

ss smear slide

○ lense

● dropstone

↓ wormtube

⌘ plant fragments

⌘ shell fragments

~ slight bioturbation

~ moderate bioturbation

~ strong bioturbation

EXPEDITION TO THE LENA AND YANA RIVERS
June-September 1995

by V. Rachold, E. Hoops, A.M. Alabyan, V.N. Korotaev and A.A. Zaitsev

Volker Rachold & Erich Hoops, Alfred Wegener Institute for Polar and Marine
Research, Research Department Potsdam, Telegrafenberg A 43, 14773
Potsdam, F.R.G.

Andrey M. Alabyan, Vladislav N. Korotaev and Alexander A. Zaitsev, Moscow State
University, Geography Department, Scientific Research Laboratory of
Erosion and Fluvial Processes, Moscow 119899 RUSSIA

TABLE OF CONTENTS

1. INTRODUCTION.....	197
2. BACKGROUND INFORMATION.....	198
3. RESEARCH PROGRAM.....	199
4. COURSE OF EXPEDITION.....	200
5. SAMPLING AND METHODS.....	202
5.1. Water samples.....	202
5.2. Suspended material.....	203
5.3. Sediment samples.....	203
6. ACKNOWLEDGEMENTS.....	203
7. REFERENCES.....	204
APPENDIX.....	205

Expedition to the Lena and Yana Rivers June-September 1995

by V. Rachold, E. Hoops, A.M. Alabyan, V.N. Korotaev and A.A. Zaitsev

1. INTRODUCTION

Distribution, thickness and drift patterns of Arctic sea ice cover control the gas and heat exchange between atmosphere and ocean thus affecting ocean circulation and the global climate system (Aagaard et al., 1985; Clark, 1990). Today the major part of sea ice is formed in the broad Eurasian shelves, especially in the Laptev Sea that is the source area for the Transpolar Drift (Nürnberg et al., 1994; Wollenburg, 1993; Dethleff et al., 1993; Kassens & Karpiy, 1994) (Fig. 1). The Laptev Sea is strongly influenced by freshwater and sediment supply of the Siberian rivers mainly the Lena river. Sediments transported by those rivers are partly incorporated into sea ice entering the Transpolar Drift (Reimnitz et al., 1994 and 1995; Stein & Korolev, 1994). For this reason material derived from the Siberian continent contributes to the sedimentation in the Arctic ocean and the north Atlantic.

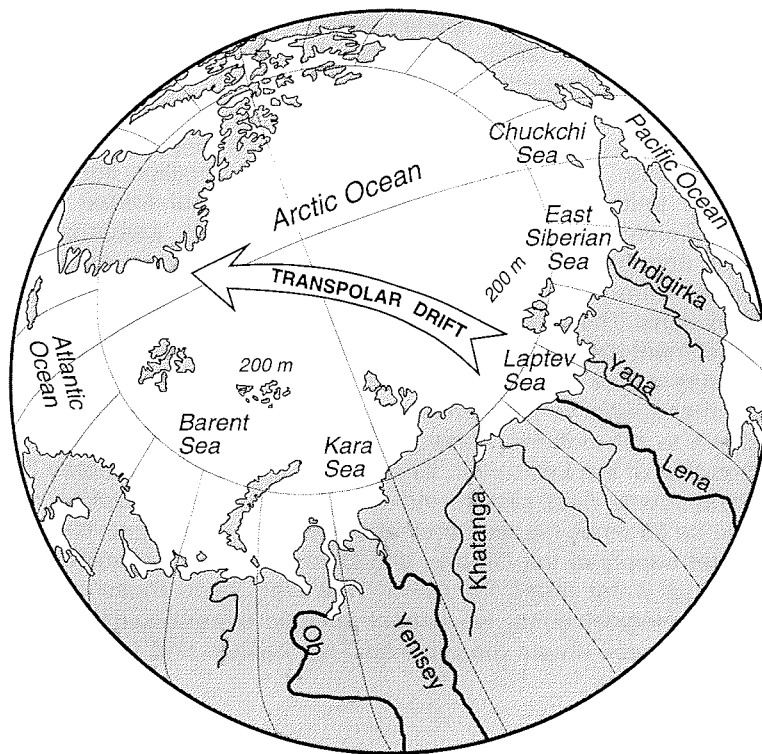


Fig. 1: Map of the Arctic Ocean showing the Transpolar Drift.

Within the framework of the Russian-German project "The Laptev Sea System", that is funded by the German ministry of education and research and the Russian ministry of research and technology, our group concentrates on the sediment transport of east Siberian rivers. The scientific goals of the investigations are

- to qualify and
- to quantify the recent and ancient material supply from the continent,
- to distinguish material transported by different rivers and
- to find characteristic signatures that allow the identification of this material in the marine sediments of the Laptev Sea shelf and the Arctic Ocean.

The Expedition to the Lena, Yana, Omoloy and Olenyok rivers organised by the Geographical Faculty of the Moscow State University in cooperation with the Alfred Wegener Institute, Research Department Potsdam, was carried from June 26 to September 7. It was the second expedition to the Siberian rivers; the first expedition took place in 1994 (Rachold et al., 1995).

2. BACKGROUND INFORMATION

In total the water supply of Siberian rivers to the Laptev Sea accounts for more than 700 km³ per year. 27 million tons of suspended sediment per year are transported mainly by the Lena river (Fig. 2).

In terms of water discharge the Lena river (520 km³ per year) is the eighth largest river in the world and the second largest of the Arctic rivers after the Yenisey (Milliman & Meade, 1983). The drainage area of 2.5 million km² is composed of three tectonic units: the Siberian platform, the Baikal folded region and the Verkhoyano-Kolymean folded region. Due to strong seasonal variations in temperature and precipitation (up to 100° C temperature difference between summer and winter) monthly water discharge and sediment transport exhibit extreme variations. The average concentration of suspended material is 40 mg/l.

The catchment area of the Yana is located in the Verkhoyano-Kolymean folded region and has a size of 0.24 million km². 99% of the sediments are transported during summer (June to September). On average once in four years the river freezes down to the bottom. Although the water discharge of the Yana is much smaller than that of the Lena river, its sediment supply to the Laptev Sea has to be taken into account. First results indicate that the concentration of suspended material can be 25 times higher than that of the Lena river (up to 1000 mg/l).

The water supply of the Omoloy and Olenyok rivers is of minor importance for the Laptev Sea water mass formation. However, since those rivers originate in remarkable geological units, we expect specific mineralogical and geochemical signals. The Olenyok drains the Siberian Trap basalts and the Omoloy cassiterite and gold ore deposits.

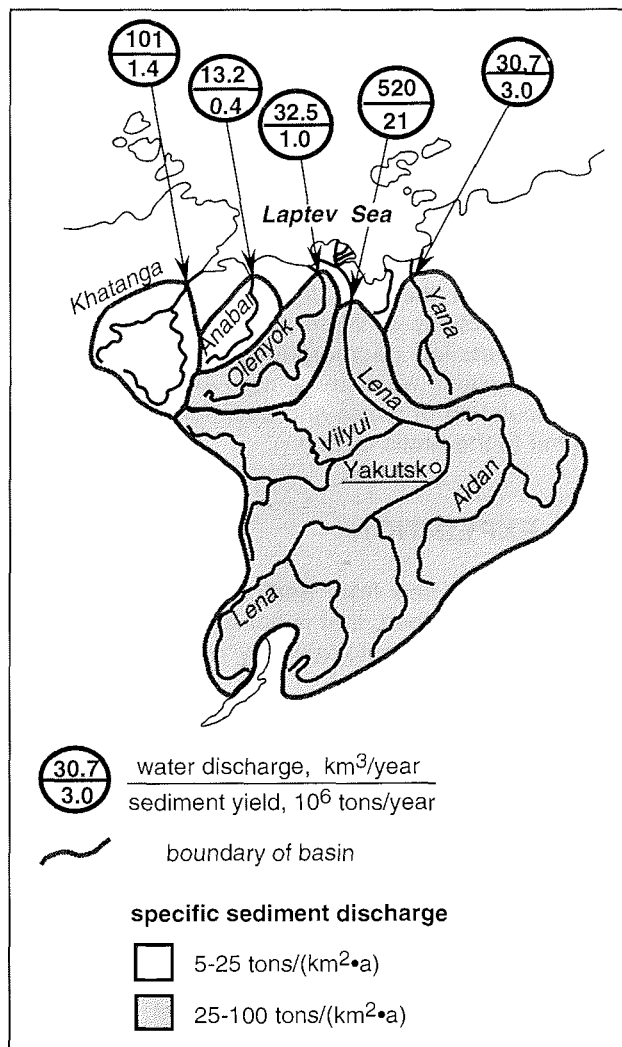


Fig. 2: Water and sediment supply to the Laptev Sea (from Alabyan et al., 1995).

3. RESEARCH PROGRAM

During the expedition water, surface sediments and suspended load of the Lena, Yana, Olenyok, Omoloy rivers and their tributaries were sampled. These samples will be analysed in the AWI by geochemical and mineralogical methods.

The analyses of the suspended load concentrate on

- major, trace and rare earth element geochemistry
- clay mineralogy,
- $\delta^{13}\text{C}$ values of the organic fraction and
- Sr isotope composition.

Surface sediments are studied for

- mineralogical composition, especially heavy minerals and
- bulk inorganic geochemistry of the fraction < 63 μm.

Water samples are analysed for

- oxygen and hydrogen isotopic composition.

Furthermore peat samples from the Lena and Yana delta are used for ¹⁴C age determination.

The Research Laboratory of Soil Erosion and Channel Processes of the Geographical Faculty, Moscow State University investigated hydrological and geomorphological features of basins, channels, confluences and deltas of the Vilyui, the Aldan, the Kirenga, the Vitim, the Lena, the Omoloy and the Yana rivers. During 1969-1995 long sections of these rivers were covered by bathymetric and sedimentologic maps. Detailed geomorphological and hydrological analyses of river channels and delta plains were performed. All these data may be considered as a basis for the calculation of water and sediment transport from Siberia to the Laptev Sea and further to the Arctic Ocean.

4. COURSE OF EXPEDITION

The German participants flew from Berlin to Moscow on June 26. During the next day in Moscow additional food, that is not available in Yakutia was bought. On June 28 the German group accompanied by one Russian participant took the aeroplane to Yakutsk.

After two days of preparing the RV "Prof. Makkaveev" in Yakutsk the first part of the expedition with two Russian and two German participants started on June 30. The ship went upstream and reached Olekminsk, the southernmost point of the expedition, on July 5. During the trip samples were taken at 10 stations (Fig. 3).

On July 9 "Prof. Makkaveev" arrived back in Yakutsk and the third Russian scientist joined the group. The next day the second leg, the expedition to the lower Lena including the Lena delta, started. The ship went northward and sampling was carried out in approximately 100 km intervals.

To obtain surface sediments of the Vilyui river we had to go up the tributary, since the lower reach of the river cuts through old Lena sediments. After going upstream with "Prof. Makkaveev" for 120 km the last 100 km were covered by a small motor boat.

Sampling the main river and the tributaries between Yakutsk and the Lena delta took about 2 weeks and on July 27 the ship arrived at Stolb island in the delta.

In the Lena delta the participants split up into two groups. While one group was sampling the different channels of the delta the other group headed to the mouth of the Olenyok river through the Olenyokskaya channel with the pilot boat "Iceberg". However, the "Iceberg" could not reach the Olenyok river because of ice in the Laptev Sea and returned to Stolb island. Our samples from the Olenyok river were taken by the crew of "Iceberg" one week later, after the ice had disappeared.

After completing the work in the Lena delta on August 8 the participants left "Prof. Makkaveev" and moved to a trade ship heading to Nizhneyansk at the Yana mouth.

The third leg, the expedition to the Yana with a fast ship of the type "Sarya", started on August 10. During 10 days the Yana river was sampled between Nizhneyansk and Verkhoyansk. Furthermore samples of most of the tributaries could be retrieved (Fig. 3).

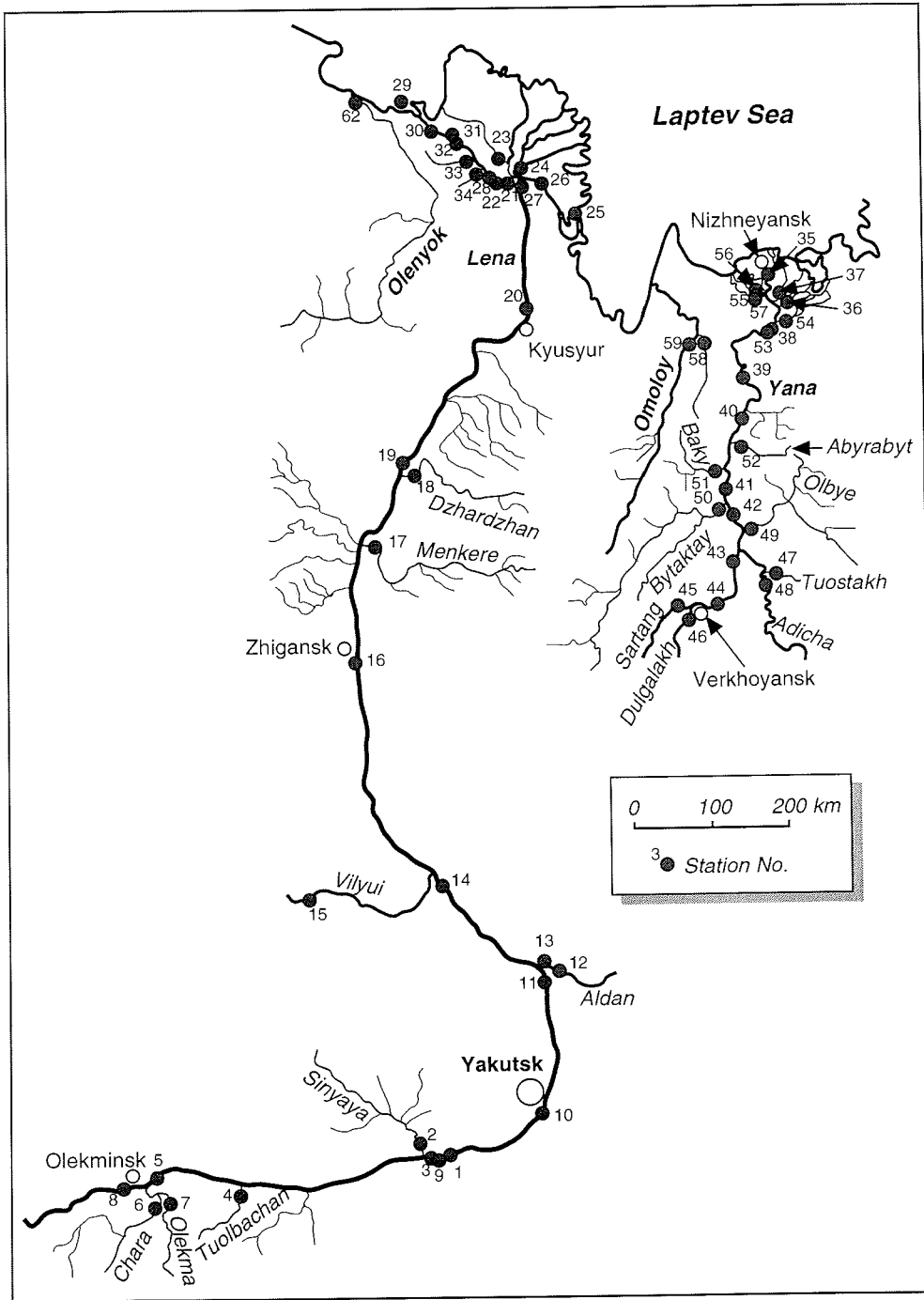


Fig. 3: Course of the expedition and locations of sampling.

To reach the Omoloy river a tank was used to cover the 90 km distance across the tundra. Since there is no road one way of the trip took us about 8 hours.

Sampling on the Yana river was completed on August 23 and two days later we flew from Nizhneyansk back to Yakutsk. After one week of preparing samples and equipment for customs we took the aeroplane to Moscow. The expedition ended in Berlin on September 7.

5. SAMPLING AND METHODS

Surface sediments, suspended load and river water were sampled at 62 stations. In general stations on the main rivers were performed as river cross sections, at which sediments were collected at 5 points and river water at 3 points. Small tributaries on the other hand were only sampled at one spot.

5.1. Water samples

For ultra-clean water sampling a Teflon watersampler with four 1l bottles was applied (Fig. 4). The sampler was lowered into the water in closed condition and opened by the fall weight. Water samples were taken at constant depth of 1.5 m.

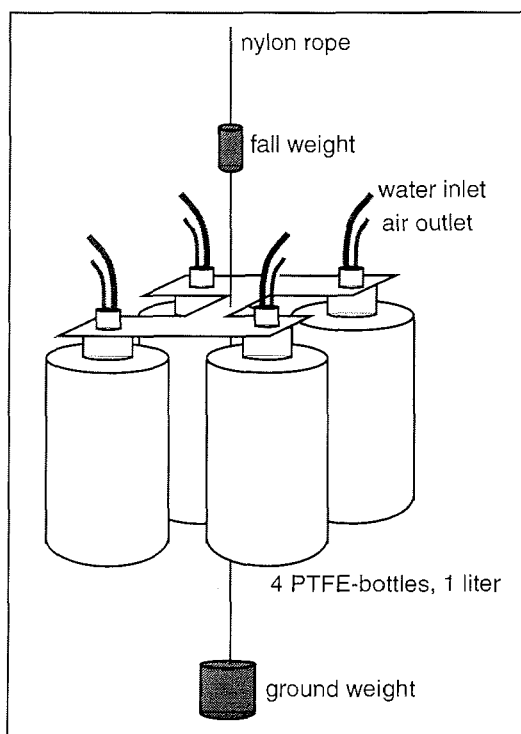


Fig. 4: PTFE water sampler.

The filtered water (0.45 μm Nucleopore filters, see below) was stored in pre-cleaned HDPE bottles for stable isotope analyses and in pre-cleaned, acidified HDPE bottles for inorganic analyses, respectively.

5.2. Suspended material

The suspended material was separated immediately after sampling by vacuum filtration. The filtered water volume varied between 0.25 and 4 l depending on sediment load. Three different types of filters were used:

- Nucleopore filters (pore size 0.45 μm) for inorganic geochemical analyses,
- cellulose acetate filters (pore size 0.45 μm) for clay mineral studies and
- glass fibre filters (pore size 0.7 μm) for analyses of the organic material.

All filters had been pre-weighted to calculate the sediment load. After air-drying the sediment loaded filters were stored dry and cold.

5.3. Sediment samples

The same heavy pale available on board RV "Professor Makkaveev", that was used during the last expedition (Rachold et al., 1995), was applied for sediment sampling. The instrument worked reasonably in the strong current of the Lena and Yana rivers and we obtained samples of disturbed surface sediments. However, the rivers have to be regarded as a dynamic system. While in one year sediments accumulates in the next year sediments are eroded at the same location. For this reason we think that the application of special equipment for sampling of undisturbed surface sediments is not required.

6. ACKNOWLEDGEMENTS

The authors wish to thank the crews of RV "Prof. Makkaveev" and "Sarya 9". Special thanks to O. M. Kirik and S. Ostgotchnov.

This study is part of the "Verbundvorhaben System Laptev See" which is funded by the "Bundesministerium für Bildung und Forschung".

7. REFERENCES

- Aagaard, K., Swift, J.H. & Carmack, E.C. (1985): *Thermohaline circulation in the Arctic Mediterranean Seas*. J. Geophys. Res. 90, 4833-4846
- Alabyan, A.M., Chalov, R.S., Korotaev, V.N., Sidorchuk, A.Y. & Zaitsev, A.A. (1995): *Natural and technogenic water and sediment supply to the Laptev Sea*. Reports on Polar Research 176, 265-271
- Clark, D.L. (1990): *Arctic ocean ice cover; geologic history and climatic significance*. Pp. 53-62 in Grantz, A., Johnson, L. & Sweeney, J.F. (ed.): *The Arctic Ocean Region*. Geol. Soc. Am., Boulder, CO
- Dethleff, D., Nürnberg, D., Reimnitz, E., Saarso, M. & Savchenko, Y.P. (1993): *East Siberian Arctic Region Expedition 92: The Laptev Sea - Its significance for Arctic sea-ice formation and transpolar sediment flux*. Reports on Polar Research 120, 1-44
- Kassens, H. & Karpiv, V. (1994): *Russian-German cooperation: the Transdrift 1 Expedition to the Laptev Sea*. Reports on Polar Research 151, Alfred Wegener Institute, Bremerhaven, 168 pp
- Milliman, J.D. & Meade, R.H. (1983): *World-wide delivery of river sediment to the oceans*. J. Geol. 91, 1-21
- Nürnberg, D., Wollenburg, I., Dethleff, D., Eicken, H., Kassens, H., Letzig, T., Reimnitz, E. & Thiede, J. (1994): *Sediments in Arctic sea ice: Implications for entrainment, transport and release*. Mar. Geol. 119, 185-214
- Rachold, V., Hermel, J. & Korotaev, V.N. (1995): *Expedition to the Lena River in July/August 1994*. Rep. Polar Research 182, 181-195
- Reimnitz, E., Dethleff, D. & Nürnberg, D. (1994): *Contrasts in Arctic shelf sea-ice regimes and some implications: Beaufort Sea versus Laptev Sea*. Mar. Geol. 119, 215-225
- Reimnitz, E., Kassens, H. & Eicken, H. (1995): *Sediment transport by Laptev Sea ice*. Reports on Polar Research 176, 71-77.
- Stein, R. & Korolev, S. (1994): *Present and past shelf-to-basin transport*. Reports on Polar Research 144, 87-100
- Wollenburg, I. (1993): *Sediment transport by Arctic Sea Ice: the recent load of lithogenic and biogenic material*. Reports on Polar Research 127, Alfred Wegener Institute, Bremerhaven, 159 pp

APPENDIX

Appendix 1: List of stations

Station	Date	Time (GMT)	Position		Description
1	01.07.1995	13:00	61°09.7'	127°23.3'	Lena R.
2	02.07.1995	1:00	61°10.5'	126°50.0'	Sinyaya R.
3	02.07.1995	6:00	61°08.1'	126°58.3'	Lena R.
4	04.07.1995	3:00	60°30.6'	122°52.6'	Tuolbachan R.
5	05.07.1995	3:00	60°27.4'	120°37.8'	Lena R.
6	05.07.1995	3:00	60°16.1'	120°59.2'	Chara R.
7	05.07.1995	3:30	60°16.1'	121°09.0'	Olyekma R.
8	06.07.1995	0:30	60°19.5'	120°15.8'	Lena R.
9	07.07.1995	8:30	61°08.1'	126°58.3'	Lena R.
10	07.07.1995	23:30	61°47.8'	129°39.4'	Lena R.
11	11.07.1995	1:30	63°16.2'	129°34.9'	Lena R.
12	11.07.1995	6:00	63°24.3'	129°50.9'	Aldan R.
13	15.07.1995	9:00	63°25.1'	129°36.4'	Aldan R.
14	17.07.1995	9:00	64°22.6'	126°30.0'	Lena R.
15	18.07.1995	12:30	63°57.8'	123°17.5'	Vilyuy R.
16	21.07.1995	5:00	66°41.1'	123°29.5'	Lena R.
17	24.07.1995	1:00	68°01.6'	123°32.1'	Menkere R.
18	24.07.1995	8:00	68°47.0'	124°06.7'	Dzhardzhan R.
19	24.07.1995	16:30	68°51.1'	123°57.8'	Lena R.
20	26.07.1995	8:00	70°81.5'	127°33.1'	Lena R.
21	27.07.1995	5:00	72°22.6'	126°29.3'	Lena Delta
22	27.07.1995	8:30	72°19.3'	126°00.0'	Lena Delta
23	27.07.1995	9:30	72°24.9'	126°26.7'	Lena Delta
24	29.07.1995	2:00	72°29.0'	126°40.0'	Lena Delta
25	30.07.1995	2:30	72°01.6'	129°07.8'	Lena Delta
26	31.07.1995	1:30	72°20.9'	127°28.7'	Lena Delta
27	02.08.1995	5:00	72°21.8'	126°41.7'	Lena River
28	02.08.1995	11:00	72°20.1'	125°44.0'	Lena Delta
29	30.07.1995	15:00	73°01.0'	121°47.0'	Laptev Sea
30	31.07.1995	15:15	72°52.7'	123°20.2'	Lena Delta
31	01.08.1995	15:45	72°36.2'	124°27.3'	Lena Delta
32	01.08.1995	16:45	72°40.3'	124°19.1'	Khmuraya R.
33	02.08.1995	7:00	72°35.8'	124°52.1'	Bolshaya R.
34	02.08.1995	11:00	72°26.3'	125°21.7'	Gagarya R.
35	08.08.1995	10:00	71°18.1'	135°59.8'	Yana Delta
36	09.08.1995	0:00	70°58.4'	136°29.4'	Yana Delta
37	09.08.1995	1:00	71°04.4'	136°17.1'	Yana Delta

Appendix 1: List of stations (continued)

Station	Date	Time (GMT)	Position		Description
38	09.08.1995	2:30	70°45.5'	136°04.0'	Yana Delta
39	09.08.1995	11:00	70°13.4'	135°06.9'	Yana R.
40	10.08.1995	8:00	69°43.1'	135°04.4'	Yana R.
41	11.08.1995	4:00	68°57.2'	134°27.8'	Yana R.
42	12.08.1995	2:00	68°36.4'	134°39.6'	Yana R.
43	12.08.1995	8:30	68°12.3'	134°54.7'	Yana R.
44	13.08.1995	0:30	67°32.9'	134°01.9'	Yana R.
45	13.08.1995	6:30	67°27.3'	133°13.1'	Sartang R.
46	13.08.1995	7:00	67°29.6'	133°14.5'	Dulgalakh R.
47	17.08.1995	5:00	67°51.9'	135°40.4'	Tuostakh R.
48	17.08.1995	5:30	67°48.7'	135°27.3'	Adicha R.
49	18.08.1995	3:00	68°24.3'	134°58.9'	Olbye R.
50	18.08.1995	12:30	68°44.6'	134°20.4'	Bytaktay R.
51	18.08.1995	23:00	69°07.3'	134°15.9'	Baky R.
52	19.08.1995	2:00	69°24.3'	134°45.5'	Abyrabyt R.
53	21.08.1995	7:30	70°45.4'	136°04.0'	Yana Delta
54	21.08.1995	8:30	70°47.0'	136°20.0'	Yana Delta
55	21.08.1995	11:00	71°47.5'	135°08.1'	Yana Delta
56	21.08.1995	22:30	71°09.7'	135°57.7'	Yana Delta
57	21.08.1995	22:50	71°07.3'	135°47.5'	Yana Delta
58	21.08.1995	12:30	70°42.3'	133°28.6'	Kyugyulyur R.
59	21.08.1995	13:00	70°42.6'	133°24.1'	Omoloy R.
60	23.08.1995	4:00	71°35.0'	136°46.5'	Laptev Sea
61	23.08.1995	4:30	71°39.5'	136°50.3'	Laptev Sea
62	13.08.1995	11:30	72°57.9'	119°57.2'	Olenyek R.

Appendix 2: List of samples

station	sample	comment
1	sediment	sandbank
2	water, sediment , filtered water, suspended material	tributary Sinyaya R.
3	water, sediment, filtered water, suspended material	river cross section Lena R.
4	water, filtered water, suspended material	tributary Tuolbachan R.
5	water, sediment , filtered water, suspended material	river cross section Lena R.
6	water, sediment , filtered water, suspended material	tributary Chara R.
7	water, sediment , filtered water, suspended material	tributary Olyekma R.
8	water, sediment , filtered water, suspended material	river cross section Lena R.
9	water, filtered water, suspended material	Lena R.
10	water, Sediment, filtered water, suspended material	river cross section Lena R.
11	water, sediment , filtered water, suspended material	river cross section Lena R.
12	water, sediment , filtered water, suspended material	river cross section Aldan R.
13	sediment	Aldan R.
14	water, sediment , filtered water, suspended material	river cross section Lena R.
15	water, sediment , filtered water, suspended material	river cross section Lena R.
16	water, sediment , filtered water, suspended material	river cross section Lena R.
17	water, sediment , filtered water, suspended material	tributary Menkere R.
18	water, sediment , filtered water, suspended material	tributary Dzhardzhan R.
19	water, sediment , filtered water, suspended material	river cross section Lena R.
20	water, sediment , filtered water, suspended material	river cross section Lena R.
21	sediment , peat	island Lena Delta
22	water, sediment , filtered water, suspended material	Lena Delta
23	water, sediment , filtered water, suspended material	Lena Delta
24	water, sediment , filtered water, suspended material	Lena Delta
25	water, sediment , filtered water, suspended material	Lena Delta
26	water, sediment , filtered water, suspended material	Lena Delta
27	water, sediment , filtered water, suspended material	Lena R.
28	sediment , peat	Lena Delta
29	sediment	Laptev Sea
30	sediment	Lena Delta
31	water, sediment , filtered water, suspended material	Lena Delta
32	sediment	tributary Khmuraya R.
33	sediment	tributary Boishaya R.
34	sediment	tributary Gagarya R.
35	water, sediment , filtered water, suspended material	Yana Delta
36	water, sediment , filtered water, suspended material	Yana Delta
37	sediment	Yana Delta

Appendix 2: List of samples (continued)

station	sample	comment
38	water, sediment , filtered water, suspended material	Yana Delta
39	water, sediment , filtered water, suspended material	river cross section Yana R.
40	water, sediment , filtered water, suspended material	river cross section Yana R.
41	water, sediment , filtered water, suspended material	river cross section Yana R.
42	water, sediment , filtered water, suspended material	river cross section Yana R.
43	water, sediment , filtered water, suspended material	river cross section Yana R.
44	water, sediment , filtered water, suspended material	river cross section Yana R.
45	water, sediment , filtered water, suspended material	tributary Sartang R.
46	water, sediment , filtered water, suspended material	tributary Dulgalakh R.
47	water, sediment , filtered water, suspended material	tributary Tuostakh R.
48	water, sediment , filtered water, suspended material	tributary Adicha R.
49	water, sediment , filtered water, suspended material	tributary Olbye R.
50	water, sediment , filtered water, suspended material	tributary Bytaktay R.
51	water, filtered water, suspended material	tributary Baky R.
52	sediment	tributary Abyrabyt R.
53	peat	Yana Delta
54	sediment	Yana Delta
55	sediment	Yana Delta
56	sediment	Yana Delta
57	sediment	Yana Delta
58	water, sediment , filtered water, suspended material	tributary Kyugyulyur R.
59	water, sediment , filtered water, suspended material	Omoloy R.
60	sediment	Laptev Sea
61	sediment	Laptev Sea
62	sediment, suspended material	Olenyek R.